

PART TWO

TWO-DIMENSIONAL FLOWS

5

LINEAR SYSTEMS

5.0 Introduction

As we've seen, in one-dimensional phase spaces the flow is extremely confined—all trajectories are forced to move monotonically or remain constant. In higher-dimensional phase spaces, trajectories have much more room to maneuver, and so a wider range of dynamical behavior becomes possible. Rather than attack all this complexity at once, we begin with the simplest class of higher-dimensional systems, namely *linear systems in two dimensions*. These systems are interesting in their own right, and, as we'll see later, they also play an important role in the classification of fixed points of *nonlinear* systems. We begin with some definitions and examples.

5.1 Definitions and Examples

A *two-dimensional linear system* is a system of the form

$$\dot{x} = ax + by$$

$$\dot{y} = cx + dy$$

where a, b, c, d are parameters. If we use boldface to denote vectors, this system can be written more compactly in matrix form as

$$\dot{\mathbf{x}} = A\mathbf{x},$$

where

$$A = \begin{pmatrix} a & b \\ c & d \end{pmatrix} \text{ and } \mathbf{x} = \begin{pmatrix} x \\ y \end{pmatrix}.$$

Such a system is *linear* in the sense that if \mathbf{x}_1 and \mathbf{x}_2 are solutions, then so is any linear combination $c_1\mathbf{x}_1 + c_2\mathbf{x}_2$. Notice that $\dot{\mathbf{x}} = \mathbf{0}$ when $\mathbf{x} = \mathbf{0}$, so $\mathbf{x}^* = \mathbf{0}$ is always a fixed point for any choice of A .

The solutions of $\dot{\mathbf{x}} = A\mathbf{x}$ can be visualized as trajectories moving on the (x, y) plane, in this context called the *phase plane*. Our first example presents the phase plane analysis of a familiar system.

EXAMPLE 5.1.1:

As discussed in elementary physics courses, the vibrations of a mass hanging from a linear spring are governed by the linear differential equation

$$m\ddot{x} + kx = 0 \quad (1)$$

where m is the mass, k is the spring constant, and x is the displacement of the mass from equilibrium (Figure 5.1.1). Give a phase plane analysis of this *simple harmonic oscillator*.

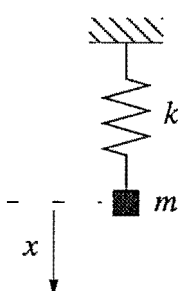


Figure 5.1.1

Solution: As you probably recall, it's easy to solve (1) analytically in terms of sines and cosines. But that's precisely what makes linear equations so special! For the *nonlinear* equations of ultimate interest to us, it's usually impossible to find an analytical solution. We want to develop methods for deducing the behavior of equations like (1) *without actually solving them*.

The motion in the phase plane is determined by a vector field that comes from the differential equation (1). To find this vector field, we note that the *state* of the system is characterized by its current position x and velocity v ; if we know the values of *both* x and v , then (1) uniquely determines the future states of the system. Therefore we rewrite (1) in terms of x and v , as follows:

$$\dot{x} = v \quad (2a)$$

$$\dot{v} = -\frac{k}{m}x. \quad (2b)$$

Equation (2a) is just the definition of velocity, and (2b) is the differential equation (1) rewritten in terms of v . To simplify the notation, let $\omega^2 = k/m$. Then (2) becomes

$$\dot{x} = v \quad (3a)$$

$$\dot{v} = -\omega^2x. \quad (3b)$$

The system (3) assigns a vector $(\dot{x}, \dot{v}) = (v, -\omega^2x)$ at each point (x, v) , and therefore represents a *vector field* on the phase plane.

For example, let's see what the vector field looks like when we're on the x -axis. Then $v = 0$ and so $(\dot{x}, \dot{v}) = (0, -\omega^2 x)$. Hence the vectors point vertically downward for positive x and vertically upward for negative x (Figure 5.1.2). As x gets larger in magnitude, the vectors $(0, -\omega^2 x)$ get longer. Similarly, on the v -axis, the vector field is $(\dot{x}, \dot{v}) = (v, 0)$, which points to the right when $v > 0$ and to the left when $v < 0$. As we move around in phase space, the vectors change direction as shown in Figure 5.1.2.

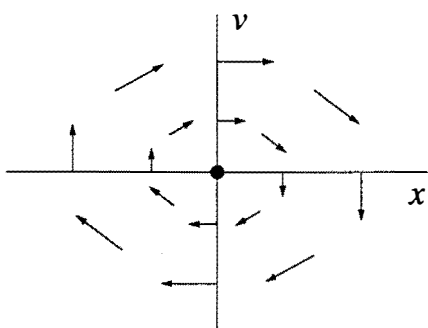


Figure 5.1.2

The flow in Figure 5.1.2 swirls about the origin. The origin is special, like the eye of a hurricane: a phase point placed there would remain motionless, because $(\dot{x}, \dot{v}) = (0, 0)$ when $(x, v) = (0, 0)$; hence the origin is a **fixed point**. But a phase point starting anywhere else would circulate around the origin and eventually return to its starting point. Such trajectories form **closed orbits**, as shown in Figure 5.1.3. Figure 5.1.3 is called the **phase portrait** of the system—it shows the overall picture of trajectories in phase space.

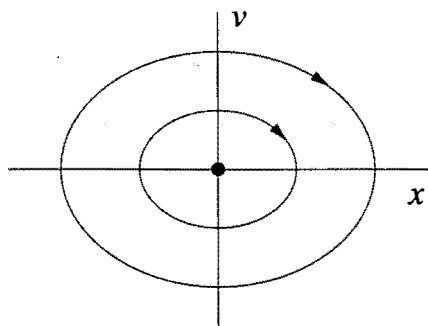


Figure 5.1.3

What do fixed points and closed orbits have to do with the original problem of a mass on a spring? The answers are beautifully simple. The fixed point $(x, v) = (0, 0)$ corresponds to static equilibrium of the system: the mass is at rest at its equilibrium position and will remain there forever, since the spring is relaxed. The closed orbits have a more interesting interpretation: they correspond to periodic motions, i.e., oscillations of the mass. To see this, just look at some points on a closed orbit (Figure 5.1.4). When the displacement x is most negative, the velocity v is zero; this corresponds to one extreme of the oscillation, where the spring is most compressed (Figure 5.1.4).

Just as in Chapter 2, it is helpful to visualize the vector field in terms of the motion of an imaginary fluid. In the present case, we imagine that a fluid is flowing steadily on the phase plane with a local velocity given by $(\dot{x}, \dot{v}) = (v, -\omega^2 x)$. Then, to find the trajectory starting at (x_0, v_0) , we place an imaginary particle or **phase point** at (x_0, v_0) and watch how it is carried around by the flow.

The flow in Figure 5.1.2 swirls about

the origin. The origin is special, like the eye of a hurricane: a phase point placed there would remain motionless, because $(\dot{x}, \dot{v}) = (0, 0)$ when $(x, v) = (0, 0)$; hence the origin is a **fixed point**. But a phase point starting anywhere else would circulate around the origin and eventually return to its starting point. Such trajectories form **closed orbits**, as shown in Figure 5.1.3. Figure 5.1.3 is called the **phase portrait** of the system—it shows the overall picture of trajectories in phase space.

What do fixed points and closed orbits have to do with the original problem of a mass on a spring? The answers are beautifully simple. The fixed point $(x, v) = (0, 0)$ corresponds to static equilibrium of the system: the mass is at rest at its equilibrium position and will remain there forever, since the spring is relaxed. The closed orbits have a more interesting interpretation: they correspond to periodic motions, i.e., oscillations of the mass. To see this, just look at some points on a closed orbit (Figure 5.1.4). When the displacement x is most negative, the velocity v is zero; this corresponds to one extreme of the oscillation, where the spring is most compressed (Figure 5.1.4).

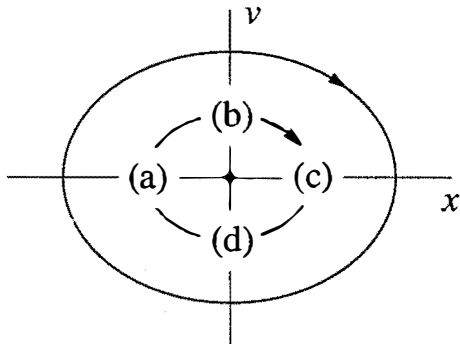
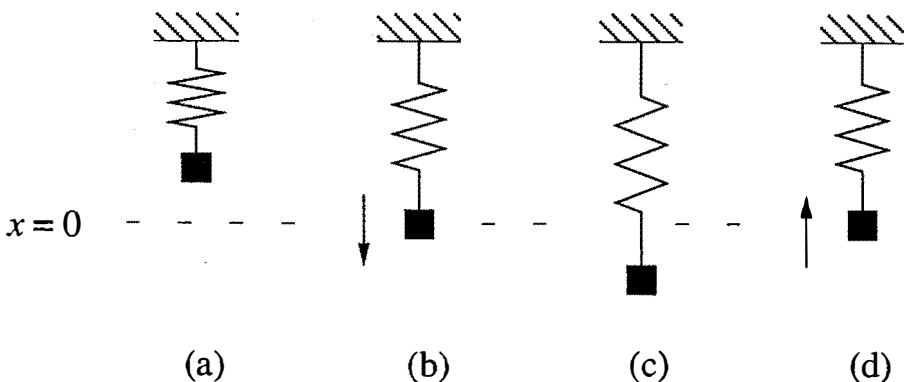


Figure 5.1.4

In the next instant as the phase point flows along the orbit, it is carried to points where x has increased and v is now positive; the mass is being pushed back toward its equilibrium position. But by the time the mass has reached $x = 0$, it has a large positive velocity (Figure 5.1.4b) and so it overshoots $x = 0$. The mass eventually comes to rest at the other end of its swing, where x is most positive and v is zero again (Figure 5.1.4c). Then the mass gets pulled up again and eventually completes the cycle (Figure 5.1.4d).

The shape of the closed orbits also has an interesting physical interpretation. The orbits in Figures 5.1.3 and 5.1.4 are actually *ellipses* given by the equation $\omega^2 x^2 + v^2 = C$, where $C \geq 0$ is a constant. In Exercise 5.1.1, you are asked to derive this geometric result, and to show that it is equivalent to conservation of energy. ■

EXAMPLE 5.1.2:

Solve the linear system $\dot{\mathbf{x}} = A\mathbf{x}$, where $A = \begin{pmatrix} a & 0 \\ 0 & -1 \end{pmatrix}$. Graph the phase portrait

as a varies from $-\infty$ to $+\infty$, showing the qualitatively different cases.

Solution: The system is

$$\begin{pmatrix} \dot{x} \\ \dot{y} \end{pmatrix} = \begin{pmatrix} a & 0 \\ 0 & -1 \end{pmatrix} \begin{pmatrix} x \\ y \end{pmatrix}.$$

Matrix multiplication yields

$$\dot{x} = ax$$

$$\dot{y} = -y$$

which shows that the two equations are **uncoupled**; there's no x in the y -equation and vice versa. In this simple case, each equation may be solved separately. The solution is

$$x(t) = x_0 e^{at} \quad (Ia)$$

$$y(t) = y_0 e^{-t}. \quad (Ib)$$

The phase portraits for different values of a are shown in Figure 5.1.5. In each case, $y(t)$ decays exponentially. When $a < 0$, $x(t)$ also decays exponentially and so all trajectories approach the origin as $t \rightarrow \infty$. However, the direction of approach depends on the size of a compared to -1 .

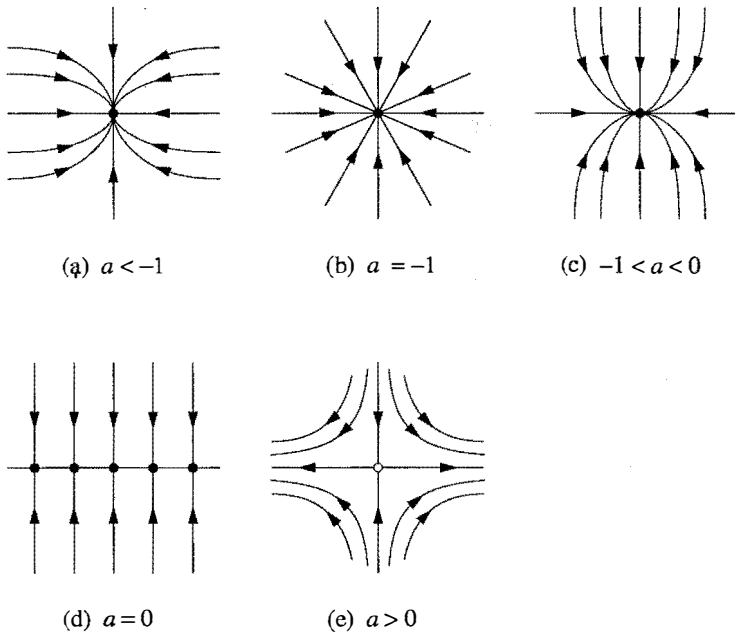


Figure 5.1.5

In Figure 5.1.5a, we have $\alpha < -1$, which implies that $x(t)$ decays more rapidly than $y(t)$. The trajectories approach the origin tangent to the *slower* direction (here, the y -direction). The intuitive explanation is that when α is very negative, the trajectory slams horizontally onto the y -axis, because the decay of $x(t)$ is almost instantaneous. Then the trajectory dawdles along the y -axis toward the origin, and so the approach is tangent to the y -axis. On the other hand, if we look *backwards* along a trajectory ($t \rightarrow -\infty$), then the trajectories all become parallel to the faster decaying direction (here, the x -direction). These conclusions are easily proved by looking at the slope $dy/dx = \dot{y}/\dot{x}$ along the trajectories; see Exercise 5.1.2. In Figure 5.1.5a, the fixed point $\mathbf{x}^* = \mathbf{0}$ is called a **stable node**.

Figure 5.1.5b shows the case $\alpha = -1$. Equation (1) shows that $y(t)/x(t) = y_0/x_0 =$ constant, and so all trajectories are straight lines through the origin. This is a very special case—it occurs because the decay rates in the two directions are precisely equal. In this case, \mathbf{x}^* is called a symmetrical node or **star**.

When $-1 < \alpha < 0$, we again have a node, but now the trajectories approach \mathbf{x}^* along the x -direction, which is the more slowly decaying direction for this range of α (Figure 5.1.5c).

Something dramatic happens when $\alpha = 0$ (Figure 5.1.5d). Now (1a) becomes $x(t) \equiv x_0$ and so there's an entire **line of fixed points** along the x -axis. All trajectories approach these fixed points along vertical lines.

Finally when $\alpha > 0$ (Figure 5.1.5e), \mathbf{x}^* becomes unstable, due to the exponential growth in the x -direction. Most trajectories veer away from \mathbf{x}^* and head out to infinity. An exception occurs if the trajectory starts on the y -axis; then it walks a tightrope to the origin. In forward time, the trajectories are asymptotic to the x -axis; in backward time, to the y -axis. Here $\mathbf{x}^* = \mathbf{0}$ is called a **saddle point**. The y -axis is called the **stable manifold** of the saddle point \mathbf{x}^* , defined as the set of initial conditions \mathbf{x}_0 such that $\mathbf{x}(t) \rightarrow \mathbf{x}^*$ as $t \rightarrow \infty$. Likewise, the **unstable manifold** of \mathbf{x}^* is the set of initial conditions such that $\mathbf{x}(t) \rightarrow \mathbf{x}^*$ as $t \rightarrow -\infty$. Here the unstable manifold is the x -axis. Note that a typical trajectory asymptotically approaches the unstable manifold as $t \rightarrow \infty$, and approaches the stable manifold as $t \rightarrow -\infty$. This sounds backwards, but it's right! ■

Stability Language

It's useful to introduce some language that allows us to discuss the stability of different types of fixed points. This language will be especially useful when we analyze fixed points of *nonlinear* systems. For now we'll be informal; precise definitions of the different types of stability will be given in Exercise 5.1.10.

We say that $\mathbf{x}^* = \mathbf{0}$ is an **attracting** fixed point in Figures 5.1.5a–c; all trajectories that start near \mathbf{x}^* approach it as $t \rightarrow \infty$. That is, $\mathbf{x}(t) \rightarrow \mathbf{x}^*$ as $t \rightarrow \infty$. In fact \mathbf{x}^* attracts *all* trajectories in the phase plane, so it could be called **globally attracting**.

There's a completely different notion of stability which relates to the behavior

of trajectories for *all* time, not just as $t \rightarrow \infty$. We say that a fixed point \mathbf{x}^* is **Liapunov stable** if all trajectories that start sufficiently close to \mathbf{x}^* remain close to it for all time. In Figures 5.1.5a–d, the origin is Liapunov stable.

Figure 5.1.5d shows that a fixed point can be Liapunov stable but not attracting. This situation comes up often enough that there is a special name for it. When a fixed point is Liapunov stable but not attracting, it is called **neutrally stable**. Nearby trajectories are neither attracted to nor repelled from a neutrally stable point. As a second example, the equilibrium point of the simple harmonic oscillator (Figure 5.1.3) is neutrally stable. Neutral stability is commonly encountered in mechanical systems in the absence of friction. Conversely, it's possible for a fixed point to be attracting but not Liapunov stable; thus, neither notion of stability implies the other. An example is given by the following vector field on the circle: $\dot{\theta} = 1 - \cos \theta$ (Figure 5.1.6). Here $\theta^* = 0$ attracts all trajectories as $t \rightarrow \infty$, but it is not Liapunov stable; there are trajectories that start infinitesimally close to θ^* but go on a very large excursion before returning to θ^* .

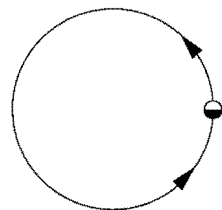


Figure 5.1.6

However, in practice the two types of stability often occur together. If a fixed point is *both* Liapunov stable and attracting, we'll call it **stable**, or sometimes **asymptotically stable**.

Finally, \mathbf{x}^* is **unstable** in Figure 5.1.5e, because it is neither attracting nor Liapunov stable.

A graphical convention: we'll use open dots to denote unstable fixed points, and solid black dots to denote Liapunov stable fixed points. This convention is consistent with that used in previous chapters.

5.2 Classification of Linear Systems

The examples in the last section had the special feature that two of the entries in the matrix A were zero. Now we want to study the general case of an arbitrary 2×2 matrix, with the aim of classifying all the possible phase portraits that can occur.

Example 5.1.2 provides a clue about how to proceed. Recall that the x and y axes played a crucial geometric role. They determined the direction of the trajectories as $t \rightarrow \pm\infty$. They also contained special **straight-line trajectories**: a trajectory starting on one of the coordinate axes stayed on that axis forever, and exhibited simple exponential growth or decay along it.

For the general case, we would like to find the analog of these straight-line trajectories. That is, we seek trajectories of the form

$$\mathbf{x}(t) = e^{\lambda t} \mathbf{v}, \quad (2)$$

where $\mathbf{v} \neq \mathbf{0}$ is some fixed vector to be determined, and λ is a growth rate, also to be determined. If such solutions exist, they correspond to exponential motion along the line spanned by the vector \mathbf{v} .

To find the conditions on \mathbf{v} and λ , we substitute $\mathbf{x}(t) = e^{\lambda t} \mathbf{v}$ into $\dot{\mathbf{x}} = A\mathbf{x}$, and obtain $\lambda e^{\lambda t} \mathbf{v} = e^{\lambda t} A\mathbf{v}$. Canceling the nonzero scalar factor $e^{\lambda t}$ yields

$$A\mathbf{v} = \lambda \mathbf{v}, \quad (3)$$

which says that the desired straight line solutions exist if \mathbf{v} is an *eigenvector* of A with corresponding *eigenvalue* λ . In this case we call the solution (2) an *eigen-solution*.

Let's recall how to find eigenvalues and eigenvectors. (If your memory needs more refreshing, see any text on linear algebra.) In general, the eigenvalues of a matrix A are given by the *characteristic equation* $\det(A - \lambda I) = 0$, where I is the identity matrix. For a 2×2 matrix

$$A = \begin{pmatrix} a & b \\ c & d \end{pmatrix},$$

the characteristic equation becomes

$$\det \begin{pmatrix} a - \lambda & b \\ c & d - \lambda \end{pmatrix} = 0.$$

Expanding the determinant yields

$$\lambda^2 - \tau\lambda + \Delta = 0 \quad (4)$$

where

$$\begin{aligned} \tau &= \text{trace}(A) = a + d, \\ \Delta &= \det(A) = ad - bc. \end{aligned}$$

Then

$$\lambda_1 = \frac{\tau + \sqrt{\tau^2 - 4\Delta}}{2}, \quad \lambda_2 = \frac{\tau - \sqrt{\tau^2 - 4\Delta}}{2} \quad (5)$$

are the solutions of the quadratic equation (4). In other words, the eigenvalues depend only on the trace and determinant of the matrix A .

The typical situation is for the eigenvalues to be distinct: $\lambda_1 \neq \lambda_2$. In this case, a theorem of linear algebra states that the corresponding eigenvectors \mathbf{v}_1 and \mathbf{v}_2 are linearly independent, and hence span the entire plane (Figure 5.2.1). In particular, any initial condition \mathbf{x}_0 can be written as a linear combination of eigenvectors, say $\mathbf{x}_0 = c_1 \mathbf{v}_1 + c_2 \mathbf{v}_2$.

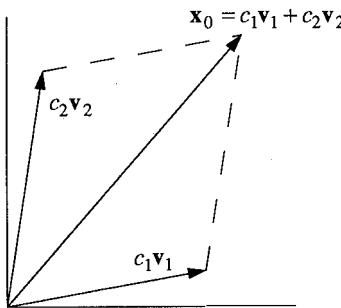


Figure 5.2.1

This observation allows us to write down the general solution for $\mathbf{x}(t)$ —it is simply

$$\mathbf{x}(t) = c_1 e^{\lambda_1 t} \mathbf{v}_1 + c_2 e^{\lambda_2 t} \mathbf{v}_2. \quad (6)$$

Why is this the general solution? First of all, it is a linear combination of solutions to $\dot{\mathbf{x}} = A\mathbf{x}$, and hence is itself a solution. Second, it satisfies the initial condition $\mathbf{x}(0) = \mathbf{x}_0$, and so by the existence and uniqueness theorem, it is the *only* solution. (See Section 6.2 for a general statement of the existence and uniqueness theorem.)

EXAMPLE 5.2.1:

Solve the initial value problem $\dot{x} = x + y$, $\dot{y} = 4x - 2y$, subject to the initial condition $(x_0, y_0) = (2, -3)$.

Solution: The corresponding matrix equation is

$$\begin{pmatrix} \dot{x} \\ \dot{y} \end{pmatrix} = \begin{pmatrix} 1 & 1 \\ 4 & -2 \end{pmatrix} \begin{pmatrix} x \\ y \end{pmatrix}.$$

First we find the eigenvalues of the matrix A . The matrix has $\tau = -1$ and $\Delta = -6$, so the characteristic equation is $\lambda^2 + \lambda - 6 = 0$. Hence

$$\lambda_1 = 2, \quad \lambda_2 = -3.$$

Next we find the eigenvectors. Given an eigenvalue λ , the corresponding eigenvector $\mathbf{v} = (v_1, v_2)$ satisfies

$$\begin{pmatrix} 1-\lambda & 1 \\ 4 & -2-\lambda \end{pmatrix} \begin{pmatrix} v_1 \\ v_2 \end{pmatrix} = \begin{pmatrix} 0 \\ 0 \end{pmatrix}.$$

For $\lambda_1 = 2$, this yields $\begin{pmatrix} -1 & 1 \\ 4 & -4 \end{pmatrix} \begin{pmatrix} v_1 \\ v_2 \end{pmatrix} = \begin{pmatrix} 0 \\ 0 \end{pmatrix}$, which has a nontrivial solution

$(v_1, v_2) = (1, 1)$, or any scalar multiple thereof. (Of course, any multiple of an eigenvector is always an eigenvector; we try to pick the simplest multiple, but any one will do.) Similarly, for $\lambda_2 = -3$, the eigenvector equation becomes $\begin{pmatrix} 4 & 1 \\ 4 & 1 \end{pmatrix} \begin{pmatrix} v_1 \\ v_2 \end{pmatrix} = \begin{pmatrix} 0 \\ 0 \end{pmatrix}$,

which has a nontrivial solution $(v_1, v_2) = (1, -4)$. In summary,

$$v_1 = \begin{pmatrix} 1 \\ 1 \end{pmatrix}, \quad v_2 = \begin{pmatrix} 1 \\ -4 \end{pmatrix}.$$

Next we write the general solution as a linear combination of eigensolutions. From (6), the general solution is

$$\mathbf{x}(t) = c_1 \begin{pmatrix} 1 \\ 1 \end{pmatrix} e^{2t} + c_2 \begin{pmatrix} 1 \\ -4 \end{pmatrix} e^{-3t}. \quad (7)$$

Finally, we compute c_1 and c_2 to satisfy the initial condition $(x_0, y_0) = (2, -3)$. At $t = 0$, (7) becomes

$$\begin{pmatrix} 2 \\ -3 \end{pmatrix} = c_1 \begin{pmatrix} 1 \\ 1 \end{pmatrix} + c_2 \begin{pmatrix} 1 \\ -4 \end{pmatrix},$$

which is equivalent to the algebraic system

$$\begin{aligned} 2 &= c_1 + c_2, \\ -3 &= c_1 - 4c_2. \end{aligned}$$

The solution is $c_1 = 1$, $c_2 = 1$. Substituting back into (7) yields

$$\begin{aligned} x(t) &= e^{2t} + e^{-3t}, \\ y(t) &= e^{2t} - 4e^{-3t} \end{aligned}$$

for the solution to the initial value problem. ■

Whew! Fortunately we don't need to go through all this to draw the phase portrait of a linear system. All we need to know are the eigenvectors and eigenvalues.

EXAMPLE 5.2.2:

Draw the phase portrait for the system of Example 5.2.1.

Solution: The system has eigenvalues $\lambda_1 = 2$, $\lambda_2 = -3$. Hence the first eigensolution grows exponentially, and the second eigensolution decays. This means the origin is a *saddle point*. Its stable manifold is the line spanned by the eigenvector $v_2 = (1, -4)$, corresponding to the decaying eigensolution. Similarly, the unstable

manifold is the line spanned by $\mathbf{v}_1 = (1, 1)$. As with all saddle points, a typical trajectory approaches the unstable manifold as $t \rightarrow \infty$, and the stable manifold as $t \rightarrow -\infty$. Figure 5.2.2 shows the phase portrait. ■

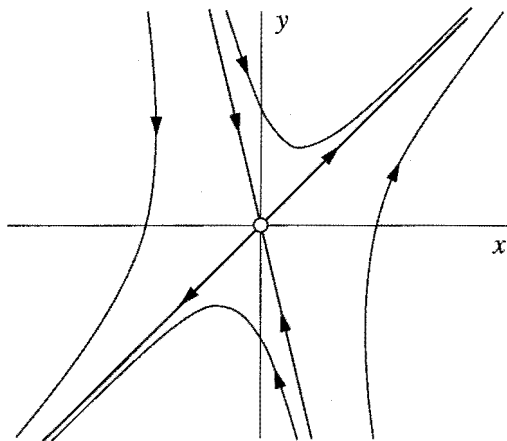
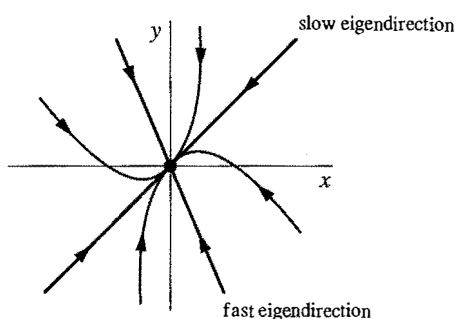


Figure 5.2.2

EXAMPLE 5.2.3:

Sketch a typical phase portrait for the case $\lambda_2 < \lambda_1 < 0$.

Solution: First suppose $\lambda_2 < \lambda_1 < 0$. Then both eigensolutions decay exponentially.



The fixed point is a stable node, as in Figures 5.1.5a and 5.1.5c, except now the eigenvectors are not mutually perpendicular, in general. Trajectories typically approach the origin tangent to the *slow eigendirection*, defined as the direction spanned by the eigenvector with the smaller $|\lambda|$. In backwards time ($t \rightarrow -\infty$), the trajectories become parallel to the fast eigendirection. Figure 5.2.3

Figure 5.2.3

shows the phase portrait. (If we reverse all the arrows in Figure 5.2.3, we obtain a typical phase portrait for an *unstable node*.) ■

EXAMPLE 5.2.4:

What happens if the eigenvalues are *complex* numbers?

Solution: If the eigenvalues are complex, the fixed point is either a **center** (Figure 5.2.4a) or a **spiral** (Figure 5.2.4b). We've already seen an example of a center

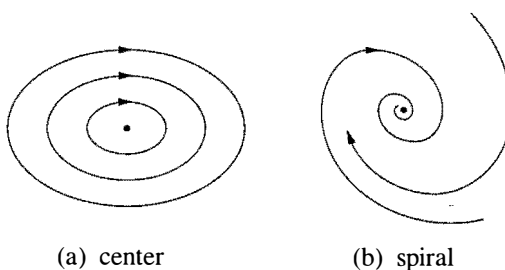


Figure 5.2.4

in the simple harmonic oscillator of Section 5.1; the origin is surrounded by a family of closed orbits. Note that centers are *neutrally stable*, since nearby trajectories are neither attracted to nor repelled from the fixed point. A spiral would occur if the harmonic oscillator were lightly damped. Then the trajectory would just fail to

close, because the oscillator loses a bit of energy on each cycle.

To justify these statements, recall that the eigenvalues are $\lambda_{1,2} = \frac{1}{2}(\tau \pm \sqrt{\tau^2 - 4\Delta})$. Thus complex eigenvalues occur when

$$\tau^2 - 4\Delta < 0.$$

To simplify the notation, let's write the eigenvalues as

$$\lambda_{1,2} = \alpha \pm i\omega$$

where

$$\alpha = \tau/2, \quad \omega = \frac{1}{2}\sqrt{4\Delta - \tau^2}.$$

By assumption, $\omega \neq 0$. Then the eigenvalues are distinct and so the general solution is still given by

$$\mathbf{x}(t) = c_1 e^{\lambda_1 t} \mathbf{v}_1 + c_2 e^{\lambda_2 t} \mathbf{v}_2.$$

But now the c 's and \mathbf{v} 's are *complex*, since the λ 's are. This means that $\mathbf{x}(t)$ involves linear combinations of $e^{(\alpha \pm i\omega)t}$. By Euler's formula, $e^{i\omega t} = \cos \omega t + i \sin \omega t$. Hence $\mathbf{x}(t)$ is a combination of terms involving $e^\alpha \cos \omega t$ and $e^\alpha \sin \omega t$. Such terms represent exponentially *decaying oscillations* if $\alpha = \text{Re}(\lambda) < 0$ and *growing oscillations* if $\alpha > 0$. The corresponding fixed points are **stable** and **unstable spirals**, respectively. Figure 5.2.4b shows the stable case.

If the eigenvalues are pure imaginary ($\alpha = 0$), then all the solutions are periodic with period $T = 2\pi/\omega$. The oscillations have fixed amplitude and the fixed point is a center.

For both centers and spirals, it's easy to determine whether the rotation is clockwise or counterclockwise; just compute a few vectors in the vector field and the sense of rotation should be obvious. ■

EXAMPLE 5.2.5:

In our analysis of the general case, we have been assuming that the eigenvalues are distinct. What happens if the eigenvalues are *equal*?

Solution: Suppose $\lambda_1 = \lambda_2 = \lambda$. There are two possibilities: either there are two independent eigenvectors corresponding to λ , or there's only one.

If there are two independent eigenvectors, then they span the plane and so *every vector is an eigenvector with this same eigenvalue λ* . To see this, write an arbitrary vector \mathbf{x}_0 as a linear combination of the two eigenvectors: $\mathbf{x}_0 = c_1 \mathbf{v}_1 + c_2 \mathbf{v}_2$. Then

$$A\mathbf{x}_0 = A(c_1 \mathbf{v}_1 + c_2 \mathbf{v}_2) = c_1 \lambda \mathbf{v}_1 + c_2 \lambda \mathbf{v}_2 = \lambda \mathbf{x}_0$$

so \mathbf{x}_0 is also an eigenvector with eigenvalue λ . Since multiplication by A simply stretches every vector by a factor λ , the matrix must be a multiple of the identity:

$$A = \begin{pmatrix} \lambda & 0 \\ 0 & \lambda \end{pmatrix}.$$

Then if $\lambda \neq 0$, all trajectories are straight lines through the origin ($\mathbf{x}(t) = e^{\lambda t} \mathbf{x}_0$) and the fixed point is a ***star node*** (Figure 5.2.5).

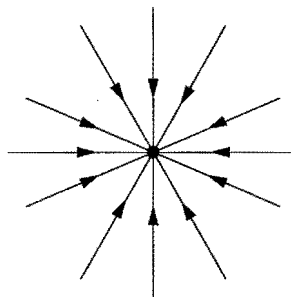


Figure 5.2.5

On the other hand, if $\lambda = 0$, the whole plane is filled with fixed points! (No surprise—the system is $\dot{\mathbf{x}} = \mathbf{0}$.)

The other possibility is that there's only one eigenvector (more accurately, the eigenspace corresponding to λ is one-dimensional.) For example, any matrix of the form $A = \begin{pmatrix} \lambda & b \\ 0 & \lambda \end{pmatrix}$, with $b \neq 0$ has only a one-dimensional eigenspace (Exercise 5.2.11).

When there's only one eigendirection, the fixed point is a ***degenerate node***. A

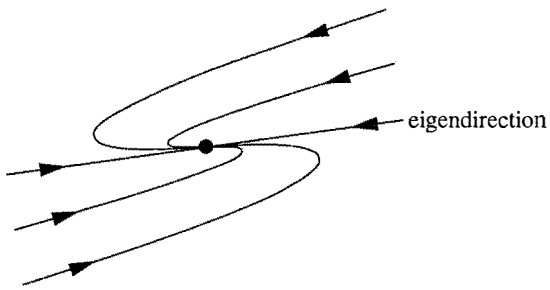


Figure 5.2.6

has two independent eigendirections; all trajectories are parallel to the slow eigendirection as $t \rightarrow \infty$, and to the fast eigendirection as $t \rightarrow -\infty$ (Figure 5.2.7a).

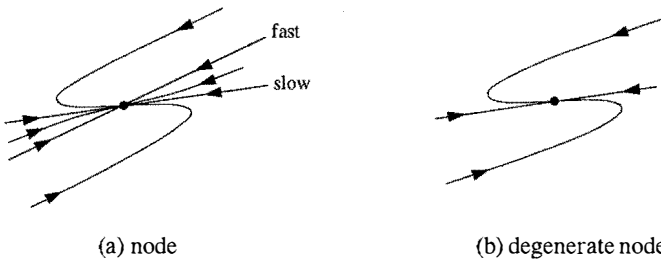


Figure 5.2.7

Now suppose we start changing the parameters of the system in such a way that the two eigendirections are scissored together. Then some of the trajectories will get squashed in the collapsing region between the two eigendirections, while the surviving trajectories get pulled around to form the degenerate node (Figure 5.2.7b).

Another way to get intuition about this case is to realize that the degenerate node is on the *borderline between a spiral and a node*. The trajectories are trying to wind around in a spiral, but they don't quite make it. ■

Classification of Fixed Points

By now you're probably tired of all the examples and ready for a simple classification scheme. Happily, there is one. We can show the type and stability of all the different fixed points on a single diagram (Figure 5.2.8).

typical phase portrait is shown in Figure 5.2.6. As $t \rightarrow +\infty$ and also as $t \rightarrow -\infty$, all trajectories become parallel to the one available eigendirection.

A good way to think about the degenerate node is to imagine that it has been created by deforming an ordinary node. The ordinary node

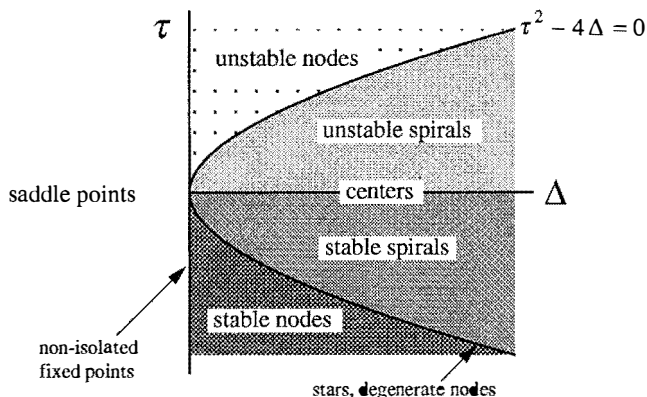


Figure 5.2.8

The axes are the trace τ and the determinant Δ of the matrix A . All of the information in the diagram is implied by the following formulas:

$$\lambda_{1,2} = \frac{1}{2} \left(\tau \pm \sqrt{\tau^2 - 4\Delta} \right), \quad \Delta = \lambda_1 \lambda_2, \quad \tau = \lambda_1 + \lambda_2.$$

The first equation is just (5). The second and third can be obtained by writing the characteristic equation in the form $(\lambda - \lambda_1)(\lambda - \lambda_2) = \lambda^2 - \tau\lambda + \Delta = 0$.

To arrive at Figure 5.2.8, we make the following observations:

If $\Delta < 0$, the eigenvalues are real and have opposite signs; hence the fixed point is a *saddle point*.

If $\Delta > 0$, the eigenvalues are either real with the same sign (*nodes*), or complex conjugate (*spirals* and *centers*). Nodes satisfy $\tau^2 - 4\Delta > 0$ and spirals satisfy $\tau^2 - 4\Delta < 0$. The parabola $\tau^2 - 4\Delta = 0$ is the borderline between nodes and spirals; star nodes and degenerate nodes live on this parabola. The stability of the nodes and spirals is determined by τ . When $\tau < 0$, both eigenvalues have negative real parts, so the fixed point is stable. Unstable spirals and nodes have $\tau > 0$. Neutrally stable centers live on the borderline $\tau = 0$, where the eigenvalues are purely imaginary.

If $\Delta = 0$, at least one of the eigenvalues is zero. Then the origin is not an isolated fixed point. There is either a whole line of fixed points, as in Figure 5.1.5d, or a plane of fixed points, if $A = 0$.

Figure 5.2.8 shows that saddle points, nodes, and spirals are the major types of fixed points; they occur in large open regions of the (Δ, τ) plane. Centers, stars, degenerate nodes, and non-isolated fixed points are *borderline cases* that occur along curves in the (Δ, τ) plane. Of these borderline cases, centers are by far the most important. They occur very commonly in frictionless mechanical systems where energy is conserved.

EXAMPLE 5.2.6:

Classify the fixed point $\mathbf{x}^* = \mathbf{0}$ for the system $\dot{\mathbf{x}} = A\mathbf{x}$, where $A = \begin{pmatrix} 1 & 2 \\ 3 & 4 \end{pmatrix}$.

Solution: The matrix has $\Delta = -2$; hence the fixed point is a saddle point. ■

EXAMPLE 5.2.7:

Redo Example 5.2.6 for $A = \begin{pmatrix} 2 & 1 \\ 3 & 4 \end{pmatrix}$.

Solution: Now $\Delta = 5$ and $\tau = 6$. Since $\Delta > 0$ and $\tau^2 - 4\Delta = 16 > 0$, the fixed point is a node. It is unstable, since $\tau > 0$. ■

5.3 Love Affairs

To arouse your interest in the classification of linear systems, we now discuss a simple model for the dynamics of love affairs (Strogatz 1988). The following story illustrates the idea.

Romeo is in love with Juliet, but in our version of this story, Juliet is a fickle lover. The more Romeo loves her, the more Juliet wants to run away and hide. But when Romeo gets discouraged and backs off, Juliet begins to find him strangely attractive. Romeo, on the other hand, tends to echo her: he warms up when she loves him, and grows cold when she hates him.

Let

$R(t)$ = Romeo's love/hate for Juliet at time t

$J(t)$ = Juliet's love/hate for Romeo at time t .

Positive values of R, J signify love, negative values signify hate. Then a model for their star-crossed romance is

$$\dot{R} = aJ$$

$$\dot{J} = -bR$$

where the parameters a and b are positive, to be consistent with the story.

The sad outcome of their affair is, of course, a neverending cycle of love and hate; the governing system has a center at $(R, J) = (0, 0)$. At least they manage to achieve simultaneous love one-quarter of the time (Figure 5.3.1).

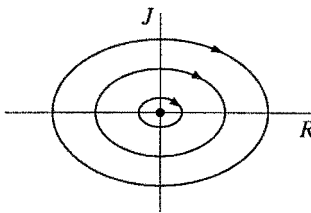


Figure 5.3.1

Now consider the forecast for lovers governed by the general linear system

$$\dot{R} = aR + bJ$$

$$\dot{J} = cR + dJ$$

where the parameters a, b, c, d may have either sign. A choice of signs specifies the romantic styles. As named by one of my students, the choice $a > 0, b > 0$ means that Romeo is an “eager beaver”—he gets excited by Juliet’s love for him, and is further spurred on by his own affectionate feelings for her. It’s entertaining to name the other three romantic styles, and to predict the outcomes for the various pairings. For example, can a “cautious lover” ($a < 0, b > 0$) find true love with an eager beaver? These and other pressing questions will be considered in the exercises.

EXAMPLE 5.3.1:

What happens when two identically cautious lovers get together?

Solution: The system is

$$\dot{R} = aR + bJ$$

$$\dot{J} = bR + aJ$$

with $a < 0, b > 0$. Here a is a measure of cautiousness (they each try to avoid throwing themselves at the other) and b is a measure of responsiveness (they both get excited by the other’s advances). We might suspect that the outcome depends on the relative size of a and b . Let’s see what happens.

The corresponding matrix is

$$A = \begin{pmatrix} a & b \\ b & a \end{pmatrix}$$

which has

$$\tau = 2a < 0, \quad \Delta = a^2 - b^2, \quad \tau^2 - 4\Delta = 4b^2 > 0.$$

Hence the fixed point $(R, J) = (0, 0)$ is a saddle point if $a^2 < b^2$ and a stable node if $a^2 > b^2$. The eigenvalues and corresponding eigenvectors are

$$\lambda_1 = a + b, \quad \mathbf{v}_1 = (1, 1), \quad \lambda_2 = a - b, \quad \mathbf{v}_2 = (1, -1).$$

Since $a + b > a - b$, the eigenvector $(1, 1)$ spans the unstable manifold when the origin is a saddle point, and it spans the slow eigendirection when the origin is a stable node. Figure 5.3.2 shows the phase portrait for the two cases.

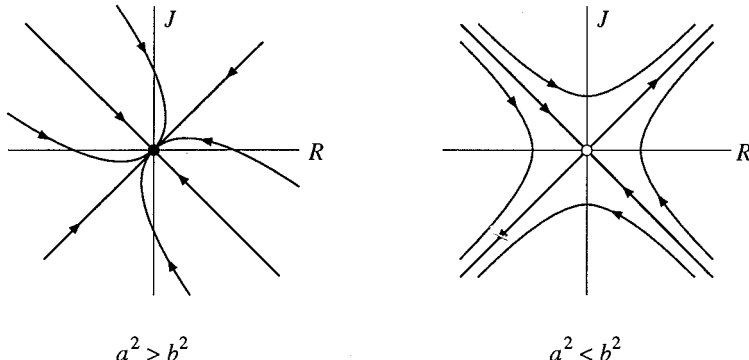


Figure 5.3.2

If $a^2 > b^2$, the relationship always fizzles out to mutual indifference. The lesson seems to be that excessive caution can lead to apathy.

If $a^2 < b^2$, the lovers are more daring, or perhaps more sensitive to each other. Now the relationship is explosive. Depending on their feelings initially, their relationship either becomes a love fest or a war. In either case, all trajectories approach the line $R = J$, so their feelings are eventually mutual. ■

EXERCISES FOR CHAPTER 5

5.1 Definitions and Examples

5.1.1 (Ellipses and energy conservation for the harmonic oscillator) Consider the harmonic oscillator $\dot{x} = v$, $\dot{v} = -\omega^2 x$.

- Show that the orbits are given by ellipses $\omega^2 x^2 + v^2 = C$, where C is any non-negative constant. (Hint: Divide the \dot{x} equation by the \dot{v} equation, separate the v 's from the x 's, and integrate the resulting separable equation.)
- Show that this condition is equivalent to conservation of energy.

5.1.2 Consider the system $\dot{x} = ax$, $\dot{y} = -y$, where $a < -1$. Show that all trajectories become parallel to the y -direction as $t \rightarrow \infty$, and parallel to the x -direction as $t \rightarrow -\infty$.

(Hint: Examine the slope $dy/dx = \dot{y}/\dot{x}$.)

Write the following systems in matrix form.

5.1.3 $\dot{x} = -y$, $\dot{y} = -x$

5.1.4 $\dot{x} = 3x - 2y$, $\dot{y} = 2y - x$

5.1.5 $\dot{x} = 0$, $\dot{y} = x + y$

5.1.6 $\dot{x} = x$, $\dot{y} = 5x + y$

Sketch the vector field for the following systems. Indicate the length and direction of the vectors with reasonable accuracy. Sketch some typical trajectories.

5.1.7 $\dot{x} = x$, $\dot{y} = x + y$

5.1.8 $\dot{x} = -2y$, $\dot{y} = x$

5.1.9 Consider the system $\dot{x} = -y$, $\dot{y} = -x$.

- Sketch the vector field.
- Show that the trajectories of the system are hyperbolas of the form $x^2 - y^2 = C$.
(Hint: Show that the governing equations imply $x\dot{x} - y\dot{y} = 0$ and then integrate both sides.)
- The origin is a saddle point; find equations for its stable and unstable manifolds.
- The system can be decoupled and solved as follows. Introduce new variables u and v , where $u = x + y$, $v = x - y$. Then rewrite the system in terms of u and v . Solve for $u(t)$ and $v(t)$, starting from an arbitrary initial condition (u_0, v_0) .
- What are the equations for the stable and unstable manifolds in terms of u and v ?
- Finally, using the answer to (d), write the general solution for $x(t)$ and $y(t)$, starting from an initial condition (x_0, y_0) .

5.1.10 (Attracting and Liapunov stable) Here are the official definitions of the various types of stability. Consider a fixed point \mathbf{x}^* of a system $\dot{\mathbf{x}} = \mathbf{f}(\mathbf{x})$.

We say that \mathbf{x}^* is **attracting** if there is a $\delta > 0$ such that $\lim_{t \rightarrow \infty} \mathbf{x}(t) = \mathbf{x}^*$ whenever $\|\mathbf{x}(0) - \mathbf{x}^*\| < \delta$. In other words, any trajectory that starts within a distance δ of \mathbf{x}^* is guaranteed to converge to \mathbf{x}^* *eventually*. As shown schematically in Figure 1, trajectories that start nearby are allowed to stray from \mathbf{x}^* in the short run, but they must approach \mathbf{x}^* in the long run.

In contrast, Liapunov stability requires that nearby trajectories remain close for *all* time. We say that \mathbf{x}^* is **Liapunov stable** if for each $\varepsilon > 0$, there is a $\delta > 0$ such that $\|\mathbf{x}(t) - \mathbf{x}^*\| < \varepsilon$ whenever $t \geq 0$ and $\|\mathbf{x}(0) - \mathbf{x}^*\| < \delta$. Thus, trajectories that start within δ of \mathbf{x}^* remain within ε of \mathbf{x}^* for all positive time (Figure 1).

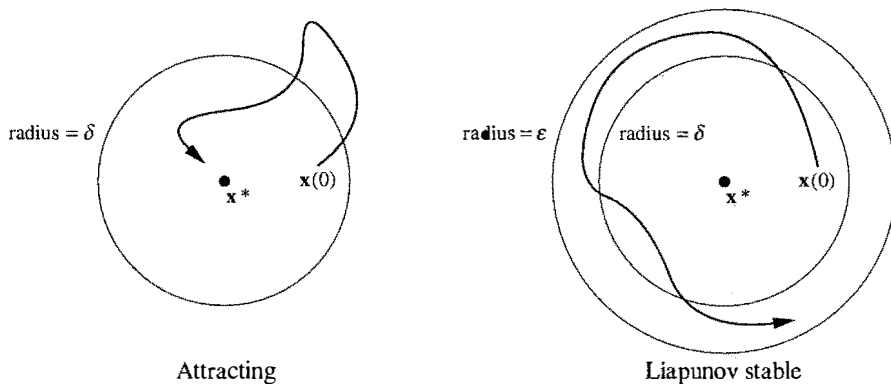


Figure 1

Finally, \mathbf{x}^* is **asymptotically stable** if it is both attracting and Liapunov stable.

For each of the following systems, decide whether the origin is attracting, Liapunov stable, asymptotically stable, or none of the above.

- | | |
|----------------------------------|--------------------------------|
| a) $\dot{x} = y, \dot{y} = -4x$ | b) $\dot{x} = 2y, \dot{y} = x$ |
| c) $\dot{x} = 0, \dot{y} = x$ | d) $\dot{x} = 0, \dot{y} = -y$ |
| e) $\dot{x} = -x, \dot{y} = -5y$ | f) $\dot{x} = x, \dot{y} = y$ |

5.1.11 (Stability proofs) Prove that your answers to 5.1.10 are correct, using the definitions of the different types of stability. (You must produce a suitable δ to prove that the origin is attracting, or a suitable $\delta(\varepsilon)$ to prove Liapunov stability.)

5.1.12 (Closed orbits from symmetry arguments) Give a simple proof that orbits are closed for the simple harmonic oscillator $\dot{x} = v, \dot{v} = -x$, using *only* the symmetry properties of the vector field. (Hint: Consider a trajectory that starts on the v -axis at $(0, -v_0)$, and suppose that the trajectory intersects the x -axis at $(x, 0)$. Then use symmetry arguments to find the subsequent intersections with the v -axis and x -axis.)

5.1.13 Why do you think a “saddle point” is called by that name? What’s the connection to real saddles (the kind used on horses)?

5.2 Classification of Linear Systems

5.2.1 Consider the system $\dot{x} = 4x - y, \dot{y} = 2x + y$.

- Write the system as $\dot{\mathbf{x}} = A\mathbf{x}$. Show that the characteristic polynomial is $\lambda^2 - 5\lambda + 6$, and find the eigenvalues and eigenvectors of A .
- Find the general solution of the system.
- Classify the fixed point at the origin.
- Solve the system subject to the initial condition $(x_0, y_0) = (3, 4)$.

5.2.2 (Complex eigenvalues) This exercise leads you through the solution of a

linear system where the eigenvalues are complex. The system is $\dot{x} = x - y$, $\dot{y} = x + y$.

- a) Find A and show that it has eigenvalues $\lambda_1 = 1+i$, $\lambda_2 = 1-i$, with eigenvectors $\mathbf{v}_1 = (i, 1)$, $\mathbf{v}_2 = (-i, 1)$. (Note that the eigenvalues are complex conjugates, and so are the eigenvectors—this is always the case for real A with complex eigenvalues.)
- b) The general solution is $\mathbf{x}(t) = c_1 e^{\lambda_1 t} \mathbf{v}_1 + c_2 e^{\lambda_2 t} \mathbf{v}_2$. So in one sense we're done! But this way of writing $\mathbf{x}(t)$ involves complex coefficients and looks unfamiliar. Express $\mathbf{x}(t)$ purely in terms of real-valued functions. (Hint: Use $e^{i\omega t} = \cos \omega t + i \sin \omega t$ to rewrite $\mathbf{x}(t)$ in terms of sines and cosines, and then separate the terms that have a prefactor of i from those that don't.)

Plot the phase portrait and classify the fixed point of the following linear systems. If the eigenvectors are real, indicate them in your sketch.

5.2.3 $\dot{x} = y$, $\dot{y} = -2x - 3y$

5.2.4 $\dot{x} = 5x + 10y$, $\dot{y} = -x - y$

5.2.5 $\dot{x} = 3x - 4y$, $\dot{y} = x - y$

5.2.6 $\dot{x} = -3x + 2y$, $\dot{y} = x - 2y$

5.2.7 $\dot{x} = 5x + 2y$, $\dot{y} = -17x - 5y$

5.2.8 $\dot{x} = -3x + 4y$, $\dot{y} = -2x + 3y$

5.2.9 $\dot{x} = 4x - 3y$, $\dot{y} = 8x - 6y$

5.2.10 $\dot{x} = y$, $\dot{y} = -x - 2y$.

- 5.2.11** Show that any matrix of the form $A = \begin{pmatrix} \lambda & b \\ 0 & \lambda \end{pmatrix}$, with $b \neq 0$, has only a one-dimensional eigenspace corresponding to the eigenvalue λ . Then solve the system $\dot{\mathbf{x}} = A\mathbf{x}$ and sketch the phase portrait.

5.2.12 (LRC circuit) Consider the circuit equation $L\ddot{I} + R\dot{I} + I/C = 0$, where $L, C > 0$ and $R \geq 0$.

- Rewrite the equation as a two-dimensional linear system.
- Show that the origin is asymptotically stable if $R > 0$ and neutrally stable if $R = 0$.
- Classify the fixed point at the origin, depending on whether $R^2C - 4L$ is positive, negative, or zero, and sketch the phase portrait in all three cases.

5.2.13 (Damped harmonic oscillator) The motion of a damped harmonic oscillator is described by $m\ddot{x} + b\dot{x} + kx = 0$, where $b > 0$ is the damping constant.

- Rewrite the equation as a two-dimensional linear system.
- Classify the fixed point at the origin and sketch the phase portrait. Be sure to show all the different cases that can occur, depending on the relative sizes of the parameters.
- How do your results relate to the standard notions of overdamped, critically damped, and underdamped vibrations?

5.2.14 (A project about random systems) Suppose we pick a linear system at

random; what's the probability that the origin will be, say, an unstable spiral? To be more specific, consider the system $\dot{\mathbf{x}} = A\mathbf{x}$, where $A = \begin{pmatrix} a & b \\ c & d \end{pmatrix}$. Suppose we pick the entries a, b, c, d independently and at random from a uniform distribution on the interval $[-1, 1]$. Find the probabilities of all the different kinds of fixed points.

To check your answers (or if you hit an analytical roadblock), try the *Monte Carlo method*. Generate millions of random matrices on the computer and have the machine count the relative frequency of saddles, unstable spirals, etc.

Are the answers the same if you use a normal distribution instead of a uniform distribution?

5.3 Love Affairs

→ **5.3.1** (Name-calling) Suggest names for the four romantic styles, determined by the signs of a and b in $\dot{R} = aR + bJ$.

5.3.2 Consider the affair described by $\dot{R} = J$, $\dot{J} = -R + J$.

a) Characterize the romantic styles of Romeo and Juliet.

b) Classify the fixed point at the origin. What does this imply for the affair?

c) Sketch $R(t)$ and $J(t)$ as functions of t , assuming $R(0) = 1$, $J(0) = 0$.

In each of the following problems, predict the course of the love affair, depending on the signs and relative sizes of a and b .

5.3.3 (Out of touch with their own feelings) Suppose Romeo and Juliet react to each other, but not to themselves: $\dot{R} = aJ$, $\dot{J} = bR$. What happens?

→ **5.3.4** (Fire and water) Do opposites attract? Analyze $\dot{R} = aR + bJ$, $\dot{J} = -bR - aJ$.

5.3.5 (Peas in a pod) If Romeo and Juliet are romantic clones ($\dot{R} = aR + bJ$, $\dot{J} = bR + aJ$), should they expect boredom or bliss?

→ **5.3.6** (Romeo the robot) Nothing could ever change the way Romeo feels about Juliet: $\dot{R} = 0$, $\dot{J} = aR + bJ$. Does Juliet end up loving him or hating him?

6

PHASE PLANE

6.0 Introduction

This chapter begins our study of two-dimensional *nonlinear* systems. First we consider some of their general properties. Then we classify the kinds of fixed points that can arise, building on our knowledge of linear systems (Chapter 5). The theory is further developed through a series of examples from biology (competition between two species) and physics (conservative systems, reversible systems, and the pendulum). The chapter concludes with a discussion of index theory, a topological method that provides global information about the phase portrait.

This chapter is mainly about fixed points. The next two chapters will discuss closed orbits and bifurcations in two-dimensional systems.

6.1 Phase Portraits

The general form of a vector field on the phase plane is

$$\dot{x}_1 = f_1(x_1, x_2)$$

$$\dot{x}_2 = f_2(x_1, x_2)$$

where f_1 and f_2 are given functions. This system can be written more compactly in vector notation as

$$\dot{\mathbf{x}} = \mathbf{f}(\mathbf{x})$$

where $\mathbf{x} = (x_1, x_2)$ and $\mathbf{f}(\mathbf{x}) = (f_1(\mathbf{x}), f_2(\mathbf{x}))$. Here \mathbf{x} represents a point in the phase plane, and $\dot{\mathbf{x}}$ is the velocity vector at that point. By flowing along the vector field, a phase point traces out a solution $\mathbf{x}(t)$, corresponding to a trajectory winding through the phase plane (Figure 6.1.1).

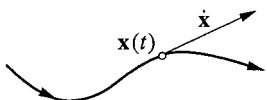


Figure 6.1.1

Furthermore, the entire phase plane is filled with trajectories, since each point can play the role of an initial condition.

For nonlinear systems, there's typically no hope of finding the trajectories analytically. Even when explicit formulas are available, they are often too complicated

to provide much insight. Instead we will try to determine the *qualitative* behavior of the solutions. Our goal is to find the system's phase portrait directly from the properties of $\mathbf{f}(\mathbf{x})$. An enormous variety of phase portraits is possible; one example is shown in Figure 6.1.2.

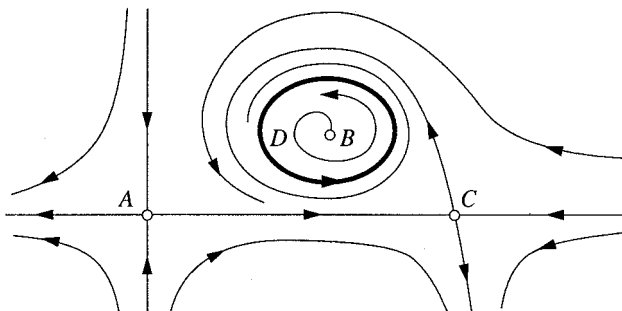


Figure 6.1.2

Some of the most salient features of any phase portrait are:

1. The **fixed points**, like A , B , and C in Figure 6.1.2. Fixed points satisfy $\mathbf{f}(\mathbf{x}^*) = \mathbf{0}$, and correspond to steady states or equilibria of the system.
2. The **closed orbits**, like D in Figure 6.1.2. These correspond to periodic solutions, i.e., solutions for which $\mathbf{x}(t+T) = \mathbf{x}(t)$ for all t , for some $T > 0$.
3. The arrangement of trajectories near the fixed points and closed orbits. For example, the flow pattern near A and C is similar, and different from that near B .
4. The stability or instability of the fixed points and closed orbits. Here, the fixed points A , B , and C are unstable, because nearby trajectories tend to move away from them, whereas the closed orbit D is stable.

Numerical Computation of Phase Portraits

Sometimes we are also interested in *quantitative* aspects of the phase portrait. Fortunately, numerical integration of $\dot{\mathbf{x}} = \mathbf{f}(\mathbf{x})$ is not much harder than that of $\dot{x} = f(x)$. The numerical methods of Section 2.8 still work, as long as we replace the numbers x and $f(x)$ by the vectors \mathbf{x} and $\mathbf{f}(\mathbf{x})$. We will always use the Runge-Kutta method, which in vector form is

$$\mathbf{x}_{n+1} = \mathbf{x}_n + \frac{1}{6}(\mathbf{k}_1 + 2\mathbf{k}_2 + 2\mathbf{k}_3 + \mathbf{k}_4)$$

where

$$\mathbf{k}_1 = \mathbf{f}(\mathbf{x}_n) \Delta t$$

$$\mathbf{k}_2 = \mathbf{f}(\mathbf{x}_n + \frac{1}{2}\mathbf{k}_1) \Delta t$$

$$\mathbf{k}_3 = \mathbf{f}(\mathbf{x}_n + \frac{1}{2}\mathbf{k}_2) \Delta t$$

$$\mathbf{k}_4 = \mathbf{f}(\mathbf{x}_n + \mathbf{k}_3) \Delta t.$$

A stepsize $\Delta t = 0.1$ usually provides sufficient accuracy for our purposes.

When plotting the phase portrait, it often helps to see a grid of representative vectors in the vector field. Unfortunately, the arrowheads and different lengths of the vectors tend to clutter such pictures. A plot of the **direction field** is clearer: short line segments are used to indicate the local direction of flow.

EXAMPLE 6.1.1:

Consider the system $\dot{x} = x + e^{-y}$, $\dot{y} = -y$. First use qualitative arguments to obtain information about the phase portrait. Then, using a computer, plot the direction field. Finally, use the Runge–Kutta method to compute several trajectories, and plot them on the phase plane.

Solution: First we find the fixed points by solving $\dot{x} = 0$, $\dot{y} = 0$ simultaneously. The only solution is $(x^*, y^*) = (-1, 0)$. To determine its stability, note that $y(t) \rightarrow 0$ as $t \rightarrow \infty$, since the solution to $\dot{y} = -y$ is $y(t) = y_0 e^{-t}$. Hence $e^{-y} \rightarrow 1$ and so in the long run, the equation for x becomes $\dot{x} \approx x + 1$; this has exponentially growing solutions, which suggests that the fixed point is unstable. In fact, if we restrict our attention to initial conditions on the x -axis, then $y_0 = 0$ and so $y(t) = 0$ for all time. Hence the flow on the x -axis is governed *strictly* by $\dot{x} = x + 1$. Therefore the fixed point is unstable.

To sketch the phase portrait, it is helpful to plot the **nullclines**, defined as the curves where either $\dot{x} = 0$ or $\dot{y} = 0$. The nullclines indicate where the flow is purely horizontal or vertical (Figure 6.1.3). For example, the flow is horizontal where $\dot{y} = 0$, and since $\dot{y} = -y$, this occurs on the line $y = 0$. Along this line, the flow is to the right where $\dot{x} = x + 1 > 0$, that is, where $x > -1$.

Similarly, the flow is vertical where $\dot{x} = x + e^{-y} = 0$, which occurs on the curve shown in Figure 6.1.3. On the upper part of the curve where $y > 0$, the flow is downward, since $\dot{y} < 0$.

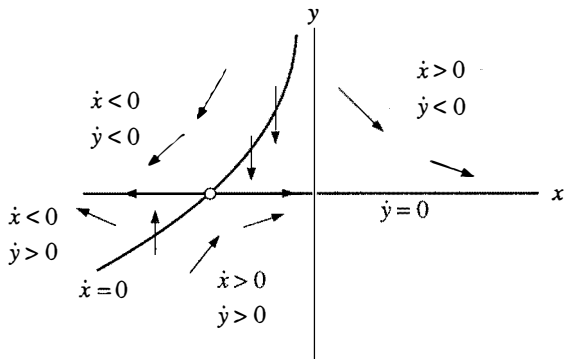


Figure 6.1.3

The nullclines also partition the plane into regions where \dot{x} and \dot{y} have various signs. Some of the typical vectors are sketched above in Figure 6.1.3. Even with the limited information obtained so far, Figure 6.1.3 gives a good sense of the overall flow pattern.

Now we use the computer to finish the problem. The direction field is indicated by the line segments in Figure 6.1.4, and several trajectories are shown. Note how the trajectories always follow the local slope.

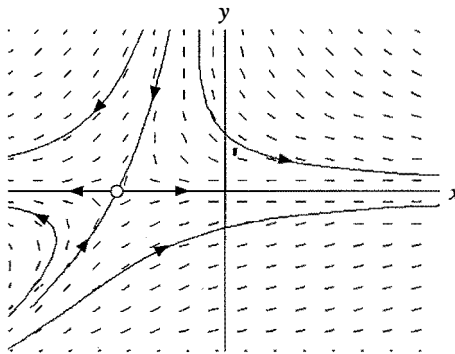


Figure 6.1.4

The fixed point is now seen to be a nonlinear version of a saddle point. ■

6.2 Existence, Uniqueness, and Topological Consequences

We have been a bit optimistic so far—at this stage, we have no guarantee that the general nonlinear system $\dot{\mathbf{x}} = \mathbf{f}(\mathbf{x})$ even *has* solutions! Fortunately the existence and uniqueness theorem given in Section 2.5 can be generalized to two-dimen-

sional systems. We state the result for n -dimensional systems, since no extra effort is involved:

Existence and Uniqueness Theorem: Consider the initial value problem $\dot{\mathbf{x}} = \mathbf{f}(\mathbf{x})$, $\mathbf{x}(0) = \mathbf{x}_0$. Suppose that \mathbf{f} is continuous and that all its partial derivatives $\partial f_i / \partial x_j$, $i, j = 1, \dots, n$, are continuous for \mathbf{x} in some open connected set $D \subset \mathbf{R}^n$. Then for $\mathbf{x}_0 \in D$, the initial value problem has a solution $\mathbf{x}(t)$ on some time interval $(-\tau, \tau)$ about $t = 0$, and the solution is unique.

In other words, existence and uniqueness of solutions are guaranteed if \mathbf{f} is continuously differentiable. The proof of the theorem is similar to that for the case $n = 1$, and can be found in most texts on differential equations. Stronger versions of the theorem are available, but this one suffices for most applications.

From now on, we'll assume that all our vector fields are smooth enough to ensure the existence and uniqueness of solutions, starting from any point in phase space.

The existence and uniqueness theorem has an important corollary: *different trajectories never intersect*. If two trajectories *did* intersect, then there would be

two solutions starting from the same point (the crossing point), and this would violate the uniqueness part of the theorem. In more intuitive language, a trajectory can't move in two directions at once.

Because trajectories can't intersect, phase portraits always have a well-groomed look to them.

Otherwise they might degenerate into a snarl of criss-crossed curves (Figure 6.2.1). The existence and uniqueness theorem prevents this from happening.

In two-dimensional phase spaces (as opposed to higher-dimensional phase spaces), these results have especially strong topological consequences. For example, suppose there is a closed orbit C in the phase plane. Then any trajectory starting inside C is trapped in there forever (Figure 6.2.2).

What is the fate of such a bounded trajectory? If there are fixed points inside C , then of course the trajectory might eventually approach one of them. But what if there *aren't* any fixed points? Your intuition may tell you that the trajectory can't meander around forever—if so, you're right.

For vector fields on the plane, the **Poincaré–Bendixson theorem** states that if a trajectory is confined to a closed, bounded region and there are no fixed points in the region, then the trajectory must

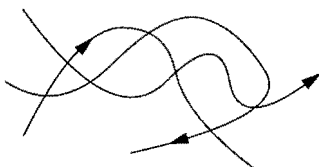


Figure 6.2.1

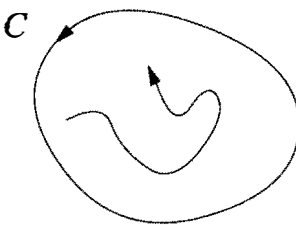


Figure 6.2.2

eventually approach a closed orbit. We'll discuss this important theorem in Section 7.3.

But that part of our story comes later. First we must become better acquainted with fixed points.

6.3 Fixed Points and Linearization

In this section we extend the *linearization* technique developed earlier for one-dimensional systems (Section 2.4). The hope is that we can approximate the phase portrait near a fixed point by that of a corresponding linear system.

Linearized System

Consider the system

$$\dot{x} = f(x, y)$$

$$\dot{y} = g(x, y)$$

and suppose that (x^*, y^*) is a fixed point, i.e.,

$$f(x^*, y^*) = 0, \quad g(x^*, y^*) = 0.$$

Let

$$u = x - x^*, \quad v = y - y^*$$

denote the components of a small disturbance from the fixed point. To see whether the disturbance grows or decays, we need to derive differential equations for u and v . Let's do the u -equation first:

$$\dot{u} = \dot{x} \quad (\text{since } x^* \text{ is a constant})$$

$$= f(x^* + u, y^* + v) \quad (\text{by substitution})$$

$$= f(x^*, y^*) + u \frac{\partial f}{\partial x} + v \frac{\partial f}{\partial y} + O(u^2, v^2, uv) \quad (\text{Taylor series expansion})$$

$$= u \frac{\partial f}{\partial x} + v \frac{\partial f}{\partial y} + O(u^2, v^2, uv) \quad (\text{since } f(x^*, y^*) = 0).$$

To simplify the notation, we have written $\partial f / \partial x$ and $\partial f / \partial y$, but please remember that these partial derivatives are to be evaluated *at the fixed point* (x^*, y^*) ; thus they are *numbers*, not functions. Also, the shorthand notation $O(u^2, v^2, uv)$ denotes *quadratic terms* in u and v . Since u and v are small, these quadratic terms are *extremely* small.

Similarly we find

$$\dot{v} = u \frac{\partial g}{\partial x} + v \frac{\partial g}{\partial y} + O(u^2, v^2, uv).$$

Hence the disturbance (u, v) evolves according to

$$\begin{pmatrix} \dot{u} \\ \dot{v} \end{pmatrix} = \begin{pmatrix} \frac{\partial f}{\partial x} & \frac{\partial f}{\partial y} \\ \frac{\partial g}{\partial x} & \frac{\partial g}{\partial y} \end{pmatrix} \begin{pmatrix} u \\ v \end{pmatrix} + \text{quadratic terms.} \quad (1)$$

The matrix

$$A = \begin{pmatrix} \frac{\partial f}{\partial x} & \frac{\partial f}{\partial y} \\ \frac{\partial g}{\partial x} & \frac{\partial g}{\partial y} \end{pmatrix}_{(x^*, y^*)}$$

is called the **Jacobian matrix** at the fixed point (x^*, y^*) . It is the multivariable analog of the derivative $f'(x^*)$ seen in Section 2.4.

Now since the quadratic terms in (1) are tiny, it's tempting to neglect them altogether. If we do that, we obtain the **linearized system**

$$\begin{pmatrix} \dot{u} \\ \dot{v} \end{pmatrix} = \begin{pmatrix} \frac{\partial f}{\partial x} & \frac{\partial f}{\partial y} \\ \frac{\partial g}{\partial x} & \frac{\partial g}{\partial y} \end{pmatrix} \begin{pmatrix} u \\ v \end{pmatrix} \quad (2)$$

whose dynamics can be analyzed by the methods of Section 5.2.

The Effect of Small Nonlinear Terms

Is it really safe to neglect the quadratic terms in (1)? In other words, does the linearized system give a qualitatively correct picture of the phase portrait near (x^*, y^*) ? The answer is *yes, as long as the fixed point for the linearized system is not one of the borderline cases* discussed in Section 5.2. In other words, if the linearized system predicts a saddle, node, or a spiral, then the fixed point *really is* a saddle, node, or spiral for the original nonlinear system. See Andronov et al. (1973) for a proof of this result, and Example 6.3.1 for a concrete illustration.

The borderline cases (centers, degenerate nodes, stars, or non-isolated fixed points) are much more delicate. They can be altered by small nonlinear terms, as we'll see in Example 6.3.2 and in Exercise 6.3.11.

EXAMPLE 6.3.1:

Find all the fixed points of the system $\dot{x} = -x + x^3$, $\dot{y} = -2y$, and use linearization to classify them. Then check your conclusions by deriving the phase portrait for the full nonlinear system.

Solution: Fixed points occur where $\dot{x} = 0$ and $\dot{y} = 0$ simultaneously. Hence we need $x = 0$ or $x = \pm 1$, and $y = 0$. Thus, there are three fixed points: $(0, 0)$, $(1, 0)$, and $(-1, 0)$. The Jacobian matrix at a general point (x, y) is

$$A = \begin{pmatrix} \frac{\partial x}{\partial x} & \frac{\partial x}{\partial y} \\ \frac{\partial y}{\partial x} & \frac{\partial y}{\partial y} \end{pmatrix} = \begin{pmatrix} -1 + 3x^2 & 0 \\ 0 & -2 \end{pmatrix}.$$

Next we evaluate A at the fixed points. At $(0,0)$, we find $A = \begin{pmatrix} -1 & 0 \\ 0 & -2 \end{pmatrix}$, so

$(0,0)$ is a stable node. At $(\pm 1, 0)$, $A = \begin{pmatrix} 2 & 0 \\ 0 & -2 \end{pmatrix}$, so both $(1,0)$ and $(-1,0)$ are saddle points.

Now because stable nodes and saddle points are not borderline cases, we can be certain that the fixed points for the full nonlinear system have been predicted correctly.

This conclusion can be checked explicitly for the nonlinear system, since the x and y equations are *uncoupled*; the system is essentially two independent first-order systems at right angles to each other. In the y -direction, all trajectories decay exponentially to $y = 0$. In the x -direction, the trajectories are attracted to $x = 0$ and repelled from $x = \pm 1$. The vertical lines $x = 0$ and $x = \pm 1$ are *invariant*, because $\dot{x} = 0$ on them; hence any trajectory that starts on these lines stays on them forever. Similarly, $y = 0$ is an invariant horizontal line. As a final observation, we note that the phase portrait must be symmetric in both the x and y axes, since the equations are invariant under the transformations $x \rightarrow -x$ and $y \rightarrow -y$. Putting all this information together, we arrive at the phase portrait shown in Figure 6.3.1.

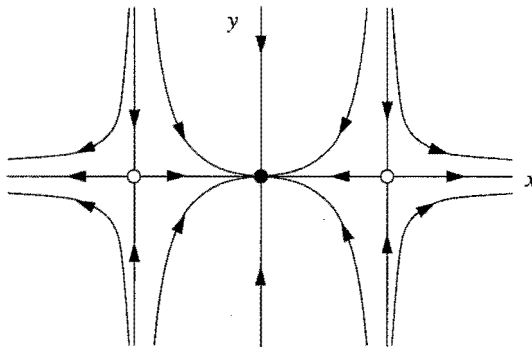


Figure 6.3.1

This picture confirms that $(0,0)$ is a stable node, and $(\pm 1,0)$ are saddles, as expected from the linearization. ■

The next example shows that small nonlinear terms can change a center into a spiral.

EXAMPLE 6.3.2:

Consider the system

$$\begin{aligned}\dot{x} &= -y + ax(x^2 + y^2) \\ \dot{y} &= x + ay(x^2 + y^2)\end{aligned}$$

where a is a parameter. Show that the linearized system *incorrectly* predicts that the origin is a center for all values of a , whereas in fact the origin is a stable spiral if $a < 0$ and an unstable spiral if $a > 0$.

Solution: To obtain the linearization about $(x^*, y^*) = (0, 0)$, we can either compute the Jacobian matrix directly from the definition, or we can take the following shortcut. For any system with a fixed point at the origin, x and y represent deviations from the fixed point, since $u = x - x^* = x$ and $v = y - y^* = y$; hence we can linearize by simply omitting nonlinear terms in x and y . Thus the linearized system is $\dot{x} = -y$, $\dot{y} = x$. The Jacobian is

$$A = \begin{pmatrix} 0 & -1 \\ 1 & 0 \end{pmatrix}$$

which has $\tau = 0$, $\Delta = 1 > 0$, so the origin is always a center, according to the linearization.

To analyze the nonlinear system, we change variables to *polar coordinates*. Let $x = r \cos \theta$, $y = r \sin \theta$. To derive a differential equation for r , we note $x^2 + y^2 = r^2$, so $xx\dot{x} + yy\dot{y} = r\dot{r}$. Substituting for \dot{x} and \dot{y} yields

$$\begin{aligned}r\dot{r} &= x(-y + ax(x^2 + y^2)) + y(x + ay(x^2 + y^2)) \\ &= a(x^2 + y^2)^2 \\ &= ar^4.\end{aligned}$$

Hence $\dot{r} = ar^3$. In Exercise 6.3.12, you are asked to derive the following differential equation for θ :

$$\dot{\theta} = \frac{xy - yx}{r^2}.$$

After substituting for \dot{x} and \dot{y} we find $\dot{\theta} = 1$. Thus in polar coordinates the original system becomes

$$\begin{aligned}\dot{r} &= ar^3 \\ \dot{\theta} &= 1.\end{aligned}$$

The system is easy to analyze in this form, because the radial and angular mo-

tions are independent. All trajectories rotate about the origin with constant angular velocity $\dot{\theta} = 1$.

The radial motion depends on a , as shown in Figure 6.3.2.

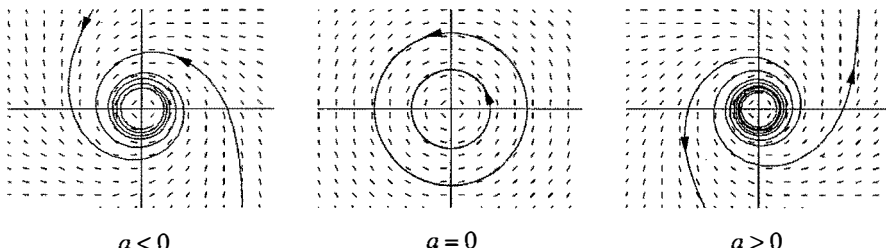


Figure 6.3.2

If $a < 0$, then $r(t) \rightarrow 0$ monotonically as $t \rightarrow \infty$. In this case, the origin is a stable spiral. (However, note that the decay is extremely slow, as suggested by the computer-generated trajectories shown in Figure 6.3.2.) If $a = 0$, then $r(t) = r_0$ for all t and the origin is a center. Finally, if $a > 0$, then $r(t) \rightarrow \infty$ monotonically and the origin is an unstable spiral.

We can see now why centers are so delicate: all trajectories are required to close *perfectly* after one cycle. The slightest miss converts the center into a spiral. ■

Similarly, stars and degenerate nodes can be altered by small nonlinearities, but unlike centers, *their stability doesn't change*. For example, a stable star may be changed into a stable spiral (Exercise 6.3.11) but not into an unstable spiral. This is plausible, given the classification of linear systems in Figure 5.2.8: stars and degenerate nodes live squarely in the stable or unstable region, whereas centers live on the razor's edge between stability and instability.

If we're only interested in *stability*, and not in the detailed geometry of the trajectories, then we can classify fixed points more coarsely as follows:

Robust cases:

Repellers (also called *sources*): both eigenvalues have positive real part.

Attractors (also called *sinks*): both eigenvalues have negative real part.

Saddles: one eigenvalue is positive and one is negative.

Marginal cases:

Centers: both eigenvalues are pure imaginary.

Higher-order and non-isolated fixed points: at least one eigenvalue is zero.

Thus, from the point of view of stability, the marginal cases are those where at least one eigenvalue satisfies $\text{Re}(\lambda) = 0$.

Hyperbolic Fixed Points, Topological Equivalence, and Structural Stability

If $\operatorname{Re}(\lambda) \neq 0$ for both eigenvalues, the fixed point is often called *hyperbolic*. (This is an unfortunate name—it sounds like it should mean “saddle point”—but it has become standard.) Hyperbolic fixed points are sturdy; their stability type is unaffected by small nonlinear terms. Nonhyperbolic fixed points are the fragile ones.

We've already seen a simple instance of hyperbolicity in the context of vector fields on the line. In Section 2.4 we saw that the stability of a fixed point was accurately predicted by the linearization, *as long as* $f'(x^*) \neq 0$. This condition is the exact analog of $\operatorname{Re}(\lambda) \neq 0$.

These ideas also generalize neatly to higher-order systems. A fixed point of an n -th-order system is *hyperbolic* if all the eigenvalues of the linearization lie off the imaginary axis, i.e., $\operatorname{Re}(\lambda_i) \neq 0$ for $i = 1, \dots, n$. The important *Hartman–Grobman theorem* states that the local phase portrait near a hyperbolic fixed point is “topologically equivalent” to the phase portrait of the linearization; in particular, the stability type of the fixed point is faithfully captured by the linearization. Here *topologically equivalent* means that there is a *homeomorphism* (a continuous deformation with a continuous inverse) that maps one local phase portrait onto the other, such that trajectories map onto trajectories and the sense of time (the direction of the arrows) is preserved.

Intuitively, two phase portraits are topologically equivalent if one is a distorted version of the other. Bending and warping are allowed, but not ripping, so closed orbits must remain closed, trajectories connecting saddle points must not be broken, etc.

Hyperbolic fixed points also illustrate the important general notion of structural stability. A phase portrait is *structurally stable* if its topology cannot be changed by an arbitrarily small perturbation to the vector field. For instance, the phase portrait of a saddle point is structurally stable, but that of a center is not: an arbitrarily small amount of damping converts the center to a spiral.

6.4 Rabbits versus Sheep

In the next few sections we'll consider some simple examples of phase plane analysis. We begin with the classic *Lotka–Volterra model of competition* between two species, here imagined to be rabbits and sheep. Suppose that both species are competing for the same food supply (grass) and the amount available is limited. Furthermore, ignore all other complications, like predators, seasonal effects, and other sources of food. Then there are two main effects we should consider:

1. Each species would grow to its carrying capacity in the absence of the other. This can be modeled by assuming logistic growth for each species (recall Section 2.3). Rabbits have a legendary ability to reproduce, so perhaps we should assign them a higher intrinsic growth rate.

2. When rabbits and sheep encounter each other, trouble starts. Sometimes the rabbit gets to eat, but more usually the sheep nudges the rabbit aside and starts nibbling (on the grass, that is). We'll assume that these conflicts occur at a rate proportional to the size of each population. (If there were twice as many sheep, the odds of a rabbit encountering a sheep would be twice as great.) Furthermore, we assume that the conflicts reduce the growth rate for each species, but the effect is more severe for the rabbits.

A specific model that incorporates these assumptions is

$$\dot{x} = x(3 - x - 2y)$$

$$\dot{y} = y(2 - x - y)$$

where

$x(t)$ = population of rabbits,

$y(t)$ = population of sheep

and $x, y \geq 0$. The coefficients have been chosen to reflect this scenario, but are otherwise arbitrary. In the exercises, you'll be asked to study what happens if the coefficients are changed.

To find the fixed points for the system, we solve $\dot{x} = 0$ and $\dot{y} = 0$ simultaneously. Four fixed points are obtained: $(0,0)$, $(0,2)$, $(3,0)$, and $(1,1)$. To classify them, we compute the Jacobian:

$$A = \begin{pmatrix} \frac{\partial \dot{x}}{\partial x} & \frac{\partial \dot{x}}{\partial y} \\ \frac{\partial \dot{y}}{\partial x} & \frac{\partial \dot{y}}{\partial y} \end{pmatrix} = \begin{pmatrix} 3 - 2x - 2y & -2x \\ -y & 2 - x - 2y \end{pmatrix}.$$

Now consider the four fixed points in turn:

$$(0,0): \text{ Then } A = \begin{pmatrix} 3 & 0 \\ 0 & 2 \end{pmatrix}.$$

The eigenvalues are $\lambda = 3, 2$ so $(0,0)$ is an *unstable node*. Trajectories leave the origin parallel to the eigenvector for $\lambda = 2$, i.e. tangential to $\mathbf{v} = (0,1)$, which spans the y -axis. (Recall the general rule: at a node, trajectories are tangential to the slow eigendirection, which is the eigendirection with the smallest $|\lambda|$.) Thus, the phase portrait near $(0,0)$ looks like Figure 6.4.1.

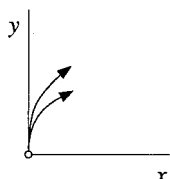


Figure 6.4.1

$$(0,2): \text{ Then } A = \begin{pmatrix} -1 & 0 \\ -2 & -2 \end{pmatrix}.$$

This matrix has eigenvalues $\lambda = -1, -2$, as can be seen from inspection, since

the matrix is triangular. Hence the fixed point is a *stable node*. Trajectories approach along the eigendirection associated with $\lambda = -1$; you can check that this direction is spanned by $\mathbf{v} = (1, -2)$. Figure 6.4.2 shows the phase portrait near the fixed point $(0, 2)$.

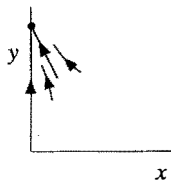


Figure 6.4.2

$(3, 0)$: Then $A = \begin{pmatrix} -3 & -6 \\ 0 & -1 \end{pmatrix}$ and $\lambda = -3, -1$.

This is also a *stable node*. The trajectories approach along the slow eigendirection spanned by $\mathbf{v} = (3, -1)$, as shown in Figure 6.4.3.

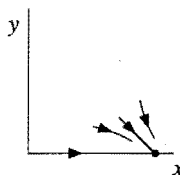


Figure 6.4.3

$(1, 1)$: Then $A = \begin{pmatrix} -1 & -2 \\ -1 & -1 \end{pmatrix}$, which has $\tau = -2$, $\Delta = -1$, and $\lambda = -1 \pm \sqrt{2}$.

Hence this is a *saddle point*. As you can check, the phase portrait near $(1, 1)$ is as shown in Figure 6.4.4.

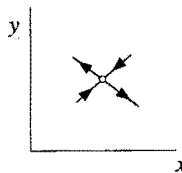


Figure 6.4.4

Combining Figures 6.4.1–6.4.4, we get Figure 6.4.5, which already conveys a good sense of the entire phase portrait. Furthermore, notice that the x and y axes contain straight-line trajectories, since $\dot{x} = 0$ when $x = 0$, and $\dot{y} = 0$ when $y = 0$.

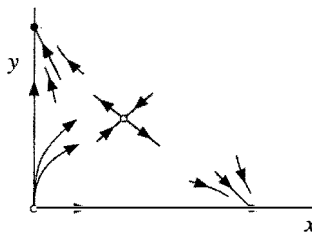


Figure 6.4.5

Now we use common sense to fill in the rest of the phase portrait (Figure 6.4.6). For example, some of the trajectories starting near the origin must go to the stable node on the x -axis, while others must go to the stable node on the y -axis. In between, there must be a special trajectory that can't decide which way to turn, and so it dives into the saddle point. This trajectory is part of the **stable manifold** of the saddle, drawn with a heavy line in Figure 6.4.6.

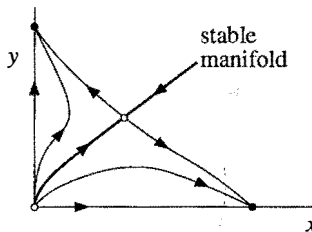


Figure 6.4.6

The other branch of the stable manifold consists of a trajectory coming in “from infinity.” A computer-generated phase portrait (Figure 6.4.7) confirms our sketch.

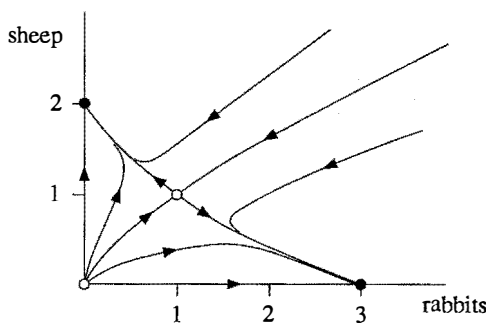


Figure 6.4.7

The phase portrait has an interesting biological interpretation. It shows that one species generally drives the other to extinction. Trajectories starting below the stable manifold lead to eventual extinction of the sheep, while those starting above lead to eventual extinction of the rabbits. This dichotomy occurs in other models of competition and has led biologists to formulate the *principle of competitive exclusion*,

which states that two species competing for the same limited resource typically cannot coexist. See Pianka (1981) for a biological discussion, and

Pielou (1969), Edelstein-Keshet (1988), or Murray (1989) for additional references and analysis.

Our example also illustrates some general mathematical concepts. Given an attracting fixed point \mathbf{x}^* , we define its **basin of attraction** to be the set of initial conditions \mathbf{x}_0 such that $\mathbf{x}(t) \rightarrow \mathbf{x}^*$ as $t \rightarrow \infty$. For instance, the basin of attraction for the node at $(3, 0)$ consists of all the points lying below the stable manifold of the saddle. This basin is shown as the shaded region in Figure 6.4.8.

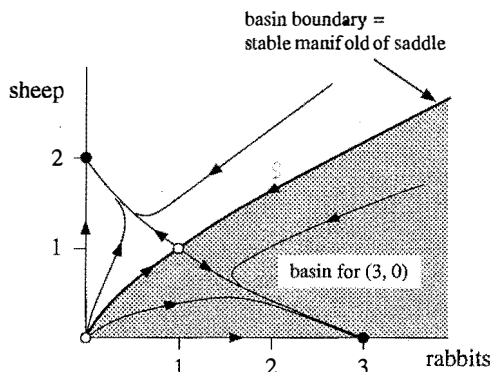


Figure 6.4.8

Because the stable manifold separates the basins for the two nodes, it is called the **basin boundary**. For the same reason, the two trajectories that comprise the stable manifold are traditionally called **separatrices**. Basins and their boundaries are important because they partition the phase space into regions of different long-term behavior.

6.5 Conservative Systems

Newton's law $F = ma$ is the source of many important second-order systems. For example, consider a particle of mass m moving along the x -axis, subject to a non-linear force $F(x)$. Then the equation of motion is

$$m\ddot{x} = F(x).$$

Notice that we are assuming that F is independent of both \dot{x} and t ; hence there is no damping or friction of any kind, and there is no time-dependent driving force.

Under these assumptions, we can show that *energy is conserved*, as follows. Let $V(x)$ denote the **potential energy**, defined by $F(x) = -dV/dx$. Then

$$m\ddot{x} + \frac{dV}{dx} = 0. \quad (1)$$

Now comes a trick worth remembering: multiply both sides by \dot{x} and notice that the left-hand side becomes an exact time-derivative!

$$m\ddot{x}\dot{x} + \frac{dV}{dx}\dot{x} = 0 \Rightarrow \frac{d}{dt}\left[\frac{1}{2}m\dot{x}^2 + V(x)\right] = 0$$

where we've used the chain rule

$$\frac{d}{dt}V(x(t)) = \frac{dV}{dx}\frac{dx}{dt}$$

in reverse. Hence, for a given solution $x(t)$, the total *energy*

$$E = \frac{1}{2}m\dot{x}^2 + V(x)$$

is constant as a function of time. The energy is often called a conserved quantity, a constant of motion, or a first integral. Systems for which a conserved quantity exists are called ***conservative systems***.

Let's be a bit more general and precise. Given a system $\dot{\mathbf{x}} = \mathbf{f}(\mathbf{x})$, a ***conserved quantity*** is a real-valued continuous function $E(\mathbf{x})$ that is constant on trajectories, i.e. $dE/dt = 0$. To avoid trivial examples, we also require that $E(\mathbf{x})$ be nonconstant on every open set. Otherwise a constant function like $E(\mathbf{x}) \equiv 0$ would qualify as a conserved quantity for every system, and so *every* system would be conservative! Our caveat rules out this silliness.

The first example points out a basic fact about conservative systems.

EXAMPLE 6.5.1:

Show that a *conservative system cannot have any attracting fixed points*.

Solution: Suppose \mathbf{x}^* were an attracting fixed point. Then all points in its basin of attraction would have to be at the same energy $E(\mathbf{x}^*)$ (because energy is constant on trajectories and all trajectories in the basin flow to \mathbf{x}^*). Hence $E(\mathbf{x})$ must be a *constant function* for \mathbf{x} in the basin. But this contradicts our definition of a conservative system, in which we required that $E(\mathbf{x})$ be nonconstant on all open sets. ■

If attracting fixed points can't occur, then what kind of fixed points *can* occur? One generally finds saddles and centers, as in the next example.

EXAMPLE 6.5.2:

Consider a particle of mass $m=1$ moving in a double-well potential $V(x) = -\frac{1}{2}x^2 + \frac{1}{4}x^4$. Find and classify all the equilibrium points for the system. Then plot the phase portrait and interpret the results physically.

Solution: The force is $-dV/dx = x - x^3$, so the equation of motion is

$$\ddot{x} = x - x^3.$$

This can be rewritten as the vector field

$$\dot{x} = y$$

$$\dot{y} = x - x^3$$

where y represents the particle's velocity. Equilibrium points occur where $(\dot{x}, \dot{y}) = (0, 0)$. Hence the equilibria are $(x^*, y^*) = (0, 0)$ and $(\pm 1, 0)$. To classify these fixed points we compute the Jacobian:

$$A = \begin{pmatrix} 0 & 1 \\ 1-3x^2 & 0 \end{pmatrix}.$$

At $(0,0)$, we have $\Delta = -1$, so the origin is a saddle point. But when $(x^*, y^*) = (\pm 1, 0)$, we find $\tau = 0$, $\Delta = 2$; hence these equilibria are predicted to be centers.

At this point you should be hearing warning bells—in Section 6.3 we saw that small nonlinear terms can easily destroy a center predicted by the linear approximation. But that's not the case here, because of energy conservation. The trajectories are closed curves defined by the **contours** of constant energy, i.e.,

$$E = \frac{1}{2}y^2 - \frac{1}{2}x^2 + \frac{1}{4}x^4 = \text{constant}.$$

Figure 6.5.1 shows the trajectories corresponding to different values of E . To decide which way the arrows point along the trajectories, we simply compute the vector (\dot{x}, \dot{y}) at a few convenient locations. For example, $\dot{x} > 0$ and $\dot{y} = 0$ on the positive y -axis, so the motion is to the right. The orientation of neighboring trajectories follows by continuity.

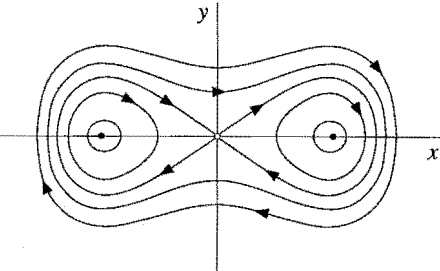


Figure 6.5.1

As expected, the system has a saddle point at $(0,0)$ and centers at $(1,0)$ and $(-1,0)$. Each of the neutrally stable centers is surrounded by a family of small closed orbits. There are also large closed orbits that encircle all three fixed points.

Thus solutions of the system are typically *periodic*, except for the equilibrium solutions and two very special trajectories: these are the trajectories that appear to start and end at the origin. More precisely, these trajectories approach the origin as $t \rightarrow \pm\infty$. Trajectories that start and end at the same fixed point are called **homoclinic orbits**. They are common in conservative systems, but are rare otherwise. Notice that a homoclinic orbit does *not* correspond to a periodic

solution, because the trajectory takes forever trying to reach the fixed point.

Finally, let's connect the phase portrait to the motion of an undamped particle in a double-well potential (Figure 6.5.2).

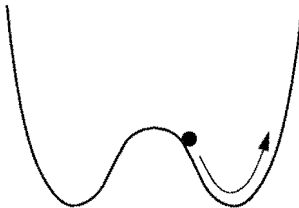


Figure 6.5.2

The neutrally stable equilibria correspond to the particle at rest at the bottom of one of the wells, and the small closed orbits represent small oscillations about these equilibria. The large orbits represent more energetic oscillations that repeatedly take the particle back and forth over the hump. Do you see what the saddle point and the homoclinic orbits mean physically? ■

EXAMPLE 6.5.3:

Sketch the graph of the energy function $E(x, y)$ for Example 6.5.2.

Solution: The graph of $E(x, y)$ is shown in Figure 6.5.3. The energy E is plotted above each point (x, y) of the phase plane. The resulting surface is often called the **energy surface** for the system.

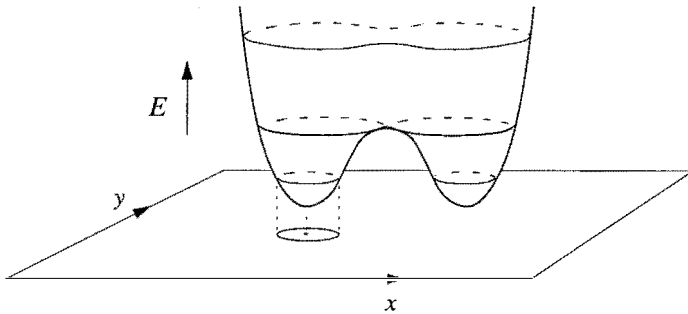


Figure 6.5.3

Figure 6.5.3 shows that the local minima of E project down to centers in the phase plane. Contours of slightly higher energy correspond to the small orbits surrounding the centers. The saddle point and its homoclinic orbits lie at even higher energy, and the large orbits that encircle all three fixed points are the most energetic of all.

It's sometimes helpful to think of the flow as occurring on the energy surface it-

self, rather than in the phase plane. But notice—the trajectories must maintain a constant height E , so they would run *around* the surface, not down it. ■

Nonlinear Centers

Centers are ordinarily very delicate but, as the examples above suggest, they are much more robust when the system is conservative. We now present a theorem about nonlinear centers in second-order conservative systems.

The theorem says that centers occur at the local minima of the energy function. This is physically plausible—one expects neutrally stable equilibria and small oscillations to occur at the bottom of *any* potential well, no matter what its shape.

Theorem 6.5.1: (Nonlinear centers for conservative systems) Consider the system $\dot{\mathbf{x}} = \mathbf{f}(\mathbf{x})$, where $\mathbf{x} = (x, y) \in \mathbf{R}^2$, and \mathbf{f} is continuously differentiable. Suppose there exists a conserved quantity $E(\mathbf{x})$ and suppose that \mathbf{x}^* is an isolated fixed point (i.e., there are no other fixed points in a small neighborhood surrounding \mathbf{x}^*). If \mathbf{x}^* is a local minimum of E , then all trajectories sufficiently close to \mathbf{x}^* are closed.

Ideas behind the proof: Since E is constant on trajectories, each trajectory is contained in some contour of E . Near a local maximum or minimum, the contours are *closed*. (We won't prove this, but Figure 6.5.3 should make it seem obvious.) The only remaining question is whether the trajectory actually goes all the way around the contour or whether it stops at a fixed point on the contour. But because we're assuming that \mathbf{x}^* is an *isolated* fixed point, there cannot be any fixed points on contours sufficiently close to \mathbf{x}^* . Hence all trajectories in a sufficiently small neighborhood of \mathbf{x}^* are closed orbits, and therefore \mathbf{x}^* is a center. ■

Two remarks about this result:

1. The theorem is valid for local *maxima* of E also. Just replace the function E by $-E$, and maxima get converted to minima; then Theorem 6.5.1 applies.
2. We need to assume that \mathbf{x}^* is isolated. Otherwise there are counterexamples due to fixed points on the energy contour—see Exercise 6.5.12.

Another theorem about nonlinear centers will be presented in the next section.

6.6 Reversible Systems

Many mechanical systems have *time-reversal symmetry*. This means that their dynamics look the same whether time runs forward or backward. For example, if you were watching a movie of an undamped pendulum swinging back and forth, you wouldn't see any physical absurdities if the movie were run backward.

In fact, any mechanical system of the form $m\ddot{x} = F(x)$ is symmetric under time reversal. If we make the change of variables $t \rightarrow -t$, the second derivative \ddot{x} stays the same and so the equation is unchanged. Of course, the velocity \dot{x} would be reversed. Let's see what this means in the phase plane. The equivalent system is

$$\begin{aligned}\dot{x} &= y \\ \dot{y} &= \frac{1}{m} F(x)\end{aligned}$$

where y is the velocity. If we make the change of variables $t \rightarrow -t$ and $y \rightarrow -y$, both equations stay the same. Hence if $(x(t), y(t))$ is a solution, then so is $(x(-t), -y(-t))$. Therefore every trajectory has a twin: they differ only by time-reversal and a reflection in the x -axis (Figure 6.6.1).

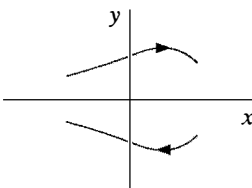


Figure 6.6.1

The trajectory above the x -axis looks just like the one below the x -axis, except the arrows are reversed.

More generally, let's define a **reversible system** to be *any* second-order system that is invariant under $t \rightarrow -t$ and $y \rightarrow -y$. For example, any system of the form

$$\begin{aligned}\dot{x} &= f(x, y) \\ \dot{y} &= g(x, y),\end{aligned}$$

where f is *odd* in y and g is *even* in y (i.e., $f(x, -y) = -f(x, y)$ and $g(x, -y) = g(x, y)$) is reversible.

Reversible systems are different from conservative systems, but they have many of the same properties. For instance, the next theorem shows that centers are robust in reversible systems as well.

Theorem 6.6.1: (Nonlinear centers for reversible systems) Suppose the origin $\mathbf{x}^* = \mathbf{0}$ is a linear center for the continuously differentiable system

$$\begin{aligned}\dot{x} &= f(x, y) \\ \dot{y} &= g(x, y),\end{aligned}$$

and suppose that the system is reversible. Then sufficiently close to the origin, all trajectories are closed curves.

Ideas behind the proof: Consider a trajectory that starts on the positive x -axis near the origin (Figure 6.6.2). Sufficiently near the origin, the flow swirls around the origin, thanks to the dominant influence of the linear center, and so the trajectory eventually intersects the *negative* x -axis. (This is the step where our proof lacks rigor, but the claim should seem plausible.)

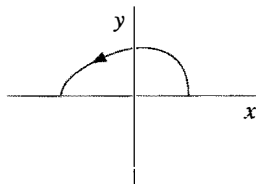


Figure 6.6.2

Now we use reversibility. By reflecting the trajectory across the x -axis, and changing the sign of t , we obtain a twin trajectory with the same endpoints but with its arrow reversed (Figure 6.6.3).

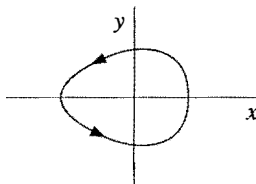


Figure 6.6.3

Together the two trajectories form a closed orbit, as desired. Hence all trajectories sufficiently close to the origin are closed. ■

EXAMPLE 6.6.1:

Show that the system

$$\dot{x} = y - y^3$$

$$\dot{y} = -x - y^2$$

has a nonlinear center at the origin, and plot the phase portrait.

Solution: We'll show that the hypotheses of the theorem are satisfied. The Jacobian at the origin is

$$A = \begin{pmatrix} 0 & 1 \\ -1 & 0 \end{pmatrix}.$$

This has $\tau = 0$, $\Delta > 0$, so the origin is a linear center. Furthermore, the system is reversible, since the equations are invariant under the transformation $t \rightarrow -t$, $y \rightarrow -y$. By Theorem 6.6.1, the origin is a *nonlinear center*.

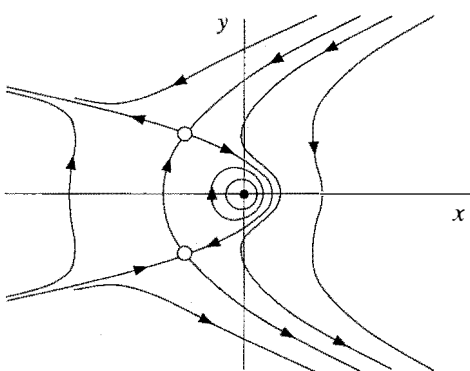


Figure 6.6.4

The other fixed points of the system are $(-1, 1)$ and $(-1, -1)$. They are saddle points, as is easily checked by computing the linearization. A computer-generated phase portrait is shown in Figure 6.6.4. It looks like some exotic sea creature, perhaps a manta ray. The reversibility symmetry is apparent. The trajectories above the x -axis have twins below the x -axis, with arrows reversed.

Notice that the twin saddle points are joined by a pair of trajectories.

They are called **heteroclinic trajectories** or **saddle connections**. Like homoclinic orbits, heteroclinic trajectories are much more common in reversible or conservative systems than in other types of systems. ■

Although we have relied on the computer to plot Figure 6.6.4, it can be sketched on the basis of qualitative reasoning alone. For example, the existence of the heteroclinic trajectories can be deduced rigorously using reversibility arguments (Exercise 6.6.6). The next example illustrates the spirit of such arguments.

EXAMPLE 6.6.2:

Using reversibility arguments alone, show that the system

$$\begin{aligned}\dot{x} &= y \\ \dot{y} &= x - x^2\end{aligned}$$

has a homoclinic orbit in the half-plane $x \geq 0$.

Solution: Consider the unstable manifold of the saddle point at the origin. This manifold leaves the origin along the vector $(1, 1)$, since this is the unstable eigen-direction for the linearization. Hence, close to the origin, part of the unstable manifold lies in the first quadrant $x, y > 0$. Now imagine a phase point with coordinates $(x(t), y(t))$ moving along the unstable manifold, starting from x, y small and positive. At first, $x(t)$ must increase since $\dot{x} = y > 0$. Also, $y(t)$ increases initially, since $\dot{y} = x - x^2 > 0$ for small x . Thus the phase point moves up and to the right. Its horizontal velocity is continually increasing, so at some time it must cross the

vertical line $x=1$. Then $\dot{y} < 0$ so $y(t)$ decreases, eventually reaching $y=0$. Figure 6.6.5 shows the situation.

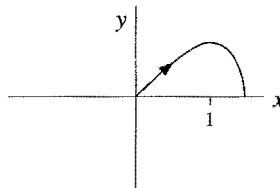


Figure 6.6.5

Now, by *reversibility*, there must be a twin trajectory with the same endpoints but with arrow reversed (Figure 6.6.6). Together the two trajectories form the desired homoclinic orbit. ■

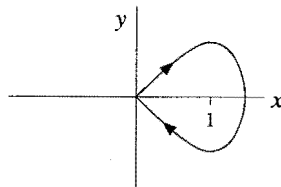


Figure 6.6.6

There is a more general definition of reversibility which extends nicely to higher-order systems. Consider any mapping $R(\mathbf{x})$ of the phase space to itself that satisfies $R^2(\mathbf{x}) = \mathbf{x}$. In other words, if the mapping is applied twice, all points go back to where they started. In our two-dimensional examples, a reflection about the x -axis (or any axis through the origin) has this property. Then the system $\dot{\mathbf{x}} = \mathbf{f}(\mathbf{x})$ is *reversible*

if it is invariant under the change of variables $t \rightarrow -t$, $\mathbf{x} \rightarrow R(\mathbf{x})$.

Our next example illustrates this more general notion of reversibility, and also highlights the main difference between reversible and conservative systems.

EXAMPLE 6.6.3:

Show that the system

$$\begin{aligned}\dot{x} &= -2 \cos x - \cos y \\ \dot{y} &= -2 \cos y - \cos x\end{aligned}$$

is reversible, but *not* conservative. Then plot the phase portrait.

Solution: The system is invariant under the change of variables $t \rightarrow -t$, $x \rightarrow -x$, and $y \rightarrow -y$. Hence the system is reversible, with $R(x, y) = (-x, -y)$ in the preceding notation.

To show that the system is not conservative, it suffices to show that it has an attracting fixed point. (Recall that a conservative system can never have an attracting fixed point—see Example 6.5.1.)

The fixed points satisfy $2 \cos x = -\cos y$ and $2 \cos y = -\cos x$. Solving these equations simultaneously yields $\cos x^* = \cos y^* = 0$. Hence there are four fixed points,

given by $(x^*, y^*) = (\pm \frac{\pi}{2}, \pm \frac{\pi}{2})$.

We claim that $(x^*, y^*) = (-\frac{\pi}{2}, -\frac{\pi}{2})$ is an attracting fixed point. The Jacobian there is

$$A = \begin{pmatrix} 2 \sin x^* & \sin y^* \\ \sin x^* & 2 \sin y^* \end{pmatrix} = \begin{pmatrix} -2 & -1 \\ -1 & -2 \end{pmatrix},$$

which has $\tau = -4$, $\Delta = 3$, $\tau^2 - 4\Delta = 4$. Therefore the fixed point is a stable node. This shows that the system is not conservative.

The other three fixed points can be shown to be an unstable node and two saddles. A computer-generated phase portrait is shown in Figure 6.6.7.

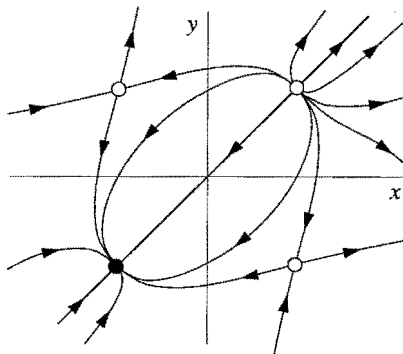


Figure 6.6.7

To see the reversibility symmetry, compare the dynamics at any two points (x, y) and $R(x, y) = (-x, -y)$. The trajectories look the same, but the arrows are reversed. In particular, the stable node at $(-\frac{\pi}{2}, -\frac{\pi}{2})$ is the twin of the unstable node at $(\frac{\pi}{2}, \frac{\pi}{2})$. ■

The system in Example 6.6.3 is closely related to a model of two superconducting Josephson junctions coupled through a resistive load (Tsang et al. 1991). For further discussion, see Exercise 6.6.9 and Example 8.7.4. Reversible, nonconservative systems also arise in the context of lasers (Politi et al. 1986) and fluid flows (Stone, Nadim, and Strogatz 1991 and Exercise 6.6.8).

6.7 Pendulum

Do you remember the first nonlinear system you ever studied in school? It was probably the pendulum. But in elementary courses, the pendulum's essential nonlinearity is sidestepped by the small-angle approximation $\sin \theta \approx \theta$. Enough of that! In this section we use phase plane methods to analyze the pendulum, even in the dreaded large-angle regime where the pendulum whirls over the top.

In the absence of damping and external driving, the motion of a pendulum is governed by

$$\frac{d^2\theta}{dt^2} + \frac{g}{L} \sin \theta = 0 \quad (1)$$

where θ is the angle from the downward vertical, g is the acceleration due to gravity, and L is the length of the pendulum (Figure 6.7.1).

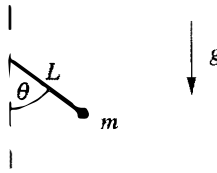


Figure 6.7.1

We nondimensionalize (1) by introducing a frequency $\omega = \sqrt{g/L}$ and a dimensionless time $\tau = \omega t$. Then the equation becomes

$$\ddot{\theta} + \sin \theta = 0 \quad (2)$$

where the overdot denotes differentiation with respect to τ . The corresponding system in the phase plane is

$$\dot{\theta} = v \quad (3a)$$

$$\dot{v} = -\sin \theta \quad (3b)$$

where v is the (dimensionless) angular velocity.

The fixed points are $(\theta^*, v^*) = (k\pi, 0)$, where k is any integer. There's no physical difference between angles that differ by 2π , so we'll concentrate on the two fixed points $(0,0)$ and $(\pi,0)$. At $(0,0)$, the Jacobian is

$$A = \begin{pmatrix} 0 & 1 \\ -1 & 0 \end{pmatrix}$$

so the origin is a linear center.

In fact, the origin is a *nonlinear* center, for two reasons. First, the system (3) is *reversible*: the equations are invariant under the transformation $\tau \rightarrow -\tau$, $v \rightarrow -v$. Then Theorem 6.6.1 implies that the origin is a nonlinear center.

Second, the system is also *conservative*. Multiplying (2) by $\dot{\theta}$ and integrating yields

$$\dot{\theta}(\ddot{\theta} + \sin \theta) = 0 \Rightarrow \frac{1}{2}\dot{\theta}^2 - \cos \theta = \text{constant.}$$

The energy function

$$E(\theta, v) = \frac{1}{2}v^2 - \cos \theta \quad (4)$$

has a local minimum at $(0, 0)$, since $E \approx \frac{1}{2}(v^2 + \theta^2) - 1$ for small (θ, v) . Hence Theorem 6.5.1 provides a second proof that the origin is a nonlinear center. (This argument also shows that the closed orbits are approximately *circular*, with $\theta^2 + v^2 \approx 2(E + 1)$.)

Now that we've beaten the origin to death, consider the fixed point at $(\pi, 0)$. The Jacobian is

$$A = \begin{pmatrix} 0 & 1 \\ 1 & 0 \end{pmatrix}.$$

The characteristic equation is $\lambda^2 - 1 = 0$. Therefore $\lambda_1 = -1$, $\lambda_2 = 1$; the fixed point is a saddle. The corresponding eigenvectors are $\mathbf{v}_1 = (1, -1)$ and $\mathbf{v}_2 = (1, 1)$.

The phase portrait near the fixed points can be sketched from the information obtained so far (Figure 6.7.2).

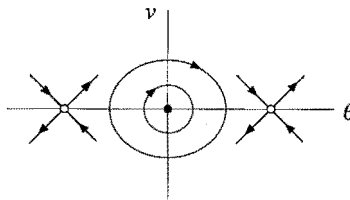


Figure 6.7.2

To fill in the picture, we include the energy contours $E = \frac{1}{2}v^2 - \cos \theta$ for different values of E . The resulting phase portrait is shown in Figure 6.7.3. The picture is

periodic in the θ -direction, as we'd expect.

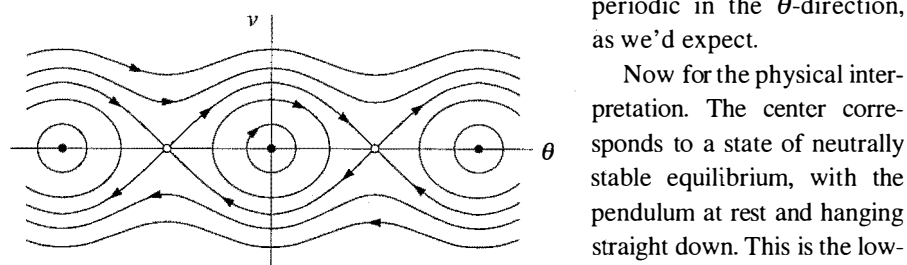


Figure 6.7.3

represent small oscillations about equilibrium, traditionally called *librations*. As E increases, the orbits grow. The critical case is $E = 1$, corresponding to the heteroclinic trajectories joining the saddles in Figure 6.7.3. The saddles represent an *inverted pendulum* at rest;

Now for the physical interpretation. The center corresponds to a state of neutrally stable equilibrium, with the pendulum at rest and hanging straight down. This is the lowest possible energy state ($E = -1$). The small orbits surrounding the center

hence the heteroclinic trajectories represent delicate motions in which the pendulum slows to a halt precisely as it approaches the inverted position. For $E > 1$, the pendulum whirls repeatedly over the top. These *rotations* should also be regarded as periodic solutions, since $\theta = -\pi$ and $\theta = +\pi$ are the same physical position.

Cylindrical Phase Space

The phase portrait for the pendulum is more illuminating when wrapped onto the surface of a cylinder (Figure 6.7.4). In fact, a cylinder is the *natural* phase space for the pendulum, because it incorporates the fundamental geometric difference between v and θ : the angular velocity v is a real number, whereas θ is an angle.

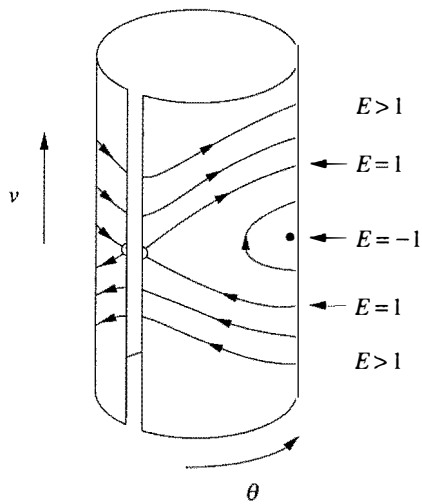


Figure 6.7.4

$E > 1$
 $E = 1$
 $E = -1$
 $E = 1$
 $E > 1$

There are several advantages to the cylindrical representation. Now the periodic whirling motions *look* periodic—they are the closed orbits that encircle the cylinder for $E > 1$. Also, it becomes obvious that the saddle points in Figure 6.7.3 are all the same physical state (an inverted pendulum at rest). The heteroclinic trajectories of Figure 6.7.3 become homoclinic orbits on the cylinder.

There is an obvious symmetry between the top and bottom half of Figure 6.7.4. For example, both homoclinic orbits have the same energy and shape. To highlight this symmetry, it is

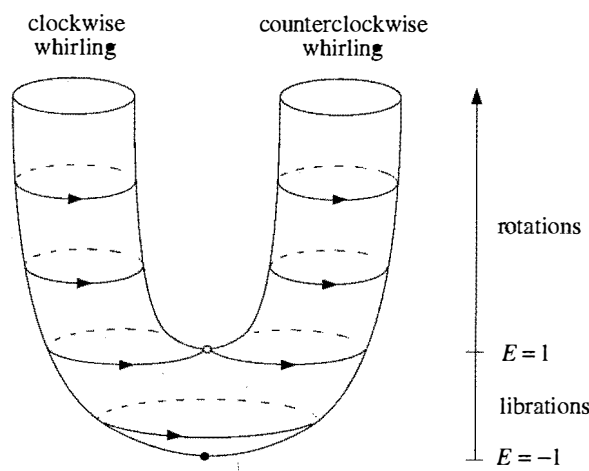


Figure 6.7.5

interesting (if a bit mind-boggling at first) to plot the *energy* vertically instead of the angular velocity v (Figure 6.7.5). Then the orbits on the cylinder remain at constant height, while the cylinder gets bent into a *U-tube*. The two arms of the tube are distinguished by the sense of rotation of the pendulum, either clockwise or counterclockwise.

wise. At low energies, this distinction no longer exists; the pendulum oscillates to and fro. The homoclinic orbits lie at $E = 1$, the borderline between rotations and librations.

At first you might think that the trajectories are drawn incorrectly on one of the arms of the U-tube. It might seem that the arrows for clockwise and counterclockwise motions should go in *opposite* directions. But if you think about the coordinate system shown in Figure 6.7.6, you'll see that the picture is correct.

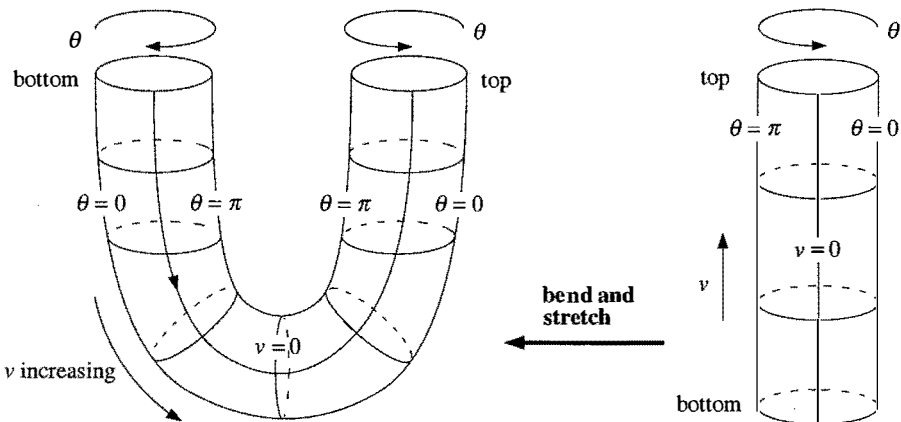


Figure 6.7.6

The point is that the direction of increasing θ has reversed when the bottom of the cylinder is bent around to form the U-tube. (Please understand that Figure 6.7.6 shows the coordinate system, not the actual trajectories; the trajectories were shown in Figure 6.7.5.)

Damping

Now let's return to the phase plane, and suppose that we add a small amount of linear damping to the pendulum. The governing equation becomes

$$\ddot{\theta} + b\dot{\theta} + \sin \theta = 0$$

where $b > 0$ is the damping strength. Then centers become stable spirals while saddles remain saddles. A computer-generated phase portrait is shown in Figure 6.7.7.

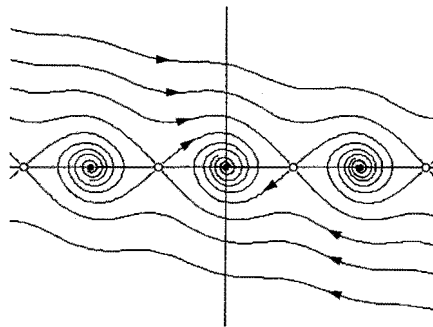


Figure 6.7.7

The picture on the U-tube is clearer. All trajectories continually lose altitude, except for the fixed points (Figure 6.7.8).

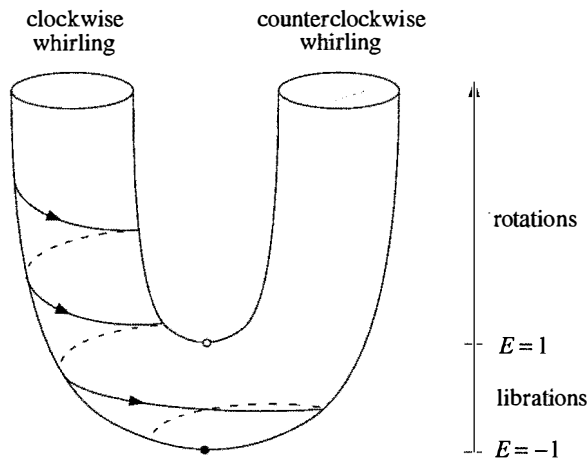


Figure 6.7.8

We can see this explicitly by computing the change in energy along a trajectory:

$$\frac{dE}{d\tau} = \frac{d}{d\tau} \left(\frac{1}{2} \dot{\theta}^2 - \cos \theta \right) = \dot{\theta} (\ddot{\theta} + \sin \theta) = -b \dot{\theta}^2 \leq 0.$$

Hence E decreases monotonically along trajectories, except at fixed points where $\dot{\theta} \equiv 0$.

The trajectory shown in Figure 6.7.8 has the following physical interpretation: the pendulum is initially whirling clockwise. As it loses energy, it has a harder time rotating over the top. The corresponding trajectory spirals down the arm of the U-tube until $E < 1$; then the pendulum doesn't have enough energy to whirl, and so it settles down into a small oscillation about the bottom. Eventually the mo-

tion damps out and the pendulum comes to rest at its stable equilibrium.

This example shows how far we can go with pictures—without invoking any difficult formulas, we were able to extract all the important features of the pendulum’s dynamics. It would be much more difficult to obtain these results analytically, and much more confusing to interpret the formulas, even if we *could* find them.

6.8 Index Theory

In Section 6.3 we learned how to linearize a system about a fixed point. Linearization is a prime example of a *local* method: it gives us a detailed microscopic view of the trajectories near a fixed point, but it can’t tell us what happens to the trajectories after they leave that tiny neighborhood. Furthermore, if the vector field starts with quadratic or higher-order terms, the linearization tells us nothing.

In this section we discuss index theory, a method that provides *global* information about the phase portrait. It enables us to answer such questions as: Must a closed trajectory always encircle a fixed point? If so, what types of fixed points are permitted? What types of fixed points can coalesce in bifurcations? The method also yields information about the trajectories near higher-order fixed points. Finally, we can sometimes use index arguments to rule out the possibility of closed orbits in certain parts of the phase plane.

The Index of a Closed Curve

The index of a closed curve C is an integer that measures the winding of the vector field on C . The index also provides information about any fixed points that might happen to lie inside the curve, as we’ll see.

This idea may remind you of a concept in electrostatics. In that subject, one often introduces a hypothetical closed surface (a “Gaussian surface”) to probe a configuration of electric charges. By studying the behavior of the electric field on the surface, one can determine the total amount of charge *inside* the surface. Amazingly, the behavior *on* the surface tells us what’s happening far away *inside* the surface! In the present context, the electric field is analogous to our vector field, the Gaussian surface is analogous to the curve C , and the total charge is analogous to the index.

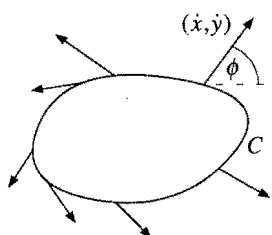


Figure 6.8.1

Now let’s make these notions precise. Suppose that $\dot{\mathbf{x}} = \mathbf{f}(\mathbf{x})$ is a smooth vector field on the phase plane. Consider a closed curve C (Figure 6.8.1). This curve is *not* necessarily a trajectory—it’s simply a loop that we’re putting in the phase plane to probe the behavior of the vector field. We also assume that C is a

"simple closed curve" (i.e., it doesn't intersect itself) and that it doesn't pass through any fixed points of the system. Then at each point \mathbf{x} on C , the vector field $\dot{\mathbf{x}} = (\dot{x}, \dot{y})$ makes a well-defined angle

$$\phi = \tan^{-1}(\dot{y}/\dot{x})$$

with the positive x -axis (Figure 6.8.1).

As \mathbf{x} moves counterclockwise around C , the angle ϕ changes *continuously* since the vector field is smooth. Also, when \mathbf{x} returns to its starting place, ϕ returns to its original direction. Hence, over one circuit, ϕ has changed by an *integer* multiple of 2π . Let $[\phi]_C$ be the net change in ϕ over one circuit. Then the *index of the closed curve* C with respect to the vector field \mathbf{f} is defined as

$$I_C = \frac{1}{2\pi} [\phi]_C.$$

Thus, I_C is the net number of counterclockwise revolutions made by the vector field as \mathbf{x} moves once counterclockwise around C .

To compute the index, we do not need to know the vector field everywhere; we only need to know it along C . The first two examples illustrate this point.

EXAMPLE 6.8.1:

Given that the vector field varies along C as shown in Figure 6.8.2, find I_C .

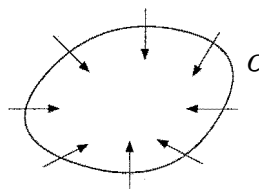
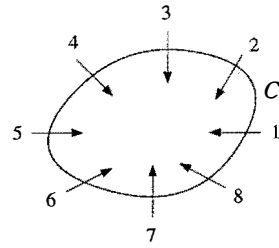


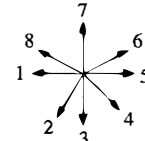
Figure 6.8.2

Solution: As we traverse C once counterclockwise, the vectors rotate through one full turn in the same sense. Hence $I_C = +1$.

If you have trouble visualizing this, here's a foolproof method. Number the vectors in counterclockwise order, starting anywhere on C (Figure 6.8.3a). Then transport these vectors (*without rotation!*) such that their tails lie at a common origin (Figure 6.8.3b). The index equals the net number of counterclockwise revolutions made by the numbered vectors.



(a)



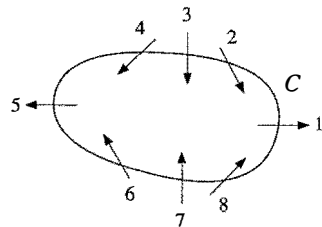
(b)

Figure 6.8.3

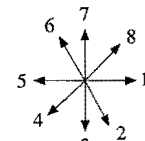
As Figure 6.8.3b shows, the vectors rotate once counterclockwise as we go in increasing order from vector #1 to vector #8. Hence $I_C = +1$. ■

EXAMPLE 6.8.2:

Given the vector field on the closed curve shown in Figure 6.8.4a, compute I_C .



(a)



(b)

Figure 6.8.4

Solution: We use the same construction as in Example 6.8.1. As we make one circuit around C , the vectors rotate through one full turn, but now in the *opposite* sense. In other words, the vectors on C rotate *clockwise* as we go around C counterclockwise. This is clear from Figure 6.8.4b; the vectors rotate clockwise as we go in increasing order from vector #1 to vector #8. Therefore $I_C = -1$. ■

In many cases, we are given equations for the vector field, rather than a picture of it. Then we have to draw the picture ourselves, and repeat the steps above. Sometimes this can be confusing, as in the next example.

EXAMPLE 6.8.3:

Given the vector field $\dot{x} = x^2y$, $\dot{y} = x^2 - y^2$, find I_C , where C is the unit circle $x^2 + y^2 = 1$.

Solution: To get a clear picture of the vector field, it is sufficient to consider a few conveniently chosen points on C . For instance, at $(x, y) = (1, 0)$, the vector is $(\dot{x}, \dot{y}) = (x^2 y, x^2 - y^2) = (0, 1)$. This vector is labeled #1 in Figure 6.8.5a. Now we move

counterclockwise around C , computing vectors as we go. At $(x, y) = \frac{1}{\sqrt{2}}(1, 1)$, we have $(\dot{x}, \dot{y}) = (x, y) = \frac{1}{2\sqrt{2}}(1, 0)$, labeled #2. The remaining vectors are found similarly. Notice that different points on the circle may be associated with the same vector; for example, vector #3 and #7 are both $(0, -1)$.

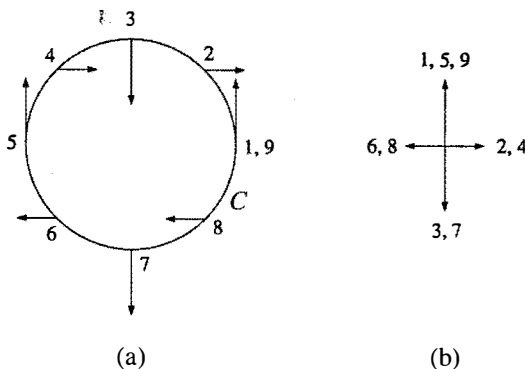


Figure 6.8.5

Now we translate the vectors over to Figure 6.8.5b. As we move from #1 to #9 in order, the vectors rotate 180° clockwise between #1 and #3, then swing back 360° counterclockwise between #3 and #7, and finally rotate 180° clockwise again between #7 and #9 as we complete the circuit of C . Thus $[\phi]_C = -\pi + 2\pi - \pi = 0$ and therefore $I_C = 0$. ■

We plotted nine vectors in this example, but you may want to plot more to see the variation of the vector field in finer detail.

Properties of the Index

Now we list some of the most important properties of the index.

1. Suppose that C can be continuously deformed into C' without passing through a fixed point. Then $I_C = I_{C'}$.

This property has an elegant proof: Our assumptions imply that as we deform C into C' , the index I_C varies *continuously*. But I_C is an integer—hence it can't change without jumping! (To put it more formally, if an integer-valued function is continuous, it must be *constant*.)

As you think about this argument, try to see where we used the assumption that the intermediate curves don't pass through any fixed points.

2. If C doesn't enclose any fixed points, then $I_C = 0$.

Proof: By property (1), we can shrink C to a tiny circle without changing the index. But ϕ is essentially constant on such a circle, because all the vectors point in nearly the same direction, thanks to the as-

sumed smoothness of the vector field (Figure 6.8.6). Hence $[\phi]_c = 0$ and therefore $I_c = 0$.



Figure 6.8.6

3. If we reverse all the arrows in the vector field by changing $t \rightarrow -t$, the index is unchanged.

Proof: All angles change from ϕ to $\phi + \pi$. Hence $[\phi]_c$ stays the same.

4. Suppose that the closed curve C is actually a *trajectory* for the system, i.e., C is a closed orbit. Then $I_c = +1$.

We won't prove this, but it should be clear from geometric intuition (Figure 6.8.7).

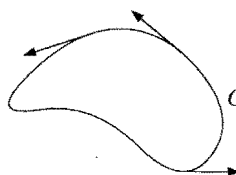


Figure 6.8.7

Notice that the vector field is everywhere tangent to C , because C is a trajectory. Hence, as x winds around C once, the tangent vector also rotates once in the same sense.

Index of a Point

The properties above are useful in several ways. Perhaps most importantly, they allow us to define the index of a fixed point, as follows.

Suppose x^* is an isolated fixed point. Then the *index* I of x^* is defined as I_c , where C is any closed curve that encloses x^* and no other fixed points. By property (1) above, I_c is independent of C and is therefore a property of x^* alone. Therefore we may drop the subscript C and use the notation I for the index of a point.

EXAMPLE 6.8.4:

Find the index of a stable node, an unstable node, and a saddle point.

Solution: The vector field near a stable node looks like the vector field of Example 6.8.1. Hence $I = +1$. The index is also $+1$ for an unstable node, because the only difference is that all the arrows are reversed; by property (3), this doesn't change the index! (This observation shows that *the index is not related to stability*,

per se.) Finally, $I = -1$ for a saddle point, because the vector field resembles that discussed in Example 6.8.2. ■

In Exercise 6.8.1, you are asked to show that spirals, centers, degenerate nodes and stars all have $I = +1$. Thus, a saddle point is truly a different animal from all the other familiar types of isolated fixed points.

The index of a curve is related in a beautifully simple way to the indices of the fixed points inside it. This is the content of the following theorem.

Theorem 6.8.1: If a closed curve C surrounds n isolated fixed points $\mathbf{x}_1^*, \dots, \mathbf{x}_n^*$, then

$$I_C = I_1 + I_2 + \dots + I_n$$

where I_k is the index of \mathbf{x}_k^* , for $k = 1, \dots, n$.

Ideas behind the proof: The argument is a familiar one, and comes up in multivariable calculus, complex variables, electrostatics, and various other subjects. We think of C as a balloon and suck most of the air out of it, being careful not to hit any of the fixed points. The result of this deformation is a new closed curve Γ , consisting of n small circles $\gamma_1, \dots, \gamma_n$ about the fixed points, and two-way bridges connecting these circles (Figure 6.8.8). Note that $I_\Gamma = I_C$, by property (1), since we didn't cross any fixed points during the deformation. Now let's compute I_Γ by considering $[\phi]_\Gamma$. There are contributions to $[\phi]_\Gamma$ from the small circles and from the two-way bridges.

The key point is that *the contributions from the bridges cancel out*: as we move around Γ , each bridge is traversed once in one direction, and later in the opposite direction. Thus we only need to consider the contributions from the small circles.

Figure 6.8.8

On γ_k , the angle ϕ changes by $[\phi]_{\gamma_k} = 2\pi I_k$, by definition of I_k . Hence

$$I_\Gamma = \frac{1}{2\pi} [\phi]_\Gamma = \frac{1}{2\pi} \sum_{k=1}^n [\phi]_{\gamma_k} = \sum_{k=1}^n I_k$$

and since $I_\Gamma = I_C$, we're done. ■

This theorem is reminiscent of Gauss's law in electrostatics, namely that the electric flux through a surface is proportional to the total charge enclosed. See Exercise 6.8.12 for a further exploration of this analogy between index and charge.

Theorem 6.8.2: Any closed orbit in the phase plane must enclose fixed points whose indices sum to +1.

Proof: Let C denote the closed orbit. From property (4) above, $I_C = +1$.

Then Theorem 6.8.1 implies $\sum_{k=1}^n I_k = +1$. ■

Theorem 6.8.2 has many practical consequences. For instance, it implies that there is always at least one fixed point inside any closed orbit in the phase plane (as you may have noticed on your own). If there is *only* one fixed point inside, it cannot be a saddle point. Furthermore, Theorem 6.8.2 can sometimes be used to rule out the possible occurrence of closed trajectories, as seen in the following examples.

EXAMPLE 6.8.5:

Show that closed orbits are impossible for the “rabbit vs. sheep” system

$$\begin{aligned}\dot{x} &= x(3 - x - 2y) \\ \dot{y} &= y(2 - x - y)\end{aligned}$$

studied in Section 6.4. Here $x, y \geq 0$.

Solution: As shown previously, the system has four fixed points: $(0, 0)$ = unstable node; $(0, 2)$ and $(3, 0)$ = stable nodes; and $(1, 1)$ = saddle point. The index at

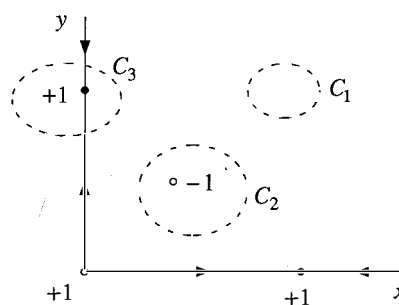


Figure 6.8.9

the index requirement? The trouble is that such orbits always cross the x -axis or the y -axis, and these axes contain straight-line trajectories. Hence C_3 violates the rule that trajectories can't cross (recall Section 6.2). ■

each of these points is shown in Figure 6.8.9. Now suppose that the system had a closed trajectory. Where could it lie? There are three qualitatively different locations, indicated by the dotted curves C_1 , C_2 , C_3 . They can be ruled out as follows: orbits like C_1 are impossible because they don't enclose any fixed points, and orbits like C_2 violate the requirement that the indices inside must sum to +1. But what is wrong with orbits like C_3 , which satisfy

EXAMPLE 6.8.6:

Show that the system $\dot{x} = xe^{-x}$, $\dot{y} = 1 + x + y^2$ has no closed orbits.

Solution: This system has no fixed points: if $\dot{x} = 0$, then $x = 0$ and so $\dot{y} = 1 + y^2 \neq 0$. By Theorem 6.8.2, closed orbits cannot exist. ■

EXERCISES FOR CHAPTER 6**6.1 Phase Portraits**

For each of the following systems, find the fixed points. Then sketch the nullclines, the vector field, and a plausible phase portrait.

6.1.1 $\dot{x} = x - y$, $\dot{y} = 1 - e^x$

6.1.2 $\dot{x} = x - x^3$, $\dot{y} = -y$

6.1.3 $\dot{x} = x(x - y)$, $\dot{y} = y(2x - y)$

6.1.4 $\dot{x} = y$, $\dot{y} = x(1 + y) - 1$

6.1.5 $\dot{x} = x(2 - x - y)$, $\dot{y} = x - y$

6.1.6 $\dot{x} = x^2 - y$, $\dot{y} = x - y$

6.1.7 (Nullcline vs. stable manifold) There's a confusing aspect of Example 6.1.1. The nullcline $\dot{x} = 0$ in Figure 6.1.3 has a similar shape and location as the stable manifold of the saddle, shown in Figure 6.1.4. But they're not the same curve! To clarify the relation between the two curves, sketch both of them on the same phase portrait.

(Computer work) Plot computer-generated phase portraits of the following systems. As always, you may write your own computer programs or use any ready-made software, e.g., *MacMath* (Hubbard and West 1992).

6.1.8 (van der Pol oscillator) $\dot{x} = y$, $\dot{y} = -x + y(1 - x^2)$

6.1.9 (Dipole fixed point) $\dot{x} = 2xy$, $\dot{y} = y^2 - x^2$

6.1.10 (Two-eyed monster) $\dot{x} = y + y^2$, $\dot{y} = -\frac{1}{2}x + \frac{1}{3}y - xy + \frac{6}{5}y^2$ (from Borrelli and Coleman 1987, p. 385.)

6.1.11 (Parrot) $\dot{x} = y + y^2$, $\dot{y} = -x + \frac{1}{5}y - xy + \frac{6}{5}y^2$ (from Borrelli and Coleman 1987, p. 384.)

6.1.12 (Saddle connections) A certain system is known to have exactly two fixed points, both of which are saddles. Sketch phase portraits in which

- there is a single trajectory that connects the saddles;
- there is no trajectory that connects the saddles.

6.1.13 Draw a phase portrait that has exactly three closed orbits and one fixed point.

6.1.14 (Series approximation for the stable manifold of a saddle point) Recall the system $\dot{x} = x + e^{-y}$, $\dot{y} = -y$ from Example 6.1.1. We showed that this system

has one fixed point, a saddle at $(-1, 0)$. Its unstable manifold is the x -axis, but its stable manifold is a curve that is harder to find. The goal of this exercise is to approximate this unknown curve.

- Let (x, y) be a point on the stable manifold, and assume that (x, y) is close to $(-1, 0)$. Introduce a new variable $u = x + 1$, and write the stable manifold as $y = a_1 u + a_2 u^2 + \bullet(u^3)$. To determine the coefficients, derive two expressions for dy/du and equate them.
- Check that your analytical result produces a curve with the same shape as the stable manifold shown in Figure 6.1.4.

6.2 Existence, Uniqueness, and Topological Consequences

6.2.1 We claimed that different trajectories can never intersect. But in many phase portraits, different trajectories appear to intersect at a fixed point. Is there a contradiction here?

6.2.2 Consider the system $\dot{x} = y$, $\dot{y} = -x + (1 - x^2 - y^2)y$.

- Let D be the open disk $x^2 + y^2 < 4$. Verify that the system satisfies the hypotheses of the existence and uniqueness theorem throughout the domain D .
- By substitution, show that $x(t) = \sin t$, $y(t) = \cos t$ is an exact solution of the system.
- Now consider a different solution, in this case starting from the initial condition $x(0) = \frac{1}{2}$, $y(0) = 0$. Without doing any calculations, explain why this solution *must* satisfy $x(t)^2 + y(t)^2 < 1$ for all $t < \infty$.

6.3 Fixed Points and Linearization

For each of the following systems, find the fixed points, classify them, sketch the neighboring trajectories, and try to fill in the rest of the phase portrait.

6.3.1 $\dot{x} = x - y$, $\dot{y} = x^2 - 4$

6.3.2 $\dot{x} = \sin y$, $\dot{y} = x - x^3$

6.3.3 $\dot{x} = 1 + y - e^{-x}$, $\dot{y} = x^3 - y$

6.3.4 $\dot{x} = y + x - x^3$, $\dot{y} = -y$

6.3.5 $\dot{x} = \sin y$, $\dot{y} = \cos x$

6.3.6 $\dot{x} = xy - 1$, $\dot{y} = x - y^3$

6.3.7 For each of the nonlinear systems above, plot a computer-generated phase portrait and compare to your approximate sketch.

6.3.8 (Gravitational equilibrium) A particle moves along a line joining two stationary masses, m_1 and m_2 , which are separated by a fixed distance a . Let x denote the distance of the particle from m_1 .

- Show that $\ddot{x} = \frac{Gm_2}{(x-a)^2} - \frac{Gm_1}{x^2}$, where G is the gravitational constant.
- Find the particle's equilibrium position. Is it stable or unstable?

6.3.9 Consider the system $\dot{x} = y^3 - 4x$, $\dot{y} = y^3 - y - 3x$.

- Find all the fixed points and classify them.
- Show that the line $x = y$ is invariant, i.e., any trajectory that starts on it stays on it.
- Show that $|x(t) - y(t)| \rightarrow 0$ as $t \rightarrow \infty$ for all other trajectories. (Hint: Form a differential equation for $x - y$.)
- Sketch the phase portrait.
- If you have access to a computer, plot an accurate phase portrait on the square domain $-20 \leq x, y \leq 20$. (To avoid numerical instability, you'll need to use a fairly small step size, because of the strong cubic nonlinearity.) Notice the trajectories seem to approach a certain curve as $t \rightarrow -\infty$; can you explain this behavior intuitively, and perhaps find an approximate equation for this curve?

6.3.10 (Dealing with a fixed point for which linearization is inconclusive) The goal of this exercise is to sketch the phase portrait for $\dot{x} = xy$, $\dot{y} = x^2 - y$.

- Show that the linearization predicts that the origin is a non-isolated fixed point.
- Show that the origin is in fact an isolated fixed point.
- Is the origin repelling, attracting, a saddle, or what? Sketch the vector field along the nullclines and at other points in the phase plane. Use this information to sketch the phase portrait.
- Plot a computer-generated phase portrait to check your answer to (c).

(Note: This problem can also be solved by a method called *center manifold theory*, as explained in Wiggins (1990) and Guckenheimer and Holmes (1983).)

6.3.11 (Nonlinear terms can change a star into a spiral) Here's another example that shows that borderline fixed points are sensitive to nonlinear terms. Consider the system in polar coordinates given by $\dot{r} = -r$, $\dot{\theta} = 1/\ln r$.

- Find $r(t)$ and $\theta(t)$ explicitly, given an initial condition (r_0, θ_0) .
- Show that $r(t) \rightarrow 0$ and $|\theta(t)| \rightarrow \infty$ as $t \rightarrow \infty$. Therefore the origin is a stable spiral for the nonlinear system.
- Write the system in x, y coordinates.
- Show that the linearized system about the origin is $\dot{x} = -x$, $\dot{y} = -y$. Thus the origin is a stable star for the linearized system.

6.3.12 (Polar coordinates) Using the identity $\theta = \tan^{-1}(y/x)$, show that $\dot{\theta} = (x\dot{y} - y\dot{x})/r^2$.

6.3.13 (Another linear center that's actually a nonlinear spiral) Consider the system $\dot{x} = -y - x^3$, $\dot{y} = x$. Show that the origin is a spiral, although the linearization predicts a center.

6.3.14 Classify the fixed point at the origin for the system $\dot{x} = -y + ax^3$, $\dot{y} = x + ay^3$, for all real values of the parameter a .

6.3.15 Consider the system $\dot{r} = r(1 - r^2)$, $\dot{\theta} = 1 - \cos \theta$, where r, θ represent polar coordinates. Sketch the phase portrait and thereby show that the fixed point $r^* = 1$, $\theta^* = 0$ is attracting but not Liapunov stable.

6.3.16 (Saddle switching and structural stability) Consider the system $\dot{x} = a + x^2 - xy$, $\dot{y} = y^2 - x^2 - 1$, where a is a parameter.

- Sketch the phase portrait for $a = 0$. Show that there is a trajectory connecting two saddle points. (Such a trajectory is called a *saddle connection*.)
- With the aid of a computer if necessary, sketch the phase portrait for $a < 0$ and $a > 0$.

Notice that for $a \neq 0$, the phase portrait has a different topological character: the saddles are no longer connected by a trajectory. The point of this exercise is that the phase portrait in (a) is *not structurally stable*, since its topology can be changed by an arbitrarily small perturbation a .

6.3.17 (Nasty fixed point) The system $\dot{x} = xy - x^2y + y^3$, $\dot{y} = y^2 + x^3 - xy^2$ has a nasty higher-order fixed point at the origin. Using polar coordinates or otherwise, sketch the phase portrait.

6.4 Rabbits versus Sheep

Consider the following “rabbits vs. sheep” problems, where $x, y \geq 0$. Find the fixed points, investigate their stability, draw the nullclines, and sketch plausible phase portraits. Indicate the basins of attraction of any stable fixed points.

6.4.1 $\dot{x} = x(3 - x - y)$, $\dot{y} = y(2 - x - y)$

6.4.2 $\dot{x} = x(3 - 2x - y)$, $\dot{y} = y(2 - x - y)$

6.4.3 $\dot{x} = x(3 - 2x - 2y)$, $\dot{y} = y(2 - x - y)$

The next three exercises deal with competition models of increasing complexity. We assume $N_1, N_2 \geq 0$ in all cases.

6.4.4 The simplest model is $\dot{N}_1 = r_1 N_1 - b_1 N_1 N_2$, $\dot{N}_2 = r_2 N_2 - b_2 N_1 N_2$.

- In what way is this model less realistic than the one considered in the text?
- Show that by suitable rescalings of N_1 , N_2 , and t , the model can be nondimensionalized to $x' = x(1 - y)$, $y' = y(\rho - x)$. Find a formula for the dimensionless group ρ .
- Sketch the nullclines and vector field for the system in (b).
- Draw the phase portrait, and comment on the biological implications.
- Show that (almost) all trajectories are curves of the form $\rho \ln x - x = \ln y - y + C$. (Hint: Derive a differential equation for dx/dy , and separate the variables.) Which trajectories are not of the stated form?

6.4.5 Now suppose that species #1 has a finite carrying capacity K_1 . Thus

$$\dot{N}_1 = r_1 N_1 (1 - N_1/K_1) - b_1 N_1 N_2$$

$$\dot{N}_2 = r_2 N_2 - b_2 N_1 N_2.$$

Nondimensionalize the model and analyze it. Show that there are two qualitatively different kinds of phase portrait, depending on the size of K_1 . (Hint: Draw the nullclines.) Describe the long-term behavior in each case.

6.4.6 Finally, suppose that both species have finite carrying capacities:

$$\dot{N}_1 = r_1 N_1 (1 - N_1/K_1) - b_1 N_1 N_2$$

$$\dot{N}_2 = r_2 N_2 (1 - N_2/K_2) - b_2 N_1 N_2.$$

- Nondimensionalize the model. How many dimensionless groups are needed?
- Show that there are four qualitatively different phase portraits, as far as long-term behavior is concerned.
- Find conditions under which the two species can stably coexist. Explain the biological meaning of these conditions. (Hint: The carrying capacities reflect the competition *within* a species, whereas the b 's reflect the competition *between* species.)

6.4.7 (Two-mode laser) According to Haken (1983, p. 129), a two-mode laser produces two different kinds of photons with numbers n_1 and n_2 . By analogy with the simple laser model discussed in Section 3.3, the rate equations are

$$\dot{n}_1 = G_1 N n_1 - k_1 n_1$$

$$\dot{n}_2 = G_2 N n_2 - k_2 n_2$$

where $N(t) = N_0 - \alpha_1 n_1 - \alpha_2 n_2$ is the number of excited atoms. The parameters $G_1, G_2, k_1, k_2, \alpha_1, \alpha_2, N_0$ are all positive.

- Discuss the stability of the fixed point $n_1^* = n_2^* = 0$.
- Find and classify any other fixed points that may exist.
- Depending on the values of the various parameters, how many qualitatively different phase portraits can occur? For each case, what does the model predict about the long-term behavior of the laser?

6.5 Conservative Systems

6.5.1 Consider the system $\ddot{x} = x^3 - x$.

- Find all the equilibrium points and classify them.
- Find a conserved quantity.
- Sketch the phase portrait.

6.5.2 Consider the system $\ddot{x} = x - x^2$.

- Find and classify the equilibrium points.

- b) Sketch the phase portrait.
- c) Find an equation for the homoclinic orbit that separates closed and nonclosed trajectories.

6.5.3 Find a conserved quantity for the system $\ddot{x} = a - e^x$, and sketch the phase portrait for $a < 0$, $a = 0$, and $a > 0$.

6.5.4 Sketch the phase portrait for the system $\ddot{x} = ax - x^2$ for $a < 0$, $a = 0$, and $a > 0$.

6.5.5 Investigate the stability of the equilibrium points of the system $\ddot{x} = (x - a)(x^2 - a)$ for all real values of the parameter a . (Hints: It might help to graph the right-hand side. An alternative is to rewrite the equation as $\ddot{x} = -V'(x)$ for a suitable potential energy function V and then use your intuition about particles moving in potentials.)

6.5.6 (Epidemic model revisited) In Exercise 3.7.6, you analyzed the Kermack–McKendrick model of an epidemic by reducing it to a certain first-order system. In this problem you'll see how much easier the analysis becomes in the phase plane. As before, let $x(t) \geq 0$ denote the size of the healthy population and $y(t) \geq 0$ denote the size of the sick population. Then the model is

$$\dot{x} = -kxy, \quad \dot{y} = kxy - \ell y$$

where $k, \ell > 0$. (The equation for $z(t)$, the number of deaths, plays no role in the x, y dynamics so we omit it.)

- a) Find and classify all the fixed points.
- b) Sketch the nullclines and the vector field.
- c) Find a conserved quantity for the system. (Hint: Form a differential equation for dy/dx . Separate the variables and integrate both sides.)
- d) Plot the phase portrait. What happens as $t \rightarrow \infty$?
- e) Let (x_0, y_0) be the initial condition. An *epidemic* is said to occur if $y(t)$ increases initially. Under what condition does an epidemic occur?

6.5.7 (General relativity and planetary orbits) The relativistic equation for the orbit of a planet around the sun is

$$\frac{d^2u}{d\theta^2} + u = \alpha + \varepsilon u^2$$

where $u = 1/r$ and r, θ are the polar coordinates of the planet in its plane of motion. The parameter α is positive and can be found explicitly from classical Newtonian mechanics; the term εu^2 is Einstein's correction. Here ε is a very small positive parameter.

- a) Rewrite the equation as a system in the (u, v) phase plane, where $v = du/d\theta$.

- b) Find all the equilibrium points of the system.
- c) Show that one of the equilibria is a center in the (u, v) phase plane, according to the linearization. Is it a *nonlinear* center?
- d) Show that the equilibrium point found in (c) corresponds to a circular planetary orbit.

Hamiltonian systems are fundamental to classical mechanics; they provide an equivalent but more geometric version of Newton's laws. They are also central to celestial mechanics and plasma physics, where dissipation can sometimes be neglected on the time scales of interest. The theory of Hamiltonian systems is deep and beautiful, but perhaps too specialized and subtle for a first course on nonlinear dynamics. See Arnold (1978), Lichtenberg and Lieberman (1992), Tabor (1989), or Hénon (1983) for introductions.

Here's the simplest instance of a Hamiltonian system. Let $H(p, q)$ be a smooth, real-valued function of two variables. The variable q is the "generalized coordinate" and p is the "conjugate momentum." (In some physical settings, H could also depend explicitly on time t , but we'll ignore that possibility.) Then a system of the form

$$\dot{q} = \partial H / \partial p, \quad \dot{p} = -\partial H / \partial q$$

is called a **Hamiltonian system** and the function H is called the **Hamiltonian**. The equations for \dot{q} and \dot{p} are called Hamilton's equations.

The next three exercises concern Hamiltonian systems.

6.5.8 (Harmonic oscillator) For a simple harmonic oscillator of mass m , spring constant k , displacement x , and momentum p , the Hamiltonian is $H = \frac{p^2}{2m} + \frac{kx^2}{2}$.

Write out Hamilton's equations explicitly. Show that one equation gives the usual definition of momentum and the other is equivalent to $F = ma$. Verify that H is the total energy.

6.5.9 Show that for any Hamiltonian system, $H(x, p)$ is a conserved quantity. (Hint: Show $\dot{H} = 0$ by applying the chain rule and invoking Hamilton's equations.) Hence the trajectories lie on the contour curves $H(x, p) = C$.

6.5.10 (Inverse-square law) A particle moves in a plane under the influence of an inverse-square force. It is governed by the Hamiltonian $H(p, r) = \frac{p^2}{2} + \frac{h^2}{2r^2} - \frac{k}{r}$

where $r > 0$ is the distance from the origin and p is the radial momentum. The parameters h and k are the angular momentum and the force constant, respectively.

a) Suppose $k > 0$, corresponding to an attractive force like gravity. Sketch the

- phase portrait in the (r, p) plane. (Hint: Graph the “effective potential” $V(r) = h^2/2r^2 - k/r$ and then look for intersections with horizontal lines of height E . Use this information to sketch the contour curves $H(p, r) = E$ for various positive and negative values of E .)
- Show that the trajectories are closed if $-k^2/2h^2 < E < 0$, in which case the particle is “captured” by the force. What happens if $E > 0$? What about $E = 0$?
 - If $k < 0$ (as in electric repulsion), show that there are no periodic orbits.

6.5.11 (Basins for damped double-well oscillator) Suppose we add a small amount of damping to the double-well oscillator of Example 6.5.2. The new system is $\dot{x} = y$, $\dot{y} = -by + x - x^3$, where $0 < b \ll 1$. Sketch the basin of attraction for the stable fixed point $(x^*, y^*) = (1, 0)$. Make the picture large enough so that the global structure of the basin is clearly indicated.

6.5.12 (Why we need to assume *isolated* minima in Theorem 6.5.1) Consider the system $\dot{x} = xy$, $\dot{y} = -x^2$.

- Show that $E = x^2 + y^2$ is conserved.
- Show that the origin is a fixed point, but not an isolated fixed point.
- Since E has a local minimum at the origin, one might have thought that the origin has to be a center. But that would be a misuse of Theorem 6.5.1; the theorem does not apply here because the origin is *not* an isolated fixed point. Show that in fact the origin is not surrounded by closed orbits, and sketch the actual phase portrait.

6.5.13 (Nonlinear centers)

- Show that the Duffing equation $\ddot{x} + x + \varepsilon x^3 = 0$ has a nonlinear center at the origin for all $\varepsilon > 0$.
- If $\varepsilon < 0$, show that all trajectories near the origin are closed. What about trajectories that are far from the origin?

6.5.14 (Glider) Consider a glider flying at speed v at an angle θ to the horizontal. Its motion is governed approximately by the dimensionless equations

$$\begin{aligned}\dot{v} &= -\sin \theta - Dv^2 \\ v\dot{\theta} &= -\cos \theta + v^2\end{aligned}$$

where the trigonometric terms represent the effects of gravity and the v^2 terms represent the effects of drag and lift.

- Suppose there is no drag ($D = 0$). Show that $v^3 - 3v \cos \theta$ is a conserved quantity. Sketch the phase portrait in this case. Interpret your results physically—what does the flight path of the glider look like?
- Investigate the case of positive drag ($D > 0$).

In the next four exercises, we return to the problem of a bead on a rotating hoop,

discussed in Section 3.5. Recall that the bead's motion is governed by

$$mr\ddot{\phi} = -b\dot{\phi} - mg \sin \phi + mr\omega^2 \sin \phi \cos \phi.$$

Previously, we could only treat the overdamped limit. The next four exercises deal with the dynamics more generally.

6.5.15 (Frictionless bead) Consider the undamped case $b=0$.

- Show that the equation can be nondimensionalized to $\phi'' = \sin \phi (\cos \phi - \gamma^{-1})$, where $\gamma = r\omega^2/g$ as before, and prime denotes differentiation with respect to dimensionless time $\tau = \omega t$.
- Draw all the qualitatively different phase portraits as γ varies.
- What do the phase portraits imply about the physical motion of the bead?

6.5.16 (Small oscillations of the bead) Return to the original dimensional variables. Show that when $b=0$ and ω is sufficiently large, the system has a symmetric pair of stable equilibria. Find the approximate frequency of small oscillations about these equilibria. (Please express your answer with respect to t , not τ .)

6.5.17 (A puzzling constant of motion for the bead) Find a conserved quantity when $b=0$. You might think that it's essentially the bead's total energy, but it isn't! Show explicitly that the bead's kinetic plus potential energy is *not* conserved. Does this make sense physically? Can you find a physical interpretation for the conserved quantity? (Hint: Think about reference frames and moving constraints.)

6.5.18 (General case for the bead) Finally, allow the damping b to be arbitrary. Define an appropriate dimensionless version of b , and plot all the qualitatively different phase portraits that occur as b and γ vary.

6.5.19 (Rabbits vs. foxes) The model $\dot{R} = aR - bRF$, $\dot{F} = -cF + dRF$ is the **Lotka–Volterra predator-prey model**. Here $R(t)$ is the number of rabbits, $F(t)$ is the number of foxes, and $a, b, c, d > 0$ are parameters.

- Discuss the biological meaning of each of the terms in the model. Comment on any unrealistic assumptions.
- Show that the model can be recast in dimensionless form as $x' = x(1-y)$, $y' = \mu y(x-1)$.
- Find a conserved quantity in terms of the dimensionless variables.
- Show that the model predicts *cycles* in the populations of both species, for almost all initial conditions.

This model is popular with many textbook writers because it's simple, but some are beguiled into taking it too seriously. Mathematical biologists dismiss the Lotka–Volterra model because it is not structurally stable, and because real predator-prey cycles typically have a characteristic amplitude. In other words, realistic

models should predict a *single* closed orbit, or perhaps finitely many, but not a continuous family of neutrally stable cycles. See the discussions in May (1972), Edelstein–Keshet (1988), or Murray (1989).

6.6 Reversible Systems

Show that each of the following systems is reversible, and sketch the phase portrait.

6.6.1 $\dot{x} = y(1 - x^2)$, $\dot{y} = 1 - y^2$

6.6.2 $\dot{x} = y$, $\dot{y} = x \cos y$

6.6.3 (Wallpaper) Consider the system $\dot{x} = \sin y$, $\dot{y} = \sin x$.

- Show that the system is reversible.
- Find and classify all the fixed points.
- Show that the lines $y = \pm x$ are invariant (any trajectory that starts on them stays on them forever).
- Sketch the phase portrait.

6.6.4 (Computer explorations) For each of the following reversible systems, try to sketch the phase portrait by hand. Then use a computer to check your sketch. If the computer reveals patterns you hadn't anticipated, try to explain them.

a) $\ddot{x} + (\dot{x})^2 + x = 3$ b) $\dot{x} = y - y^3$, $\dot{y} = x \cos y$ c) $\dot{x} = \sin y$, $\dot{y} = y^2 - x$

6.6.5 Consider equations of the form $\dot{x} + f(\dot{x}) + g(x) = 0$, where f is an even function, and both f and g are smooth.

- Show that the equation is invariant under the pure time-reversal symmetry $t \rightarrow -t$.
- Show that the equilibrium points cannot be stable nodes or spirals.

6.6.6 (Manta ray) Use qualitative arguments to deduce the “manta ray” phase portrait of Example 6.6.1.

- Plot the nullclines $\dot{x} = 0$ and $\dot{y} = 0$.
- Find the sign of \dot{x} , \dot{y} in different regions of the plane.
- Calculate the eigenvalues and eigenvectors of the saddle points at $(-1, \pm 1)$.
- Consider the unstable manifold of $(-1, -1)$. By making an argument about the signs of \dot{x} , \dot{y} , prove that this unstable manifold intersects the negative x -axis. Then use reversibility to prove the existence of a heteroclinic trajectory connecting $(-1, -1)$ to $(-1, 1)$.
- Using similar arguments, prove that another heteroclinic trajectory exists, and sketch several other trajectories to fill in the phase portrait.

6.6.7 (Oscillator with both positive and negative damping) Show that the system $\ddot{x} + x\dot{x} + x = 0$ is reversible and plot the phase portrait.

6.6.8 (Reversible system on a cylinder) While studying chaotic streamlines inside a drop immersed in a steady Stokes flow, Stone et al. (1991) encountered the system

$$\dot{x} = \frac{\sqrt{2}}{4} x(x-1)\sin\phi, \quad \dot{\phi} = \frac{1}{2} \left[\beta - \frac{1}{\sqrt{2}} \cos\phi - \frac{1}{8\sqrt{2}} x \cos\phi \right]$$

where $0 \leq x \leq 1$ and $-\pi \leq \phi < \pi$.

Since the system is 2π -periodic in ϕ , it may be considered as a vector field on a *cylinder*. (See Section 6.7 for another vector field on a cylinder.) The x -axis runs along the cylinder, and the ϕ -axis wraps around it. Note that the cylindrical phase space is finite, with edges given by the circles $x=0$ and $x=1$.

- a) Show that the system is reversible.
- b) Verify that for $\frac{9}{8\sqrt{2}} > \beta > \frac{1}{\sqrt{2}}$, the system has three fixed points on the cylinder, one of which is a saddle. Show that this saddle is connected to itself by a homoclinic orbit that winds around the waist of the cylinder. Using reversibility, prove that there is a *band of closed orbits* sandwiched between the circle $x=0$ and the homoclinic orbit. Sketch the phase portrait on the cylinder, and check your results by numerical integration.
- c) Show that as $\beta \rightarrow \frac{1}{\sqrt{2}}$ from above, the saddle point moves toward the circle $x=0$, and the homoclinic orbit tightens like a noose. Show that all the closed orbits disappear when $\beta = \frac{1}{\sqrt{2}}$.
- d) For $0 < \beta < \frac{1}{\sqrt{2}}$, show that there are two saddle points on the edge $x=0$. Plot the phase portrait on the cylinder.

6.6.9 (Josephson junction array) As discussed in Exercises 4.6.4 and 4.6.5, the equations

$$\frac{d\phi_k}{d\tau} = \Omega + a \sin \phi_k + \frac{1}{N} \sum_{j=1}^N \sin \phi_j, \text{ for } k = 1, 2,$$

arise as the dimensionless circuit equations for a resistively loaded array of Josephson junctions.

- a) Let $\theta_k = \phi_k - \frac{\pi}{2}$, and show that the resulting system for θ_k is reversible.
- b) Show that there are four fixed points (mod 2π) when $|\Omega/(a+1)| < 1$, and none when $|\Omega/(a+1)| > 1$.
- c) Using the computer, explore the various phase portraits that occur for $a=1$, as Ω varies over the interval $0 \leq \Omega \leq 3$.

For more about this system, see Tsang et al. (1991).

6.6.10 Is the origin a nonlinear center for the system $\dot{x} = -y - x^2$, $\dot{y} = x$?

6.6.11 (Rotational dynamics and a phase portrait on a sphere) The rotational dynamics of an object in a shear flow are governed by

$$\dot{\theta} = \cot \phi \cos \theta, \quad \dot{\phi} = (\cos^2 \phi + A \sin^2 \phi) \sin \theta,$$

where θ and ϕ are spherical coordinates that describe the orientation of the object. Our convention here is that $-\pi < \theta \leq \pi$ is the “longitude,” i.e., the angle around the z -axis, and $-\frac{\pi}{2} \leq \phi \leq \frac{\pi}{2}$ is the “latitude,” i.e., the angle measured northward from the equator. The parameter A depends on the shape of the object.

- a) Show that the equations are reversible in two ways: under $t \rightarrow -t$, $\theta \rightarrow -\theta$ and under $t \rightarrow -t$, $\phi \rightarrow -\phi$.
- b) Investigate the phase portraits when A is positive, zero, and negative. You may sketch the phase portraits as Mercator projections (treating θ and ϕ as rectangular coordinates), but it’s better to visualize the motion on the sphere, if you can.
- c) Relate your results to the tumbling motion of an object in a shear flow. What happens to the orientation of the object as $t \rightarrow \infty$?

6.7 Pendulum

6.7.1 (Damped pendulum) Find and classify the fixed points of $\ddot{\theta} + b\dot{\theta} + \sin \theta = 0$ for all $b > 0$, and plot the phase portraits for the qualitatively different cases.

6.7.2 (Pendulum driven by constant torque) The equation $\ddot{\theta} + \sin \theta = \gamma$ describes the dynamics of an undamped pendulum driven by a constant torque, or an undamped Josephson junction driven by a constant bias current.

- a) Find all the equilibrium points and classify them as γ varies.
- b) Sketch the nullclines and the vector field.
- c) Is the system conservative? If so, find a conserved quantity. Is the system reversible?
- d) Sketch the phase portrait on the plane as γ varies.
- e) Find the approximate frequency of small oscillations about any centers in the phase portrait.

6.7.3 (Nonlinear damping) Analyze $\ddot{\theta} + (1 + a \cos \theta)\dot{\theta} + \sin \theta = 0$, for all $a \geq 0$.

6.7.4 (Period of the pendulum) Suppose a pendulum governed by $\ddot{\theta} + \sin \theta = 0$ is swinging with an amplitude α . Using some tricky manipulations, we are going to derive a formula for $T(\alpha)$, the period of the pendulum.

- a) Using conservation of energy, show that $\dot{\theta}^2 = 2(\cos \theta - \cos \alpha)$ and hence that

$$T = 4 \int_{\theta_0}^{\alpha} \frac{d\theta}{[2(\cos \theta - \cos \alpha)]^{1/2}}.$$

- b) Using the half-angle formula, show that $T = 4 \int_0^{\alpha} \frac{d\theta}{[4(\sin^2 \frac{1}{2}\alpha - \sin^2 \frac{1}{2}\theta)]^{1/2}}$.
- c) The formulas in parts (a) and (b) have the disadvantage that α appears in both the integrand and the upper limit of integration. To remove the α -dependence

from the limits of integration, we introduce a new angle ϕ that runs from 0 to $\frac{\pi}{2}$ when θ runs from 0 to α . Specifically, let $(\sin \frac{1}{2}\alpha) \sin \phi = \sin \frac{1}{2}\theta$. Using this substitution, rewrite (b) as an integral with respect to ϕ . Thereby derive the exact result

$$T = 4 \int_0^{\pi/2} \frac{d\phi}{\cos \frac{1}{2}\theta} = 4K(\sin^2 \frac{1}{2}\alpha),$$

where the *complete elliptic integral of the first kind* is defined as

$$K(m) = \int_0^{\pi/2} \frac{d\phi}{(1 - m \sin^2 \phi)^{1/2}}, \text{ for } 0 \leq m < 1.$$

d) By expanding the elliptic integral using the binomial series and integrating term-by-term, show that

$$T(\alpha) = 2\pi \left[1 + \frac{1}{16} \alpha^2 + O(\alpha^4) \right] \text{ for } \alpha \ll 1.$$

Note that larger swings take longer.

6.7.5 (Numerical solution for the period) Redo Exercise 6.7.4 using either numerical integration of the differential equation, or numerical evaluation of the elliptic integral. Specifically, compute the period $T(\alpha)$, where α runs from 0 to 180° in steps of 10° .

6.8 Index Theory

6.8.1 Show that each of the following fixed points has an index equal to +1.

- a) stable spiral b) unstable spiral c) center d) star e) degenerate node

(Unusual fixed points) For each of the following systems, locate the fixed points and calculate the index. (Hint: Draw a small closed curve C around the fixed point and examine the variation of the vector field on C .)

6.8.2 $\dot{x} = x^2, \dot{y} = y$

6.8.3 $\dot{x} = y - x, \dot{y} = x^2$

6.8.4 $\dot{x} = y^3, \dot{y} = x$

6.8.5 $\dot{x} = xy, \dot{y} = x + y$

6.8.6 A closed orbit in the phase plane encircles S saddles, N nodes, F spirals, and C centers, all of the usual type. Show that $N + F + C = 1 + S$.

6.8.7 (Ruling out closed orbits) Use index theory to show that the system $\dot{x} = x(4 - y - x^2), \dot{y} = y(x - 1)$ has no closed orbits.

6.8.8 A smooth vector field on the phase plane is known to have exactly three closed orbits. Two of the cycles, say C_1 and C_2 , lie inside the third cycle C_3 . However, C_1 does not lie inside C_2 , nor vice-versa.

- a) Sketch the arrangement of the three cycles.

- b) Show that there must be at least one fixed point in the region bounded by C_1 , C_2 , C_3 .

6.8.9 A smooth vector field on the phase plane is known to have exactly two closed trajectories, one of which lies inside the other. The inner cycle runs clockwise, and the outer one runs counterclockwise. True or False: There must be at least one fixed point in the region between the cycles. If true, prove it. If false, provide a simple counterexample.

6.8.10 (Open-ended question for the topologically minded) Does Theorem 6.8.2 hold for surfaces other than the plane? Check its validity for various types of closed orbits on a torus, cylinder, and sphere.

6.8.11 (Complex vector fields) Let $z = x + iy$. Explore the complex vector fields $\dot{z} = z^k$ and $\dot{z} = (\bar{z})^k$, where $k > 0$ is an integer and $\bar{z} = x - iy$ is the complex conjugate of z .

- Write the vector fields in both Cartesian and polar coordinates, for the cases $k = 1, 2, 3$.
- Show that the origin is the only fixed point, and compute its index.
- Generalize your results to arbitrary integer $k > 0$.

6.8.12 (“Matter and antimatter”) There’s an intriguing analogy between bifurcations of fixed points and collisions of particles and anti-particles. Let’s explore this in the context of index theory. For example, a two-dimensional version of the saddle-node bifurcation is given by $\dot{x} = a + x^2$, $\dot{y} = -y$, where a is a parameter.

- Find and classify all the fixed points as a varies from $-\infty$ to $+\infty$.
- Show that the sum of the indices of all the fixed points is conserved as a varies.
- State and prove a generalization of this result, for systems of the form $\dot{\mathbf{x}} = \mathbf{f}(\mathbf{x}, \alpha)$, where $\mathbf{x} \in \mathbb{R}^2$ and α is a parameter.

6.8.13 (Integral formula for the index of a curve) Consider a smooth vector field $\dot{x} = f(x, y)$, $\dot{y} = g(x, y)$ on the plane, and let C be a simple closed curve that does not pass through any fixed points. As usual, let $\phi = \tan^{-1}(\dot{y}/\dot{x})$ as in Figure 6.8.1.

- Show that $d\phi = (f dg - g df)/(f^2 + g^2)$.
- Derive the integral formula

$$I_C = \frac{1}{2\pi} \oint_C \frac{f dg - g df}{f^2 + g^2}.$$

6.8.14 Consider the family of linear systems $\dot{x} = x \cos \alpha - y \sin \alpha$, $\dot{y} = x \sin \alpha + y \cos \alpha$, where α is a parameter that runs over the range $0 \leq \alpha \leq \pi$. Let C be a simple closed curve that does not pass through the origin.

- a) Classify the fixed point at the origin as a function of α .
- b) Using the integral derived in Exercise 6.8.13, show that I_C is *independent* of α .
- c) Let C be a circle centered at the origin. Compute I_C explicitly by evaluating the integral for any convenient choice of α .

7

LIMIT CYCLES

7.0 Introduction

A *limit cycle* is an isolated closed trajectory. *Isolated* means that neighboring trajectories are not closed; they spiral either toward or away from the limit cycle (Figure 7.0.1).

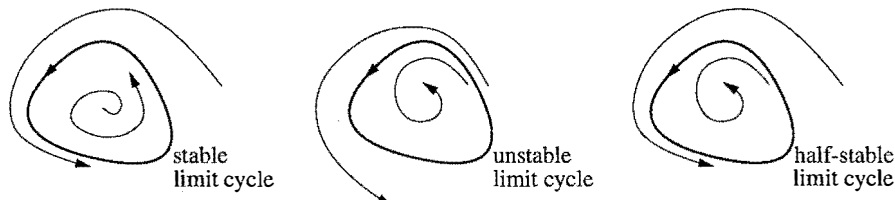


Figure 7.0.1

If all neighboring trajectories approach the limit cycle, we say the limit cycle is *stable* or *attracting*. Otherwise the limit cycle is *unstable*, or in exceptional cases, *half-stable*.

Stable limit cycles are very important scientifically—they model systems that exhibit self-sustained oscillations. In other words, these systems oscillate even in the absence of external periodic forcing. Of the countless examples that could be given, we mention only a few: the beating of a heart; the periodic firing of a pacemaker neuron; daily rhythms in human body temperature and hormone secretion; chemical reactions that oscillate spontaneously; and dangerous self-excited vibrations in bridges and airplane wings. In each case, there is a standard oscillation of some preferred period, waveform, and amplitude. If the system is perturbed slightly, it always returns to the standard cycle.

Limit cycles are inherently nonlinear phenomena; they can't occur in linear sys-

tems. Of course, a linear system $\dot{\mathbf{x}} = A\mathbf{x}$ can have closed orbits, but they won't be *isolated*; if $\mathbf{x}(t)$ is a periodic solution, then so is $c\mathbf{x}(t)$ for any constant $c \neq 0$. Hence $\mathbf{x}(t)$ is surrounded by a one-parameter family of closed orbits (Figure 7.0.2).

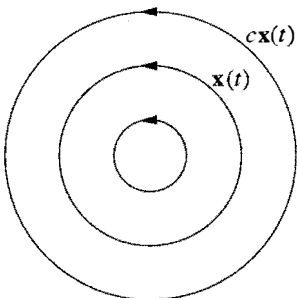


Figure 7.0.2

Consequently, the amplitude of a linear oscillation is set entirely by its initial conditions; any slight disturbance to the amplitude will persist forever. In contrast, limit cycle oscillations are determined by the structure of the system itself.

The next section presents two examples of systems with limit cycles. In the first case, the limit cycle is obvious by inspection, but normally it's difficult to tell whether a given system has a limit cycle, or indeed any closed orbits, from the governing equations alone. Sections 7.2–7.4 present some techniques for ruling out closed orbits or for

proving their existence. The remainder of the chapter discusses analytical methods for approximating the shape and period of a closed orbit and for studying its stability.

7.1 Examples

It's straightforward to construct examples of limit cycles if we use polar coordinates.

EXAMPLE 7.1.1: A SIMPLE LIMIT CYCLE

Consider the system

$$\dot{r} = r(1 - r^2), \quad \dot{\theta} = 1 \quad (1)$$

where $r \geq 0$. The radial and angular dynamics are uncoupled and so can be analyzed separately. Treating $\dot{r} = r(1 - r^2)$ as a vector field on the line, we see that $r^* = 0$ is an unstable fixed point and $r^* = 1$ is stable (Figure 7.1.1).

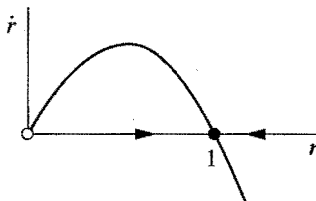


Figure 7.1.1

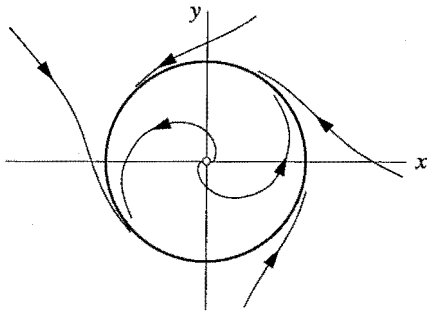


Figure 7.1.2

Hence, back in the phase plane, all trajectories (except $r^* = 0$) approach the unit circle $r^* = 1$ monotonically. Since the motion in the θ -direction is simply rotation at constant angular velocity, we see that all trajectories spiral asymptotically toward a limit cycle at $r = 1$ (Figure 7.1.2).

It is also instructive to plot solutions as functions of t . For instance, in Figure 7.1.3 we plot $x(t) = r(t) \cos \theta(t)$ for a trajectory starting outside the limit cycle.

As expected, the solution settles down to a sinusoidal oscillation of constant amplitude, corresponding to the limit cycle solution $x(t) = \cos(t + \theta_0)$ of (1). ■

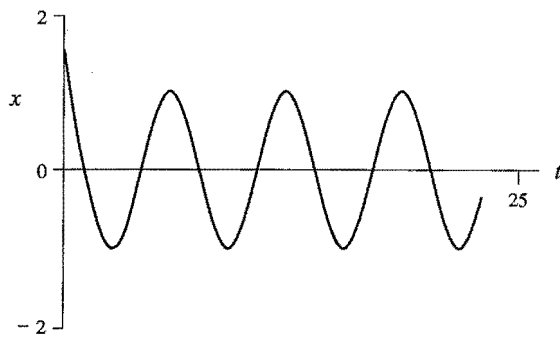


Figure 7.1.3

EXAMPLE 7.1.2: VAN DER POL OSCILLATOR

A less transparent example, but one that played a central role in the development of nonlinear dynamics, is given by the *van der Pol equation*

$$\ddot{x} + \mu(x^2 - 1)\dot{x} + x = 0 \quad (2)$$

where $\mu \geq 0$ is a parameter. Historically, this equation arose in connection with the nonlinear electrical circuits used in the first radios (see Exercise 7.1.6 for the circuit). Equation (2) looks like a simple harmonic oscillator, but with a **nonlinear damping** term $\mu(x^2 - 1)\dot{x}$. This term acts like ordinary positive damping for $|x| > 1$, but like *negative damping* for $|x| < 1$. In other words, it causes large-amplitude oscillations to decay, but it pumps them back up if they become too small.

As you might guess, the system eventually settles into a self-sustained oscillation where the energy dissipated over one cycle balances the energy pumped in. This idea can be made rigorous, and with quite a bit of work, one can prove that *the van der Pol equation has a unique, stable limit cycle for each $\mu > 0$* . This result follows from a more general theorem discussed in Section 7.4.

To give a concrete illustration, suppose we numerically integrate (2) for $\mu = 1.5$, starting from $(x, \dot{x}) = (0.5, 0)$ at $t = 0$. Figure 7.1.4 plots the solution in the phase plane and Figure 7.1.5 shows the graph of $x(t)$. Now, in contrast to Example 7.1.1, the limit cycle is not a circle and the stable waveform is not a sine wave. ■

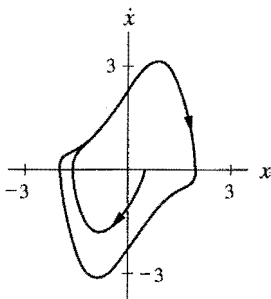


Figure 7.1.4

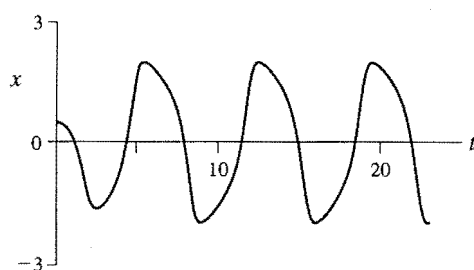


Figure 7.1.5

7.2 Ruling Out Closed Orbits

Suppose we have a strong suspicion, based on numerical evidence or otherwise, that a particular system has no periodic solutions. How could we prove this? In the last chapter we mentioned one method, based on index theory (see Examples 6.8.5 and 6.8.6). Now we present three other ways of ruling out closed orbits. They are of limited applicability, but they're worth knowing about, in case you get lucky.

Gradient Systems

Suppose the system can be written in the form $\dot{\mathbf{x}} = -\nabla V$, for some continuously differentiable, single-valued scalar function $V(\mathbf{x})$. Such a system is called a **gradient system** with **potential function** V .

Theorem 7.2.1: Closed orbits are impossible in gradient systems.

Proof: Suppose there were a closed orbit. We obtain a contradiction by considering the change in V after one circuit. On the one hand, $\Delta V = 0$ since V is single-valued. But on the other hand,

$$\begin{aligned}\Delta V &= \int_0^T \frac{dV}{dt} dt \\ &= \int_0^T (\nabla V \cdot \dot{\mathbf{x}}) dt \\ &= - \int_0^T \|\dot{\mathbf{x}}\|^2 dt \\ &< 0\end{aligned}$$

(unless $\dot{\mathbf{x}} \equiv \mathbf{0}$, in which case the trajectory is a fixed point, not a closed orbit). This contradiction shows that closed orbits can't exist in gradient systems. ■

The trouble with Theorem 7.2.1 is that most two-dimensional systems are *not* gradient systems. (Although, curiously, all vector fields *on the line* are gradient systems; this gives another explanation for the absence of oscillations noted in Sections 2.6 and 2.7.)

EXAMPLE 7.2.1:

Show that there are no closed orbits for the system $\dot{x} = \sin y$, $\dot{y} = x \cos y$.

Solution: The system is a gradient system with potential function $V(x, y) = -x \sin y$, since $\dot{x} = -\partial V / \partial x$ and $\dot{y} = -\partial V / \partial y$. By Theorem 7.2.1, there are no closed orbits. ■

How can you tell whether a system is a gradient system? And if it is, how do you find its potential function V ? See Exercises 7.2.5 and 7.2.6.

Even if the system is not a gradient system, similar techniques may still work, as in the following example. We examine the change in an energy-like function after one circuit around the putative closed orbit, and derive a contradiction.

EXAMPLE 7.2.2:

Show that the nonlinearly damped oscillator $\ddot{x} + (\dot{x})^3 + x = 0$ has no periodic solutions.

Solution: Suppose that there were a periodic solution $x(t)$ of period T . Consider the energy function $E(x, \dot{x}) = \frac{1}{2}(x^2 + \dot{x}^2)$. After one cycle, x and \dot{x} return to their starting values, and therefore $\Delta E = 0$ around any closed orbit.

On the other hand, $\Delta E = \int_0^T \dot{E} dt$. If we can show this integral is nonzero, we've reached a contradiction. Note that $\dot{E} = \dot{x}(x + \ddot{x}) = \dot{x}(-\dot{x}^3) = -\dot{x}^4 \leq 0$. Therefore $\Delta E = - \int_0^T (\dot{x})^4 dt \leq 0$, with equality only if $\dot{x} \equiv 0$. But $\dot{x} \equiv 0$ would mean the trajectory is a fixed point, contrary to the original assumption that it's a closed orbit. Thus ΔE is strictly negative, which contradicts $\Delta E = 0$. Hence there are no periodic solutions. ■

Liapunov Functions

Even for systems that have nothing to do with mechanics, it is occasionally possible to construct an energy-like function that decreases along trajectories. Such a function is called a Liapunov function. If a Liapunov function exists, then closed orbits are forbidden, by the same reasoning as in Example 7.2.2.

To be more precise, consider a system $\dot{\mathbf{x}} = \mathbf{f}(\mathbf{x})$ with a fixed point at \mathbf{x}^* . Suppose that we can find a **Liapunov function**, i.e., a continuously differentiable, real-valued function $V(\mathbf{x})$ with the following properties:

1. $V(\mathbf{x}) > 0$ for all $\mathbf{x} \neq \mathbf{x}^*$, and $V(\mathbf{x}^*) = 0$. (We say that V is *positive definite*.)
2. $\dot{V} < 0$ for all $\mathbf{x} \neq \mathbf{x}^*$. (All trajectories flow “downhill” toward \mathbf{x}^* .)

Then \mathbf{x}^* is globally asymptotically stable: for all initial conditions, $\mathbf{x}(t) \rightarrow \mathbf{x}^*$ as $t \rightarrow \infty$. In particular the system has no closed orbits. (For a proof, see Jordan and Smith 1987.)

The intuition is that all trajectories move monotonically down the graph of $V(\mathbf{x})$ toward \mathbf{x}^* (Figure 7.2.1).

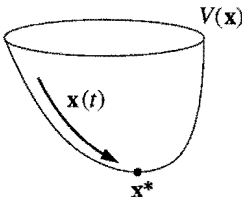


Figure 7.2.1

The solutions can't get stuck anywhere else because if they did, V would stop changing, but by assumption, $\dot{V} < 0$ everywhere except at \mathbf{x}^* .

Unfortunately, there is no systematic way to construct Liapunov functions. Divine inspiration is usually required, although sometimes one can work backwards. Sums of squares occasionally work, as in the following example.

EXAMPLE 7.2.3:

By constructing a Liapunov function, show that the system $\dot{x} = -x + 4y$, $\dot{y} = -x - y^3$ has no closed orbits.

Solution: Consider $V(x, y) = x^2 + ay^2$, where a is a parameter to be chosen later. Then $\dot{V} = 2x\dot{x} + 2ay\dot{y} = 2x(-x + 4y) + 2ay(-x - y^3) = -2x^2 + (8 - 2a)xy - 2ay^4$. If we choose $a = 4$, the xy term disappears and $\dot{V} = -2x^2 - 8y^4$. By inspection, $V > 0$ and $\dot{V} < 0$ for all $(x, y) \neq (0, 0)$. Hence $V = x^2 + 4y^2$ is a Liapunov

function and so there are no closed orbits. In fact, all trajectories approach the origin as $t \rightarrow \infty$. ■

Dulac's Criterion

The third method for ruling out closed orbits is based on Green's theorem, and is known as Dulac's criterion.

Dulac's Criterion: Let $\dot{\mathbf{x}} = \mathbf{f}(\mathbf{x})$ be a continuously differentiable vector field defined on a simply connected subset R of the plane. If there exists a continuously differentiable, real-valued function $g(\mathbf{x})$ such that $\nabla \cdot (g\dot{\mathbf{x}})$ has one sign throughout R , then there are no closed orbits lying entirely in R .

Proof: Suppose there were a closed orbit C lying entirely in the region R . Let A denote the region inside C (Figure 7.2.2). Then Green's theorem yields

$$\iint_A \nabla \cdot (g\dot{\mathbf{x}}) dA = \oint_C g\dot{\mathbf{x}} \cdot \mathbf{n} d\ell$$

where \mathbf{n} is the outward normal and $d\ell$ is the element of arc length along C . Look first at the double integral on the left: it must be *nonzero*, since $\nabla \cdot (g\dot{\mathbf{x}})$ has one sign in R . On the other hand, the line integral on the right equals *zero* since $\dot{\mathbf{x}} \cdot \mathbf{n} = 0$ everywhere, by the assumption that C is a trajectory (the tangent vector $\dot{\mathbf{x}}$ is orthogonal to \mathbf{n}). This contradiction implies that no such C can exist. ■

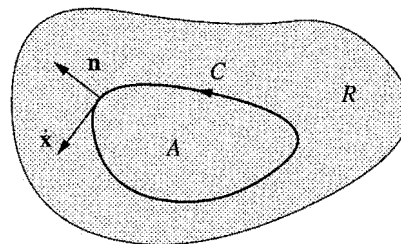


Figure 7.2.2

Dulac's criterion suffers from the same drawback as Liapunov's method: there is no algorithm for finding $g(\mathbf{x})$. Candidates that occasionally work are $g=1$, $1/x^a y^b$, e^{ax} , and e^{ay} .

EXAMPLE 7.2.4:

Show that the system $\dot{x} = x(2 - x - y)$, $\dot{y} = y(4x - x^2 - 3)$ has no closed orbits in the positive quadrant $x, y > 0$.

Solution: A hunch tells us to pick $g = 1/xy$. Then

$$\begin{aligned}\nabla \cdot (g\dot{\mathbf{x}}) &= \frac{\partial}{\partial x}(g\dot{x}) + \frac{\partial}{\partial y}(g\dot{y}) \\ &= \frac{\partial}{\partial x}\left(\frac{2-x-y}{y}\right) + \frac{\partial}{\partial y}\left(\frac{4x-x^2-3}{x}\right) \\ &= -1/y \\ &< 0.\end{aligned}$$

Since the region $x, y > 0$ is simply connected and g and \mathbf{f} satisfy the required smoothness conditions, Dulac's criterion implies there are no closed orbits in the positive quadrant. ■

EXAMPLE 7.2.5:

Show that the system $\dot{x} = y$, $\dot{y} = -x - y + x^2 + y^2$ has no closed orbits.

Solution: Let $g = e^{-2x}$. Then $\nabla \cdot (g\dot{\mathbf{x}}) = -2e^{-2x}y + e^{-2x}(-1+2y) = -e^{-2x} < 0$. By Dulac's criterion, there are no closed orbits. ■

7.3 Poincaré–Bendixson Theorem

Now that we know how to rule out closed orbits, we turn to the opposite task: finding methods to *establish that closed orbits exist* in particular systems. The following theorem is one of the few results in this direction. It is also one of the key theoretical results in nonlinear dynamics, because it implies that chaos can't occur in the phase plane, as discussed briefly at the end of this section.

Poincaré–Bendixson Theorem: Suppose that:

- (1) R is a closed, bounded subset of the plane;
- (2) $\dot{\mathbf{x}} = \mathbf{f}(\mathbf{x})$ is a continuously differentiable vector field on an open set containing R ;
- (3) R does not contain any fixed points; and
- (4) There exists a trajectory C that is “confined” in R , in the sense that it starts in R and stays in R for all future time (Figure 7.3.1).

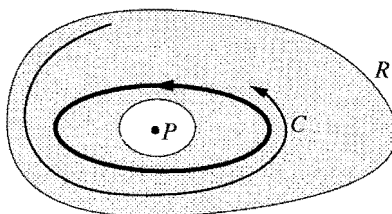


Figure 7.3.1

The proof of this theorem is subtle, and requires some advanced ideas from topol-

ogy. For details, see Perko (1991), Coddington and Levinson (1955), Hurewicz (1958), or Cesari (1963).

In Figure 7.3.1, we have drawn R as a ring-shaped region because any closed orbit must encircle a fixed point (P in Figure 7.3.1) and no fixed points are allowed in R .

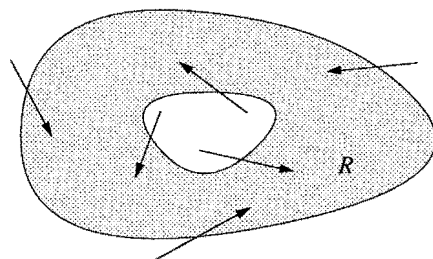


Figure 7.3.2

When applying the Poincaré–Bendixson theorem, it's easy to satisfy conditions (1)–(3); condition (4) is the tough one. How can we be sure that a confined trajectory C exists? The standard trick is to construct a **trapping region** R , i.e., a closed connected set such that the vector field points “inward” everywhere on the boundary of R (Figure 7.3.2). Then *all* trajectories in R are confined. If we can also arrange that there are no fixed points in R , then the Poincaré–Bendixson theorem ensures that R contains a closed orbit.

The Poincaré–Bendixson theorem can be difficult to apply in practice. One convenient case occurs when the system has a simple representation in polar coordinates, as in the following example.

EXAMPLE 7.3.1:

Consider the system

$$\begin{aligned}\dot{r} &= r(1 - r^2) + \mu r \cos \theta \\ \dot{\theta} &= 1.\end{aligned}\tag{1}$$

When $\mu = 0$, there's a stable limit cycle at $r = 1$, as discussed in Example 7.1.1. Show that a closed orbit still exists for $\mu > 0$, as long as μ is sufficiently small.

Solution: We seek two concentric circles with radii r_{\min} and r_{\max} , such that $\dot{r} < 0$ on the outer circle and $\dot{r} > 0$ on the inner circle. Then the annulus $0 < r_{\min} \leq r \leq r_{\max}$ will be our desired trapping region. Note that there are no fixed points in the annulus since $\dot{\theta} > 0$; hence if r_{\min} and r_{\max} can be found, the Poincaré–Bendixson theorem will imply the existence of a closed orbit.

To find r_{\min} , we require $\dot{r} = r(1 - r^2) + \mu r \cos \theta > 0$ for all θ . Since $\cos \theta \geq -1$, a sufficient condition for r_{\min} is $1 - r^2 - \mu > 0$. Hence any $r_{\min} < \sqrt{1 - \mu}$ will work, as long as $\mu < 1$ so that the square root makes sense. We should choose r_{\min} as large as possible, to hem in the limit cycle as tightly as we can. For instance, we could pick $r_{\min} = 0.999\sqrt{1 - \mu}$. (Even $r_{\min} = \sqrt{1 - \mu}$ works, but more careful rea-

soning is required.) By a similar argument, the flow is inward on the outer circle if $r_{\max} = 1.001\sqrt{1+\mu}$.

Therefore a closed orbit exists for all $\mu < 1$, and it lies somewhere in the annulus $0.999\sqrt{1-\mu} < r < 1.001\sqrt{1+\mu}$. ■

The estimates used in Example 7.3.1 are conservative. In fact, the closed orbit can exist even if $\mu \geq 1$. Figure 7.3.3 shows a computer-generated phase portrait of (1) for $\mu = 1$. In Exercise 7.3.8, you're asked to explore what happens for larger μ , and in particular, whether there's a critical μ beyond which the closed orbit disappears. It's also possible to obtain some analytical insight about the closed orbit for small μ (Exercise 7.3.9).

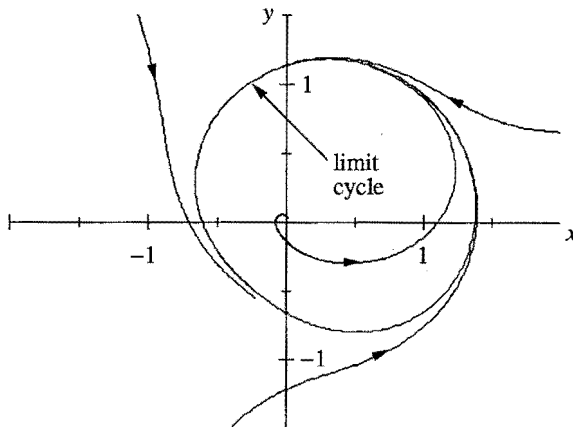


Figure 7.3.3

When polar coordinates are inconvenient, we may still be able to find an appropriate trapping region by examining the system's nullclines, as in the next example.

EXAMPLE 7.3.2:

In the fundamental biochemical process called *glycolysis*, living cells obtain energy by breaking down sugar. In intact yeast cells as well as in yeast or muscle extracts, glycolysis can proceed in an *oscillatory* fashion, with the concentrations of various intermediates waxing and waning with a period of several minutes. For reviews, see Chance et al. (1973) or Goldbeter (1980).

A simple model of these oscillations has been proposed by Sel'kov (1968). In dimensionless form, the equations are

$$\begin{aligned}\dot{x} &= -x + ay + x^2y \\ \dot{y} &= b - ay - x^2y\end{aligned}$$

where x and y are the concentrations of ADP (adenosine diphosphate) and F6P (fructose-6-phosphate), and $a, b > 0$ are kinetic parameters. Construct a trapping region for this system.

Solution: First we find the nullclines. The first equation shows that $\dot{x} = 0$ on the curve $y = x/(a + x^2)$ and the second equation shows that $\dot{y} = 0$ on the curve $y = b/(a + x^2)$. These nullclines are sketched in Figure 7.3.4, along with some representative vectors.

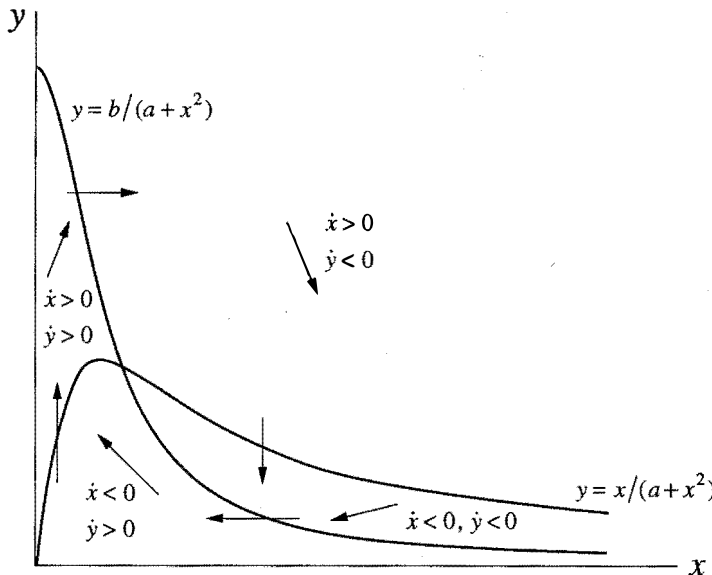


Figure 7.3.4

How did we know how to sketch these vectors? By definition, the arrows are vertical on the $\dot{x} = 0$ nullcline, and horizontal on the $\dot{y} = 0$ nullcline. The direction of flow is determined by the signs of \dot{x} and \dot{y} . For instance, in the region above both nullclines, the governing equations imply $\dot{x} > 0$ and $\dot{y} < 0$, so the arrows point down and to the right, as shown in Figure 7.3.4.

Now consider the region bounded by the dashed line shown in Figure 7.3.5. We claim that it's a trapping region. To verify this, we have to show that all the vectors on the boundary point into the box. On the horizontal and vertical sides, there's no problem: the claim follows from Figure 7.3.4. The tricky part of the construction is the diagonal line of slope -1 extending from the point $(b, b/a)$ to the nullcline $y = x/(a + x^2)$. Where did this come from?

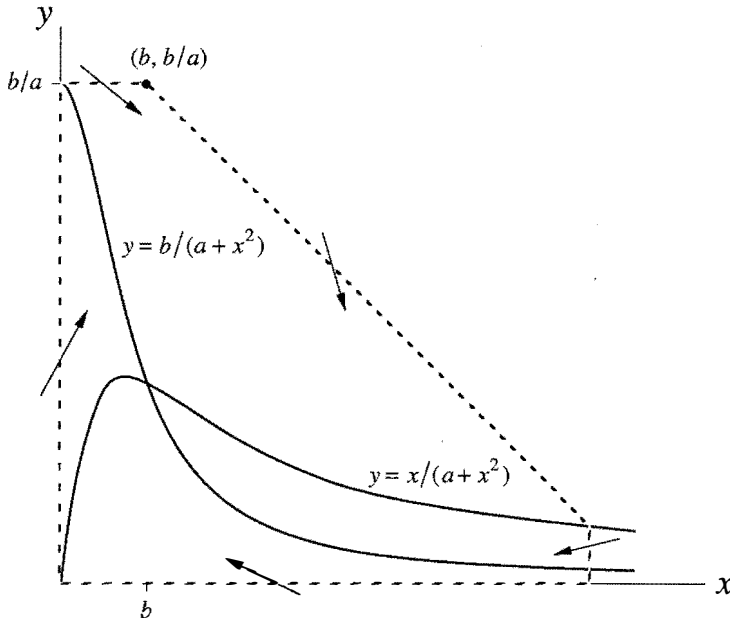


Figure 7.3.5

To get the right intuition, consider \dot{x} and \dot{y} in the limit of very large x . Then $\dot{x} \approx x^2 y$ and $\dot{y} \approx -x^2 y$, so $\dot{y}/\dot{x} = dy/dx \approx -1$ along trajectories. Hence the vector field at large x is roughly parallel to the diagonal line. This suggests that in a more precise calculation, we should compare the sizes of \dot{x} and $-\dot{y}$, for some sufficiently large x .

In particular, consider $\dot{x} - (-\dot{y})$. We find

$$\begin{aligned}\dot{x} - (-\dot{y}) &= -x + ay + x^2 y + (b - ay - x^2 y) \\ &= b - x.\end{aligned}$$

Hence

$$-\dot{y} > \dot{x} \text{ if } x > b.$$

This inequality implies that the vector field points inward on the diagonal line in Figure 7.3.5, because dy/dx is more negative than -1 , and therefore the vectors are steeper than the diagonal line. Thus the region is a trapping region, as claimed. ■

Can we conclude that there is a closed orbit inside the trapping region? No! There is a fixed point in the region (at the intersection of the nullclines), and so the conditions of the Poincaré–Bendixson theorem are not satisfied. But if this fixed point is a *repeller*, then we *can* prove the existence of a closed orbit by considering

the modified “punctured” region shown in Figure 7.3.6. (The hole is infinitesimal, but drawn larger for clarity.)

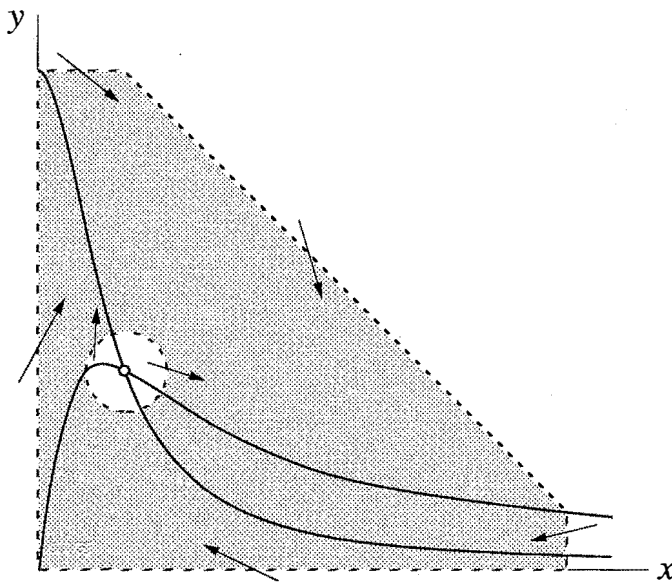


Figure 7.3.6

The repeller drives all neighboring trajectories into the shaded region, and since this region is free of fixed points, the Poincaré–Bendixson theorem applies.

Now we find conditions under which the fixed point is a repeller.

EXAMPLE 7.3.3:

Once again, consider the glycolytic oscillator $\dot{x} = -x + ay + x^2y$, $\dot{y} = b - ay - x^2y$ of Example 7.3.2. Prove that a closed orbit exists if a and b satisfy an appropriate condition, to be determined. (As before, $a, b > 0$.)

Solution: By the argument above, it suffices to find conditions under which the fixed point is a repeller, i.e., an unstable node or spiral. In general, the Jacobian is

$$A = \begin{pmatrix} -1 + 2xy & a + x^2 \\ -2xy & -(a + x^2) \end{pmatrix}.$$

After some algebra, we find that at the fixed point

$$x^* = b, \quad y^* = \frac{b}{a + b^2},$$

the Jacobian has determinant $\Delta = a + b^2 > 0$ and trace

$$\tau = - \frac{b^4 + (2a-1)b^2 + (a+a^2)}{a+b^2}.$$

Hence the fixed point is unstable for $\tau > 0$, and stable for $\tau < 0$. The dividing line $\tau = 0$ occurs when

$$b^2 = \frac{1}{2}(1 - 2a \pm \sqrt{1 - 8a}).$$

This defines a curve in (a, b) space, as shown in Figure 7.3.7.

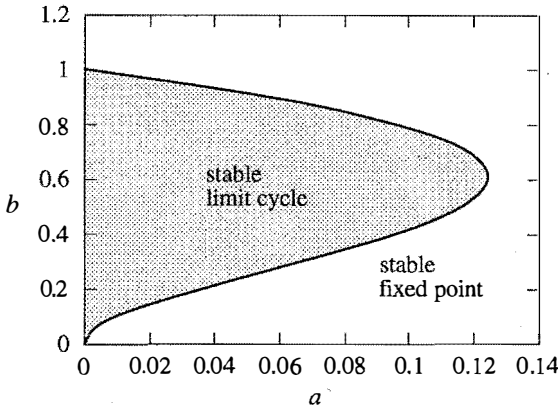


Figure 7.3.7

For parameters in the region corresponding to $\tau > 0$, we are guaranteed that the system has a closed orbit—numerical integration shows that it is actually a stable limit cycle. Figure 7.3.8 shows a computer-generated phase portrait for the typical case $a = 0.08$, $b = 0.6$. ■

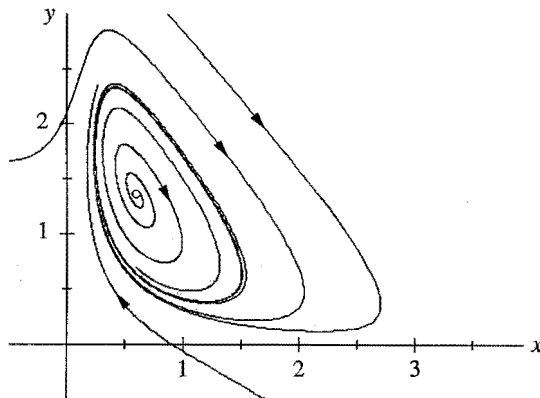


Figure 7.3.8

No Chaos in the Phase Plane

The Poincaré–Bendixson theorem is one of the central results of nonlinear dynamics. It says that the dynamical possibilities in the phase plane are very limited: if a trajectory is confined to a closed, bounded region that contains no fixed points, then the trajectory must eventually approach a closed orbit. Nothing more complicated is possible.

This result depends crucially on the two-dimensionality of the plane. In higher-dimensional systems ($n \geq 3$), the Poincaré–Bendixson theorem no longer applies, and something radically new can happen: trajectories may wander around forever in a bounded region without settling down to a fixed point or a closed orbit. In some cases, the trajectories are attracted to a complex geometric object called a *strange attractor*, a fractal set on which the motion is aperiodic and sensitive to tiny changes in the initial conditions. This sensitivity makes the motion unpredictable in the long run. We are now face to face with *chaos*. We'll discuss this fascinating topic soon enough, but for now you should appreciate that the Poincaré–Bendixson theorem implies that chaos can never occur in the phase plane.

7.4 Liénard Systems

In the early days of nonlinear dynamics, say from about 1920 to 1950, there was a great deal of research on nonlinear oscillations. The work was initially motivated by the development of radio and vacuum tube technology, and later it took on a mathematical life of its own. It was found that many oscillating circuits could be modeled by second-order differential equations of the form

$$\ddot{x} + f(x)\dot{x} + g(x) = 0, \quad (1)$$

now known as *Liénard's equation*. This equation is a generalization of the van der Pol oscillator $\ddot{x} + \mu(x^2 - 1)\dot{x} + x = 0$ mentioned in Section 7.1. It can also be interpreted mechanically as the equation of motion for a unit mass subject to a nonlinear damping force $-f(x)\dot{x}$ and a nonlinear restoring force $-g(x)$.

Liénard's equation is equivalent to the system

$$\begin{aligned}\dot{x} &= y \\ \dot{y} &= -g(x) - f(x)y.\end{aligned} \quad (2)$$

The following theorem states that this system has a unique, stable limit cycle under appropriate hypotheses on f and g . For a proof, see Jordan and Smith (1987), Grimshaw (1990), or Perko (1991).

Liénard's Theorem: Suppose that $f(x)$ and $g(x)$ satisfy the following conditions:

- (1) $f(x)$ and $g(x)$ are continuously differentiable for all x ;
- (2) $g(-x) = -g(x)$ for all x (i.e., $g(x)$ is an *odd* function);
- (3) $g(x) > 0$ for $x > 0$;
- (4) $f(-x) = f(x)$ for all x (i.e., $f(x)$ is an *even* function);
- (5) The odd function $F(x) = \int_0^x f(u) du$ has exactly one positive zero at $x = a$, is negative for $0 < x < a$, is positive and nondecreasing for $x > a$, and $F(x) \rightarrow \infty$ as $x \rightarrow \infty$.

Then the system (2) has a unique, stable limit cycle surrounding the origin in the phase plane.

This result should seem plausible. The assumptions on $g(x)$ mean that the restoring force acts like an ordinary spring, and tends to reduce any displacement, whereas the assumptions on $f(x)$ imply that the damping is negative at small $|x|$ and positive at large $|x|$. Since small oscillations are pumped up and large oscillations are damped down, it is not surprising that the system tends to settle into a self-sustained oscillation of some intermediate amplitude.

EXAMPLE 7.4.1:

Show that the van der Pol equation has a unique, stable limit cycle.

Solution: The van der Pol equation $\ddot{x} + \mu(x^2 - 1)\dot{x} + x = 0$ has $f(x) = \mu(x^2 - 1)$ and $g(x) = x$, so conditions (1)–(4) of Liénard's theorem are clearly satisfied. To check condition (5), notice that

$$F(x) = \mu\left(\frac{1}{3}x^3 - x\right) = \frac{1}{3}\mu x(x^2 - 3).$$

Hence condition (5) is satisfied for $a = \sqrt{3}$. Thus the van der Pol equation has a unique, stable limit cycle. ■

There are several other classical results about the existence of periodic solutions for Liénard's equation and its relatives. See Stoker (1950), Minorsky (1962), Andronov et al. (1973), and Jordan and Smith (1987).

7.5 Relaxation Oscillations

It's time to change gears. So far in this chapter, we have focused on a qualitative question: Given a particular two-dimensional system, does it have any periodic solutions? Now we ask a quantitative question: Given that a closed orbit exists, what can we say about its shape and period? In general, such problems can't be solved exactly, but we can still obtain useful approximations if some parameter is large or small.

We begin by considering the van der Pol equation

$$\ddot{x} + \mu(x^2 - 1)\dot{x} + x = 0$$

for $\mu \gg 1$. In this *strongly nonlinear* limit, we'll see that the limit cycle consists of an extremely slow buildup followed by a sudden discharge, followed by another slow buildup, and so on. Oscillations of this type are often called **relaxation oscillations**, because the “stress” accumulated during the slow buildup is “relaxed” during the sudden discharge. Relaxation oscillations occur in many other scientific contexts, from the stick-slip oscillations of a bowed violin string to the periodic firing of nerve cells driven by a constant current (Edelstein-Keshet 1988, Murray 1989, Rinzel and Ermentrout 1989).

EXAMPLE 7.5.1:

Give a phase plane analysis of the van der Pol equation for $\mu \gg 1$.

Solution: It proves convenient to introduce different phase plane variables from the usual “ $\dot{x} = y$, $\dot{y} = \dots$ ”. To motivate the new variables, notice that

$$\ddot{x} + \mu\dot{x}(x^2 - 1) = \frac{d}{dt}\left(\dot{x} + \mu\left[\frac{1}{3}x^3 - x\right]\right).$$

So if we let

$$F(x) = \frac{1}{3}x^3 - x, \quad w = \dot{x} + \mu F(x), \tag{1}$$

the van der Pol equation implies that

$$\dot{w} = \ddot{x} + \mu\dot{x}(x^2 - 1) = -x. \tag{2}$$

Hence the van der Pol equation is equivalent to (1), (2), which may be rewritten as

$$\begin{aligned} \dot{x} &= w - \mu F(x) \\ \dot{w} &= -x. \end{aligned} \tag{3}$$

One further change of variables is helpful. If we let

$$y = \frac{w}{\mu}$$

then (3) becomes

$$\begin{aligned} \dot{x} &= \mu[y - F(x)] \\ \dot{y} &= -\frac{1}{\mu}x. \end{aligned} \tag{4}$$

Now consider a typical trajectory in the (x, y) phase plane. The nullclines are the key to understanding the motion. We claim that all trajectories behave like that shown in Figure 7.5.1; starting from any point except the origin, the trajectory zaps horizontally onto the **cubic nullcline** $y = F(x)$. Then it crawls down the nullcline until it comes to the knee (point B in Figure 7.5.1), after which it zaps over to the other branch of the cubic at C. This is followed by another crawl along the cubic until it reaches the next jumping-off point at D, and the motion continues periodically after that.

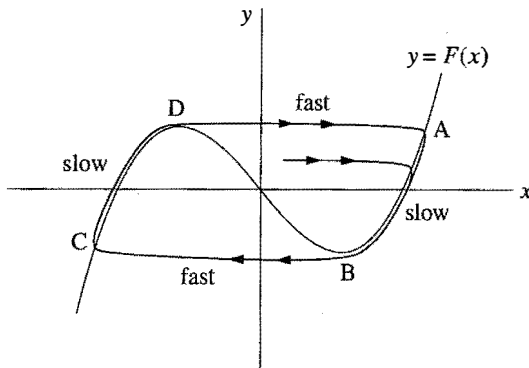


Figure 7.5.1

until the trajectory reaches the next jumping-off point at D, and the motion continues periodically after that.

To justify this picture, suppose that the initial condition is not too close to the cubic nullcline, i.e., suppose $y - F(x) \sim O(1)$. Then (4) implies $|\dot{x}| \sim O(\mu) \gg 1$ whereas $|\dot{y}| \sim O(\mu^{-1}) \ll 1$; hence the velocity is enormous in the horizontal direction and tiny in the vertical direction, so trajectories move practically horizontally. If the initial condition is *above* the nullcline, then $y - F(x) > 0$ and therefore $\dot{x} > 0$; thus the trajectory moves sideways *toward* the nullcline. However, once the trajectory gets so close that $y - F(x) \sim O(\mu^{-2})$, then \dot{x} and \dot{y} become comparable, both being $O(\mu^{-1})$. What happens then? The trajectory crosses the nullcline vertically, as shown in Figure 7.5.1, and then moves slowly along the backside of the branch, with a velocity of size $O(\mu^{-1})$, until it reaches the knee and can jump sideways again. ■

This analysis shows that the limit cycle has two **widely separated time scales**: the crawls require $\Delta t \sim O(\mu)$ and the jumps require $\Delta t \sim O(\mu^{-1})$. Both time scales are apparent in the waveform of $x(t)$ shown in Figure 7.5.2, obtained by numerical integration of the van der Pol equation for $\mu = 10$ and initial condition $(x_0, y_0) = (2, 0)$.

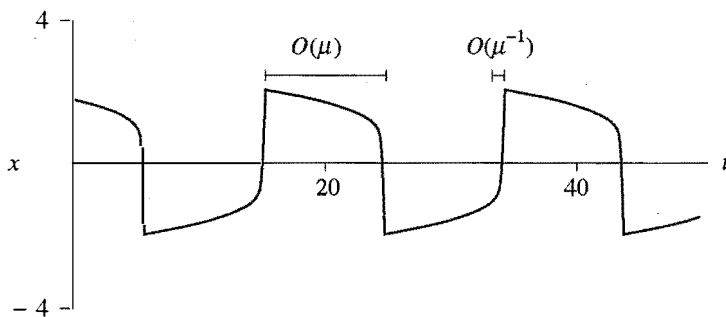


Figure 7.5.2

EXAMPLE 7.5.2:

Estimate the period of the limit cycle for the van der Pol equation for $\mu \gg 1$.

Solution: The period T is essentially the time required to travel along the two **slow branches**, since the time spent in the jumps is negligible for large μ .

By symmetry, the time spent on each branch is the same. Hence $T \approx 2 \int_{x_A}^{x_B} dt$. To derive an expression for dt , note that on the slow branches, $y \approx F(x)$ and thus

$$\frac{dy}{dt} \approx F'(x) \frac{dx}{dt} = (x^2 - 1) \frac{dx}{dt}.$$

But since $dy/dt = -x/\mu$ from (4), we find $dx/dt = -x/\mu(x^2 - 1)$. Therefore

$$dt \approx -\frac{\mu(x^2 - 1)}{x} dx \quad (5)$$

on a slow branch. As you can check (Exercise 7.5.1), the positive branch begins at $x_A = 2$ and ends at $x_B = 1$. Hence

$$T \approx 2 \int_2^1 \frac{-\mu}{x} (x^2 - 1) dx = 2\mu \left[\frac{x^2}{2} - \ln x \right]_1^2 = \mu [3 - 2 \ln 2], \quad (6)$$

which is $O(\mu)$ as expected. ■

The formula (6) can be refined. With much more work, one can show that $T \approx \mu [3 - 2 \ln 2] + 2\alpha\mu^{-1/3} + \dots$, where $\alpha \approx 2.338$ is the smallest root of $\text{Ai}(-\alpha) = 0$. Here $\text{Ai}(x)$ is a special function called the Airy function. This correction term comes from an estimate of the time required to turn the corner between

the jumps and the crawls. See Grimshaw (1990, pp. 161–163) for a readable derivation of this wonderful formula, discovered by Mary Cartwright (1952). See also Stoker (1950) for more about relaxation oscillations.

One last remark: We have seen that a relaxation oscillation has two time scales that operate *sequentially*—a slow buildup is followed by a fast discharge. In the next section we will encounter problems where two time scales operate *concurrently*, and that makes the problems a bit more subtle.

7.6 Weakly Nonlinear Oscillators

This section deals with equations of the form

$$\ddot{x} + x + \varepsilon h(x, \dot{x}) = 0 \quad (1)$$

where $0 \leq \varepsilon \ll 1$ and $h(x, \dot{x})$ is an arbitrary smooth function. Such equations represent small perturbations of the linear oscillator $\ddot{x} + x = 0$ and are therefore called **weakly nonlinear oscillators**. Two fundamental examples are the van der Pol equation

$$\ddot{x} + x + \varepsilon(x^2 - 1)\dot{x} = 0, \quad (2)$$

(now in the limit of small nonlinearity), and the **Duffing equation**

$$\ddot{x} + x + \varepsilon x^3 = 0. \quad (3)$$

To illustrate the kinds of phenomena that can arise, Figure 7.6.1 shows a computer-generated solution of the van der Pol equation in the (x, \dot{x}) phase plane, for $\varepsilon = 0.1$ and an initial condition close to the origin. The trajectory is a slowly winding spiral; it takes many cycles for the amplitude to grow substantially. Eventually

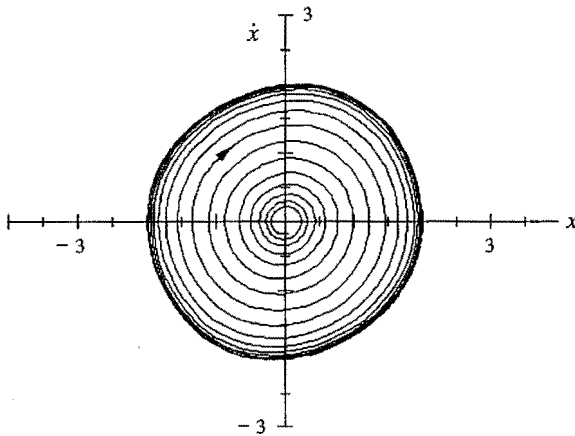


Figure 7.6.1

the trajectory asymptotes to an approximately circular limit cycle whose radius is close to 2.

We'd like to be able to predict the shape, period, and radius of this limit cycle. Our analysis will exploit the fact that the oscillator is "close to" a simple harmonic oscillator, which we understand completely.

Regular Perturbation Theory and Its Failure

As a first approach, we seek solutions of (1) in the form of a power series in ε . Thus if $x(t, \varepsilon)$ is a solution, we expand it as

$$x(t, \varepsilon) = x_0(t) + \varepsilon x_1(t) + \varepsilon^2 x_2(t) + \dots, \quad (4)$$

where the unknown functions $x_k(t)$ are to be determined from the governing equation and the initial conditions. The hope is that all the important information is captured by the first few terms—ideally, the first *two*—and that the higher-order terms represent only tiny corrections. This technique is called ***regular perturbation theory***. It works well on certain classes of problems (for instance, Exercise 7.3.9), but as we'll see, it runs into trouble here.

To expose the source of the difficulties, we begin with a practice problem that can be solved exactly. Consider the weakly damped linear oscillator

$$\ddot{x} + 2\varepsilon \dot{x} + x = 0, \quad (5)$$

with initial conditions

$$x(0) = 0, \quad \dot{x}(0) = 1. \quad (6)$$

Using the techniques of Chapter 5, we find the exact solution

$$x(t, \varepsilon) = (1 - \varepsilon^2)^{-1/2} e^{-\varepsilon t} \sin[(1 - \varepsilon^2)^{1/2} t]. \quad (7)$$

Now let's solve the same problem using perturbation theory. Substitution of (4) into (5) yields

$$\frac{d^2}{dt^2} (x_0 + \varepsilon x_1 + \dots) + 2\varepsilon \frac{d}{dt} (x_0 + \varepsilon x_1 + \dots) + (x_0 + \varepsilon x_1 + \dots) = 0. \quad (8)$$

If we group the terms according to powers of ε , we get

$$[\ddot{x}_0 + x_0] + \varepsilon [\ddot{x}_1 + 2\dot{x}_0 + x_1] + O(\varepsilon^2) = 0. \quad (9)$$

Since (9) is supposed to hold for *all* sufficiently small ε , the coefficients of each power of ε must vanish separately. Thus we find

$$O(1): \ddot{x}_0 + x_0 = 0 \quad (10)$$

$$O(\varepsilon): \ddot{x}_1 + 2\dot{x}_0 + x_1 = 0. \quad (11)$$

(We're ignoring the $O(\varepsilon^2)$ and higher equations, in the optimistic spirit mentioned earlier.)

The appropriate initial conditions for these equations come from (6). At $t = 0$, (4) implies that $0 = x_0(0) + \varepsilon x_1(0) + \dots$; this holds for all ε , so

$$x_0(0) = 0, \quad x_1(0) = 0. \quad (12)$$

By applying a similar argument to $\dot{x}(0)$ we obtain

$$\dot{x}_0(0) = 1, \quad \dot{x}_1(0) = 0. \quad (13)$$

Now we solve the initial-value problems one by one; they fall like dominoes. The solution of (10), subject to the initial conditions $x_0(0) = 0$, $\dot{x}_0(0) = 1$, is

$$x_0(t) = \sin t. \quad (14)$$

Plugging this solution into (11) gives

$$\ddot{x}_1 + x_1 = -2 \cos t. \quad (15)$$

Here's the first sign of trouble: the right-hand side of (15) is a **resonant** forcing. The solution of (15) subject to $x_1(0) = 0$, $\dot{x}_1(0) = 0$ is

$$x_1(t) = -t \sin t, \quad (16)$$

which is a **secular** term, i.e., a term that *grows* without bound as $t \rightarrow \infty$.

In summary, the solution of (5), (6) according to perturbation theory is

$$x(t, \varepsilon) = \sin t - \varepsilon t \sin t + O(\varepsilon^2). \quad (17)$$

How does this compare with the exact solution (7)? In Exercise 7.6.1, you are asked to show that the two formulas agree in the following sense: If (7) is expanded as power series in ε , the first two terms are given by (17). In fact, (17) is the beginning of a *convergent* series expansion for the true solution. For any fixed t , (17) provides a good approximation as long as ε is small enough—specifically, we need $\varepsilon t \ll 1$ so that the correction term (which is actually $O(\varepsilon^2 t^2)$) is negligible.

But normally we are interested in the behavior for *fixed* ε , not fixed t . In that case we can only expect the perturbation approximation to work for times $t \ll O(1/\varepsilon)$. To illustrate this limitation, Figure 7.6.2 plots the exact solution (7) and the perturbation series (17) for $\varepsilon = 0.1$. As expected, the perturbation series works reasonably well if $t \ll \frac{1}{\varepsilon} = 10$, but it breaks down after that.

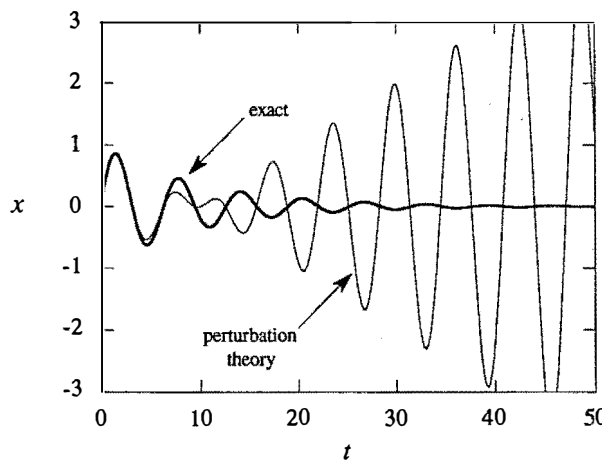


Figure 7.6.2

In many situations we'd like our approximation to capture the true solution's qualitative behavior for all t , or at least for large t . By this criterion, (17) is a failure, as Figure 7.6.2 makes obvious. There are two major problems:

1. The true solution (7) exhibits **two time scales**: a fast time $t \sim O(1)$ for the sinusoidal oscillations and a slow time $t \sim 1/\varepsilon$ over which the amplitude decays. Equation (17) completely misrepresents the slow time scale behavior. In particular, because of the secular term $t \sin t$, (17) falsely suggests that the solution grows with time whereas we know from (7) that the amplitude $A = (1 - \varepsilon^2)^{-1/2} e^{-\varepsilon t}$ decays exponentially.

The discrepancy occurs because $e^{-\varepsilon t} = 1 - \varepsilon t + O(\varepsilon^2 t^2)$, so to this order in ε , it appears (incorrectly) that the amplitude increases with t . To get the correct result, we'd need to calculate an *infinite* number of terms in the series. That's worthless; we want series approximations that work well with just one or two terms.

2. The frequency of the oscillations in (7) is $\omega = (1 - \varepsilon^2)^{1/2} \approx 1 - \frac{1}{2}\varepsilon^2$, which is shifted slightly from the frequency $\omega = 1$ of (17). After a very long time $t \sim O(1/\varepsilon^2)$, this frequency error will have a significant cumulative effect. Note that this is a third, *super-slow* time scale!

Two-Timing

The elementary example above reveals a more general truth: There are going to be (at least) two time scales in weakly nonlinear oscillators. We've already met this phenomenon in Figure 7.6.1, where the amplitude of the spiral grew very slowly compared to the cycle time. An analytical method called **two-timing** builds in the fact of two time scales from the start, and produces better approximations

than regular perturbation theory. In fact, more than two times can be used, but we'll stick to the simplest case.

To apply two-timing to (1), let $\tau = t$ denote the fast $O(1)$ time, and let $T = \varepsilon t$ denote the slow time. We'll treat these two times as if they were *independent* variables. In particular, functions of the slow time T will be regarded as *constants* on the fast time scale τ . It's hard to justify this idea rigorously, but it works! (Here's an analogy: it's like saying that your height is constant on the time scale of a day. Of course, over many months or years your height can change dramatically, especially if you're an infant or a pubescent teenager, but over one day your height stays constant, to a good approximation.)

Now we turn to the mechanics of the method. We expand the solution of (1) as a series

$$x(t, \varepsilon) = x_0(\tau, T) + \varepsilon x_1(\tau, T) + O(\varepsilon^2). \quad (18)$$

The time derivatives in (1) are transformed using the chain rule:

$$\dot{x} = \frac{dx}{dt} = \frac{\partial x}{\partial \tau} + \frac{\partial x}{\partial T} \frac{\partial T}{\partial t} = \frac{\partial x}{\partial \tau} + \varepsilon \frac{\partial x}{\partial T}. \quad (19)$$

A subscript notation for differentiation is more compact; thus we write (19) as

$$\dot{x} = \partial_\tau x + \varepsilon \partial_T x. \quad (20)$$

After substituting (18) into (20) and collecting powers of ε , we find

$$\dot{x} = \partial_\tau x_0 + \varepsilon (\partial_T x_0 + \partial_\tau x_1) + O(\varepsilon^2). \quad (21)$$

Similarly,

$$\ddot{x} = \partial_{\tau\tau} x_0 + \varepsilon (\partial_{T\tau} x_0 + 2 \partial_{TT} x_0) + O(\varepsilon^2). \quad (22)$$

To illustrate the method, let's apply it to our earlier test problem.

EXAMPLE 7.6.1:

Use two-timing to approximate the solution to the damped linear oscillator $\ddot{x} + 2\varepsilon \dot{x} + x = 0$, with initial conditions $x(0) = 0$, $\dot{x}(0) = 1$.

Solution: After substituting (21) and (22) for \dot{x} and \ddot{x} , we get

$$\partial_{\tau\tau} x_0 + \varepsilon (\partial_{T\tau} x_0 + 2 \partial_{TT} x_0) + 2\varepsilon \partial_\tau x_0 + x_0 + \varepsilon x_1 + O(\varepsilon^2) = 0. \quad (23)$$

Collecting powers of ε yields a pair of differential equations:

$$O(1): \partial_{\tau\tau} x_0 + x_0 = 0 \quad (24)$$

$$O(\varepsilon) : \partial_{\tau\tau}x_1 + 2\partial_{T\tau}x_0 + 2\partial_Tx_0 + x_1 = 0. \quad (25)$$

Equation (24) is just a simple harmonic oscillator. Its general solution is

$$x_0 = A \sin \tau + B \cos \tau, \quad (26)$$

but now comes the interesting part: *The “constants” A and B are actually functions of the slow time T*. Here we are invoking the above-mentioned ideas that τ and T should be regarded as independent variables, with functions of T behaving like constants on the fast time scale τ .

To determine $A(T)$ and $B(T)$, we need to go to the next order of ε . Substituting (26) into (25) gives

$$\begin{aligned} \partial_{\tau\tau}x_1 + x_1 &= -2(\partial_{T\tau}x_0 + \partial_Tx_0) \\ &= -2(A' + A)\cos \tau + 2(B' + B)\sin \tau \end{aligned} \quad (27)$$

where the prime denotes differentiation with respect to T .

Now we face the same predicament that ruined us after (15). As in that case, the right-hand side of (27) is a resonant forcing that will produce *secular terms* like $\tau \sin \tau$ and $\tau \cos \tau$ in the solution for x_1 . These terms would lead to a convergent but useless series expansion for x . Since we want an approximation free from secular terms, *we set the coefficients of the resonant terms to zero*—this maneuver is characteristic of all two-timing calculations. Here it yields

$$A' + A = 0 \quad (28)$$

$$B' + B = 0. \quad (29)$$

The solutions of (28) and (29) are

$$\begin{aligned} A(T) &= A(0)e^{-T} \\ B(T) &= B(0)e^{-T}. \end{aligned}$$

The last step is to find the initial values $A(0)$ and $B(0)$. They are determined by (18), (26), and the given initial conditions $x(0) = 0$, $\dot{x}(0) = 1$, as follows. Equation (18) gives $0 = x(0) = x_0(0,0) + \varepsilon x_1(0,0) + O(\varepsilon^2)$. To satisfy this equation for all sufficiently small ε , we must have

$$x_0(0,0) = 0 \quad (30)$$

and $x_1(0,0) = 0$. Similarly,

$$1 = \dot{x}(0) = \partial_Tx_0(0,0) + \varepsilon(\partial_Tx_0(0,0) + \partial_Tx_1(0,0)) + O(\varepsilon^2)$$

so

$$\partial_Tx_0(0,0) = 1 \quad (31)$$

and $\partial_T x_0(0,0) + \partial_\tau x_1(0,0) = 0$. Combining (26) and (30) we find $B(0) = 0$; hence $B(T) \equiv 0$. Similarly, (26) and (31) imply $A(0) = 1$, so $A(T) = e^{-T}$. Thus (26) becomes

$$x_0(\tau, T) = e^{-T} \sin \tau. \quad (32)$$

Hence

$$\begin{aligned} x &= e^{-T} \sin \tau + O(\varepsilon) \\ &= e^{-\varepsilon t} \sin t + O(\varepsilon) \end{aligned} \quad (33)$$

is the approximate solution predicted by two-timing. ■

Figure 7.6.3 compares the two-timing solution (33) to the exact solution (7) for $\varepsilon = 0.1$. The two curves are almost indistinguishable, even though ε is not terribly small. This is a characteristic feature of the method—it often works better than it has any right to.

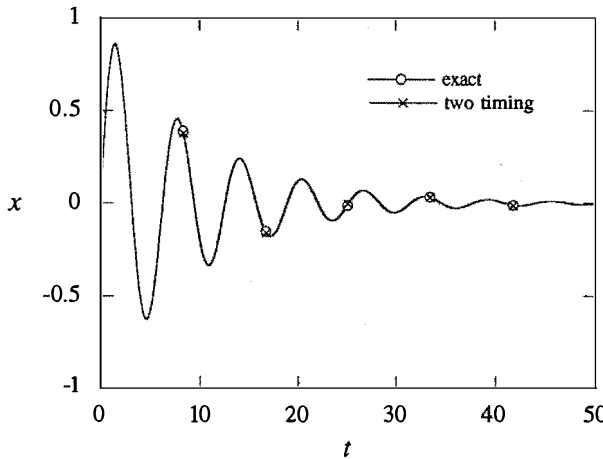


Figure 7.6.3

If we wanted to go further with Example 7.6.1, we could either solve for x_i and higher-order corrections, or introduce a super-slow time $\mathfrak{I} = \varepsilon^2 t$ to investigate the long-term phase shift caused by the $O(\varepsilon^2)$ error in frequency. But Figure 7.6.3 shows that we already have a good approximation.

OK, enough practice problems! Now that we have calibrated the method, let's unleash it on a genuine nonlinear problem.

EXAMPLE 7.6.2:

Use two-timing to show that the van der Pol oscillator (2) has a stable limit cycle that is nearly circular, with a radius $= 2 + O(\varepsilon)$ and a frequency $\omega = 1 + O(\varepsilon^2)$.

Solution: The equation is $\ddot{x} + x + \varepsilon(x^2 - 1)\dot{x} = 0$. Using (21) and (22) and collecting powers of ε , we find the following equations:

$$\partial_{\tau\tau}x_0 + x_0 = 0 \quad (34)$$

$$\partial_{\tau\varepsilon}x_1 + x_1 = -2\partial_{\tau T}x_0 - (x_0^2 - 1)\partial_\tau x_0. \quad (35)$$

As always, the $O(1)$ equation is a simple harmonic oscillator. Its general solution can be written as (26), or alternatively, as

$$x_0 = r(T) \cos(\tau + \phi(T)) \quad (36)$$

where $r(T)$ and $\phi(T)$ are the *slowly-varying amplitude and phase* of x_0 .

To find equations governing r and ϕ , we insert (36) into (35). This yields

$$\begin{aligned} \partial_{\tau\tau}x_1 + x_1 &= -2(r' \sin(\tau + \phi) + r\phi' \cos(\tau + \phi)) \\ &\quad - r \sin(\tau + \phi)[r^2 \cos^2(\tau + \phi) - 1]. \end{aligned} \quad (37)$$

As before, we need to avoid resonant terms on the right-hand side. These are terms proportional to $\cos(\tau + \phi)$ and $\sin(\tau + \phi)$. Some terms of this form already appear explicitly in (37). But—and this is the important point—there is also a resonant term lurking in $\sin(\tau + \phi)\cos^2(\tau + \phi)$, because of the trigonometric identity

$$\sin(\tau + \phi)\cos^2(\tau + \phi) = \frac{1}{4}[\sin(\tau + \phi) + \sin 3(\tau + \phi)]. \quad (38)$$

(Exercise 7.6.10 reminds you how to derive such identities, but usually we won't need them—shortcuts are available, as we'll see.) After substituting (38) into (37), we get

$$\begin{aligned} \partial_{\tau\tau}x_1 + x_1 &= \left[-2r' + r - \frac{1}{4}r^3\right] \sin(\tau + \phi) \\ &\quad + [-2r\phi'] \cos(\tau + \phi) - \frac{1}{4}r^3 \sin 3(\tau + \phi). \end{aligned} \quad (39)$$

To avoid secular terms, we require

$$-2r' + r - \frac{1}{4}r^3 = 0 \quad (40)$$

$$-2r\phi' = 0. \quad (41)$$

First consider (40). It may be rewritten as a vector field

$$r' = \frac{1}{8}r(4 - r^2) \quad (42)$$

on the half-line $r \geq 0$. Following the methods of Chapter 2 or Example 7.1.1, we see that $r^* = 0$ is an unstable fixed point and $r^* = 2$ is a stable fixed point. Hence $r(T) \rightarrow 2$ as $T \rightarrow \infty$. Secondly, (41) implies $\phi' = 0$, so $\phi(T) = \phi_0$ for some constant ϕ_0 . Hence $x_0(\tau, T) \rightarrow 2\cos(\tau + \phi_0)$ and therefore

$$x(t) \rightarrow 2 \cos(t + \phi_0) + O(\varepsilon) \quad (43)$$

as $t \rightarrow \infty$. Thus $x(t)$ approaches a stable limit cycle of radius $= 2 + O(\varepsilon)$.

To find the frequency implied by (43), let $\theta = t + \phi(T)$ denote the argument of the cosine. Then the angular frequency ω is given by

$$\omega = \frac{d\theta}{dt} = 1 + \frac{d\phi}{dT} \frac{dT}{dt} = 1 + \varepsilon \phi' = 1, \quad (44)$$

through first order in ε . Hence $\omega = 1 + O(\varepsilon^2)$; if we want an explicit formula for this $O(\varepsilon^2)$ correction term, we'd need to introduce a super-slow time $\mathfrak{T} = \varepsilon^2 t$, or we could use the Poincaré–Lindstedt method, as discussed in the exercises. ■

Averaged Equations

The same steps occur again and again in problems about weakly nonlinear oscillators. We can save time by deriving some general formulas.

Consider the equation for a general weakly nonlinear oscillator:

$$\ddot{x} + x + \varepsilon h(x, \dot{x}) = 0. \quad (45)$$

The usual two-timing substitutions give

$$O(1): \partial_{\tau\tau} x_0 + x_0 = 0 \quad (46)$$

$$O(\varepsilon): \partial_{\tau\tau} x_1 + x_1 = -2\partial_{\tau\tau} x_0 - h \quad (47)$$

where now $h = h(x_0, \partial_\tau x_0)$. As in Example 7.6.2, the solution of the $O(1)$ equation is

$$x_0 = r(T) \cos(\tau + \phi(T)). \quad (48)$$

Our goal is to derive differential equations for r' and ϕ' , analogous to (40) and (41). We'll find these equations by insisting, as usual, that there be no terms proportional to $\cos(\tau + \phi)$ and $\sin(\tau + \phi)$ on the right-hand side of (47). Substituting (48) into (47), we see that this right-hand side is

$$2[r' \sin(\tau + \phi) + r\phi' \cos(\tau + \phi)] - h \quad (49)$$

where now $h = h(r \cos(\tau + \phi), -r \sin(\tau + \phi))$.

To extract the terms in h proportional to $\cos(\tau + \phi)$ and $\sin(\tau + \phi)$, we borrow some ideas from Fourier analysis. (If you're unfamiliar with Fourier analysis, don't worry—we'll derive all that we need in Exercise 7.6.12.) Notice that h is a 2π -periodic function of $\tau + \phi$. Let

$$\theta = \tau + \phi.$$

Fourier analysis tells us that $h(\theta)$ can be written as a **Fourier series**

$$h(\theta) = \sum_{k=0}^{\infty} a_k \cos k\theta + \sum_{k=1}^{\infty} b_k \sin k\theta \quad (50)$$

where the **Fourier coefficients** are given by

$$\begin{aligned} a_0 &= \frac{1}{2\pi} \int_0^{2\pi} h(\theta) d\theta \\ a_k &= \frac{1}{\pi} \int_0^{2\pi} h(\theta) \cos k\theta d\theta, \quad k \geq 1 \\ b_k &= \frac{1}{\pi} \int_0^{2\pi} h(\theta) \sin k\theta d\theta, \quad k \geq 1. \end{aligned} \quad (51)$$

Hence (49) becomes

$$2[r' \sin \theta + r\phi' \cos \theta] - \sum_{k=0}^{\infty} a_k \cos k\theta - \sum_{k=1}^{\infty} b_k \sin k\theta. \quad (52)$$

The only resonant terms in (52) are $[2r' - b_1] \sin \theta$ and $[2r\phi' - a_1] \cos \theta$. Therefore, to avoid secular terms we need $r' = b_1/2$ and $r\phi' = a_1/2$. Using the expressions in (51) for a_1 and b_1 , we obtain

$$\begin{aligned} r' &= \frac{1}{2\pi} \int_0^{2\pi} h(\theta) \sin \theta d\theta \equiv \langle h \sin \theta \rangle \\ r\phi' &= \frac{1}{2\pi} \int_0^{2\pi} h(\theta) \cos \theta d\theta \equiv \langle h \cos \theta \rangle \end{aligned} \quad (53)$$

where the angled brackets $\langle \cdot \rangle$ denote an average over one cycle of θ .

The equations in (53) are called the **averaged** or **slow-time equations**. To use them, we write out $h = h(r \cos(\tau + \phi), -r \sin(\tau + \phi)) = h(r \cos \theta, -r \sin \theta)$ explicitly, and then compute the relevant averages over the fast variable θ , treating the slow variable r as constant. Here are some averages that appear often:

$$\begin{aligned} \langle \cos \rangle &= \langle \sin \rangle = 0, \quad \langle \sin \cos \rangle = 0, \quad \langle \cos^3 \rangle = \langle \sin^3 \rangle = 0, \quad \langle \cos^{2n+1} \rangle = \langle \sin^{2n+1} \rangle = 0, \\ \langle \cos^2 \rangle &= \langle \sin^2 \rangle = \frac{1}{2}, \quad \langle \cos^4 \rangle = \langle \sin^4 \rangle = \frac{3}{8}, \quad \langle \cos^2 \sin^2 \rangle = \frac{1}{8}, \\ \langle \cos^{2n} \rangle &= \langle \sin^{2n} \rangle = \frac{1 \cdot 3 \cdot 5 \cdots (2n-1)}{2 \cdot 4 \cdot 6 \cdots (2n)}, \quad n \geq 1. \end{aligned} \quad (54)$$

Other averages can either be derived from these, or found by direct integration. For instance,

$$\langle \cos^2 \sin^4 \rangle = \langle (1 - \sin^2) \sin^4 \rangle = \langle \sin^4 \rangle - \langle \sin^6 \rangle = \frac{3}{8} - \frac{15}{48} = \frac{1}{16}$$

and

$$\langle \cos^3 \sin \rangle = \frac{1}{2\pi} \int_0^{2\pi} \cos^3 \theta \sin \theta d\theta = -\frac{1}{2\pi} [\cos^4 \theta]_0^{2\pi} = 0.$$

EXAMPLE 7.6.3:

Consider the van der Pol equation $\ddot{x} + x + \varepsilon(x^2 - 1)\dot{x} = 0$, subject to the initial conditions $x(0) = 1$, $\dot{x}(0) = 0$. Find the averaged equations, and then solve them to obtain an approximate formula for $x(t, \varepsilon)$. Compare your result to a numerical solution of the full equation, for $\varepsilon = 0.1$.

Solution: The van der Pol equation has $h = (x^2 - 1)\dot{x} = (r^2 \cos^2 \theta - 1)(-r \sin \theta)$. Hence (53) becomes

$$\begin{aligned} r' &= \langle h \sin \theta \rangle = \langle (r^2 \cos^2 \theta - 1)(-r \sin \theta) \sin \theta \rangle \\ &= r \langle \sin^2 \theta \rangle - r^3 \langle \cos^2 \theta \sin^2 \theta \rangle \\ &= \frac{1}{2} r - \frac{1}{8} r^3 \end{aligned}$$

and

$$\begin{aligned} r\phi' &= \langle h \cos \theta \rangle = \langle (r^2 \cos^2 \theta - 1)(-r \sin \theta) \cos \theta \rangle \\ &= r \langle \sin \theta \cos \theta \rangle - r^3 \langle \cos^3 \theta \sin \theta \rangle \\ &= 0 - 0 = 0. \end{aligned}$$

These equations match those found in Example 7.6.2, as they should.

The initial conditions $x(0) = 1$ and $\dot{x}(0) = 0$ imply $r(0) \approx \sqrt{x(0)^2 + \dot{x}(0)^2} = 1$ and $\phi(0) \approx \tan^{-1}(\dot{x}(0)/x(0)) - \tau = 0 - 0 = 0$. Since $\phi' = 0$, we find $\phi(T) \equiv 0$. To find $r(T)$, we solve $r' = \frac{1}{2} r - \frac{1}{8} r^3$ subject to $r(0) = 1$. The differential equation separates to

$$\int \frac{8dr}{r(4-r^2)} = \int dT.$$

After integrating by partial fractions and using $r(0) = 1$, we find

$$r(T) = 2(1+3e^{-T})^{-1/2}. \quad (55)$$

Hence

$$\begin{aligned} x(t, \varepsilon) &\sim x_0(\tau, T) + O(\varepsilon) \\ &= \frac{2}{\sqrt{1+3e^{-\varepsilon t}}} \cos t + O(\varepsilon). \end{aligned} \quad (56)$$

Equation (56) describes the transient dynamics of the oscillator as it spirals out to its limit cycle. Notice that $r(T) \rightarrow 2$ as $T \rightarrow \infty$, as in Example 7.6.2.

In Figure 7.6.4 we plot the “exact” solution of the van der Pol equation, obtained by numerical integration for $\varepsilon = 0.1$ and initial conditions $x(0) = 1$, $\dot{x}(0) = 0$. For comparison, the slowly-varying amplitude $r(T)$ predicted by (55) is also shown. The agreement is striking. Alternatively, we could have plotted the whole solution (56) instead of just its envelope; then the two curves would be virtually indistinguishable, like those in Figure 7.6.3. ■

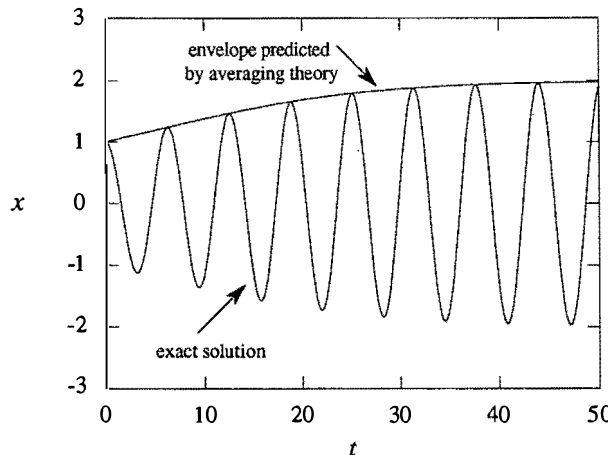


Figure 7.6.4

Now we consider an example in which the frequency of an oscillator depends on its amplitude. This is a common phenomenon, and one that is intrinsically *non-linear*—it cannot occur for linear oscillators.

EXAMPLE 7.6.4:

Find an approximate relation between the amplitude and frequency of the Duffing oscillator $\ddot{x} + x + \varepsilon x^3 = 0$, where ε can have either sign. Interpret the results physically.

Solution: Here $h = x^3 = r^3 \cos^3 \theta$. Equation (53) becomes

$$r' = \langle h \sin \theta \rangle = r^3 \langle \cos^3 \theta \sin \theta \rangle = 0$$

and

$$r\phi' = \langle h \cos \theta \rangle = r^3 \langle \cos^4 \theta \rangle = \frac{3}{8} r^3.$$

Hence $r(T) \equiv a$, for some constant a , and $\phi' = \frac{3}{8} a^2$. As in Example 7.6.2, the frequency ω is given by

$$\omega = 1 + \varepsilon \phi' = 1 + \frac{3}{8} \varepsilon a^2 + O(\varepsilon^2). \quad (57)$$

Now for the physical interpretation. The Duffing equation describes the undamped motion of a unit mass attached to a nonlinear spring with restoring force $F(x) = -x - \varepsilon x^3$. We can use our intuition about ordinary linear springs if we write $F(x) = -kx$, where the spring stiffness is now dependent on x :

$$k = k(x) = 1 + \varepsilon x^2.$$

Suppose $\varepsilon > 0$. Then the spring gets *stiffer* as the displacement x increases—this is called a **hardening spring**. On physical grounds we'd expect it to *increase* the frequency of the oscillations, consistent with (57). For $\varepsilon < 0$ we have a **softening spring**, exemplified by the pendulum (Exercise 7.6.15).

It also makes sense that $r' = 0$. The Duffing equation is a conservative system and for all ε sufficiently small, it has a *nonlinear center* at the origin (Exercise 6.5.13). Since all orbits close to the origin are periodic, there can be no long-term change in amplitude, consistent with $r' = 0$. ■

Validity of Two-Timing

We conclude with a few comments about the validity of the two-timing method. The rule of thumb is that the one-term approximation x_0 will be within $O(\varepsilon)$ of the true solution x for all times up to and including $t \sim O(1/\varepsilon)$, assuming that both x and x_0 start from the same initial condition. If x is a periodic solution, the situation is even better: x_0 remains within $O(\varepsilon)$ of x for *all* t .

But for precise statements and rigorous results about these matters, and for discussions of the subtleties that can occur, you should consult more advanced treatments, such as Guckenheimer and Holmes (1983) or Grimshaw (1990). Those authors use the *method of averaging*, an alternative approach that yields the same results as two-timing. See Exercise 7.6.25 for an introduction to this powerful technique.

Also, we have been very loose about the sense in which our formulas approximate the true solutions. The relevant notion is that of *asymptotic* approximation. For introductions to asymptotics, see Lin and Segel (1988) or Bender and Orszag (1978).

EXERCISES FOR CHAPTER 7

7.1 Examples

Sketch the phase portrait for each of the following systems. (As usual, r, θ denote polar coordinates.)

$$\mathbf{7.1.1} \quad \dot{r} = r^3 - 4r, \dot{\theta} = 1$$

$$\mathbf{7.1.2} \quad \dot{r} = r(1-r^2)(9-r^2), \dot{\theta} = 1$$

$$\mathbf{7.1.3} \quad \dot{r} = r(1-r^2)(4-r^2), \dot{\theta} = 2-r^2 \quad \mathbf{7.1.4} \quad \dot{r} = r \sin r, \dot{\theta} = 1$$

7.1.5 (From polar to Cartesian coordinates) Show that the system $\dot{r} = r(1-r^2)$, $\dot{\theta} = 1$ is equivalent to

$$\dot{x} = x - y - x(x^2 + y^2), \quad \dot{y} = x + y - y(x^2 + y^2),$$

where $x = r \cos \theta$, $y = r \sin \theta$. (Hint: $\dot{x} = \frac{d}{dt}(r \cos \theta) = \dot{r} \cos \theta - r \dot{\theta} \sin \theta$.)

7.1.6 (Circuit for van der Pol oscillator) Figure 1 shows the “tetrode multivibrator” circuit used in the earliest commercial radios and analyzed by van der Pol.

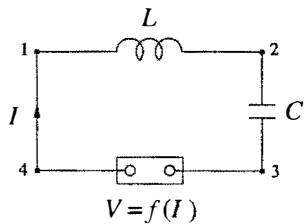


Figure 1

In van der Pol's day, the active element was a vacuum tube; today it would be a semiconductor device. It acts like an ordinary resistor when I is high, but like a negative resistor (energy source) when I is low. Its current-voltage characteristic $V = f(I)$ resembles a cubic function, as discussed below.

Suppose a source of current is attached to the circuit and then withdrawn. What equations govern the subsequent evolution of the current and the various voltages?

- Let $V = V_{32} = -V_{23}$ denote the voltage drop from point 3 to point 2 in the circuit.
Show that $\dot{V} = -I/C$ and $V = L\dot{I} + f(I)$.
- Show that the equations in (a) are equivalent to

$$\frac{dw}{d\tau} = -x, \quad \frac{dx}{d\tau} = w - \mu F(x)$$

where $x = L^{1/2}I$, $w = C^{1/2}V$, $\tau = (LC)^{-1/2}t$, and $F(x) = f(L^{-1/2}x)$.

In Section 7.5, we'll see that this system for (w, x) is equivalent to the van der Pol equation, if $F(x) = \frac{1}{3}x^3 - x$. Thus the circuit produces self-sustained oscillations.

7.1.7 (Waveform) Consider the system $\dot{r} = r(4-r^2)$, $\dot{\theta} = 1$, and let $x(t) = r(t)\cos \theta(t)$. Given the initial condition $x(0) = 0.1$, $y(0) = 0$, sketch the approximate waveform of $x(t)$, without obtaining an explicit expression for it.

7.1.8 (A circular limit cycle) Consider $\ddot{x} + a\dot{x}(x^2 + \dot{x}^2 - 1) + x = 0$, where $a > 0$.

- Find and classify all the fixed points.
- Show that the system has a circular limit cycle, and find its amplitude and period.
- Determine the stability of the limit cycle.

- d) Give an argument which shows that the limit cycle is unique, i.e., there are no other periodic trajectories.

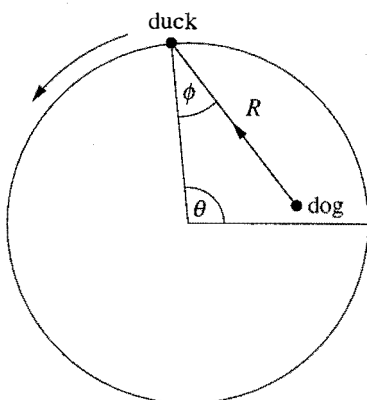
7.1.9 (Circular pursuit problem) A dog at the center of circular pond sees a duck swimming along the edge. The dog chases the duck by always swimming straight toward it. In other words, the dog's velocity vector always lies along the line connecting it to the duck. Meanwhile, the duck takes evasive action by swimming around the circumference as fast as it can, always moving counterclockwise.

- a) Assuming the pond has unit radius and both animals swim at the same constant speed, derive a pair of differential equations for the path of the dog. (Hint: Use the coordinate system shown in Figure 2 and find equations for $dR/d\theta$ and $d\phi/d\theta$.) Analyze the system. Can you solve it explicitly? Does the dog ever catch the duck?

- b) Now suppose the dog swims k times faster than the duck. Derive the differential equations for the dog's path.
c) If $k = \frac{1}{2}$, what does the dog end up doing in the long run?

Note: This problem has a long and intriguing history, dating back to the mid-1800s at least. It is much more difficult than similar **pursuit problems**—there is no known solution for the path of the dog in part (a), in terms of elementary functions. See Davis (1962, pp. 113–125) for a nice analysis and a guide to the literature.

Figure 2



7.2 Ruling Out Closed Orbits

Plot the phase portraits of the following gradient systems $\dot{\mathbf{x}} = -\nabla V$.

7.2.1 $V = x^2 + y^2$

7.2.2 $V = x^2 - y^2$

7.2.3 $V = e^x \sin y$

- 7.2.4** Show that all vector fields on the line are gradient systems. Is the same true of vector fields on the circle?

- 7.2.5** Let $\dot{x} = f(x, y)$, $\dot{y} = g(x, y)$ be a smooth vector field defined on the phase plane.

- a) Show that if this is a gradient system, then $\partial f / \partial y = \partial g / \partial x$.
b) Is the condition in (a) also sufficient?

- 7.2.6** Given that a system is a gradient system, here's how to find its potential function V . Suppose that $\dot{x} = f(x, y)$, $\dot{y} = g(x, y)$. Then $\dot{\mathbf{x}} = -\nabla V$ implies

$f(x, y) = -\partial V / \partial x$ and $g(x, y) = -\partial V / \partial y$. These two equations may be “partially integrated” to find V . Use this procedure to find V for the following gradient systems.

- $\dot{x} = y^2 + y \cos x, \quad \dot{y} = 2xy + \sin x$
- $\dot{x} = 3x^2 - 1 - e^{2y}, \quad \dot{y} = -2xe^{2y}$

7.2.7 Consider the system $\dot{x} = y + 2xy, \dot{y} = x + x^2 - y^2$.

- Show that $\partial f / \partial y = \partial g / \partial x$. (Then Exercise 7.2.5(a) implies this is a gradient system.)
- Find V .
- Sketch the phase portrait.

7.2.8 Show that the trajectories of a gradient system always cross the equipotentials at right angles (except at fixed points).

7.2.9 For each of the following systems, decide whether it is a gradient system. If so, find V and sketch the phase portrait. On a separate graph, sketch the equipotentials $V = \text{constant}$. (If the system is not a gradient system, go on to the next question.)

- $\dot{x} = y + x^2y, \quad \dot{y} = -x + 2xy$
- $\dot{x} = 2x, \quad \dot{y} = 8y$
- $\dot{x} = -2xe^{x^2+y^2}, \quad \dot{y} = -2ye^{x^2+y^2}$

7.2.10 Show that the system $\dot{x} = y - x^3, \dot{y} = -x - y^3$ has no closed orbits, by constructing a Liapunov function $V = ax^2 + by^2$ with suitable a, b .

7.2.11 Show that $V = ax^2 + 2bxy + cy^2$ is positive definite if and only if $a > 0$ and $ac - b^2 > 0$. (This is a useful criterion that allows us to test for positive definiteness when the quadratic form V includes a “cross term” $2bxy$.)

7.2.12 Show that $\dot{x} = -x + 2y^3 - 2y^4, \dot{y} = -x - y + xy$ has no periodic solutions. (Hint: Choose a, m , and n such that $V = x^m + ay^n$ is a Liapunov function.)

7.2.13 Recall the competition model

$$\dot{N}_1 = r_1 N_1 (1 - N_1/K_1) - b_1 N_1 N_2, \quad \dot{N}_2 = r_2 N_2 (1 - N_2/K_2) - b_2 N_1 N_2,$$

of Exercise 6.4.6. Using Dulac’s criterion with the weighting function $g = (N_1 N_2)^{-1}$, show that the system has no periodic orbits in the first quadrant $N_1, N_2 > 0$.

7.2.14 Consider $\dot{x} = x^2 - y - 1, \dot{y} = y(x - 2)$.

- Show that there are three fixed points and classify them.

- b) By considering the three straight lines through pairs of fixed points, show that there are no closed orbits.
 c) Sketch the phase portrait.

7.2.15 Consider the system $\dot{x} = x(2 - x - y)$, $\dot{y} = y(4x - x^2 - 3)$. We know from Example 7.2.4 that this system has no closed orbits.

- a) Find the three fixedpoints and classify them.
 b) Sketch the phase portrait.

7.2.16 If R is not simply connected, then the conclusion of Dulac's criterion is no longer valid. Find a counterexample.

7.2.17 Assume the hypotheses of Dulac's criterion, except now suppose that R is topologically equivalent to an annulus, i.e., it has exactly one hole in it. Using Green's theorem, show that there exists *at most* one closed orbit in R . (This result can be useful sometimes as a way of proving that a closed orbit is unique.)

7.3 Poincaré–Bendixson Theorem

- 7.3.1** Consider $\dot{x} = x - y - x(x^2 + 5y^2)$, $\dot{y} = x + y - y(x^2 + y^2)$.
- Classify the fixed point at the origin.
 - Rewrite the system in polar coordinates, using $r\dot{r} = x\dot{x} + y\dot{y}$ and $\dot{\theta} = (x\dot{y} - y\dot{x})/r^2$.
 - Determine the circle of maximum radius, r_1 , centered on the origin such that all trajectories have a radially *outward* component on it.
 - Determine the circle of minimum radius, r_2 , centered on the origin such that all trajectories have a radially *inward* component on it.
 - Prove that the system has a limit cycle somewhere in the trapping region $r_1 \leq r \leq r_2$.

7.3.2 Using numerical integration, compute the limit cycle of Exercise 7.3.1 and verify that it lies in the trapping region you constructed.

7.3.3 Show that the system $\dot{x} = x - y - x^3$, $\dot{y} = x + y - y^3$ has a periodic solution.

7.3.4 Consider the system

$$\dot{x} = x(1 - 4x^2 - y^2) - \frac{1}{2}y(1 + x), \quad \dot{y} = y(1 - 4x^2 - y^2) + 2x(1 + x).$$

- Show that the origin is an unstable fixed point.
- By considering \dot{V} , where $V = (1 - 4x^2 - y^2)^2$, show that all trajectories approach the ellipse $4x^2 + y^2 = 1$ as $t \rightarrow \infty$.

7.3.5 Show that the system $\dot{x} = -x - y + x(x^2 + 2y^2)$, $\dot{y} = x - y + y(x^2 + 2y^2)$ has at least one periodic solution.

7.3.6 Consider the oscillator equation $\ddot{x} + F(x, \dot{x})\dot{x} + x = 0$, where $F(x, \dot{x}) < 0$ if $r \leq a$ and $F(x, \dot{x}) > 0$ if $r \geq b$, where $r^2 = x^2 + \dot{x}^2$.

- Give a physical interpretation of the assumptions on F .
- Show that there is at least one closed orbit in the region $a < r < b$.

7.3.7 Consider $\dot{x} = y + ax(1 - 2b - r^2)$, $\dot{y} = -x + ay(1 - r^2)$, where a and b are parameters ($0 < a \leq 1$, $0 \leq b < \frac{1}{2}$) and $r^2 = x^2 + y^2$.

- Rewrite the system in polar coordinates.
- Prove that there is at least one limit cycle, and that if there are several, they all have the same period $T(a, b)$.
- Prove that for $b = 0$ there is only one limit cycle.

7.3.8 Recall the system $\dot{r} = r(1 - r^2) + \mu r \cos \theta$, $\dot{\theta} = 1$ of Example 7.3.1. Using the computer, plot the phase portrait for various values of $\mu > 0$. Is there a critical value μ_c at which the closed orbit ceases to exist? If so, estimate it. If not, prove that a closed orbit exists for all $\mu > 0$.

7.3.9 (Series approximation for a closed orbit) In Example 7.3.1, we used the Poincaré–Bendixson Theorem to prove that the system $\dot{r} = r(1 - r^2) + \mu r \cos \theta$, $\dot{\theta} = 1$ has a closed orbit in the annulus $\sqrt{1 - \mu} < r < \sqrt{1 + \mu}$ for all $\mu < 1$.

- To approximate the shape $r(\theta)$ of the orbit for $\mu \ll 1$, assume a power series solution of the form $r(\theta) = 1 + \mu r_1(\theta) + O(\mu^2)$. Substitute the series into a differential equation for $dr/d\theta$. Neglect all $O(\mu^2)$ terms, and thereby derive a simple differential equation for $r_1(\theta)$. Solve this equation explicitly for $r_1(\theta)$. (The approximation technique used here is called regular perturbation theory; see Section 7.6.)
- Find the maximum and minimum r on your approximate orbit, and hence show that it lies in the annulus $\sqrt{1 - \mu} < r < \sqrt{1 + \mu}$, as expected.
- Use a computer to calculate $r(\theta)$ numerically for various small μ , and plot the results on the same graph as your analytical approximation for $r(\theta)$. How does the maximum error depend on μ ?

7.3.10 Consider the two-dimensional system $\dot{\mathbf{x}} = A\mathbf{x} - r^2\mathbf{x}$, where $r = \|\mathbf{x}\|$ and A is a 2×2 constant real matrix with complex eigenvalues $\alpha \pm i\omega$. Prove that there exists at least one limit cycle for $\alpha > 0$ and that there are none for $\alpha < 0$.

7.3.11 (Cycle graphs) Suppose $\dot{\mathbf{x}} = \mathbf{f}(\mathbf{x})$ is a smooth vector field on \mathbf{R}^2 . An improved version of the Poincaré–Bendixson theorem states that if a trajectory is trapped in a compact region, then it must approach a fixed point, a limit cycle, or something exotic called a *cycle graph* (an invariant set containing a finite number of fixed points connected by a finite number of trajectories, all oriented either

clockwise or counterclockwise). Cycle graphs are rare in practice; here's a contrived but simple example.

- a) Plot the phase portrait for the system

$$\dot{r} = r(1 - r^2)[r^2 \sin^2 \theta + (r^2 \cos^2 \theta - 1)^2]$$

$$\dot{\theta} = r^2 \sin^2 \theta + (r^2 \cos^2 \theta - 1)^2$$

where r, θ are polar coordinates. (Hint: Note the common factor in the two equations; examine where it vanishes.)

- b) Sketch x vs. t for a trajectory starting away from the unit circle. What happens as $t \rightarrow \infty$?

7.4 Liénard Systems

- † 7.4.1** Show that the equation $\ddot{x} + \mu(x^2 - 1)\dot{x} + \tanh x = 0$, for $\mu > 0$, has exactly one periodic solution, and classify its stability.

- † 7.4.2** Consider the equation $\ddot{x} + \mu(x^4 - 1)\dot{x} + x = 0$.

- a) Prove that the system has a unique stable limit cycle if $\mu > 0$.
- b) Using a computer, plot the phase portrait for the case $\mu = 1$.
- c) If $\mu < 0$, does the system still have a limit cycle? If so, is it stable or unstable?

7.5 Relaxation Oscillations

- 7.5.1** For the van der Pol oscillator with $\mu \gg 1$, show that the positive branch of the cubic nullcline begins at $x_A = 2$ and ends at $x_B = 1$.

- 7.5.2** In Example 7.5.1, we used a tricky phase plane (often called the *Liénard plane*) to analyze the van der Pol oscillator for $\mu \gg 1$. Try to redo the analysis in the standard phase plane where $\dot{x} = y$, $\dot{y} = -x - \mu(x^2 - 1)$. What is the advantage of the Liénard plane?

- 7.5.3** Estimate the period of the limit cycle of $\ddot{x} + k(x^2 - 4)\dot{x} + x = 1$ for $k \gg 1$.

- 7.5.4** (Piecewise-linear nullclines) Consider the equation $\ddot{x} + \mu f(x)\dot{x} + x = 0$, where $f(x) = -1$ for $|x| < 1$ and $f(x) = 1$ for $|x| \geq 1$.

- a) Show that the system is equivalent to $\dot{x} = \mu(y - F(x))$, $\dot{y} = -x/\mu$, where $F(x)$ is the piecewise-linear function

$$F(x) = \begin{cases} x + 2, & x \leq -1 \\ -x, & |x| \leq 1 \\ x - 2, & x \geq 1 \end{cases}$$

- b) Graph the nullclines.
- c) Show that the system exhibits relaxation oscillations for $\mu \gg 1$, and plot the limit cycle in the (x, y) plane.
- d) Estimate the period of the limit cycle for $\mu \gg 1$.

7.5.5 Consider the equation $\ddot{x} + \mu(|x| - 1)\dot{x} + x = 0$. Find the approximate period of the limit cycle for $\mu \gg 1$.

7.5.6 (Biased van der Pol) Suppose the van der Pol oscillator is biased by a constant force: $\ddot{x} + \mu(x^2 - 1)\dot{x} + x = a$, where a can be positive, negative, or zero. (Assume $\mu > 0$ as usual.)

- a) Find and classify all the fixed points.
- b) Plot the nullclines in the Liénard plane. Show that if they intersect on the *middle* branch of the cubic nullcline, the corresponding fixed point is unstable.
- c) For $\mu \gg 1$, show that the system has a stable limit cycle if and only if $|a| < a_c$, where a_c is to be determined. (Hint: Use the Liénard plane.)
- d) Sketch the phase portrait for a slightly greater than a_c . Show that the system is *excitable* (it has a globally attracting fixed point, but certain disturbances can send the system on a long excursion through phase space before returning to the fixed point; compare Exercise 4.5.3.)

This system is closely related to the Fitzhugh–Nagumo model of neural activity; see Murray (1989) or Edelstein–Keshet (1988) for an introduction.

7.5.7 (Cell cycle) Tyson (1991) proposed an elegant model of the cell division cycle, based on interactions between the proteins cdc2 and cyclin. He showed that the model's mathematical essence is contained in the following set of dimensionless equations:

$$\dot{u} = b(v - u)(\alpha + u^2) - u, \quad \dot{v} = c - u,$$

where u is proportional to the concentration of the active form of a cdc2-cyclin complex, and v is proportional to the total cyclin concentration (monomers and dimers). The parameters $b \gg 1$ and $\alpha \ll 1$ are fixed and satisfy $8\alpha b < 1$; and c is adjustable.

- a) Sketch the nullclines.
- b) Show that the system exhibits relaxation oscillations for $c_1 < c < c_2$, where c_1 and c_2 are to be determined approximately. (It is too hard to find c_1 and c_2 exactly, but a good approximation can be achieved if you assume $8\alpha b \ll 1$.)
- c) Show that the system is excitable if c is slightly less than c_1 .

7.6 Weakly Nonlinear Oscillators

7.6.1 Show that if (7.6.7) is expanded as a power series in ε , we recover (7.6.17).

7.6.2 (Calibrating regular perturbation theory) Consider the initial value problem $\ddot{x} + x + \varepsilon x = 0$, with $x(0) = 1$, $\dot{x}(0) = 0$.

- Obtain the exact solution to the problem.
- Using regular perturbation theory, find x_0 , x_1 , and x_2 in the series expansion $x(t, \varepsilon) = x_0(t) + \varepsilon x_1(t) + \varepsilon^2 x_2(t) + O(\varepsilon^3)$.
- Does the perturbation solution contain secular terms? Did you expect to see any? Why?

7.6.3 (More calibration) Consider the initial value problem $\ddot{x} + x = \varepsilon$, with $x(0) = 1$, $\dot{x}(0) = 0$.

- Solve the problem exactly.
- Using regular perturbation theory, find x_0 , x_1 , and x_2 in the series expansion $x(t, \varepsilon) = x_0(t) + \varepsilon x_1(t) + \varepsilon^2 x_2(t) + O(\varepsilon^3)$.
- Explain why the perturbation solution does or doesn't contain secular terms.

For each of the following systems $\ddot{x} + x + \varepsilon h(x, \dot{x}) = 0$, with $0 < \varepsilon \ll 1$, calculate the averaged equations (7.6.53) and analyze the long-term behavior of the system. Find the amplitude and frequency of any limit cycles for the original system. If possible, solve the averaged equations explicitly for $x(t, \varepsilon)$, given the initial conditions $x(0) = a$, $\dot{x}(0) = 0$.

7.6.4 $h(x, \dot{x}) = x$

7.6.5 $h(x, \dot{x}) = x\dot{x}^2$

7.6.6 $h(x, \dot{x}) = \dot{x}\dot{x}$

7.6.7 $h(x, \dot{x}) = (x^4 - 1)\dot{x}$

7.6.8 $h(x, \dot{x}) = (|x| - 1)\dot{x}$

7.6.9 $h(x, \dot{x}) = (x^2 - 1)\dot{x}^3$

7.6.10 Derive the identity $\sin \theta \cos^2 \theta = \frac{1}{4}[\sin \theta + \sin 3\theta]$ as follows: Use the complex representations

$$\cos \theta = \frac{e^{i\theta} + e^{-i\theta}}{2}, \quad \sin \theta = \frac{e^{i\theta} - e^{-i\theta}}{2i},$$

multiply everything out, and then collect terms. This is always the most straightforward method of deriving such identities, and you don't have to remember any others.

7.6.11 (Higher harmonics) Notice the third harmonic $\sin 3(\tau + \phi)$ in Equation (7.6.39). The generation of *higher harmonics* is a characteristic feature of non-linear systems. To find the effect of such terms, return to Example 7.6.2 and solve for x_1 , assuming that the original system had initial conditions $x(0) = 2$, $\dot{x}(0) = 0$.

7.6.12 (Deriving the Fourier coefficients) This exercise leads you through the derivation of the formulas (7.6.51) for the Fourier coefficients. For convenience,

let brackets denote the average of a function: $\langle f(\theta) \rangle \equiv \frac{1}{2\pi} \int_0^{2\pi} f(\theta) d\theta$ for any 2π -periodic function f . Let k and m be arbitrary integers.

- a) Using integration by parts, complex exponentials, trig identities, or otherwise, derive the *orthogonality relations*

$$\langle \cos k\theta \sin m\theta \rangle = 0, \text{ for all } k, m;$$

$$\langle \cos k\theta \cos m\theta \rangle = \langle \sin k\theta \sin m\theta \rangle = 0, \text{ for all } k \neq m;$$

$$\langle \cos^2 k\theta \rangle = \langle \sin^2 k\theta \rangle = \frac{1}{2}, \text{ for } k \neq 0.$$

- b) To find a_k for $k \neq 0$, multiply both sides of (7.6.50) by $\cos m\theta$ and average both sides term by term over the interval $[0, 2\pi]$. Now using the orthogonality relations from part (a), show that *all the terms on the right-hand side cancel out, except the $k = m$ term!* Deduce that $\langle h(\theta) \cos k\theta \rangle = \frac{1}{2} a_k$, which is equivalent to the formula for a_k in (7.6.51).
c) Similarly, derive the formulas for b_k and a_0 .

7.6.13 (Exact period of a conservative oscillator) Consider the Duffing oscillator $\ddot{x} + x + \varepsilon x^3 = 0$, where $0 < \varepsilon \ll 1$, $x(0) = a$, and $\dot{x}(0) = 0$.

- a) Using conservation of energy, express the oscillation period $T(\varepsilon)$ as a certain integral.
b) Expand the integrand as a power series in ε , and integrate term by term to obtain an approximate formula $T(\varepsilon) = c_0 + c_1 \varepsilon + c_2 \varepsilon^2 + O(\varepsilon^3)$. Find c_0 , c_1 , c_2 and check that c_0 , c_1 are consistent with (7.6.57).

7.6.14 (Computer test of two-timing) Consider the equation $\ddot{x} + \varepsilon \dot{x}^3 + x = 0$.

- a) Derive the averaged equations.
b) Given the initial conditions $x(0) = a$, $\dot{x}(0) = 0$, solve the averaged equations and thereby find an approximate formula for $x(t, \varepsilon)$.
c) Solve $\ddot{x} + \varepsilon \dot{x}^3 + x = 0$ numerically for $a = 1$, $\varepsilon = 2$, $0 \leq t \leq 50$, and plot the result on the same graph as your answer to part (b). Notice the impressive agreement, even though ε is not small!

7.6.15 (Pendulum) Consider the pendulum equation $\ddot{x} + \sin x = 0$.

- a) Using the method of Example 7.6.4, show that the frequency of small oscillations of amplitude $a \ll 1$ is given by $\omega \approx 1 - \frac{1}{16} a^2$. (Hint: $\sin x \approx x - \frac{1}{6} x^3$, where $\frac{1}{6} x^3$ is a “small” perturbation.)
b) Is this formula for ω consistent with the exact results obtained in Exercise 6.7.4?

7.6.16 (Amplitude of the van der Pol oscillator via Green’s theorem) Here’s another way to determine the radius of the nearly circular limit cycle of the van der

Pol oscillator $\ddot{x} + \varepsilon \dot{x}(x^2 - 1) + x = 0$, in the limit $\varepsilon \ll 1$. Assume that the limit cycle is a circle of unknown radius a about the origin, and invoke the normal form of Green's theorem (i.e., the 2-D divergence theorem):

$$\oint_C \mathbf{v} \cdot \mathbf{n} d\ell = \iint_A \nabla \cdot \mathbf{v} dA$$

where C is the cycle and A is the region enclosed. By substituting $\mathbf{v} = \dot{\mathbf{x}} = (\dot{x}, \dot{y})$ and evaluating the integrals, show that $a \approx 2$.

7.6.17 (Playing on a swing) A simple model for a child playing on a swing is

$$\ddot{x} + (1 + \varepsilon\gamma + \varepsilon \cos 2t) \sin x = 0$$

where ε and γ are parameters, and $0 < \varepsilon \ll 1$. The variable x measures the angle between the swing and the downward vertical. The term $1 + \varepsilon\gamma + \varepsilon \cos 2t$ models the effects of gravity and the periodic pumping of the child's legs at approximately twice the natural frequency of the swing. The question is: Starting near the fixed point $x = 0$, $\dot{x} = 0$, can the child get the swing going by pumping her legs this way, or does she need a push?

- a) For small x , the equation may be replaced by $\ddot{x} + (1 + \varepsilon\gamma + \varepsilon \cos 2t)x = 0$. Show that the averaged equations (7.6.53) become

$$r' = \frac{1}{4}r \sin 2\phi, \quad \phi' = \frac{1}{2}(\gamma + \frac{1}{2}\cos 2\phi),$$

where $x = r \cos \theta = r(T) \cos(t + \phi(T))$, $\dot{x} = -r \sin \theta = -r(T) \sin(t + \phi(T))$, and prime denotes differentiation with respect to slow time $T = \varepsilon t$. Hint: To average terms like $\cos 2t \cos \theta \sin \theta$ over one cycle of θ , recall that $t = \theta - \phi$ and use trig identities:

$$\begin{aligned} \langle \cos 2t \cos \theta \sin \theta \rangle &= \frac{1}{2} \langle \cos(2\theta - 2\phi) \sin 2\theta \rangle \\ &= \frac{1}{2} \langle (\cos 2\theta \cos 2\phi + \sin 2\theta \sin 2\phi) \sin 2\theta \rangle \\ &= \frac{1}{4} \sin 2\phi. \end{aligned}$$

- b) Show that the fixed point $r = 0$ is unstable to exponentially growing oscillations, i.e., $r(T) = r_0 e^{kT}$ with $k > 0$, if $|\gamma| < \gamma_c$ where γ_c is to be determined. (Hint: For r near 0, $\phi' \gg r'$ so ϕ equilibrates relatively rapidly.)
c) For $|\gamma| < \gamma_c$, write a formula for the growth rate k in terms of γ .
d) How do the solutions to the averaged equations behave if $|\gamma| > \gamma_c$?
e) Interpret the results physically.

7.6.18 (Mathieu equation and a super-slow time scale) Consider the **Mathieu equation** $\ddot{x} + (a + \varepsilon \cos t)x = 0$ with $a \approx 1$. Using two-timing with a slow time

$T = \varepsilon^2 t$, show that the solution becomes unbounded as $t \rightarrow \infty$ if $1 - \frac{1}{12} \varepsilon^2 + O(\varepsilon^4) \leq a \leq 1 + \frac{5}{12} \varepsilon^2 + O(\varepsilon^4)$.

7.6.19 (Poincaré–Lindstedt method) This exercise guides you through an improved version of perturbation theory known as the **Poincaré–Lindstedt method**. Consider the Duffing equation $\ddot{x} + x + \varepsilon x^3 = 0$, where $0 < \varepsilon \ll 1$, $x(0) = a$, and $\dot{x}(0) = 0$. We know from phase plane analysis that the true solution $x(t, \varepsilon)$ is periodic; our goal is to find an approximate formula for $x(t, \varepsilon)$ that is valid for all t . The key idea is to regard the frequency ω as *unknown* in advance, and to solve for it by demanding that $x(t, \varepsilon)$ contains no secular terms.

- Define a new time $\tau = \omega t$ such that the solution has period 2π with respect to τ . Show that the equation transforms to $\omega^2 x'' + x + \varepsilon x^3 = 0$.
- Let $x(\tau, \varepsilon) = x_0(\tau) + \varepsilon x_1(\tau) + \varepsilon^2 x_2(\tau) + O(\varepsilon^3)$ and $\omega = 1 + \varepsilon \omega_1 + \varepsilon^2 \omega_2 + O(\varepsilon^3)$. (We know already that $\omega_0 = 1$ since the solution has frequency $\omega = 1$ when $\varepsilon = 0$.) Substitute these series into the differential equation and collect powers of ε . Show that

$$O(1): x_0'' + x_0 = 0$$

$$O(\varepsilon): x_1'' + x_1 = -2\omega_1 x_0'' - x_0^3.$$

- Show that the initial conditions become $x_0(0) = a$, $\dot{x}_0(0) = 0$; $x_k(0) = \dot{x}_k(0) = 0$ for all $k > 0$.
- Solve the $O(1)$ equation for x_0 .
- Show that after substitution of x_0 and the use of a trigonometric identity, the $O(\varepsilon)$ equation becomes $x_1'' + x_1 = (2\omega_1 a - \frac{3}{4} a^3) \cos \tau - \frac{1}{4} a^3 \cos 3\tau$. Hence, to avoid secular terms, we need $\omega_1 = \frac{3}{8} a^2$.
- Solve for x_1 .

Two comments: (1) This exercise shows that the Duffing oscillator has a frequency that depends on amplitude: $\omega = 1 + \frac{3}{8} \varepsilon a^2 + O(\varepsilon^2)$, in agreement with (7.6.57). (2) The Poincaré–Lindstedt method is good for approximating periodic solutions, but that's *all* it can do; if you want to explore transients or non-periodic solutions, you can't use this method. Use two-timing or averaging theory instead.

7.6.20 Show that if we had used regular perturbation to solve Exercise 7.6.19, we would have obtained $x(t, \varepsilon) = a \cos t + \varepsilon a^3 \left[-\frac{3}{8} t \sin t + \frac{1}{32} (\cos 3t - \cos t) \right] + O(\varepsilon^2)$. Why is this solution inferior?

7.6.21 Using the Poincaré–Lindstedt method, show that the frequency of the limit cycle for the van der Pol oscillator $\ddot{x} + \varepsilon(x^2 - 1)\dot{x} + x = 0$ is given by

$$\omega = 1 - \frac{1}{16} \varepsilon^2 + O(\varepsilon^3).$$

7.6.22 (Asymmetric spring) Use the Poincaré–Lindstedt method to find the first few terms in the expansion for the solution of $\ddot{x} + x + \varepsilon x^2 = 0$, with $x(0) = a$, $\dot{x}(0) = 0$. Show that the center of oscillation is at $x \approx \frac{1}{2} \varepsilon a^2$, approximately.

7.6.23 Find the approximate relation between amplitude and frequency for the periodic solutions of $\ddot{x} - \varepsilon x \dot{x} + x = 0$.

7.6.24 (Computer algebra) Using Mathematica, Maple, or some other computer algebra package, apply the Poincaré–Lindstedt method to the problem $\ddot{x} + x - \varepsilon x^3 = 0$, with $x(0) = a$, and $\dot{x}(0) = 0$. Find the frequency ω of periodic solutions, up to and including the $O(\varepsilon^3)$ term.

7.6.25 (The method of averaging) Consider the weakly nonlinear oscillator $\ddot{x} + x + \varepsilon h(x, \dot{x}, t) = 0$. Let $x(t) = r(t)\cos(t + \phi(t))$, $\dot{x} = -r(t)\sin(t + \phi(t))$. This change of variables should be regarded as a definition of $r(t)$ and $\phi(t)$.

- a) Show that $\dot{r} = \varepsilon h \sin(t + \phi)$, $r\dot{\phi} = \varepsilon h \cos(t + \phi)$. (Hence r and ϕ are slowly varying for $0 < \varepsilon \ll 1$, and thus $x(t)$ is a sinusoidal oscillation modulated by a slowly drifting amplitude and phase.)
- b) Let $\langle r \rangle(t) = \bar{r}(t) = \frac{1}{2\pi} \int_{t-\pi}^{t+\pi} r(\tau) d\tau$ denote the running average of r over one cycle of the sinusoidal oscillation. Show that $d\langle r \rangle/dt = \langle dr/dt \rangle$, i.e., it doesn't matter whether we differentiate or time-average first.
- c) Show that $d\langle r \rangle/dt = \varepsilon \langle h[r \cos(t + \phi), -r \sin(t + \phi), t] \sin(t + \phi) \rangle$.
- d) The result of part (c) is exact, but not helpful because the left-hand side involves $\langle r \rangle$ whereas the right-hand side involves r . Now comes the key approximation: replace r and ϕ by their averages over one cycle. Show that $r(t) = \bar{r}(t) + O(\varepsilon)$ and $\phi(t) = \bar{\phi}(t) + O(\varepsilon)$, and therefore

$$d\bar{r}/dt = \varepsilon \langle h[\bar{r} \cos(t + \bar{\phi}), -\bar{r} \sin(t + \bar{\phi}), t] \sin(t + \bar{\phi}) \rangle + O(\varepsilon^2)$$

$$\bar{r} d\bar{\phi}/dt = \varepsilon \langle h[\bar{r} \cos(t + \bar{\phi}), -\bar{r} \sin(t + \bar{\phi}), t] \cos(t + \bar{\phi}) \rangle + O(\varepsilon^2)$$

where the barred quantities are to be treated as constants inside the averages. These equations are just the *averaged equations* (7.6.53), derived by a different approach in the text. It is customary to drop the overbars; one usually doesn't distinguish between slowly varying quantities and their averages.

7.6.26 (Calibrating the method of averaging) Consider the equation $\dot{x} = -\varepsilon x \sin^2 t$, with $0 \leq \varepsilon \ll 1$ and $x = x_0$ at $t = 0$.

- a) Find the *exact* solution to the equation.
- b) Let $\bar{x}(t) = \frac{1}{2\pi} \int_{t-\pi}^{t+\pi} x(\tau) d\tau$. Show that $x(t) = \bar{x}(t) + O(\varepsilon)$. Use the method of averaging to find an approximate differential equation satisfied by \bar{x} , and solve it.
- c) Compare the results of parts (a) and (b); how large is the error incurred by averaging?

8

S

BIFFURCATIONS REVISITED

8.0 Introduction

This chapter extends our earlier work on bifurcations (Chapter 3). As we move up from one-dimensional to two-dimensional systems, we still find that fixed points can be created or destroyed or destabilized as parameters are varied—but now the same is true of closed orbits as well. Thus we can begin to *describe the ways in which oscillations can be turned on or off*.

In this broader context, what exactly do we mean by a bifurcation? The usual definition involves the concept of “topological equivalence” (Section 6.3): if the phase portrait changes its topological structure as a parameter is varied, we say that a **bifurcation** has occurred. Examples include changes in the number or stability of fixed points, closed orbits, or saddle connections as a parameter is varied.

This chapter is organized as follows: for each bifurcation, we start with a simple prototypical example, and then graduate to more challenging examples, either briefly or in separate sections. Models of genetic switches, chemical oscillators, driven pendula and Josephson junctions are used to illustrate the theory.

8.1 Saddle-Node, Transcritical, and Pitchfork Bifurcations

The bifurcations of fixed points discussed in Chapter 3 have analogs in two dimensions (and indeed, in *all* dimensions). Yet it turns out that nothing really new happens when more dimensions are added—all the action is confined to a one-dimensional subspace along which the bifurcations occur, while in the extra dimensions the flow is either simple attraction or repulsion from that subspace, as we’ll see below.

Saddle-Node Bifurcation

The saddle-node bifurcation is the basic mechanism for the creation and destruction of fixed points. Here's the prototypical example in two dimensions:

$$\begin{aligned}\dot{x} &= \mu - x^2 \\ \dot{y} &= -y.\end{aligned}\tag{1}$$

In the x -direction we see the bifurcation behavior discussed in Section 3.1, while in the y -direction the motion is exponentially damped.

Consider the phase portrait as μ varies. For $\mu > 0$, Figure 8.1.1 shows that there are two fixed points, a stable node at $(x^*, y^*) = (\sqrt{\mu}, 0)$ and a saddle at $(-\sqrt{\mu}, 0)$. As μ decreases, the saddle and node approach each other, then collide when $\mu = 0$, and finally disappear when $\mu < 0$.

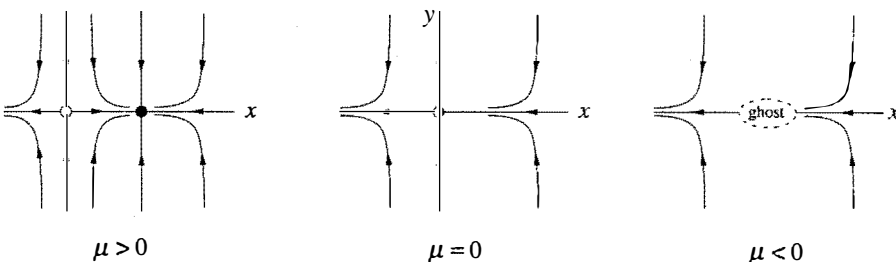


Figure 8.1.1

Even after the fixed points have annihilated each other, they continue to influence the flow—as in Section 4.3, they leave a *ghost*, a bottleneck region that sucks trajectories in and delays them before allowing passage out the other side. For the same reasons as in Section 4.3, the time spent in the bottleneck generically increases as $(\mu - \mu_c)^{-1/2}$, where μ_c is the value at which the saddle-node bifurcation occurs.

Some applications of this scaling law in condensed-matter physics are discussed by Strogatz and Westervelt (1989).

Figure 8.1.1 is representative of the following more general situation. Consider a two-dimensional system $\dot{x} = f(x, y)$, $\dot{y} = g(x, y)$ that depends on a parameter μ . Suppose that for some value of μ the nullclines intersect as shown in Figure 8.1.2. Notice that each intersection corresponds to a fixed point

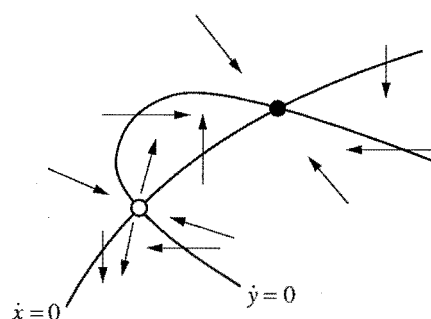


Figure 8.1.2

since $\dot{x} = 0$ and $\dot{y} = 0$ simultaneously. Thus, to see how the fixed points move as μ changes, we just have to watch the intersections. Now suppose that the nullclines pull away from each other as μ varies, becoming *tangent* at $\mu = \mu_c$. Then the fixed points approach each other and collide when $\mu = \mu_c$; after the nullclines pull apart, there are no intersections and the fixed points disappear with a bang. The point is that *all* saddle-node bifurcations have this character locally.

EXAMPLE 8.1.1:

The following system has been discussed by Griffith (1971) as a model for a genetic control system. The activity of a certain gene is assumed to be directly induced by two copies of the protein for which it codes. In other words, the gene is stimulated by its own product, potentially leading to an autocatalytic feedback process. In dimensionless form, the equations are

$$\begin{aligned}\dot{x} &= -ax + y \\ \dot{y} &= \frac{x^2}{1+x^2} - by\end{aligned}$$

where x and y are proportional to the concentrations of the protein and the messenger RNA from which it is translated, respectively, and $a, b > 0$ are parameters that govern the rate of degradation of x and y .

Show that the system has three fixed points when $a < a_c$, where a_c is to be determined. Show that two of these fixed points coalesce in a saddle-node bifurcation when $a = a_c$. Then sketch the phase portrait for $a < a_c$, and give a biological interpretation.

Solution: The nullclines are given by the line $y = ax$ and the sigmoidal curve

$$y = \frac{x^2}{b(1+x^2)}$$

as sketched in Figure 8.1.3. Now suppose we vary a while holding b fixed. This is simple to visualize, since a is the slope of the line. For small a there are three intersections, as in Figure 8.1.3. As a increases, the top two intersections approach each other and collide when the line intersects the curve tangentially. For larger values of a , those fixed points disappear, leaving the origin as the only fixed point.

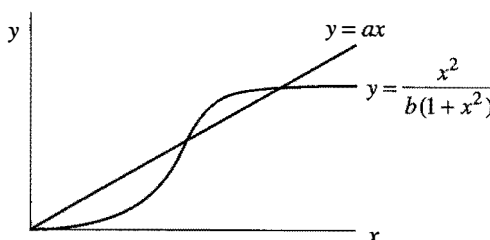


Figure 8.1.3

To find a_c , we compute the

fixed points directly and find where they coalesce. The nullclines intersect when

$$ax = \frac{x^2}{b(1+x^2)}.$$

One solution is $x^* = 0$, in which case $y^* = 0$. The other intersections satisfy the quadratic equation

$$ab(1+x^2) = x \quad (2)$$

which has two solutions

$$x^* = \frac{1 \pm \sqrt{1 - 4a^2b^2}}{2ab}$$

if $1 - 4a^2b^2 > 0$, i.e., $2ab < 1$. These solutions coalesce when $2ab = 1$. Hence

$$a_c = 1/2b.$$

For future reference, note that the fixed point $x^* = 1$ at the bifurcation.

The nullclines (Figure 8.1.4) provide a lot of information about the phase portrait for $a < a_c$. The vector field is vertical on the line $y = ax$ and horizontal on the sigmoidal curve. Other arrows can be sketched by noting the signs of \dot{x} and \dot{y} . It appears that the middle fixed point is a saddle and the other two are sinks. To confirm this, we turn now to the classification of the fixed points.

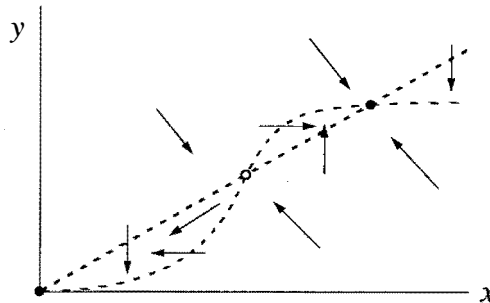


Figure 8.1.4

The Jacobian matrix at (x, y) is

$$A = \begin{pmatrix} -a & 1 \\ \frac{2x}{(1+x^2)^2} & -b \end{pmatrix}.$$

A has trace $\tau = -(a+b) < 0$ so all the fixed points are either sinks or saddles, depending on the value of the determinant Δ . At $(0,0)$, $\Delta = ab > 0$, so the origin is always a stable fixed point. In fact, it is a *stable node*, since $\tau^2 - 4\Delta = (a-b)^2 > 0$

(except in the degenerate case $a = b$, which we disregard). At the other two fixed points, Δ looks messy but it can be simplified using (2). We find

$$\Delta = ab - \frac{2x^*}{(1+(x^*)^2)^2} = ab \left[1 - \frac{2}{1+(x^*)^2} \right] = ab \left[\frac{(x^*)^2 - 1}{1+(x^*)^2} \right].$$

So $\Delta < 0$ for the “middle” fixed point, which has $0 < x^* < 1$; this is a *saddle point*. The fixed point with $x^* > 1$ is always a *stable node*, since $\Delta < ab$ and therefore $\tau^2 - 4\Delta > (a-b)^2 > 0$.

The phase portrait is plotted in Figure 8.1.5. By looking back at Figure 8.1.4, we can see that the unstable manifold of the saddle is necessarily trapped in the narrow channel between the two nullclines. More importantly, the *stable* manifold separates the plane into two regions, each a basin of attraction for a sink.

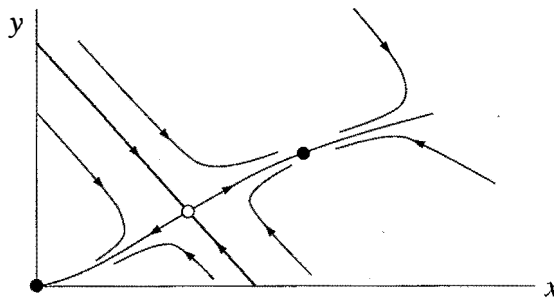


Figure 8.1.5

The biological interpretation is that the system can act like a *biochemical switch*, but only if the mRNA and protein degrade slowly enough—specifically, their decay rates must satisfy $ab < 1/2$. In this case, there are two stable steady states: one at the origin, meaning that the gene is silent and there is no protein around to turn it on; and one where x and y are large, meaning that the gene is active and sustained by the high level of protein. The stable manifold of the saddle acts like a threshold; it determines whether the gene turns on or off, depending on the initial values of x and y . ■

As advertised, the flow in Figure 8.1.5 is qualitatively similar to that in the idealized Figure 8.1.1. All trajectories relax rapidly onto the unstable manifold of the saddle, which plays a completely analogous role to the x -axis in Figure 8.1.1.

Thus, in many respects, the bifurcation is a fundamentally one-dimensional event, with the fixed points sliding toward each other along the unstable manifold like beads on a string. *This is why we spent so much time looking at bifurcations in one-dimensional systems*—they’re the building blocks of analogous bifurcations in higher dimensions. (The fundamental role of one-dimensional systems can be jus-

tified rigorously by “center manifold theory”—see Wiggins (1990) for an introduction.)

Transcritical and Pitchfork Bifurcations

Using the same idea as above, we can also construct prototypical examples of transcritical and pitchfork bifurcations at a stable fixed point. In the x -direction the dynamics are given by the normal forms discussed in Chapter 3, and in the y -direction the motion is exponentially damped. This yields the following examples:

$$\begin{aligned}\dot{x} &= \mu x - x^2, & \dot{y} &= -y \quad (\text{transcritical}) \\ \dot{x} &= \mu x - x^3, & \dot{y} &= -y \quad (\text{supercritical pitchfork}) \\ \dot{x} &= \mu x + x^3, & \dot{y} &= -y \quad (\text{subcritical pitchfork})\end{aligned}$$

The analysis in each case follows the same pattern, so we’ll discuss only the supercritical pitchfork, and leave the other two cases as exercises.

EXAMPLE 8.1.2:

Plot the phase portraits for the supercritical pitchfork system $\dot{x} = \mu x - x^3$, $\dot{y} = -y$, for $\mu < 0$, $\mu = 0$, and $\mu > 0$.

Solution: For $\mu < 0$, the only fixed point is a stable node at the origin. For $\mu = 0$, the origin is still stable, but now we have very slow (algebraic) decay along the x -direction instead of exponential decay; this is the phenomenon of “critical slowing down” discussed in Section 3.4 and Exercise 2.4.9. For $\mu > 0$, the origin loses stability and gives birth to two new stable fixed points symmetrically located at $(x^*, y^*) = (\pm\sqrt{\mu}, 0)$. By computing the Jacobian at each point, you can check that the origin is a saddle and the other two fixed points are stable nodes. The phase portraits are shown in Figure 8.1.6. ■

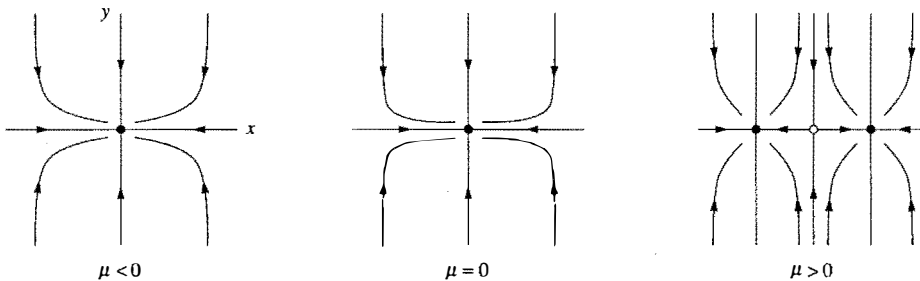


Figure 8.1.6

As mentioned in Chapter 3, pitchfork bifurcations are common in systems that have a symmetry. Here’s an example.

EXAMPLE 8.1.3:

Show that a supercritical pitchfork bifurcation occurs at the origin in the system

$$\dot{x} = \mu x + y + \sin x$$

$$\dot{y} = x - y$$

and determine the bifurcation value μ_c . Plot the phase portrait near the origin for μ slightly greater than μ_c .

Solution: The system is invariant under the change of variables $x \rightarrow -x$, $y \rightarrow -y$, so the phase portrait must be symmetric under reflection through the origin. The origin is a fixed point for all μ , and its Jacobian is

$$A = \begin{pmatrix} \mu+1 & 1 \\ 1 & -1 \end{pmatrix}$$

which has $\tau = \mu$ and $\Delta = -(\mu + 2)$. Hence the origin is a stable fixed point if $\mu < -2$ and a saddle if $\mu > -2$. This suggests that a pitchfork bifurcation occurs at $\mu_c = -2$. To confirm this, we seek a symmetric pair of fixed points close to the origin for μ close to μ_c . (Note that at this stage we don't know whether the bifurcation is sub- or supercritical.) The fixed points satisfy $y = x$ and hence $(\mu + 1)x + \sin x = 0$. One solution is $x = 0$, but we've found that already. Now suppose x is small and nonzero, and expand the sine as a power series. Then

$$(\mu + 1)x + x - \frac{x^3}{3!} + O(x^5) = 0.$$

After dividing through by x and neglecting higher-order terms, we get $\mu + 2 - x^2/6 \approx 0$. Hence there is a pair of fixed points with $x^* \approx \pm \sqrt{6(\mu + 2)}$ for μ slightly greater than -2 . Thus a *supercritical* pitchfork bifurcation occurs at $\mu_c = -2$. (If the bifurcation had been subcritical, the pair of fixed points would exist when the origin was stable, not after it has become a saddle.) Because the bifurcation is supercritical, we know the new fixed points are stable *without even checking*.

To draw the phase portrait near $(0,0)$ for μ slightly greater than -2 , it's helpful to find the eigenvectors of the Jacobian at the origin. This can be done exactly, but a simple approximation is that the Jacobian is close to that *at the bifurcation*. Thus

$$A \approx \begin{pmatrix} -1 & 1 \\ 1 & -1 \end{pmatrix}$$

which has eigenvectors $(1, 1)$ and $(1, -1)$, with eigenvalues $\lambda = 0$ and $\lambda = -2$, respectively. For μ slightly greater than -2 , the origin becomes a saddle and so the

zero eigenvalue becomes slightly positive. This information implies the phase portrait shown in Figure 8.1.7.

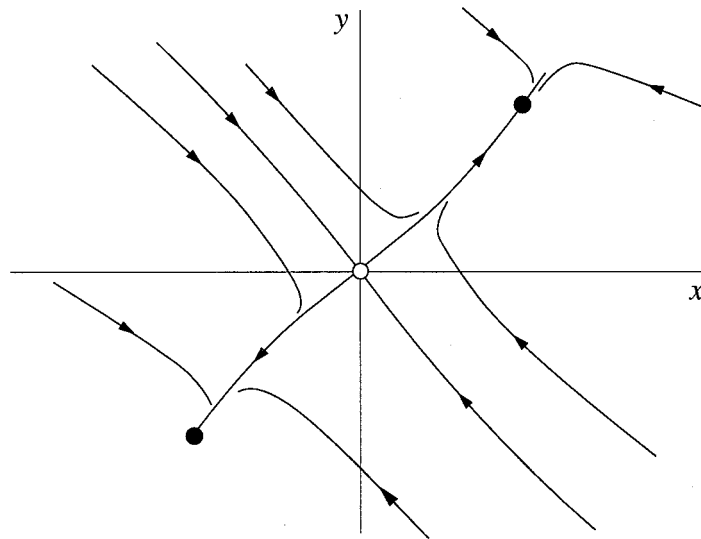


Figure 8.1.7

Note that because of the approximations we've made, this picture is only valid *locally* in both parameter and phase space—if we're not near the origin and if μ is not close to μ_c , all bets are off. ■

In all of the examples above, the bifurcation occurs when $\Delta = 0$, or equivalently, when one of the eigenvalues equals zero. More generally, the saddle-node, transcritical, and pitchfork bifurcations are all examples of *zero-eigenvalue bifurcations*. (There are other examples, but these are the most common.) Such bifurcations always involve the collision of two or more fixed points.

In the next section we'll consider a fundamentally new kind of bifurcation, one that has no counterpart in one-dimensional systems. It provides a way for a fixed point to lose stability without colliding with any other fixed points.

8.2 Hopf Bifurcations

Suppose a two-dimensional system has a stable fixed point. What are all the possible ways it could lose stability as a parameter μ varies? The eigenvalues of the Jacobian are the key. If the fixed point is stable, the eigenvalues λ_1, λ_2 must both lie in the left half-plane $\operatorname{Re} \lambda < 0$. Since the λ 's satisfy a quadratic equation with real coefficients, there are two possible pictures: either the eigenvalues are both real and negative (Figure 8.2.1a) or they are complex conjugates (Figure 8.2.1b). To

destabilize the fixed point, we need one or both of the eigenvalues to cross into the right half-plane as μ varies.

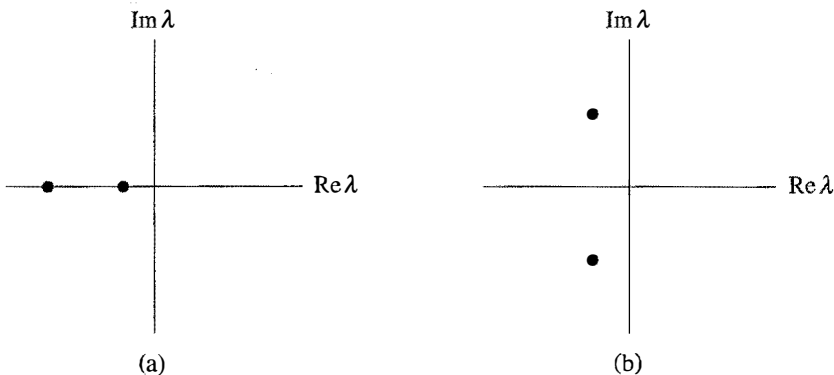


Figure 8.2.1

In Section 8.1 we explored the cases in which a real eigenvalue passes through $\lambda = 0$. These were just our old friends from Chapter 3, namely the saddle-node, transcritical, and pitchfork bifurcations. Now we consider the other possible scenario, in which two complex conjugate eigenvalues simultaneously cross the imaginary axis into the right half-plane.

Supercritical Hopf Bifurcation

Suppose we have a physical system that settles down to equilibrium through exponentially damped oscillations. In other words, small disturbances decay after “ringing” for a while (Figure 8.2.2a). Now suppose that the decay rate depends on a control parameter μ . If the decay becomes slower and slower and finally changes to *growth* at a critical value μ_c , the equilibrium state will lose stability. In many cases the resulting motion is a small-amplitude, sinusoidal, limit cycle oscillation about the former steady state (Figure 8.2.2b). Then we say that the system has undergone a **supercritical Hopf bifurcation**.

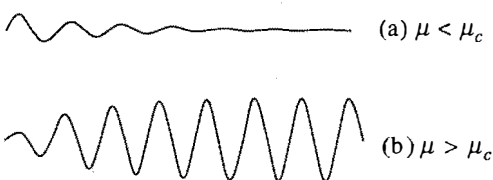


Figure 8.2.2

In terms of the flow in phase space, a supercritical Hopf bifurcation occurs when a stable spiral changes into an unstable spiral surrounded by a small, nearly elliptical limit cycle. Hopf bifurcations can occur in phase spaces of any dimension $n \geq 2$, but as in

the rest of this chapter, we’ll restrict ourselves to two dimensions.

A simple example of a supercritical Hopf bifurcation is given by the following system:

$$\dot{r} = \mu r - r^3$$

$$\dot{\theta} = \omega + br^2.$$

There are three parameters: μ controls the stability of the fixed point at the origin, ω gives the frequency of infinitesimal oscillations, and b determines the dependence of frequency on amplitude for larger amplitude oscillations.

Figure 8.2.3 plots the phase portraits for μ above and below the bifurcation. When $\mu < 0$ the origin $r = 0$ is a stable spiral whose sense of rotation depends on the sign of ω . For $\mu = 0$ the origin is still a stable spiral, though a very weak one: the decay is only algebraically fast. (This case was shown in Figure 6.3.2. Recall that the linearization wrongly predicts a center at the origin.) Finally, for $\mu > 0$ there is an unstable spiral at the origin and a stable circular limit cycle at $r = \sqrt{\mu}$.

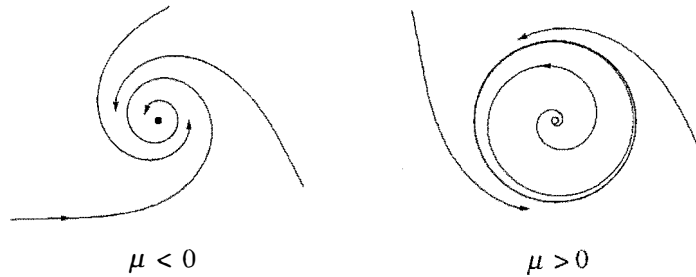


Figure 8.2.3

To see how the eigenvalues behave during the bifurcation, we rewrite the system in Cartesian coordinates; this makes it easier to find the Jacobian. We write $x = r \cos \theta$, $y = r \sin \theta$. Then

$$\begin{aligned}\dot{x} &= \dot{r} \cos \theta - r \dot{\theta} \sin \theta \\ &= (\mu r - r^3) \cos \theta - r(\omega + br^2) \sin \theta \\ &= (\mu - [x^2 + y^2])x - (\omega + b[x^2 + y^2])y \\ &= \mu x - \omega y + \text{cubic terms}\end{aligned}$$

and similarly

$$\dot{y} = \omega x + \mu y + \text{cubic terms.}$$

So the Jacobian at the origin is

$$A = \begin{pmatrix} \mu & -\omega \\ \omega & \mu \end{pmatrix},$$

which has eigenvalues

$$\lambda = \mu \pm i\omega.$$

As expected, the eigenvalues cross the imaginary axis from left to right as μ increases from negative to positive values.

Rules of Thumb

Our idealized case illustrates two rules that hold *generically* for supercritical Hopf bifurcations:

1. The size of the limit cycle grows continuously from zero, and increases proportional to $\sqrt{\mu - \mu_c}$, for μ close to μ_c .
2. The frequency of the limit cycle is given approximately by $\omega = \text{Im } \lambda$, evaluated at $\mu = \mu_c$. This formula is exact at the birth of the limit cycle, and correct within $\mathcal{O}(\mu - \mu_c)$ for μ close to μ_c . The period is therefore $T = (2\pi/\text{Im } \lambda) + \mathcal{O}(\mu - \mu_c)$.

But our idealized example also has some artifactual properties. First, in Hopf bifurcations encountered in practice, the limit cycle is elliptical, not circular, and its shape becomes distorted as μ moves away from the bifurcation point. Our example is only typical topologically, not geometrically. Second, in our idealized case the eigenvalues move on horizontal lines as μ varies, i.e., $\text{Im } \lambda$ is strictly independent of μ . Normally, the eigenvalues would follow a curvy path and cross the imaginary axis with nonzero slope (Figure 8.2.4).

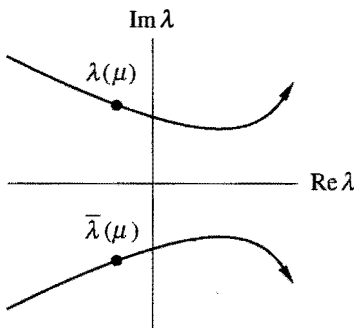


Figure 8.2.4

Subcritical Hopf Bifurcation

Like pitchfork bifurcations, Hopf bifurcations come in both super- and subcritical varieties. The subcritical case is always much more dramatic, and potentially dangerous in engineering applications. After the bifurcation, the trajectories must *jump* to a *distant* attractor, which may be a fixed point, another limit cycle, infinity, or—in

three and higher dimensions—a chaotic attractor. We'll see a concrete example of this last, most interesting case when we study the Lorenz equations (Chapter 9).

But for now, consider the two-dimensional example

$$\dot{r} = \mu r + r^3 - r^5$$

$$\dot{\theta} = \omega + br^2.$$

The important difference from the earlier supercritical case is that the cubic term r^3 is now *destabilizing*; it helps to drive trajectories away from the origin.

The phase portraits are shown in Figure 8.2.5. For $\mu < 0$ there are two attractors, a stable limit cycle and a stable fixed point at the origin. Between them lies an unstable cycle, shown as a dashed curve in Figure 8.2.5; it's the player to watch in this scenario. As μ increases, the unstable cycle tightens like a noose around the fixed point. A ***subcritical Hopf bifurcation*** occurs at $\mu = 0$, where the unstable cycle shrinks to zero amplitude and engulfs the origin, rendering it unstable. For $\mu > 0$, the large-amplitude limit cycle is suddenly the only attractor in town. Solutions that used to remain near the origin are now forced to grow into large-amplitude oscillations.

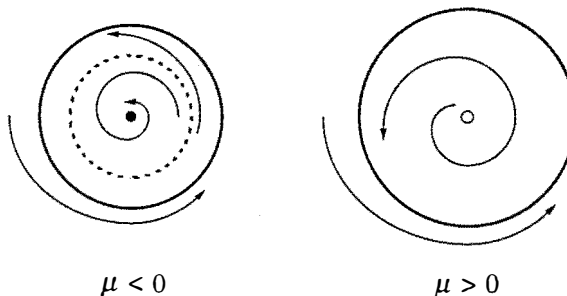


Figure 8.2.5

Note that the system exhibits *hysteresis*: once large-amplitude oscillations have begun, they cannot be turned off by bringing μ back to zero. In fact, the large oscillations will persist until $\mu = -1/4$ where the stable and unstable cycles collide and annihilate. This destruction of the large-amplitude cycle occurs via another type of bifurcation, to be discussed in Section 8.4.

Subcritical Hopf bifurcations occur in the dynamics of nerve cells (Rinzel and Ermentrout 1989), in aeroelastic flutter and other vibrations of airplane wings (Dowell and Ilgamova 1988, Thompson and Stewart 1986), and in instabilities of fluid flows (Drazin and Reid 1981).

Subcritical, Supercritical, or Degenerate Bifurcation?

Given that a Hopf bifurcation occurs, how can we tell if it's sub- or supercritical? The linearization doesn't provide a distinction: in both cases, a pair of eigen-

values moves from the left to the right half-plane.

An analytical criterion exists, but it can be difficult to use (see Exercises 8.2.12–15 for some tractable cases). A quick and dirty approach is to use the computer. If a small, attracting limit cycle appears immediately after the fixed point goes unstable, and if its amplitude shrinks back to zero as the parameter is reversed, the bifurcation is supercritical; otherwise, it's probably subcritical, in which case the nearest attractor might be far from the fixed point, and the system may exhibit hysteresis as the parameter is reversed. Of course, computer experiments are not proofs and you should check the numerics carefully before making any firm conclusions.

Finally, you should also be aware of a *degenerate Hopf bifurcation*. An example is given by the damped pendulum $\ddot{x} + \mu\dot{x} + \sin x = 0$. As we change the damping μ from positive to negative, the fixed point at the origin changes from a stable to an unstable spiral. However at $\mu = 0$ we do *not* have a true Hopf bifurcation because there are no limit cycles on either side of the bifurcation. Instead, at $\mu = 0$ we have a continuous band of closed orbits surrounding the origin. These are not limit cycles! (Recall that a limit cycle is an *isolated* closed orbit.)

This degenerate case typically arises when a nonconservative system suddenly becomes conservative at the bifurcation point. Then the fixed point becomes a nonlinear center, rather than the weak spiral required by a Hopf bifurcation. See Exercise 8.2.11 for another example.

EXAMPLE 8.2.1:

Consider the system $\dot{x} = \mu x - y + xy^2$, $\dot{y} = x + \mu y + y^3$. Show that a Hopf bifurcation occurs at the origin as μ varies. Is the bifurcation subcritical, supercritical, or degenerate?

Solution: The Jacobian at the origin is $A = \begin{pmatrix} \mu & -1 \\ 1 & \mu \end{pmatrix}$, which has $\tau = 2\mu$, $\Delta = \mu^2 + 1 > 0$, and $\lambda = \mu \pm i$. Hence, as μ increases through zero, the origin changes from a stable spiral to an unstable spiral. This suggests that some kind of Hopf bifurcation takes place at $\mu = 0$.

To decide whether the bifurcation is subcritical, supercritical, or degenerate, we use simple reasoning and numerical integration. If we transform the system to polar coordinates, we find that

$$\dot{r} = \mu r + ry^2,$$

as you should check. Hence $\dot{r} \geq \mu r$. This implies that for $\mu > 0$, $r(t)$ grows *at least*

as fast as $r_0 e^{\mu t}$. In other words, all trajectories are repelled out to infinity! So there are certainly no closed orbits for $\mu > 0$. In particular, the unstable spiral is not surrounded by a stable limit cycle; hence the bifurcation cannot be supercritical.

Could the bifurcation be degenerate? That would require that the origin be a nonlinear center when $\mu = 0$. But \dot{r} is strictly positive away from the x -axis, so closed orbits are still impossible.

By process of elimination, we expect that the bifurcation is *subcritical*. This is confirmed by Figure 8.2.6, which is a computer-generated phase portrait for $\mu = -0.2$.

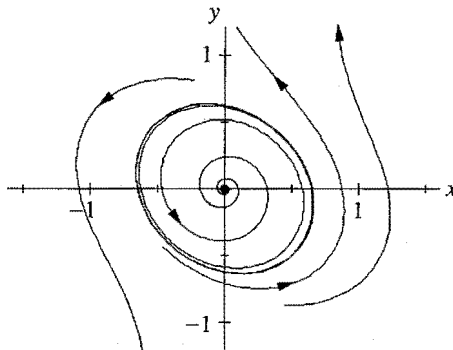


Figure 8.2.6

Note that an *unstable* limit cycle surrounds the stable fixed point, just as we expect in a subcritical bifurcation. Furthermore, the cycle is nearly elliptical and surrounds a gently winding spiral—these are typical features of *either* kind of Hopf bifurcation. ■

8.3 Oscillating Chemical Reactions

For an application of Hopf bifurcations, we now consider a class of experimental systems known as *chemical oscillators*. These systems are remarkable, both for their spectacular behavior and for the story behind their discovery. After presenting this background information, we analyze a simple model proposed recently for oscillations in the chlorine dioxide–iodine–malonic acid reaction. The definitive reference on chemical oscillations is the book edited by Field and Burger (1985). See also Epstein et al. (1983), Winfree (1987b) and Murray (1989).

Belousov's "Supposedly Discovered Discovery"

In the early 1950s the Russian biochemist Boris Belousov was trying to create a test tube caricature of the Krebs cycle, a metabolic process that occurs in living

cells. When he mixed citric acid and bromate ions in a solution of sulfuric acid, and in the presence of a cerium catalyst, he observed to his astonishment that the mixture became yellow, then faded to colorless after about a minute, then returned to yellow a minute later, then became colorless again, and continued to oscillate dozens of times before finally reaching equilibrium after about an hour.

Today it comes as no surprise that chemical reactions can oscillate spontaneously—such reactions have become a standard demonstration in chemistry classes, and you may have seen one yourself. (For recipes, see Winfree (1980).) But in Belousov's day, his discovery was so radical that he couldn't get his work published. It was thought that all solutions of chemical reagents must go *monotonically* to equilibrium, because of the laws of thermodynamics. Belousov's paper was rejected by one journal after another. According to Winfree (1987b, p.161), one editor even added a snide remark about Belousov's "supposedly discovered discovery" to the rejection letter.

Belousov finally managed to publish a brief abstract in the obscure proceedings of a Russian medical meeting (Belousov 1959), although his colleagues weren't aware of it until years later. Nevertheless, word of his amazing reaction circulated among Moscow chemists in the late 1950s, and in 1961 a graduate student named Zhabotinsky was assigned by his adviser to look into it. Zhabotinsky confirmed that Belousov was right all along, and brought this work to light at an international conference in Prague in 1968, one of the few times that Western and Soviet scientists were allowed to meet. At that time there was a great deal of interest in biological and biochemical oscillations (Chance et al. 1973) and the BZ reaction, as it came to be called, was seen as a manageable model of those more complex systems.

The analogy to biology turned out to be surprisingly close: Zaikin and Zhabotinsky (1970) and Winfree (1972) observed beautiful propagating *waves* of oxidation in thin unstirred layers of BZ reagent, and found that these waves annihilate upon collision, just like waves of excitation in neural or cardiac tissue. The waves always take the shape of expanding concentric rings or spirals (Color plate 1). Spiral waves are now recognized to be a ubiquitous feature of chemical, biological, and physical excitable media; in particular, spiral waves and their three-dimensional analogs, "scroll waves" (Front cover illustration) appear to be implicated in certain cardiac arrhythmias, a problem of great medical importance (Winfree 1987b).

Boris Belousov would be pleased to see what he started.

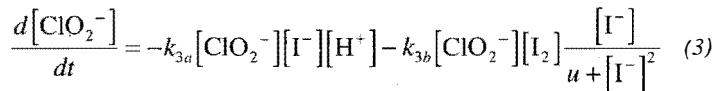
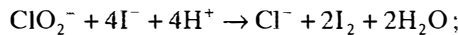
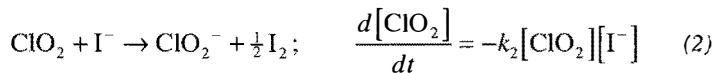
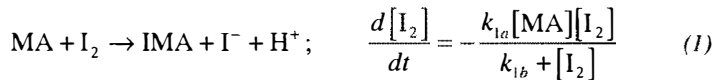
In 1980, he and Zhabotinsky were awarded the Lenin Prize, the Soviet Union's highest medal, for their pioneering work on oscillating reactions. Unfortunately, Belousov had passed away ten years earlier.

For more about the history of the BZ reaction, see Winfree (1984, 1987b). An English translation of Belousov's original paper from 1951 appears in Field and Burger (1985).

Chlorine Dioxide-Iodine-Malonic Acid Reaction

The mechanisms of chemical oscillations can be very complex. The BZ reaction is thought to involve more than twenty elementary reaction steps, but luckily many of them equilibrate rapidly—this allows the kinetics to be reduced to as few as three differential equations. See Tyson (1985) for this reduced system and its analysis.

In a similar spirit, Lengyel et al. (1990) have proposed and analyzed a particularly elegant model of another oscillating reaction, the chlorine dioxide-iodine-malonic acid ($\text{ClO}_2 - \text{I}_2 - \text{MA}$) reaction. Their experiments show that the following three reactions and empirical rate laws capture the behavior of the system:



Typical values of the concentrations and kinetic parameters are given in Lengyel et al. (1990) and Lengyel and Epstein (1991).

Numerical integrations of (1)–(3) show that the model exhibits oscillations that closely resemble those observed experimentally. However this model is still too complicated to handle analytically. To simplify it, Lengyel et al. (1990) use a result found in their simulations: Three of the reactants (MA , I_2 , and ClO_2) vary much more slowly than the intermediates I^- and ClO_2^- , which change by several orders of magnitude during an oscillation period. By approximating the concentrations of the slow reactants as *constants* and making other reasonable simplifications, they reduce the system to a two-variable model. (Of course, since this approximation neglects the slow consumption of the reactants, the model will be unable to account for the eventual approach to equilibrium.) After suitable nondimensionalization, the model becomes

$$\dot{x} = a - x - \frac{4xy}{1+x^2} \quad (4)$$

$$\dot{y} = bx \left(1 - \frac{y}{1+x^2}\right) \quad (5)$$

where x and y are the dimensionless concentrations of I^- and ClO_2^- . The parameters $a, b > 0$ depend on the empirical rate constants and on the concentrations assumed for the slow reactants.

We begin the analysis of (4), (5) by constructing a trapping region and applying the Poincaré–Bendixson theorem. Then we'll show that the chemical oscillations arise from a supercritical Hopf bifurcation.

EXAMPLE 8.3.1:

Prove that the system (4), (5) has a closed orbit in the positive quadrant $x, y > 0$ if a and b satisfy certain constraints, to be determined.

Solution: As in Example 7.3.2, the nullclines help us to construct a trapping region. Equation (4) shows that $\dot{x} = 0$ on the curve

$$y = \frac{(a-x)(1+x^2)}{4x} \quad (6)$$

and (5) shows that $\dot{y} = 0$ on the y -axis and on the parabola $y = 1 + x^2$. These nullclines are sketched in Figure 8.3.1, along with some representative vectors.

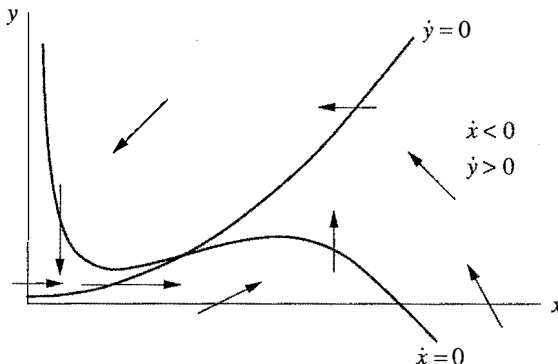


Figure 8.3.1

(We've taken some pedagogical license with Figure 8.3.1; the curvature of the nullcline (6) has been exaggerated to highlight its shape, and to give us more room to draw the vectors.)

Now consider the dashed box shown in Figure 8.3.2. It's a trapping region because all the vectors on the boundary point into the box.

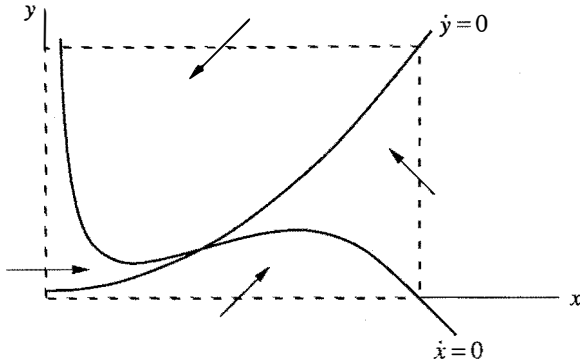


Figure 8.3.2

We can't apply the Poincaré–Bendixson theorem yet, because there's a fixed point

$$x^* = a/5, \quad y^* = 1 + (x^*)^2 = 1 + (a/5)^2$$

inside the box at the intersection of the nullclines. But now we argue as in Example 7.3.3: if the fixed point turns out to be a *repeller*, we *can* apply the Poincaré–Bendixson theorem to the “punctured” box obtained by removing the fixed point.

All that remains is to see under what conditions (if any) the fixed point is a repeller. The Jacobian at (x^*, y^*) is

$$\frac{1}{1+(x^*)^2} \begin{pmatrix} 3(x^*)^2 - 5 & -4x^* \\ 2b(x^*)^2 & -bx^* \end{pmatrix}.$$

(We've used the relation $y^* = 1 + (x^*)^2$ to simplify some of the entries in the Jacobian.) The determinant and trace are given by

$$\Delta = \frac{5bx^*}{1+(x^*)^2} > 0, \quad \tau = \frac{3(x^*)^2 - 5 - bx^*}{1+(x^*)^2}.$$

We're in luck—since $\Delta > 0$, the fixed point is never a saddle. Hence (x^*, y^*) is a repeller if $\tau > 0$, i.e., if

$$b < b_c \equiv 3a/5 - 25/a. \tag{7}$$

When (7) holds, the Poincaré–Bendixson theorem implies the existence of a closed orbit somewhere in the punctured box. ■

EXAMPLE 8.3.2:

Using numerical integration, show that a Hopf bifurcation occurs at $b = b_c$ and

decide whether the bifurcation is sub- or supercritical.

Solution: The analytical results above show that as b decreases through b_c , the fixed point changes from a stable spiral to an unstable spiral; this is the signature of a Hopf bifurcation. Figure 8.3.3 plots two typical phase portraits. (Here we have chosen $a = 10$; then (7) implies $b_c = 3.5$.) When $b > b_c$, all trajectories spiral into the stable fixed point (Figure 8.3.3a), while for $b < b_c$ they are attracted to a stable limit cycle (Figure 8.3.3b).

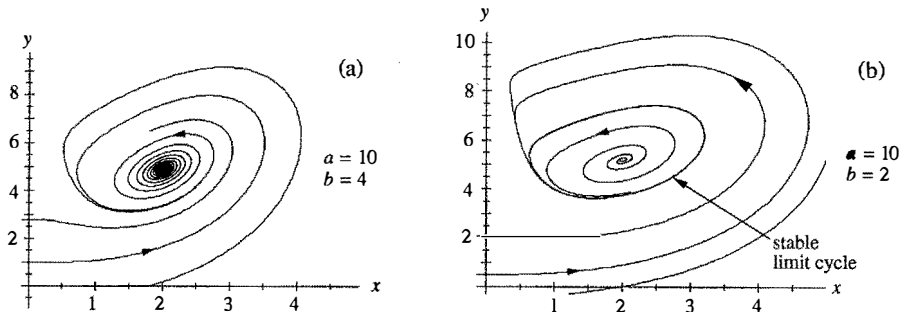


Figure 8.3.3

Hence the bifurcation is *supercritical*—after the fixed point loses stability, it is surrounded by a stable limit cycle. Moreover, by plotting phase portraits as $b \rightarrow b_c$ from below, we could confirm that the limit cycle shrinks continuously to a point, as required. ■

Our results are summarized in the stability diagram in Figure 8.3.4. The boundary between the two regions is given by the Hopf bifurcation locus $b = 3a/5 - 25/a$.

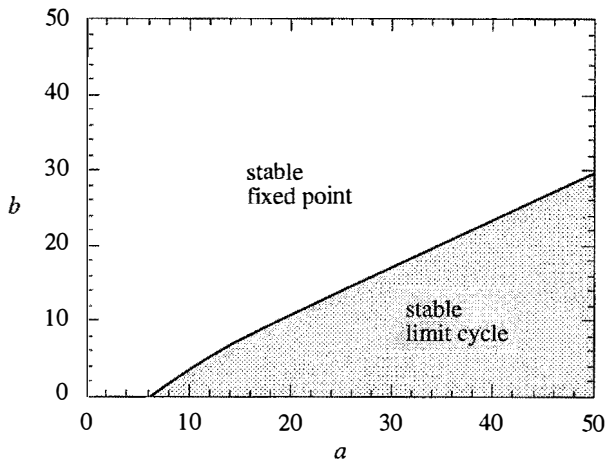


Figure 8.3.4

EXAMPLE 8.3.3:

Approximate the period of the limit cycle for b slightly less than b_c .

Solution: The frequency is approximated by the imaginary part of the eigenvalues at the bifurcation. As usual, the eigenvalues satisfy $\lambda^2 - \tau\lambda + \Delta = 0$. Since $\tau = 0$ and $\Delta > 0$ at $b = b_c$, we find

$$\lambda = \pm i\sqrt{\Delta}.$$

But at b_c ,

$$\Delta = \frac{5b_c x^*}{1+(x^*)^2} = \frac{5\left(\frac{3a}{5} - \frac{25}{a}\right)\left(\frac{a}{5}\right)}{1+(a/5)^2} = \frac{15a^2 - 625}{a^2 + 25}.$$

Hence $\omega \approx \Delta^{1/2} = [(15a^2 - 625)/(a^2 + 25)]^{1/2}$ and therefore

$$\begin{aligned} T &= 2\pi/\omega \\ &= 2\pi[(a^2 + 25)/(15a^2 - 625)]^{1/2}. \end{aligned}$$

A graph of $T(a)$ is shown in Figure 8.3.5. As $a \rightarrow \infty$, $T \rightarrow 2\pi/\sqrt{15} \approx 1.63$. ■

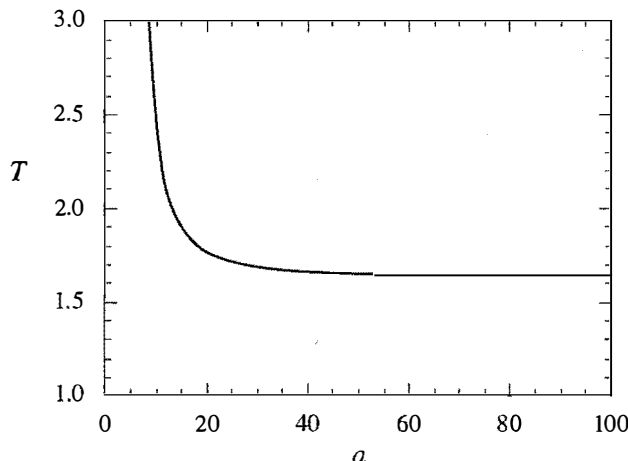


Figure 8.3.5

8.4 Global Bifurcations of Cycles

In two-dimensional systems, there are four common ways in which limit cycles are created or destroyed. The Hopf bifurcation is the most famous, but the other three deserve their day in the sun. They are harder to detect because they involve large

regions of the phase plane rather than just the neighborhood of a single fixed point. Hence they are called ***global bifurcations***. In this section we offer some prototypical examples of global bifurcations, and then compare them to one another and to the Hopf bifurcation. A few of their scientific applications are discussed in Sections 8.5 and 8.6 and in the exercises.

Saddle-node Bifurcation of Cycles

A bifurcation in which two limit cycles coalesce and annihilate is called a ***fold*** or ***saddle-node bifurcation of cycles***, by analogy with the related bifurcation of fixed points. An example occurs in the system

$$\dot{r} = \mu r + r^3 - r^5$$

$$\dot{\theta} = \omega + br^2$$

studied in Section 8.2. There we were interested in the subcritical Hopf bifurcation at $\mu = 0$; now we concentrate on the dynamics for $\mu < 0$.

It is helpful to regard the radial equation $\dot{r} = \mu r + r^3 - r^5$ as a one-dimensional system. As you should check, this system undergoes a saddle-node bifurcation of fixed points at $\mu_c = -1/4$. Now returning to the two-dimensional system, these fixed points correspond to circular ***limit cycles***. Figure 8.4.1 plots the “radial phase portraits” and the corresponding behavior in the phase plane.

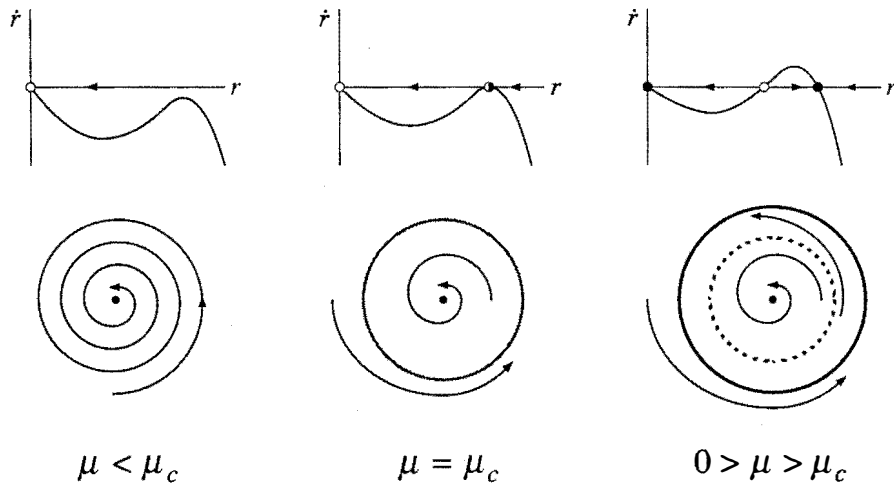


Figure 8.4.1

At μ_c a half-stable cycle is born out of the clear blue sky. As μ increases it splits into a pair of limit cycles, one stable, one unstable. Viewed in the other direction, a stable and unstable cycle collide and disappear as μ decreases through μ_c . Notice that the origin remains stable throughout; it does not participate in this bifurcation.

For future reference, note that at birth the cycle has $O(1)$ amplitude, in contrast to the Hopf bifurcation, where the limit cycle has small amplitude proportional to $(\mu - \mu_c)^{1/2}$.

Infinite-period Bifurcation

Consider the system

$$\dot{r} = r(1 - r^2)$$

$$\dot{\theta} = \mu - \sin \theta$$

where $\mu \geq 0$. This system combines two one-dimensional systems that we have studied previously in Chapters 3 and 4. In the radial direction, all trajectories (except $r^* = 0$) approach the unit circle monotonically as $t \rightarrow \infty$. In the angular direction, the motion is everywhere counterclockwise if $\mu > 1$, whereas there are two invariant rays defined by $\sin \theta = \mu$ if $\mu < 1$. Hence as μ decreases through $\mu_c = 1$, the phase portraits change as in Figure 8.4.2.

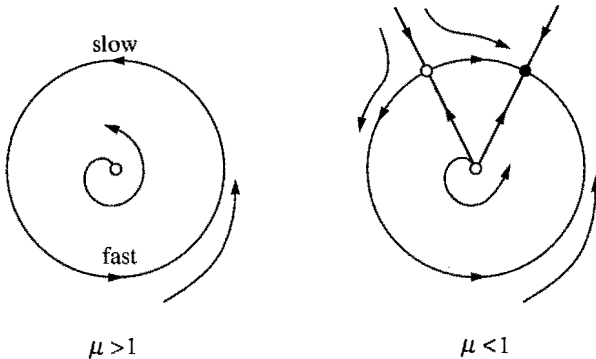


Figure 8.4.2

As μ decreases, the limit cycle $r=1$ develops a bottleneck at $\theta = \pi/2$ that becomes increasingly severe as $\mu \rightarrow 1^+$. The oscillation period lengthens and finally becomes infinite at $\mu_c = 1$, when a fixed point appears on the circle; hence the term **infinite-period bifurcation**. For $\mu < 1$, the fixed point splits into a saddle and a node.

As the bifurcation is approached, the amplitude of the oscillation stays $O(1)$ but the period increases like $(\mu - \mu_c)^{-1/2}$, for the reasons discussed in Section 4.3.

Homoclinic Bifurcation

In this scenario, part of a limit cycle moves closer and closer to a saddle point. At the bifurcation the cycle touches the saddle point and becomes a homoclinic or-

bit. This is another kind of infinite-period bifurcation; to avoid confusion, we'll call it a *saddle-loop* or *homoclinic bifurcation*.

It is hard to find an analytically transparent example, so we resort to the computer. Consider the system

$$\begin{aligned}\dot{x} &= y \\ \dot{y} &= \mu y + x - x^2 + xy.\end{aligned}$$

Figure 8.4.3 plots a series of phase portraits before, during, and after the bifurcation; only the important features are shown.

Numerically, the bifurcation is found to occur at $\mu_c \approx -0.8645$. For $\mu < \mu_c$, say $\mu = -0.92$, a stable limit cycle passes close to a saddle point at the origin (Figure 8.4.3a). As μ increases to μ_c , the limit cycle swells (Figure 8.4.3b) and bangs into the saddle, creating a homoclinic orbit (Figure 8.4.3c). Once $\mu > \mu_c$, the saddle connection breaks and the loop is destroyed (Figure 8.4.3d).

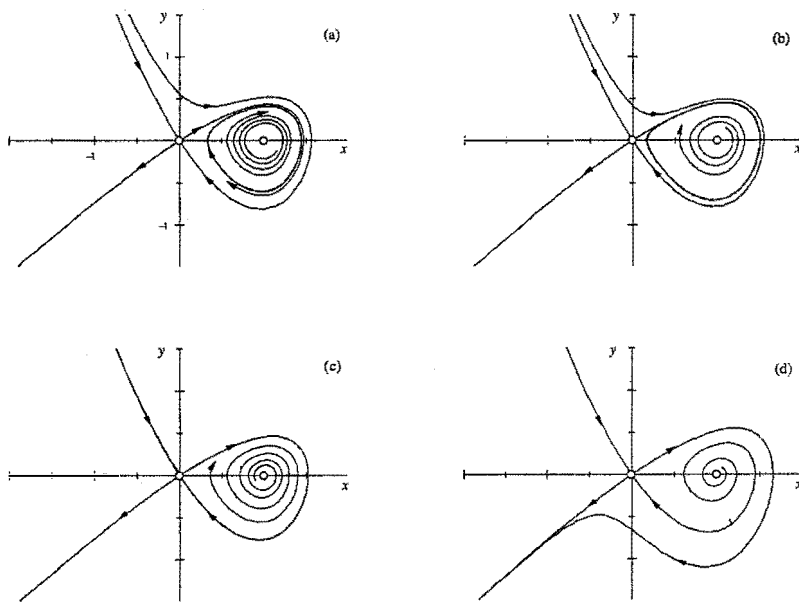


Figure 8.4.3

The key to this bifurcation is the behavior of the unstable manifold of the saddle. Look at the branch of the unstable manifold that leaves the origin to the north-east: after it loops around, it either hits the origin (Figure 8.4.3c) or veers off to one side or the other (Figures 8.4.3a, d).

Scaling Laws

For each of the bifurcations given here, there are characteristic *scaling laws* that govern the amplitude and period of the limit cycle as the bifurcation is approached. Let μ denote some dimensionless measure of the distance from the bifurcation, and assume that $\mu \ll 1$. The generic scaling laws for bifurcations of cycles in two-dimensional systems are given in Table 7.4.1.

	Amplitude of stable limit cycle	Period of cycle
Supercritical Hopf	$O(\mu^{1/2})$	$O(1)$
Saddle-node bifurcation of cycles	$O(1)$	$O(1)$
Infinite-period	$O(1)$	$O(\mu^{-1/2})$
Homoclinic	$O(1)$	$O(\ln \mu)$

Table 7.4.1

All of these laws have been explained previously, except those for the homoclinic bifurcation. The scaling of the period in that case is obtained by estimating the time required for a trajectory to pass by a saddle point (see Exercise 8.4.12 and Gaspard 1990).

Exceptions to these rules can occur, but only if there is some symmetry or other special feature that renders the problem nongeneric, as in the following example.

EXAMPLE 8.4.1:

The van der Pol oscillator $\ddot{x} + \varepsilon \dot{x}(x^2 - 1) + x = 0$ does not seem to fit anywhere in Table 7.4.1. At $\varepsilon = 0$, the eigenvalues at the origin are pure imaginary ($\lambda = \pm i$), suggesting that a Hopf bifurcation occurs at $\varepsilon = 0$. But we know from Section 7.6 that for $0 < \varepsilon \ll 1$, the system has a limit cycle of amplitude $r \approx 2$. Thus the cycle is born “full grown,” not with size $O(\varepsilon^{1/2})$ as predicted by the scaling law. What’s the explanation?

Solution: The bifurcation at $\varepsilon = 0$ is degenerate. The nonlinear term $\varepsilon \dot{x}x^2$ vanishes at precisely the same parameter value as the eigenvalues cross the imaginary axis. That’s a nongeneric coincidence if there ever was one!

We can rescale x to remove this degeneracy. Write the equation as $\ddot{x} + x + \varepsilon x^2 \dot{x} - \varepsilon \dot{x} = 0$. Let $u^2 = \varepsilon x^2$ to remove the ε -dependence of the nonlinear term. Then $u = \varepsilon^{1/2}x$ and the equation becomes

$$\ddot{u} + u + u^2 \dot{u} - \varepsilon \dot{u} = 0.$$

Now the nonlinear term is not destroyed when the eigenvalues become pure imaginary. From Section 7.6 the limit cycle solution is $x(t, \varepsilon) \approx 2 \cos t$ for $0 < \varepsilon \ll 1$. In terms of u this becomes

$$u(t, \varepsilon) \approx (2\sqrt{\varepsilon}) \cos t.$$

Hence the amplitude grows like $\varepsilon^{1/2}$, just as expected for a Hopf bifurcation. ■

The scaling laws given here were derived by thinking about prototypical examples in *two-dimensional* systems. In higher-dimensional phase spaces, the corresponding bifurcations obey the same scaling laws, but with two caveats: (1) Many *additional* bifurcations of limit cycles become possible; thus our table is no longer exhaustive. (2) The homoclinic bifurcation becomes much more subtle to analyze. It often creates chaotic dynamics in its aftermath (Guckenheimer and Holmes 1983, Wiggins 1990).

All of this begs the question: Why should you care about these scaling laws? Suppose you're an experimental scientist and the system you're studying exhibits a stable limit cycle oscillation. Now suppose you change a control parameter and the oscillation stops. By examining the scaling of the period and amplitude near this bifurcation, you can learn something about the system's dynamics (which are usually not known precisely, if at all). In this way, possible models can be eliminated or supported. For an example in physical chemistry, see Gaspard (1990).

8.5 Hysteresis in the Driven Pendulum and Josephson Junction

This section deals with a physical problem in which both homoclinic and infinite-period bifurcations arise. The problem was introduced back in Sections 4.4 and 4.6. At that time we were studying the dynamics of a damped pendulum driven by a constant torque, or equivalently, its high-tech analog, a superconducting Josephson junction driven by a constant current. Because we weren't ready for two-dimensional systems, we reduced both problems to vector fields on the circle by looking at the heavily *overdamped limit* of negligible mass (for the pendulum) or negligible capacitance (for the Josephson junction).

Now we're ready to tackle the full two-dimensional problem. As we claimed at the end of Section 4.6, for sufficiently weak damping the pendulum and the Josephson junction can exhibit intriguing hysteresis effects, thanks to the coexistence of a stable limit cycle and a stable fixed point. In physical terms, the pendulum can settle into either a rotating solution where it whirls over the top, or a stable rest state where gravity balances the applied torque. The final state depends on the initial conditions. Our goal now is to understand how this bistability comes about.

We will phrase our discussion in terms of the Josephson junction, but will mention the pendulum analog whenever it seems helpful.

Governing Equations

As explained in Section 4.6, the governing equation for the Josephson junction is

$$\frac{\hbar C}{2e} \ddot{\phi} + \frac{\hbar}{2eR} \dot{\phi} + I_c \sin \phi = I_B \quad (1)$$

where \hbar is Planck's constant divided by 2π , e is the charge on the electron, I_B is the constant bias current, C , R , and I_c are the junction's capacitance, resistance, and critical current, and $\phi(t)$ is the phase difference across the junction.

To highlight the role of damping, we nondimensionalize (1) differently from in Section 4.6. Let

$$\tilde{t} = \left(\frac{2eI_c}{\hbar C} \right)^{1/2} t, \quad I = \frac{I_B}{I_c}, \quad \alpha = \left(\frac{\hbar}{2eI_c R^2 C} \right)^{1/2}. \quad (2)$$

Then (1) becomes

$$\phi'' + \alpha \phi' + \sin \phi = I \quad (3)$$

where α and I are the dimensionless damping and applied current, and the prime denotes differentiation with respect to \tilde{t} . Here $\alpha > 0$ on physical grounds, and we may choose $I \geq 0$ without loss of generality (otherwise, redefine $\phi \rightarrow -\phi$).

Let $y = \phi'$. Then the system becomes

$$\begin{aligned} \phi' &= y \\ y' &= I - \sin \phi - \alpha y. \end{aligned} \quad (4)$$

As in Section 6.7 the phase space is a *cylinder*, since ϕ is an angular variable and y is a real number (best thought of as an angular velocity).

Fixed Points

The fixed points of (4) satisfy $y^* = 0$ and $\sin \phi^* = I$. Hence there are two fixed points on the cylinder if $I < 1$, and none if $I > 1$. When the fixed points exist, one is a saddle and the other is a sink, since the Jacobian

$$A = \begin{pmatrix} 0 & 1 \\ -\cos \phi^* & -\alpha \end{pmatrix}$$

has $\tau = -\alpha < 0$ and $\Delta = \cos \phi^* = \pm \sqrt{1 - I^2}$. When $\Delta > 0$, we have a stable node if

$\tau^2 - 4\Delta = \alpha^2 - 4\sqrt{1-I^2} > 0$, i.e., if the damping is strong enough or if I is close to 1; otherwise the sink is a stable spiral. At $I = 1$ the stable node and the saddle coalesce in a *saddle-node bifurcation of fixed points*.

Existence of a Closed Orbit

What happens when $I > 1$? There are no more fixed points available; something new has to happen. We claim that *all trajectories are attracted to a unique, stable limit cycle*.

The first step is to show that a periodic solution exists. The argument uses a clever idea introduced by Poincaré long ago. Watch carefully—this idea will come up frequently in our later work.

Consider the nullcline $y = \alpha^{-1}(I - \sin \phi)$ where $y' = 0$. The flow is downward above the nullcline and upward below it (Figure 8.5.1).

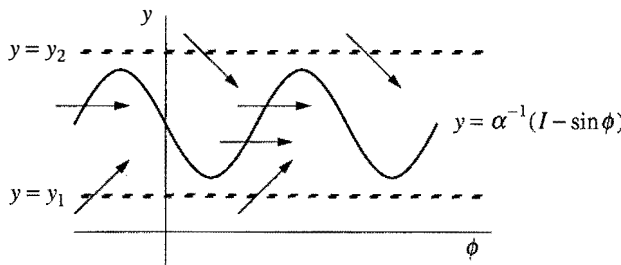


Figure 8.5.1

In particular, all trajectories eventually enter the strip $y_1 \leq y \leq y_2$ (Figure 8.5.1), and stay in there forever. (Here y_1 and y_2 are any fixed numbers such that $0 < y_1 < (I-1)/\alpha$ and $y_2 > (I+1)/\alpha$.) Inside the strip, the flow is always to the right, because $y > 0$ implies $\phi' > 0$.

Also, since $\phi = 0$ and $\phi = 2\pi$ are equivalent on the cylinder, we may as well confine our attention to the rectangular box $0 \leq \phi \leq 2\pi$, $y_1 \leq y \leq y_2$. This box contains all the information about the long-term behavior of the flow (Figure 8.5.2).

Now consider a trajectory that starts at a height y on the left side of the box, and follow it until it intersects the right side of the box at some new height $P(y)$, as shown in Figure 8.5.2. The mapping from y to $P(y)$ is called the *Poincaré map*. It tells us how the height of a trajectory changes after one lap around the cylinder (Figure 8.5.3).

Figure 8.5.2

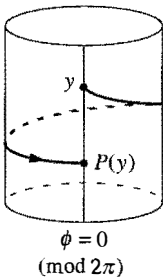


Figure 8.5.3

The Poincaré map is also called the *first-return map*, because if a trajectory starts at a height y on the line $\phi = 0$ (mod 2π), then $P(y)$ is its height when it returns to that line for the first time.

Now comes the key point: we can't compute $P(y)$ explicitly, but if we can show that there's a point y^* such that $P(y^*) = y^*$, then the corresponding trajectory will be a closed orbit (because it returns to the same location on the cylinder after one lap).

To show that such a y^* must exist, we need to know what the graph of $P(y)$ looks like, at least roughly. Consider a trajectory that starts at $y = y_1$, $\phi = 0$. We claim that

$$P(y_1) > y_1.$$

This follows because the flow is strictly upward at first, and the trajectory can never return to the line $y = y_1$, since the flow is everywhere upward on that line (recall Figures 8.5.1 and 8.5.2). By the same kind of argument,

$$P(y_2) < y_2.$$

Furthermore, $P(y)$ is a *continuous* function. This follows from the theorem that solutions of differential equations depend continuously on initial conditions, if the vector field is smooth enough.

And finally, $P(y)$ is a *monotonic* function. (By drawing pictures, you can convince yourself that if $P(y)$ were not monotonic, two trajectories would cross—and that's forbidden.) Taken together, these results imply that $P(y)$ has the shape shown in Figure 8.5.4.

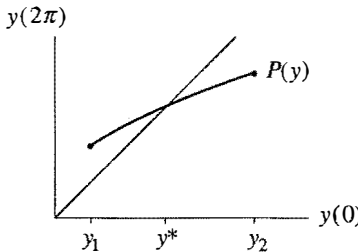


Figure 8.5.4

By the intermediate value theorem (or common sense), the graph of $P(y)$ must cross the 45° diagonal somewhere; that intersection is our desired y^* .

Uniqueness of the Limit Cycle

The argument above proves the *existence* of a closed orbit, and almost proves its uniqueness. But we haven't excluded the possibility that $P(y) \equiv y$ on some in-

terval, in which case there would be a band of infinitely many closed orbits.

To nail down the uniqueness part of our claim, we recall from Section 6.7 that there are two topologically different kinds of periodic orbits on a cylinder: ***librations*** and ***rotations*** (Figure 8.5.5).

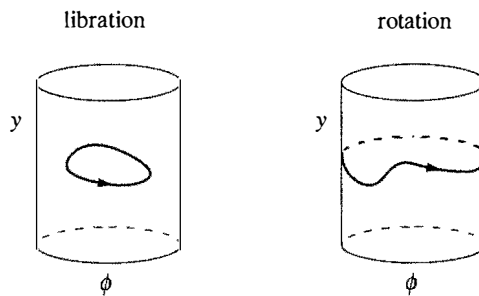


Figure 8.5.5

For $I > 1$, librations are impossible because any libration must encircle a fixed point, by index theory—but there are no fixed points when $I > 1$. Hence we only need to consider rotations.

Suppose there were two different rotations. The phase portrait on the cylinder would have to look like Figure 8.5.6.

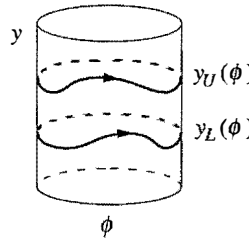


Figure 8.5.6

One of the rotations would have to lie *strictly above* the other because trajectories can't cross. Let $y_U(\phi)$ and $y_L(\phi)$ denote the “upper” and “lower” rotations, where $y_U(\phi) > y_L(\phi)$ for all ϕ .

The existence of two such rotations leads to a contradiction, as shown by the following energy argument. Let

$$E = \frac{1}{2}y^2 - \cos \phi. \quad (5)$$

After one circuit around any rotation $y(\phi)$, the change in energy ΔE must vanish. Hence

$$0 = \Delta E = \int_0^{2\pi} \frac{dE}{d\phi} d\phi. \quad (6)$$

But (5) implies

$$\frac{dE}{d\phi} = y \frac{dy}{d\phi} + \sin \phi \quad (7)$$

and

$$\frac{dy}{d\phi} = \frac{y'}{\phi'} = \frac{I - \sin \phi - \alpha y}{y}, \quad (8)$$

from (4). Substituting (8) into (7) gives $dE/d\phi = I - \alpha y$. Thus (6) implies

$$0 = \int_0^{2\pi} (I - \alpha y) d\phi$$

on any rotation $y(\phi)$. Equivalently, any rotation must satisfy

$$\int_0^{2\pi} y(\phi) d\phi = \frac{2\pi I}{\alpha}. \quad (9)$$

But since $y_U(\phi) > y_L(\phi)$,

$$\int_0^{2\pi} y_U(\phi) d\phi > \int_0^{2\pi} y_L(\phi) d\phi,$$

and so (9) can't hold for *both* rotations.

This contradiction proves that the rotation for $I > 1$ is unique, as claimed.

Homoclinic Bifurcation

Suppose we slowly decrease I , starting from some value $I > 1$. What happens to the rotating solution? Think about the pendulum: as the driving torque is reduced, the pendulum struggles more and more to make it over the top. At some critical value $I_c < 1$, the torque is insufficient to overcome gravity and damping, and the pendulum can no longer whirl. Then the rotation disappears and all solutions damp out to the rest state.

Our goal now is to visualize the corresponding bifurcation in phase space. In Exercise 8.5.2, you're asked to show (by numerical computation of the phase portrait) that if α is sufficiently small, the stable limit cycle is destroyed in a *homoclinic bifurcation* (Section 8.4). The following schematic drawings summarize the results you should get.

First suppose $I_c < I < 1$. The system is bistable: a sink coexists with a stable limit cycle (Figure 8.5.7).

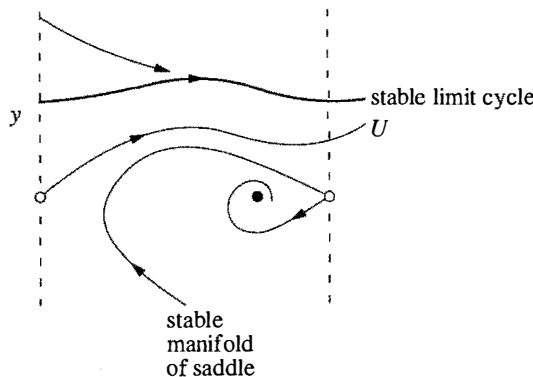


Figure 8.5.7

Keep your eye on the trajectory labeled U in Figure 8.5.7. It is a branch of the unstable manifold of the saddle. As $t \rightarrow \infty$, U asymptotically approaches the stable limit cycle.

As I decreases, the stable limit cycle moves down and squeezes U closer to the stable manifold of the saddle. When $I = I_c$, the limit cycle merges with U in a homoclinic bifurcation. Now U is a homoclinic orbit—it joins the saddle to itself (Figure 8.5.8).

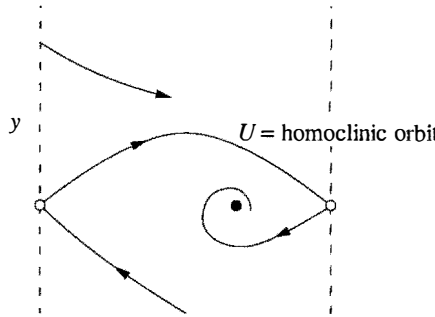


Figure 8.5.8

Finally, when $I < I_c$, the saddle connection breaks and U spirals into the sink (Figure 8.5.9).

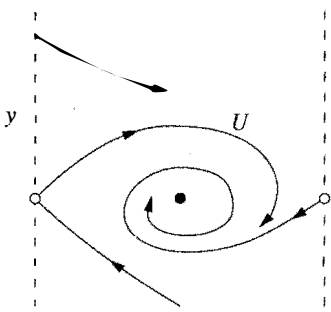


Figure 8.5.9

The scenario described here is valid only if the dimensionless damping α is sufficiently small. We know that something different has to happen for large α . After all, when α is infinite we are in the overdamped limit studied in Section 4.6. Our analysis there showed that the periodic solution is destroyed by an *infinite-period bifurcation* (a saddle and a node are born on the former limit cycle). So it's plausible that an infinite-period bifurcation should also occur if α is large but finite. These intuitive ideas are confirmed by numerical integration (Exercise 8.5.2).

Putting it all together, we arrive at the stability diagram shown in Figure 8.5.10. Three types of bifurcations occur: homoclinic and infinite-period bifurcations of periodic orbits, and a saddle-node bifurcation of fixed points.

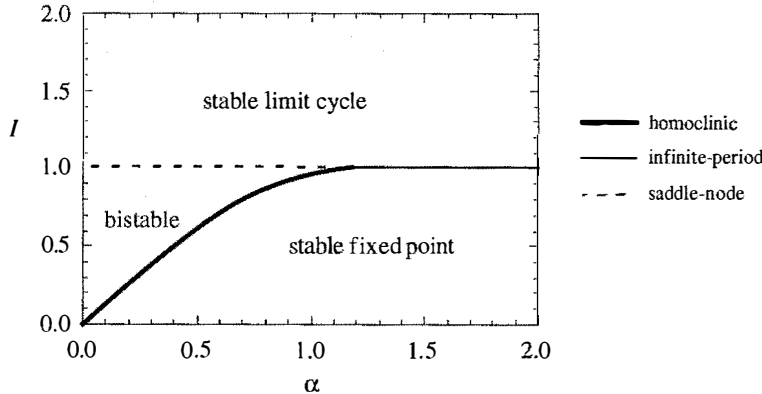


Figure 8.5.10

Our argument leading to Figure 8.5.10 has been heuristic. For rigorous proofs, see Levi et al. (1978). Also, Guckenheimer and Holmes (1983, p. 202) derive an analytical approximation for the homoclinic bifurcation curve for $\alpha \ll 1$, using an advanced technique known as Melnikov's method. They show that the bifurcation curve is tangent to the line $I = 4\alpha/\pi$ as $\alpha \rightarrow 0$. Even if α is not so small, this approximation works nicely, thanks to the straightness of the homoclinic bifurcation curve in Figure 8.5.10.

Hysteretic Current-Voltage Curve

Figure 8.5.10 explains why lightly damped Josephson junctions have hysteretic $I - V$ curves. Suppose α is small and I is initially below the homoclinic bifurca-

tion (thick line in Figure 8.5.10). Then the junction will be operating at the stable fixed point, corresponding to the zero-voltage state. As I is increased, nothing changes until I exceeds 1. Then the stable fixed point disappears in a saddle-node bifurcation, and the junction jumps into a nonzero voltage state (the limit cycle).

If I is brought back down, the limit cycle persists below $I = 1$ but its frequency tends to zero continuously as I_c is approached. Specifically, the frequency tends to zero like $[\ln(I - I_c)]^{-1}$, just as expected from the scaling law discussed in Section 8.4. Now recall from Section 4.6 that the junction's dc-voltage is proportional to its oscillation frequency. Hence, the voltage also returns to zero continuously as $I \rightarrow I_c^+$ (Figure 8.5.11).

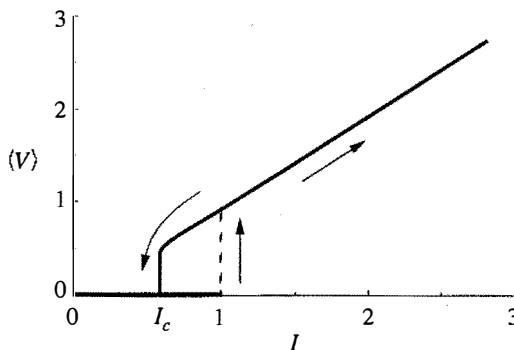


Figure 8.5.11

In practice, the voltage appears to jump discontinuously back to zero, but that is to be expected because $[\ln(I - I_c)]^{-1}$ has *infinite derivatives of all orders* at I_c ! (See Exercise 8.5.1.) The steepness of the curve makes it impossible to resolve the continuous return to zero. For instance, in experiments on pendula, Sullivan and Zimmerman (1971) measured the mechanical analog of the $I - V$ curve—namely, the curve relating the rotation rate to the applied torque. Their data show a jump back to zero rotation rate at the bifurcation.

8.6 Coupled Oscillators and Quasiperiodicity

Besides the plane and the cylinder, another important two-dimensional phase space is the **torus**. It is the natural phase space for systems of the form

$$\dot{\theta}_1 = f_1(\theta_1, \theta_2)$$

$$\dot{\theta}_2 = f_2(\theta_1, \theta_2)$$

where f_1 and f_2 are periodic in both arguments.

For instance, a simple model of *coupled oscillators* is given by

$$\begin{aligned}\dot{\theta}_1 &= \omega_1 + K_1 \sin(\theta_2 - \theta_1) \\ \dot{\theta}_2 &= \omega_2 + K_2 \sin(\theta_1 - \theta_2),\end{aligned}\quad (1)$$

where θ_1, θ_2 are the *phases* of the oscillators, $\omega_1, \omega_2 > 0$ are their *natural frequencies*, and $K_1, K_2 \geq 0$ are *coupling constants*. Equation (1) has been used to model the interaction between human circadian rhythms and the sleep-wake cycle (Strogatz 1986, 1987).

An intuitive way to think about (1) is to imagine two friends jogging on a circular track. Here $\theta_1(t), \theta_2(t)$ represent their positions on the track, and ω_1, ω_2 are proportional to their preferred running speeds. If they were uncoupled, then each would run at his or her preferred speed and the faster one would periodically overtake the slower one (as in Example 4.2.1). But these are *friends*—they want to run around *together*! So they need to compromise, with each adjusting his or her speed as necessary.

If their preferred speeds are too different, phase-locking will be impossible and they may want to find new running partners.

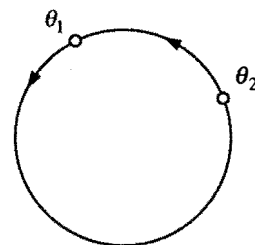


Figure 8.6.1

Here we consider (1) more abstractly, to illustrate some general features of flows on the torus and also to provide an example of a saddle-node bifurcation of cycles (Section 8.4). To visualize the flow, imagine two points running around a circle at instantaneous rates $\dot{\theta}_1, \dot{\theta}_2$ (Figure 8.6.1). Alternatively, we could imagine a *single* point tracing out a trajectory on a torus with coordinates θ_1, θ_2 (Figure 8.6.2). The coordinates are analogous to latitude and longitude.

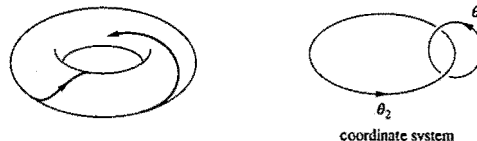


Figure 8.6.2

But since the curved surface of a torus makes it hard to draw phase portraits, we prefer to use an equivalent representation: a *square with periodic boundary conditions*. Then if a trajectory runs off an edge, it magically reappears on the opposite edge, as in some video games (Figure 8.6.3).

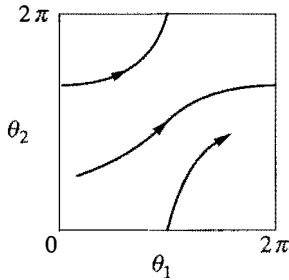


Figure 8.6.3

Uncoupled System

Even the seemingly trivial case of uncoupled oscillators ($K_1, K_2 = 0$) holds some surprises. Then (1) reduces to $\dot{\theta}_1 = \omega_1, \dot{\theta}_2 = \omega_2$. The corresponding trajectories on the square are straight lines with constant slope $d\theta_2/d\theta_1 = \omega_2/\omega_1$. There are two qualitatively different cases, depending on whether the slope is a rational or an irrational number.

If the slope is **rational**, then $\omega_1/\omega_2 = p/q$ for some integers p, q with no common factors. In this case *all trajectories are closed orbits* on the torus, because θ_1 completes p revolutions in the same time that θ_2 completes q revolutions. For example, Figure 8.6.4 shows a trajectory on the square with $p = 3, q = 2$.

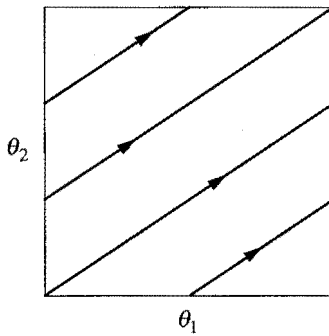


Figure 8.6.4

When plotted on the torus, the same trajectory gives . . . a **trefoil knot**! Figure 8.6.5 shows a trefoil, alongside a top view of a torus with a trefoil wound around it.

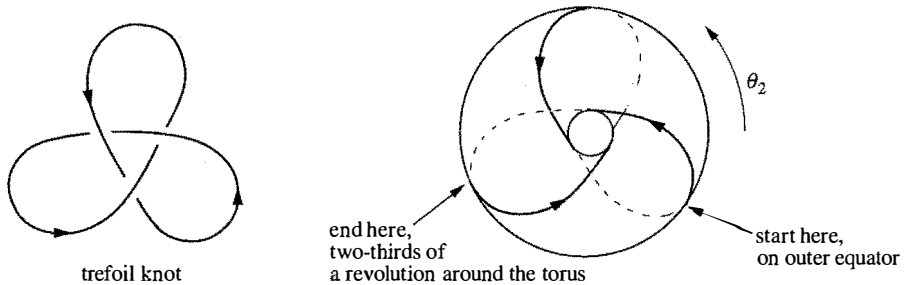


Figure 8.6.5

Do you see why this knot corresponds to $p = 3, q = 2$? Follow the knotted trajectory in Figure 8.6.5, and count the number of revolutions made by θ_2 during the time that θ_1 makes one revolution, where θ_1 is latitude and θ_2 is longitude. Starting on the outer equator, the trajectory moves onto the top surface, dives into the hole, travels along the bottom surface, and then reappears on the outer equator, *two-thirds* of the way around the torus. Thus θ_2 makes *two-thirds* of a revolution while θ_1 makes one revolution; hence $p = 3, q = 2$.

In fact the trajectories are always knotted if $p, q \geq 2$ have no common factors. The resulting curves are called *p:q torus knots*.

The second possibility is that the slope is *irrational* (Figure 8.6.6). Then the flow is said to be *quasiperiodic*. Every trajectory winds around endlessly on the torus, never intersecting itself and yet never quite closing.

How can we be sure the trajectories never close? Any closed trajectory necessarily makes an integer number of revolutions in both θ_1 and θ_2 ; hence the slope would have to be rational, contrary to assumption.

Furthermore, when the slope is irrational, each trajectory is *dense* on the torus: in other words, each trajectory comes arbitrarily close to any given point on the torus. This is *not* to say that the trajectory passes *through* each point; it just comes arbitrarily close (Exercise 8.6.3).

Quasiperiodicity is significant because it is a new type of long-term behavior. Unlike the earlier entries (fixed point, closed orbit, homoclinic and heteroclinic orbits and cycles), quasiperiodicity occurs only on the torus.

Coupled System

Now consider (1) in the coupled case where $K_1, K_2 > 0$. The dynamics can be deciphered by looking at the *phase difference* $\phi = \theta_1 - \theta_2$. Then (1) yields

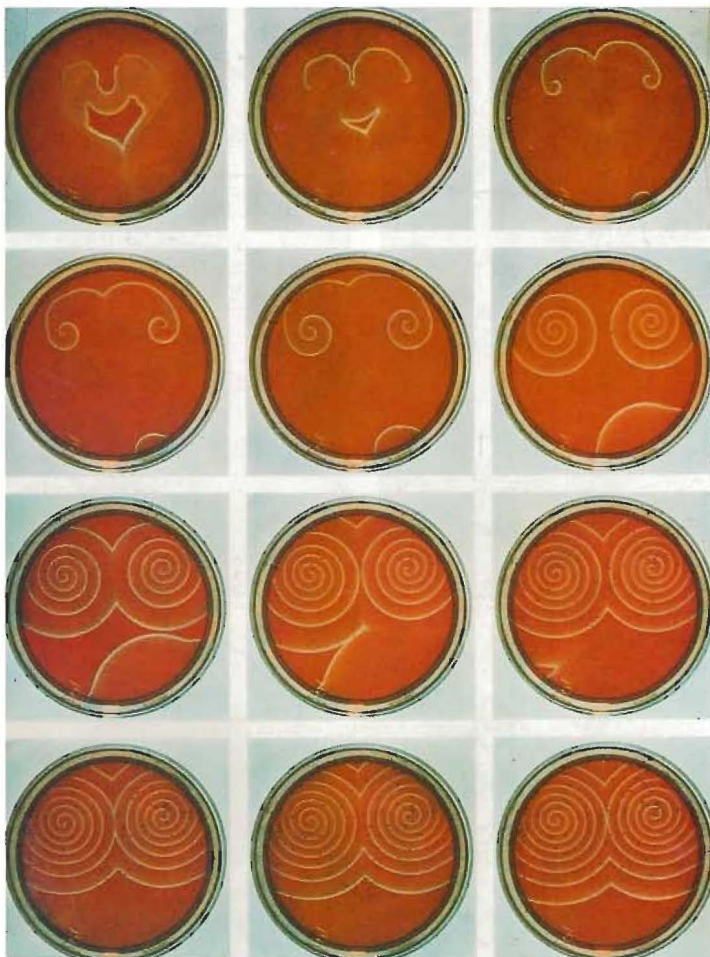


Plate 1: Spiral waves of chemical activity in a shallow dish of the Belousov-Zhabotinsky reaction (Section 8.3). These snapshots read from left to right and top to bottom. The complicated initial condition shown in the upper left was created by touching the liquid with a hot wire, thereby inducing an expanding circular wave of oxidation, and then disrupting this wave by gently rocking the dish. As time evolves, the blue waves propagate by diffusion through the motionless reddish-orange liquid. Whenever two waves collide, they annihilate each other, like grassfires rushing head on. Ultimately the system organizes itself into a pair of counterrotating spirals. Reproduced from Winfree (1974). Photographs by Fritz Goro.

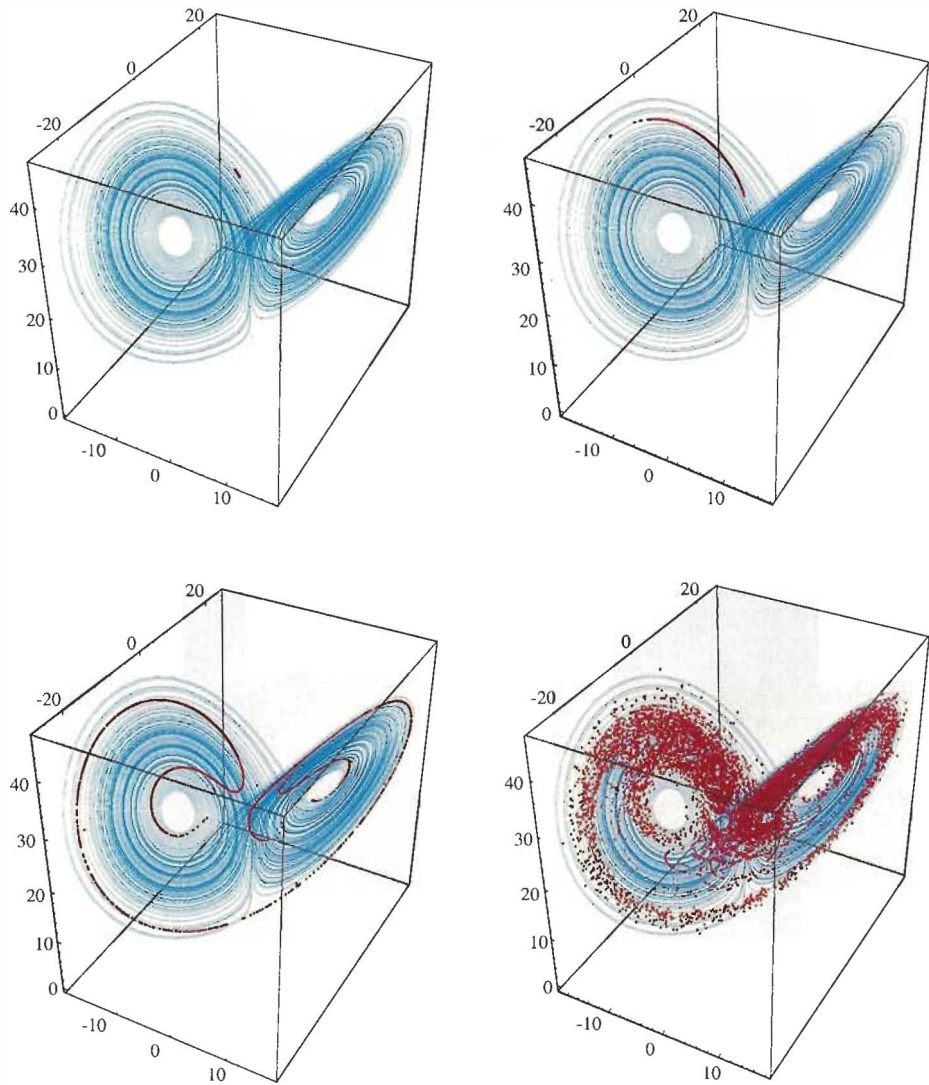


Plate 2: Divergence of nearby trajectories on the Lorenz attractor (Section 9.3). The Lorenz attractor is shown in blue. The red points show the evolution of a small blob of 10,000 nearby initial conditions, at times $t = 3, 6, 9$, and 15 . As each point moves according to the Lorenz equations, the blob is stretched into a long thin filament, which then wraps around the attractor. Ultimately the points spread over much of the attractor, showing that the final state could be almost anywhere, even though the initial conditions were almost identical. This sensitive dependence on initial conditions is the signature of a chaotic system.

Plate inspired by a similar illustration in Crutchfield et al. (1986). Numerical integration and computer graphics by Thanos Siapas, using Equation (9.2.1) with parameters $\sigma = 10$, $b = 8/3$, $r = 28$.

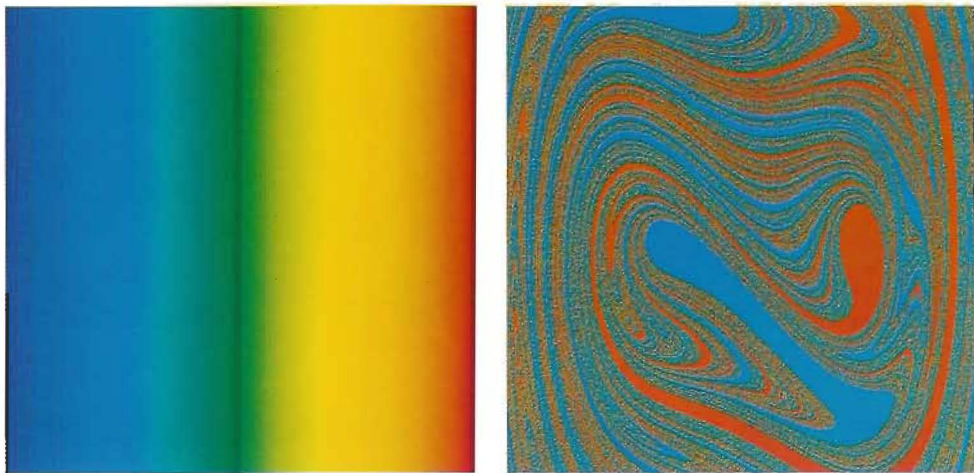


Plate 3: Fractal basin boundaries for the periodically forced double-well oscillator

$$x' = y, \quad y' = x - x^3 - \delta y + F \cos \omega t,$$

with $\delta=0.25$, $F=0.25$, $\omega=1$ (Section 12.5). For these parameter values, the system has two periodic attractors, corresponding to forced oscillations confined to the left or right well.

(a) Color map: The square region $-2.5 \leq x, y \leq 2.5$ is subdivided into 900×900 cells, and each cell is color-coded according to the x -position of its center point.

(b) Basins of attraction: Each cell is color-coded according to its fate after many drive cycles. Roughly speaking, if the trajectory ends up oscillating in the right well, the original cell is colored red; if it ends up in the left well, it is colored blue. More precisely, given an initial point (x_0, y_0) at the center of a cell, the state $(x(t), y(t))$ is computed at $t=73 \times 2\pi/\omega$ (that is, after 73 drive cycles), and the original cell is color-coded by the value of $x(t)$. The basins have a complicated shape, and the boundary between them is fractal (Moon and Li 1985). Near the boundary, slight variations in initial conditions can lead to totally different outcomes.

Computations by Thanos Siapas on a Thinking Machines CM-5 parallel computer using a fifth-order Runge–Kutta–Fehlberg method.

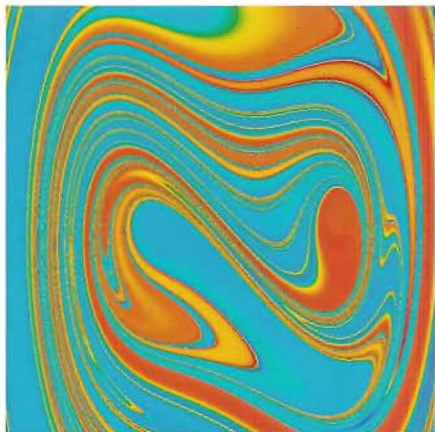
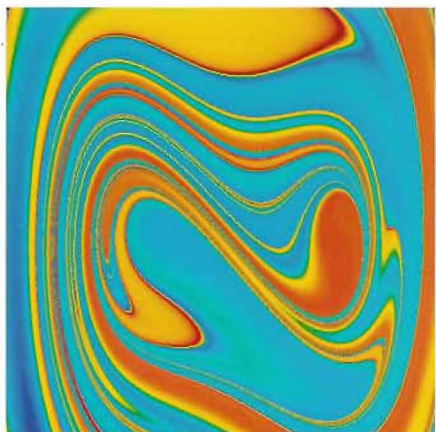
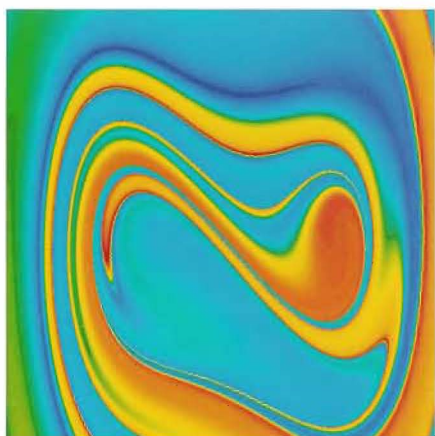
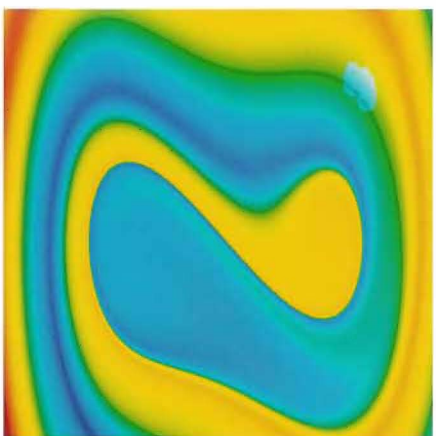


Plate 4: Maps of the short-term behavior of the periodically forced double-well oscillator. Equations, parameters, and color code as in Plate 3. However, instead of showing the system's asymptotic behavior, these plates show the color-coded value of $x(t)$ after only 1, 2, 3, and 4 drive cycles, respectively. The red and blue regions correspond to initial conditions that converge rapidly to one of the two attractors. A rainbow of colors is found near the basin boundary, because those initial conditions lead to trajectories that linger far from either attractor during the time shown.

$$\begin{aligned}\dot{\phi} &= \dot{\theta}_1 - \dot{\theta}_2 \\ &= \omega_1 - \omega_2 - (K_1 + K_2) \sin \phi,\end{aligned}\quad (2)$$

which is just the nonuniform oscillator studied in Section 4.3. By drawing the standard picture (Figure 8.6.7), we see that there are two fixed points for (2) if $|\omega_1 - \omega_2| < K_1 + K_2$ and none if $|\omega_1 - \omega_2| > K_1 + K_2$. A saddle-node bifurcation occurs when $|\omega_1 - \omega_2| = K_1 + K_2$.

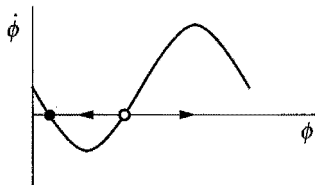


Figure 8.6.7

Suppose for now that there are two fixed points, defined implicitly by

$$\sin \phi^* = \frac{\omega_1 - \omega_2}{K_1 + K_2}.$$

As Figure 8.6.7 shows, all trajectories of (2) asymptotically approach the stable fixed point. Therefore, back on the torus, the trajectories of (1) approach a stable **phase-locked** solution in which the oscillators are separated by a constant phase difference ϕ^* . The phase-locked solution is *periodic*; in fact, both oscillators run at a constant frequency given by $\omega^* = \dot{\theta}_1 = \dot{\theta}_2 = \omega_2 + K_2 \sin \phi^*$. Substituting for $\sin \phi^*$ yields

$$\omega^* = \frac{K_1 \omega_2 + K_2 \omega_1}{K_1 + K_2}.$$

This is called the **compromise frequency** because it lies between the natural frequencies of the two oscillators (Figure 8.6.8).

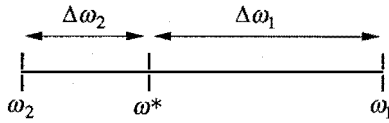


Figure 8.6.8

The compromise is not generally halfway; instead the frequencies are shifted by an amount proportional to the coupling strengths, as shown by the identity

$$\left| \frac{\Delta\omega_1}{\Delta\omega_2} \right| = \left| \frac{\omega_1 - \omega^*}{\omega_2 - \omega^*} \right| = \left| \frac{K_1}{K_2} \right|.$$

Now we're ready to plot the phase portrait on the torus (Figure 8.6.9). The stable and unstable locked solutions appear as diagonal lines of slope 1, since $\dot{\theta}_1 = \dot{\theta}_2 = \omega^*$.

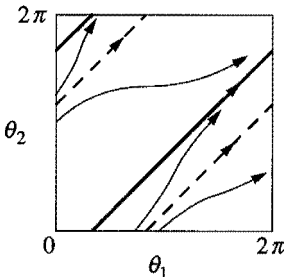


Figure 8.6.9

If we pull the natural frequencies apart, say by detuning one of the oscillators, then the locked solutions approach each other and coalesce when $|\omega_1 - \omega_2| = K_1 + K_2$. Thus the locked solution is destroyed in a *saddle-node bifurcation of cycles* (Section 8.4). After the bifurcation, the flow is like that in the uncoupled case studied earlier: we have either quasiperiodic or rational flow, depending on the parameters. The only difference is that now the trajectories on the square are curvy, not straight.

8.7 Poincaré Maps

In Section 8.5 we used a Poincaré map to prove the existence of a periodic orbit for the driven pendulum and Josephson junction. Now we discuss Poincaré maps more generally.

Poincaré maps are useful for studying swirling flows, such as the flow near a periodic orbit (or as we'll see later, the flow in some chaotic systems). Consider an n -dimensional system $\dot{\mathbf{x}} = \mathbf{f}(\mathbf{x})$. Let S be an $n-1$ dimensional *surface of section* (Figure 8.7.1). S is required to be transverse to the flow, i.e., all trajectories starting on S flow through it, not parallel to it.

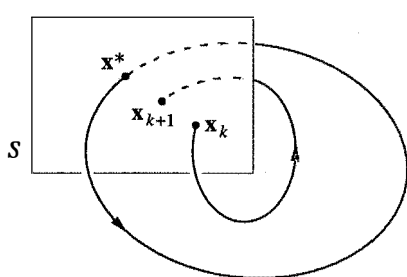


Figure 8.7.1

The *Poincaré map* P is a mapping from S to itself, obtained by following trajectories from one intersection with S to the next. If $\mathbf{x}_k \in S$ denotes the k th in-

tersection, then the Poincaré map is defined by

$$\mathbf{x}_{k+1} = P(\mathbf{x}_k).$$

Suppose that \mathbf{x}^* is a *fixed point* of P , i.e., $P(\mathbf{x}^*) = \mathbf{x}^*$. Then a trajectory starting at \mathbf{x}^* returns to \mathbf{x}^* after some time T , and is therefore a *closed orbit* for the original system $\dot{\mathbf{x}} = \mathbf{f}(\mathbf{x})$. Moreover, by looking at the behavior of P near this fixed point, we can determine the stability of the closed orbit.

Thus the Poincaré map converts problems about closed orbits (which are difficult) into problems about fixed points of a mapping (which are easier in principle, though not always in practice). The snag is that it's typically impossible to find a formula for P . For the sake of illustration, we begin with two examples for which P can be computed explicitly.

EXAMPLE 8.7.1:

Consider the vector field given in polar coordinates by $\dot{r} = r(1 - r^2)$, $\dot{\theta} = 1$. Let S be the positive x -axis, and compute the Poincaré map. Show that the system has a unique periodic orbit and classify its stability.

Solution: Let r_0 be an initial condition on S . Since $\dot{\theta} = 1$, the first return to S occurs after a *time of flight* $t = 2\pi$. Then $r_1 = P(r_0)$, where r_1 satisfies

$$\int_{r_0}^{r_1} \frac{dr}{r(1-r^2)} = \int_0^{2\pi} dt = 2\pi.$$

Evaluation of the integral (Exercise 8.7.1) yields $r_1 = [1 + e^{-4\pi}(r_0^{-2} - 1)]^{-1/2}$. Hence $P(r) = [1 + e^{-4\pi}(r^{-2} - 1)]^{-1/2}$. The graph of P is plotted in Figure 8.7.2.

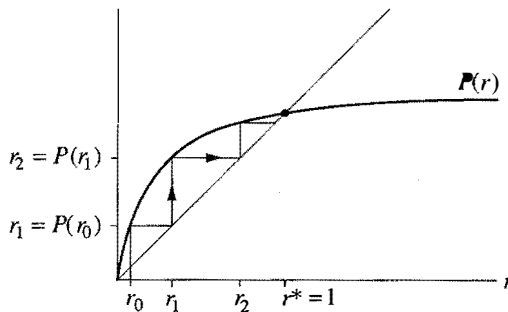


Figure 8.7.2

A fixed point occurs at $r^* = 1$ where the graph intersects the 45° line. The *cobweb* construction in Figure 8.7.2 enables us to iterate the map graphically. Given an input r_k , draw a vertical line until it intersects the graph of P ; that height is the out-

put r_{k+1} . To iterate, we make r_{k+1} the new input by drawing a horizontal line until it intersects the 45° diagonal line. Then repeat the process. Convince yourself that this construction works; we'll be using it often.

The cobweb shows that the fixed point $r^* = 1$ is stable and unique. No surprise, since we knew from Example 7.1.1 that this system has a stable limit cycle at $r = 1$. ■

EXAMPLE 8.7.2:

A sinusoidally forced RC -circuit can be written in dimensionless form as $\dot{x} + x = A \sin \omega t$, where $\omega > 0$. Using a Poincaré map, show that this system has a unique, globally stable limit cycle.

Solution: This is one of the few time-dependent systems we've discussed in this book. Such systems can always be made time-independent by adding a new variable. Here we introduce $\theta = \omega t$ and regard the system as a vector field on a cylinder: $\dot{\theta} = \omega$, $\dot{x} + x = A \sin \theta$. Any vertical line on the cylinder is an appropriate section S ; we choose $S = \{(\theta, x) : \theta = 0 \bmod 2\pi\}$. Consider an initial condition on S given by $\theta(0) = 0$, $x(0) = x_0$. Then the time of flight between successive intersections is $t = 2\pi/\omega$. In physical terms, we strobe the system once per drive cycle and look at the consecutive values of x .

To compute P , we need to solve the differential equation. Its general solution is a sum of homogeneous and particular solutions: $x(t) = c_1 e^{-t} + c_2 \sin \omega t + c_3 \cos \omega t$. The constants c_2 and c_3 can be found explicitly, but the important point is that they depend on A and ω but *not* on the initial condition x_0 ; only c_1 depends on x_0 . To make the dependence on x_0 explicit, observe that at $t = 0$, $x = x_0 = c_1 + c_3$. Thus

$$x(t) = (x_0 - c_3)e^{-t} + c_2 \sin \omega t + c_3 \cos \omega t.$$

Then P is defined by $x_1 = P(x_0) = x(2\pi/\omega)$. Substitution yields

$$\begin{aligned} P(x_0) &= x(2\pi/\omega) = (x_0 - c_3)e^{-2\pi/\omega} + c_3 \\ &= x_0 e^{-2\pi/\omega} + c_4 \end{aligned}$$

where $c_4 = c_3(1 - e^{-2\pi/\omega})$.

The graph of P is a straight line with a slope $e^{-2\pi/\omega} < 1$ as shown in Figure 8.7.3.

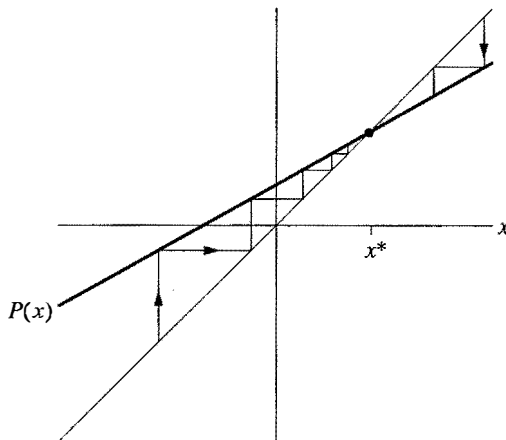


Figure 8.7.3

Since P has slope less than 1, it intersects the diagonal at a unique point. Furthermore, the cobweb shows that the deviation of x_k from the fixed point is reduced by a constant factor with each iteration. Hence the fixed point is unique and globally stable.

In physical terms, the circuit always settles into the same forced oscillation, regardless of the initial conditions. This is a familiar result from elementary physics, looked at in a new way. ■

Linear Stability of Periodic Orbits

Now consider the general case: Given a system $\dot{\mathbf{x}} = \mathbf{f}(\mathbf{x})$ with a closed orbit, how can we tell whether the orbit is stable or not? Equivalently, we ask whether the corresponding fixed point \mathbf{x}^* of the Poincaré map is stable. Let \mathbf{v}_0 be an infinitesimal perturbation such that $\mathbf{x}^* + \mathbf{v}_0$ is in S . Then after the first return to S ,

$$\begin{aligned}\mathbf{x}^* + \mathbf{v}_1 &= P(\mathbf{x}^* + \mathbf{v}_0) \\ &= P(\mathbf{x}^*) + [DP(\mathbf{x}^*)]\mathbf{v}_0 + O(\|\mathbf{v}_0\|^2)\end{aligned}$$

where $DP(\mathbf{x}^*)$ is an $(n-1) \times (n-1)$ matrix called the *linearized Poincaré map* at \mathbf{x}^* . Since $\mathbf{x}^* = P(\mathbf{x}^*)$, we get

$$\mathbf{v}_1 = [DP(\mathbf{x}^*)]\mathbf{v}_0$$

assuming that we can neglect the small $O(\|\mathbf{v}_0\|^2)$ terms.

The desired stability criterion is expressed in terms of the eigenvalues λ_j of $DP(\mathbf{x}^*)$: *The closed orbit is linearly stable if and only if $|\lambda_j| < 1$ for all $j = 1, \dots, n-1$.*

To understand this criterion, consider the generic case where there are no repeated eigenvalues. Then there is a basis of eigenvectors $\{\mathbf{e}_j\}$ and so we can write $\mathbf{v}_0 = \sum_{j=1}^{n-1} v_j \mathbf{e}_j$ for some scalars v_j . Hence

$$\mathbf{v}_1 = (DP(\mathbf{x}^*)) \sum_{j=1}^{n-1} v_j \mathbf{e}_j = \sum_{j=1}^{n-1} v_j \lambda_j \mathbf{e}_j.$$

Iterating the linearized map k times gives

$$\mathbf{v}_k = \sum_{j=1}^{n-1} v_j (\lambda_j)^k \mathbf{e}_j.$$

Hence, if all $|\lambda_j| < 1$, then $\|\mathbf{v}_k\| \rightarrow 0$ geometrically fast. This proves that \mathbf{x}^* is linearly stable. Conversely, if $|\lambda_j| > 1$ for some j , then perturbations along \mathbf{e}_j grow, so \mathbf{x}^* is unstable. A borderline case occurs when the largest eigenvalue has magnitude $|\lambda_m| = 1$; this occurs at bifurcations of periodic orbits, and then a nonlinear stability analysis is required.

The λ_j are called the *characteristic* or *Floquet multipliers* of the periodic orbit. (Strictly speaking, these are the *nontrivial* multipliers; there is always an additional trivial multiplier $\lambda \equiv 1$ corresponding to perturbations *along* the periodic orbit. We have ignored such perturbations since they just amount to time-translation.)

In general, the characteristic multipliers can only be found by numerical integration (see Exercise 8.7.10). The following examples are two of the rare exceptions.

EXAMPLE 8.7.3:

Find the characteristic multiplier for the limit cycle of Example 8.7.1.

Solution: We linearize about the fixed point $r^* = 1$ of the Poincaré map. Let $r = 1 + \eta$, where η is infinitesimal. Then $\dot{r} = \dot{\eta} = (1 + \eta)(1 - (1 + \eta)^2)$. After neglecting $O(\eta^2)$ terms, we get $\dot{\eta} = -2\eta$. Thus $\eta(t) = \eta_0 e^{-2t}$. After a time of flight $t = 2\pi$, the new perturbation is $\eta_1 = e^{-4\pi} \eta_0$. Hence $e^{-4\pi}$ is the characteristic multiplier. Since $|e^{-4\pi}| < 1$, the limit cycle is linearly stable. ■

For this simple two-dimensional system, the linearized Poincaré map degenerates to a 1×1 matrix, i.e., a number. Exercise 8.7.1 asks you to show explicitly that

$P'(r^*) = e^{-4\pi}$, as expected from the general theory above.

Our final example comes from a recent analysis of coupled Josephson junctions.

EXAMPLE 8.7.4:

The N -dimensional system

$$\dot{\phi}_i = \Omega + a \sin \phi_i + \frac{1}{N} \sum_{j=1}^N \sin \phi_j, \quad (1)$$

for $i = 1, \dots, N$, describes the dynamics of a series array of overdamped Josephson junctions in parallel with a resistive load (Tsang et al. 1991). For technological reasons, there is great interest in the solution where all the junctions oscillate in phase. This *in-phase* solution is given by $\phi_1(t) = \phi_2(t) = \dots = \phi_N(t) = \phi^*(t)$, where $\phi^*(t)$ denotes the common waveform. Find conditions under which the in-phase solution is periodic, and calculate the characteristic multipliers of this solution.

Solution: For the in-phase solution, all N equations reduce to

$$\frac{d\phi^*}{dt} = \Omega + (a+1) \sin \phi^*. \quad (2)$$

This has a periodic solution (on the circle) if and only if $|\Omega| > |a+1|$. To determine the stability of the in-phase solution, let $\phi_i(t) = \phi^*(t) + \eta_i(t)$, where the $\eta_i(t)$ are infinitesimal perturbations. Then substituting ϕ_i into (1) and dropping quadratic terms in η yields

$$\dot{\eta}_i = [a \cos \phi^*(t)] \eta_i + [\cos \phi^*(t)] \frac{1}{N} \sum_{j=1}^N \eta_j. \quad (3)$$

We don't have $\phi^*(t)$ explicitly, but that doesn't matter, thanks to two tricks. First, the linear system decouples if we change variables to

$$\begin{aligned} \mu &= \frac{1}{N} \sum_{j=1}^N \eta_j, \\ \xi_i &= \eta_{i+1} - \eta_i, \quad i = 1, \dots, N-1. \end{aligned}$$

Then $\dot{\xi}_i = [a \cos \phi^*(t)] \xi_i$. Separation of variables yields

$$\frac{d\xi_i}{\xi_i} = [a \cos \phi^*(t)] dt = \frac{[a \cos \phi^*] d\phi^*}{\Omega + (a+1) \sin \phi^*},$$

where we've used (2) to eliminate dt . (That was the second trick.)

Now we compute the change in the perturbations after one circuit around the closed orbit ϕ^* :

$$\oint \frac{d\xi_i}{\xi_i} = \int_0^{2\pi} \frac{[a \cos \phi^*] d\phi^*}{\Omega + (a+1) \sin \phi^*}$$
$$\Rightarrow \ln \frac{\xi_i(T)}{\xi_i(0)} = \frac{a}{a+1} \ln [\Omega + (a+1) \sin \phi^*]_0^{2\pi} = 0.$$

Hence $\xi_i(T) = \xi_i(0)$. Similarly, we can show that $\mu(T) = \mu(0)$. Thus $\eta_i(T) = \eta_i(0)$ for all i ; all perturbations are unchanged after one cycle! Therefore all the characteristic multipliers $\lambda_j = 1$. ■

This calculation shows that the in-phase state is (linearly) neutrally stable. That's discouraging technologically—one would like the array to lock into coherent oscillation, thereby greatly increasing the output power over that available from a single junction.

Since the calculation above is based on linearization, you might wonder whether the neglected nonlinear terms could stabilize the in-phase state. In fact they don't: a reversibility argument shows that the in-phase state is not attracting, even if the nonlinear terms are kept (Exercise 8.7.11).

EXERCISES FOR CHAPTER 8

8.1 Saddle-Node, Transcritical, and Pitchfork Bifurcations

8.1.1 For the following prototypical examples, plot the phase portraits as μ varies:

- $\dot{x} = \mu x - x^2$, $\dot{y} = -y$ (transcritical bifurcation)
- $\dot{x} = \mu x + x^3$, $\dot{y} = -y$ (subcritical pitchfork bifurcation)

For each of the following systems, find the eigenvalues at the stable fixed point as a function of μ , and show that one of the eigenvalues tends to zero as $\mu \rightarrow 0$.

8.1.2 $\dot{x} = \mu - x^2$, $\dot{y} = -y$

8.1.3 $\dot{x} = \mu x - x^2$, $\dot{y} = -y$

8.1.4 $\dot{x} = \mu x + x^3$, $\dot{y} = -y$

8.1.5 Prove that at any zero-eigenvalue bifurcation in two dimensions, the nullclines always intersect tangentially. (Hint: Consider the geometrical meaning of the rows in the Jacobian matrix.)

8.1.6 Consider the system $\dot{x} = y - 2x$, $\dot{y} = \mu + x^2 - y$.

- Sketch the nullclines.
- Find and classify the bifurcations that occur as μ varies.
- Sketch the phase portrait as a function of μ .

8.1.7 Find and classify all bifurcations for the system $\dot{x} = y - ax$, $\dot{y} = -by + x/(1+x)$.

8.1.8 (Bead on rotating hoop, revisited) In Section 3.5, we derived the following dimensionless equation for the motion of a bead on a rotating hoop:

$$\varepsilon \frac{d^2\phi}{d\tau^2} = -\frac{d\phi}{d\tau} - \sin\phi + \gamma \sin\phi \cos\phi.$$

Here $\varepsilon > 0$ is proportional to the mass of the bead, and $\gamma > 0$ is related to the spin rate of the hoop. Previously we restricted our attention to the overdamped limit $\varepsilon \rightarrow 0$.

- Now allow any $\varepsilon > 0$. Find and classify all bifurcations that occur as ε and γ vary.
- Plot the stability diagram in the positive quadrant of the ε, γ plane.

8.1.9 Plot the stability diagram for the system $\ddot{x} + b\dot{x} - kx + x^3 = 0$, where b and k can be positive, negative, or zero. Label the bifurcation curves in the (b, k) plane.

8.1.10 (Budworms vs. the forest) Ludwig et al. (1978) proposed a model for the effects of spruce budworm on the balsam fir forest. In Section 3.7, we considered the dynamics of the budworm population; now we turn to the dynamics of the forest. The condition of the forest is assumed to be characterized by $S(t)$, the average size of the trees, and $E(t)$, the “energy reserve” (a generalized measure of the forest’s health). In the presence of a constant budworm population B , the forest dynamics are given by

$$\dot{S} = r_S S \left(1 - \frac{S}{K_S} \frac{K_E}{E} \right), \quad \dot{E} = r_E E \left(1 - \frac{E}{K_E} \right) - P \frac{B}{S},$$

where $r_S, r_E, K_S, K_E, P > 0$ are parameters.

- Interpret the terms in the model biologically.
- Nondimensionalize the system.
- Sketch the nullclines. Show that there are two fixed points if B is small, and none if B is large. What type of bifurcation occurs at the critical value of B ?
- Sketch the phase portrait for both large and small values of B .

B.1.11 In a study of isothermal autocatalytic reactions, Gray and Scott (1985) considered a hypothetical reaction whose kinetics are given in dimensionless form by

$$\dot{u} = a(1-u) - uv^2, \quad \dot{v} = uv^2 - (a+k)v,$$

where $a, k > 0$ are parameters. Show that saddle-node bifurcations occur at $k = -a \pm \frac{1}{2}\sqrt{a}$.

8.1.12 (Interacting bar magnets) Consider the system

$$\dot{\theta}_1 = K \sin(\theta_1 - \theta_2) - \sin \theta_1$$

$$\dot{\theta}_2 = K \sin(\theta_2 - \theta_1) - \sin \theta_2$$

where $K \geq 0$. For a rough physical interpretation, suppose that two bar magnets are confined to a plane, but are free to rotate about a common pin joint, as shown in Figure 1. Let θ_1, θ_2 denote the angular orientations of the north poles of the magnets. Then the term $K \sin(\theta_2 - \theta_1)$ represents a repulsive force that tries to keep the two north poles 180° apart. This repulsion is opposed by the $\sin \theta$ terms, which model external magnets that pull the north poles of both bar magnets to the east. If the inertia of the magnets is negligible compared to viscous damping, then the equations above are a decent approximation to the true dynamics.

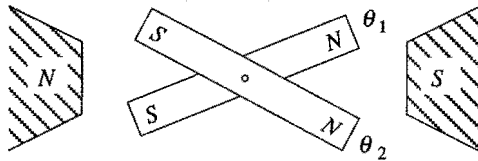


Figure 1

- Find and classify all the fixed points of the system.
- Show that a bifurcation occurs at $K = \frac{1}{2}$. What type of bifurcation is it? (Hint: Recall that $\sin(a - b) = \cos b \sin a - \sin b \cos a$.)
- Show that the system is a “gradient” system, in the sense that $\dot{\theta}_i = -\partial V/\partial \theta_i$, for some potential function $V(\theta_1, \theta_2)$, to be determined.
- Use part (c) to prove that the system has no periodic orbits.
- Sketch the phase portrait for $0 < K < \frac{1}{2}$, and then for $K > \frac{1}{2}$.

8.1.13 (Laser model) In Exercise 3.3.1 we introduced the laser model

$$\dot{n} = GnN - kn$$

$$\dot{N} = -GnN - fN + p$$

where $N(t)$ is the number of excited atoms and $n(t)$ is the number of photons in the laser field. The parameter G is the gain coefficient for stimulated emission, k is the decay rate due to loss of photons by mirror transmission, scattering, etc., f is the decay rate for spontaneous emission, and p is the pump strength. All parameters are positive, except p , which can have either sign. For more information, see Milonni and Eberly (1988).

- Nondimensionalize the system.
- Find and classify all the fixed points.
- Sketch all the qualitatively different phase portraits that occur as the dimensionless parameters are varied.
- Plot the stability diagram for the system. What types of bifurcation occur?

8.2 Hopf Bifurcations

8.2.1 Consider the biased van der Pol oscillator $\ddot{x} + \mu(x^2 - 1)\dot{x} + x = a$. Find the curves in (μ, a) space at which Hopf bifurcations occur.

The next three exercises deal with the system $\dot{x} = -y + \mu x + xy^2$, $\dot{y} = x + \mu y - x^2$.

8.2.2 By calculating the linearization at the origin, show that the system $\dot{x} = -y + \mu x + xy^2$, $\dot{y} = x + \mu y - x^2$ has pure imaginary eigenvalues when $\mu = 0$.

8.2.3 (Computer work) By plotting phase portraits on the computer, show that the system $\dot{x} = -y + \mu x + xy^2$, $\dot{y} = x + \mu y - x^2$ undergoes a Hopf bifurcation at $\mu = 0$. Is it subcritical, supercritical, or degenerate?

8.2.4 (A heuristic analysis) The system $\dot{x} = -y + \mu x + xy^2$, $\dot{y} = x + \mu y - x^2$ can be analyzed in a rough, intuitive way as follows.

- Rewrite the system in polar coordinates.
- Show that if $r \ll 1$, then $\dot{\theta} \approx 1$ and $\dot{r} \approx \mu r + \frac{1}{2}r^3 + \dots$, where the terms omitted are oscillatory and have essentially zero time-average around one cycle.
- The formulas in part (b) suggest the presence of an unstable limit cycle of radius $r \approx \sqrt{-8\mu}$ for $\mu < 0$. Confirm that prediction numerically. (Since we assumed that $r \ll 1$, the prediction is expected to hold only if $|\mu| \ll 1$.)

The reasoning above is shaky. See Drazin (1992, pp. 188–190) for a proper analysis via the Poincaré–Lindstedt method.

For each of the following systems, a Hopf bifurcation occurs at the origin when $\mu = 0$. Using a computer, plot the phase portrait and determine whether the bifurcation is subcritical or supercritical.

8.2.5 $\dot{x} = y + \mu x$, $\dot{y} = -x + \mu y - x^2 y$

8.2.6 $\dot{x} = \mu x + y - x^3$, $\dot{y} = -x + \mu y + 2y^3$

8.2.7 $\dot{x} = \mu x + y - x^2$, $\dot{y} = -x + \mu y + 2x^2$

8.2.8 (Predator-prey model) Odell (1980) considered the system

$$\dot{x} = x[x(1-x) - y], \quad \dot{y} = y(x-a),$$

where $x \geq 0$ is the dimensionless population of the prey, $y \geq 0$ is the dimension-

less population of the predator, and $a \geq 0$ is a control parameter.

- Sketch the nullclines in the first quadrant $x, y \geq 0$.
- Show that the fixed points are $(0, 0)$, $(1, 0)$, and $(a, a - a^2)$, and classify them.
- Sketch the phase portrait for $a > 1$, and show that the predators go extinct.
- Show that a Hopf bifurcation occurs at $a_c = \frac{1}{2}$. Is it subcritical or supercritical?
- Estimate the frequency of limit cycle oscillations for a near the bifurcation.
- Sketch all the topologically different phase portraits for $0 < a < 1$.

The article by Odell (1980) is worth looking up. It is an outstanding pedagogical introduction to the Hopf bifurcation and phase plane analysis in general.

8.2.9 Consider the predator-prey model

$$\dot{x} = x \left(b - x - \frac{y}{1+x} \right), \quad \dot{y} = y \left(\frac{x}{1+x} - ay \right),$$

where $x, y \geq 0$ are the populations and $a, b > 0$ are parameters.

- Sketch the nullclines and discuss the bifurcations that occur as b varies.
- Show that a positive fixed point $x^* > 0, y^* > 0$ exists for all $a, b > 0$. (Don't try to find the fixed point explicitly; use a graphical argument instead.)
- Show that a Hopf bifurcation occurs at the positive fixed point if

$$a = a_c = \frac{4(b-2)}{b^2(b+2)}$$

and $b > 2$. (Hint: A necessary condition for a Hopf bifurcation to occur is $\tau = 0$, where τ is the trace of the Jacobian matrix at the fixed point. Show that $\tau = 0$ if and only if $2x^* = b - 2$. Then use the fixed point conditions to express a_c in terms of x^* . Finally, substitute $x^* = (b-2)/2$ into the expression for a_c and you're done.)

- Using a computer, check the validity of the expression in (c) and determine whether the bifurcation is subcritical or supercritical. Plot typical phase portraits above and below the Hopf bifurcation.

8.2.10 (Bacterial respiration) Fairén and Velarde (1979) considered a model for respiration in a bacterial culture. The equations are

$$\dot{x} = B - x - \frac{xy}{1+qx^2}, \quad \dot{y} = A - \frac{xy}{1+qx^2}$$

where x and y are the levels of nutrient and oxygen, respectively, and $A, B, q > 0$ are parameters. Investigate the dynamics of this model. As a start, find all the fixed points and classify them. Then consider the nullclines and try to construct a trapping region. Can you find conditions on A, B, q under which the system has a stable limit cycle? Use numerical integration, the Poincaré–Bendixson theorem, results about Hopf bifurcations, or whatever else seems useful. (This question is deliber-

ately open-ended and could serve as a class project; see how far you can go.)

8.2.11 (Degenerate bifurcation, not Hopf) Consider the damped Duffing oscillator $\ddot{x} + \mu\dot{x} + x - x^3 = 0$.

- Show that the origin changes from a stable to an unstable spiral as μ decreases through zero.
- Plot the phase portraits for $\mu > 0$, $\mu = 0$, and $\mu < 0$, and show that the bifurcation at $\mu = 0$ is a degenerate version of the Hopf bifurcation.

8.2.12 (Analytical criterion to decide if a Hopf bifurcation is subcritical or supercritical) Any system at a Hopf bifurcation can be put into the following form by suitable changes of variables:

$$\dot{x} = -\omega y + f(x, y), \quad \dot{y} = \omega x + g(x, y),$$

where f and g contain only higher-order nonlinear terms that vanish at the origin. As shown by Guckenheimer and Holmes (1983, pp. 152–156), one can decide whether the bifurcation is subcritical or supercritical by calculating the sign of the following quantity:

$$16a = f_{xxx} + f_{xxy} + g_{xx} + g_{yyy} \\ + \frac{1}{\omega} [f_{xy}(f_{xx} + f_{yy}) - g_{xy}(g_{xx} + g_{yy}) - f_{xx}g_{xx} + f_{yy}g_{yy}]$$

where the subscripts denote partial derivatives evaluated at $(0, 0)$. The criterion is: If $a < 0$, the bifurcation is supercritical; if $a > 0$, the bifurcation is subcritical.

- Calculate a for the system $\dot{x} = -y + xy^2$, $\dot{y} = x - x^2$.
- Use part (a) to decide which type of Hopf bifurcation occurs for $\dot{x} = -y + \mu x + xy^2$, $\dot{y} = x + \mu y - x^2$ at $\mu = 0$. (Compare the results of Exercises 8.2.2–8.2.4.)

(You might be wondering what a measures. Roughly speaking, a is the coefficient of the cubic term in the equation $\dot{r} = ar^3$ governing the radial dynamics at the bifurcation. Here r is a slightly transformed version of the usual polar coordinate. For details, see Guckenheimer and Holmes (1983) or Grimshaw (1990).)

For each of the following systems, a Hopf bifurcation occurs at the origin when $\mu = 0$. Use the analytical criterion of Exercise 8.2.12 to decide if the bifurcation is sub- or supercritical. Confirm your conclusions on the computer.

8.2.13 $\dot{x} = y + \mu x$, $\dot{y} = -x + \mu y - x^2 y$

8.2.14 $\dot{x} = \mu x + y - x^3$, $\dot{y} = -x + \mu y + 2y^3$

8.2.15 $\dot{x} = \mu x + y - x^2$, $\dot{y} = -x + \mu y + 2x^2$

8.2.16 In Example 8.2.1, we argued that the system $\dot{x} = \mu x - y + xy^2$,

$\dot{y} = x + \mu y + y^3$ undergoes a subcritical Hopf bifurcation at $\mu = 0$. Use the analytical criterion to confirm that the bifurcation is subcritical.

8.3 Oscillating Chemical Reactions

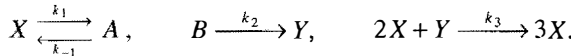
8.3.1 (Brusselator) The Brusselator is a simple model of a hypothetical chemical oscillator, named after the home of the scientists who proposed it. (This is a common joke played by the chemical oscillator community; there is also the “Oregonator,” “Palo Altonator,” etc.) In dimensionless form, its kinetics are

$$\begin{aligned}\dot{x} &= 1 - (b+1)x + ax^2y \\ \dot{y} &= bx - ax^2y\end{aligned}$$

where $a, b > 0$ are parameters and $x, y \geq 0$ are dimensionless concentrations.

- a) Find all the fixed points, and use the Jacobian to classify them.
- b) Sketch the nullclines, and thereby construct a trapping region for the flow.
- c) Show that a Hopf bifurcation occurs at some parameter value $b = b_c$, where b_c is to be determined.
- d) Does the limit cycle exist for $b > b_c$ or $b < b_c$? Explain, using the Poincaré–Bendixson theorem.
- e) Find the approximate period of the limit cycle for $b \approx b_c$.

8.3.2 Schnackenberg (1979) considered the following hypothetical model of a chemical oscillator:



After using the Law of Mass Action and nondimensionalizing, Schnackenberg reduced the system to

$$\begin{aligned}\dot{x} &= a - x + x^2y \\ \dot{y} &= b - x^2y\end{aligned}$$

where $a, b > 0$ are parameters and $x, y > 0$ are dimensionless concentrations.

- a) Show that all trajectories eventually enter a certain trapping region, to be determined. Make the trapping region as small as possible. (Hint: Examine the ratio \dot{y}/\dot{x} for large x .)
- b) Show that the system has a unique fixed point, and classify it.
- c) Show that the system undergoes a Hopf bifurcation when $b - a = (a + b)^3$.
- d) Is the Hopf bifurcation subcritical or supercritical? Use a computer to decide.
- e) Plot the stability diagram in a, b space. (Hint: It is a bit confusing to plot the curve $b - a = (a + b)^3$, since this requires analyzing a cubic. As in Section 3.7, the *parametric form* of the bifurcation curve comes to the rescue. Show that the bifurcation curve can be expressed as

$$a = \frac{1}{2}x * (1 - (x^*)^2), \quad b = \frac{1}{2}x * (1 + (x^*)^2)$$

where $x^* > 0$ is the x -coordinate of the fixed point. Then plot the bifurcation curve from these parametric equations. This trick is discussed in Murray (1989).)

8.3.3 (Relaxation limit of a chemical oscillator) Analyze the model for the chlorine dioxide–iodine–malonic acid oscillator, (8.3.4), (8.3.5), in the limit $b \ll 1$. Sketch the limit cycle in the phase plane and estimate its period.

8.4 Global Bifurcations of Cycles

8.4.1 Consider the system $\dot{r} = r(1 - r^2)$, $\dot{\theta} = \mu - \sin \theta$ for μ slightly greater than 1. Let $x = r \cos \theta$ and $y = r \sin \theta$. Sketch the waveforms of $x(t)$ and $y(t)$. (These are typical of what one might see experimentally for a system on the verge of an infinite-period bifurcation.)

8.4.2 Discuss the bifurcations of the system $\dot{r} = r(\mu - \sin r)$, $\dot{\theta} = 1$ as μ varies.

8.4.3 (Homoclinic bifurcation) Using numerical integration, find the value of μ at which the system $\dot{x} = \mu x + y - x^2$, $\dot{y} = -x + \mu y + 2x^2$ undergoes a homoclinic bifurcation. Sketch the phase portrait just above and below the bifurcation.

8.4.4 (Second-order phase-locked loop) Using a computer, explore the phase portrait of $\dot{\theta} + (1 - \mu \cos \theta)\dot{\theta} + \sin \theta = 0$ for $\mu \geq 0$. For some values of μ , you should find that the system has a stable limit cycle. Classify the bifurcations that create and destroy the cycle as μ increases from 0.

Exercises 8.4.5–8.4.11 deal with the *forced Duffing oscillator* in the limit where the forcing, detuning, damping, and nonlinearity are all weak:

$$\ddot{x} + x + \varepsilon(bx^3 + k\dot{x} - ax - F \cos t) = 0,$$

where $0 < \varepsilon \ll 1$, $b > 0$ is the nonlinearity, $k > 0$ is the damping, a is the detuning, and $F > 0$ is the forcing strength. This system is a small perturbation of a harmonic oscillator, and can therefore be handled with the methods of Section 7.6. We have postponed the problem until now because saddle-node bifurcations of cycles arise in its analysis.

8.4.5 (Averaged equations) Show that the averaged equations (7.6.53) for the system are

$$r' = -\frac{1}{2}(kr + F \cos \phi), \quad \phi' = -\frac{1}{8}(4a - 3br^2 + \frac{4F}{r} \cos \phi),$$

where $x = r \cos(t + \phi)$, $\dot{x} = -r \sin(t + \phi)$, and prime denotes differentiation with respect to slow time $T = \varepsilon t$, as usual. (If you skipped Section 7.6, accept these equations on faith.)

8.4.6 (Correspondence between averaged and original systems) Show that fixed points for the averaged system correspond to phase-locked periodic solutions for the original forced oscillator. Show further that saddle-node bifurcations of fixed points for the averaged system correspond to saddle-node bifurcations of cycles for the oscillator.

8.4.7 (No periodic solutions for averaged system) Regard (r, ϕ) as polar coordinates in the phase plane. Show that the averaged system has no closed orbits. (Hint: Use Dulac's criterion with $g(r, \phi) = r$. Let $\mathbf{x}' = (r', r\phi')$. Compute $\nabla \cdot (r\mathbf{x}') = \frac{\partial}{\partial r}(rr') + \frac{1}{r} \frac{\partial}{\partial \phi}(r^2\phi')$ and show that it has one sign.)

8.4.8 (No sources for averaged system) The result of the previous exercise shows that we only need to study the fixed points of the averaged system to determine its long-term behavior. By calculating $\nabla \cdot \mathbf{x}' = \frac{\partial}{\partial r}(r') + \frac{1}{r} \frac{\partial}{\partial \phi}(r\phi')$, show that the fixed points cannot be sources; only sinks and saddles are possible.

8.4.9 (Resonance curves and cusp catastrophe) In this exercise you are asked to determine how the equilibrium amplitude of the driven oscillations depends on the other parameters.

- Show that the fixed points satisfy $r^2 \left[k^2 + (\frac{3}{4}br^2 - a)^2 \right] = F^2$.
- From now on, assume that k and F are fixed. Graph r vs. a for the linear oscillator ($b = 0$). This is the familiar resonance curve.
- Graph r vs. a for the nonlinear oscillator ($b \neq 0$). Show that the curve is single-valued for small nonlinearity, say $b < b_c$, but triple-valued for large nonlinearity ($b > b_c$), and find an explicit formula for b_c . (Thus we obtain the intriguing conclusion that the driven oscillator can have three limit cycles for some values of a and b !)
- Show that if r is plotted as a surface above the (a, b) plane, the result is a cusp catastrophe surface (recall Section 3.6).

8.4.10 Now for the hard part: analyze the bifurcations of the averaged system.

- Plot the nullclines $r' = 0$ and $\phi' = 0$ in the phase plane, and study how their intersections change as the detuning a is increased from negative values to large positive values.
- Assuming that $b > b_c$, show that as a increases, the number of *stable* fixed points changes from one to two and then back to one again.

8.4.11 (Numerical exploration) Fix the parameters $k = 1$, $b = \frac{4}{3}$, $F = 2$.

- Using numerical integration, plot the phase portrait for the averaged system with a increasing from negative to positive values.
- Show that for $a = 2.8$, there are two stable fixed points.
- Go back to the original forced Duffing equation. Numerically integrate it and plot $x(t)$ as a increases slowly from $a = -1$ to $a = 5$, and then decreases

slowly back to $\alpha = -1$. You should see a dramatic hysteresis effect with the limit cycle oscillation suddenly jumping up in amplitude at one value of α , and then back down at another.

8.4.12 (Scaling near a homoclinic bifurcation) To find how the period of a closed orbit scales as a homoclinic bifurcation is approached, we estimate the time it takes for a trajectory to pass by a saddle point (this time is much longer than all others in the problem). Suppose the system is given locally by $\dot{x} \approx \lambda_u x$, $\dot{y} \approx -\lambda_s y$. Let a trajectory pass through the point $(\mu, 1)$, where $\mu \ll 1$ is the distance from the stable manifold. How long does it take until the trajectory has escaped from the saddle, say out to $x(t) \approx 1$? (See Gaspard (1990) for a detailed discussion.)

8.5 Hysteresis in the Driven Pendulum and Josephson Junction

8.5.1 Show that $[\ln(I - I_c)]^{-1}$ has infinite derivatives of all orders at I_c . (Hint: Consider $f(I) = (\ln I)^{-1}$ and try to derive a formula for $f^{(n+1)}(I)$ in terms of $f^{(n)}(I)$, where $f^{(n)}(I)$ denotes the n th derivative of $f(I)$.)

8.5.2 Consider the driven pendulum $\phi'' + \alpha\phi' + \sin\phi = I$. By numerical computation of the phase portrait, verify that if α is fixed and sufficiently small, the system's stable limit cycle is destroyed in a homoclinic bifurcation as I decreases. Show that if α is too large, the bifurcation is an infinite-period bifurcation instead.

8.5.3 (Logistic equation with periodically varying carrying capacity) Consider the logistic equation $\dot{N} = rN(1 - N/K(t))$, where the carrying capacity is positive, smooth, and T -periodic in t .

- Using a Poincaré map argument like that in the text, show that the system has at least one stable limit cycle of period T , contained in the strip $K_{\min} \leq N \leq K_{\max}$.
- Is the cycle necessarily unique?

8.6 Coupled Oscillators and Quasiperiodicity

† **8.6.1** (“Oscillator death” and bifurcations on a torus) In a paper on systems of neural oscillators, Ermentrout and Kopell (1990) illustrated the notion of “oscillator death” with the following model:

$$\dot{\theta}_1 = \omega_1 + \sin\theta_1 \cos\theta_2, \quad \dot{\theta}_2 = \omega_2 + \sin\theta_2 \cos\theta_1,$$

where $\omega_1, \omega_2 \geq 0$.

- Sketch all the qualitatively different phase portraits that arise as ω_1, ω_2 vary.
- Find the curves in ω_1, ω_2 parameter space along which bifurcations occur, and classify the various bifurcations.
- Plot the stability diagram in ω_1, ω_2 parameter space.

8.6.2 Reconsider the system (8.6.1):

$$\dot{\theta}_1 = \omega_1 + K_1 \sin(\theta_2 - \theta_1), \quad \dot{\theta}_2 = \omega_2 + K_2 \sin(\theta_1 - \theta_2).$$

- a) Show that the system has no fixed points, given that $\omega_1, \omega_2 > 0$ and $K_1, K_2 > 0$.
- b) Find a conserved quantity for the system. (Hint: Solve for $\sin(\theta_2 - \theta_1)$ in two ways. The existence of a conserved quantity shows that this system is a non-generic flow on the torus; normally there would not be any conserved quantities.)
- c) Suppose that $K_1 = K_2$. Show that the system can be nondimensionalized to

$$d\theta_1/d\tau = 1 + a \sin(\theta_2 - \theta_1), \quad d\theta_2/d\tau = \omega + a \sin(\theta_1 - \theta_2).$$

- d) Find the *winding number* $\lim_{\tau \rightarrow \infty} \theta_1(\tau)/\theta_2(\tau)$ analytically. (Hint: Evaluate the long-time averages $\langle d(\theta_1 + \theta_2)/d\tau \rangle$ and $\langle d(\theta_1 - \theta_2)/d\tau \rangle$, where the brackets are defined by $\langle f \rangle \equiv \lim_{T \rightarrow \infty} \frac{1}{T} \int_0^T f(\tau) d\tau$. For another approach, see Guckenheimer and Holmes (1983, p. 299).)

8.6.3 (Irrational flow yields dense orbits) Consider the flow on the torus given by $\dot{\theta}_1 = \omega_1$, $\dot{\theta}_2 = \omega_2$, where ω_1/ω_2 is irrational. Show each trajectory is **dense**; i.e., given any point p on the torus, any initial condition q , and any $\varepsilon > 0$, there is some $t < \infty$ such that the trajectory starting at q passes within a distance ε of p .

8.6.4 Consider the system

$$\dot{\theta}_1 = E - \sin \theta_1 + K \sin(\theta_2 - \theta_1), \quad \dot{\theta}_2 = E + \sin \theta_2 + K \sin(\theta_1 - \theta_2)$$

where $E, K \geq 0$.

- a) Find and classify all the fixed points.
- b) Show that if E is large enough, the system has periodic solutions on the torus. What type of bifurcation creates the periodic solutions?
- c) Find the bifurcation curve in (E, K) space at which these periodic solutions are created.

A generalization of this system to $N \gg 1$ phases has been proposed as a model of switching in charge-density waves (Strogatz et al. 1988, 1989).

8.6.5 (Plotting Lissajous figures) Using a computer, plot the curve whose parametric equations are $x(t) = \sin t$, $y(t) = \sin \omega t$, for the following rational and irrational values of the parameter ω :

- | | | |
|--------------------------------|-----------------------------------|---|
| (a) $\omega = 3$ | (b) $\omega = \frac{2}{3}$ | (c) $\omega = \frac{5}{3}$ |
| (d) $\omega = \sqrt{2}$ | (e) $\omega = \pi$ | (f) $\omega = \frac{1}{2}(1 + \sqrt{5})$. |

The resulting curves are called *Lissajous figures*. In the old days they were displayed on oscilloscopes by using two ac signals of different frequencies as inputs.

8.6.6 (Explaining Lissajous figures) Lissajous figures are one way to visualize the knots and quasiperiodicity discussed in the text. To see this, consider a pair of uncoupled harmonic oscillators described by the four-dimensional system $\ddot{x} + x = 0$, $\ddot{y} + \omega^2 y = 0$.

- Show that if $x = A(t) \sin \theta(t)$, $y = B(t) \sin \phi(t)$, then $\dot{A} = \dot{B} = 0$ (so A, B are constants) and $\dot{\theta} = 1$, $\dot{\phi} = \omega$.
- Explain why (a) implies that trajectories are typically confined to two-dimensional tori in a four-dimensional phase space.
- How are the Lissajous figures related to the trajectories of this system?

8.6.7 (Mechanical example of quasiperiodicity) The equations

$$m\ddot{r} = \frac{h^2}{mr^3} - k, \quad \dot{\theta} = \frac{h}{mr^2}$$

govern the motion of a mass m subject to a central force of constant strength $k > 0$. Here r, θ are polar coordinates and $h > 0$ is a constant (the angular momentum of the particle).

- Show that the system has a solution $r = r_0$, $\dot{\theta} = \omega_\theta$, corresponding to uniform circular motion at a radius r_0 and frequency ω_θ . Find formulas for r_0 and ω_θ .
- Find the frequency ω_r of small radial oscillations about the circular orbit.
- Show that these small radial oscillations correspond to quasiperiodic motion by calculating the winding number ω_r/ω_θ .
- Show by a geometric argument that the motion is either periodic or quasiperiodic for *any* amplitude of radial oscillation. (To say it in a more interesting way, the motion is never chaotic.)
- Can you think of a mechanical realization of this system?

8.6.8 Solve the equations of Exercise 8.6.7 on a computer, and plot the particle's path in the plane with polar coordinates r, θ .

8.7 Poincaré Maps

8.7.1 Use partial fractions to evaluate the integral $\int_{r_0}^r \frac{dr}{r(1-r^2)}$ that arises in Example 8.7.1, and show that $r_1 = [1 + e^{-4\pi}(r_0^{-2} - 1)]^{-1/2}$. Then confirm that $P'(r^*) = e^{-4\pi}$, as expected from Example 8.7.3.

† **8.7.2** Consider the vector field on the cylinder given by $\dot{\theta} = 1$, $\dot{y} = ay$. Define an appropriate Poincaré map and find a formula for it. Show that the system has a periodic orbit. Classify its stability for all real values of a .

8.7.3 (Overdamped system forced by a square wave) Consider an overdamped linear oscillator (or an RC -circuit) forced by a square wave. The system can be nondimensionalized to $\dot{x} + x = F(t)$, where $F(t)$ is a square wave of period T . To be more specific, suppose

$$F(t) = \begin{cases} +A, & 0 < t < T/2 \\ -A, & T/2 < t < T \end{cases}$$

for $t \in (0, T)$, and then $F(t)$ is periodically repeated for all other t . The goal is to show that all trajectories of the system approach a unique periodic solution. We could try to solve for $x(t)$ but that gets a little messy. Here's an approach based on the Poincaré map—the idea is to "strobe" the system once per cycle.

- a) Let $x(0) = x_0$. Show that $x(T) = x_0 e^{-T} - A(1 - e^{-T/2})^2$.
- b) Show that the system has a unique periodic solution, and that it satisfies $x_0 = -A \tanh(T/4)$.
- c) Interpret the limits of $x(T)$ as $T \rightarrow 0$ and $T \rightarrow \infty$. Explain why they're plausible.
- d) Let $x_1 = x(T)$, and define the Poincaré map P by $x_1 = P(x_0)$. More generally, $x_{n+1} = P(x_n)$. Plot the graph of P .
- e) Using a cobweb picture, show that P has a globally stable fixed point. (Hence the original system eventually settles into a periodic response to the forcing.)

8.7.4 A Poincaré map for the system $\dot{x} + x = A \sin \omega t$ was shown Figure 8.7.3, for a particular choice of parameters. Given that $\omega > 0$, can you deduce the sign of A ? If not, explain why not.

8.7.5 (Another driven overdamped system) By considering an appropriate Poincaré map, prove that the system $\dot{\theta} + \sin \theta = \sin t$ has at least two periodic solutions. Can you say anything about their stability? (Hint: Regard the system as a vector field on a cylinder: $i = 1$, $\dot{\theta} = \sin t - \sin \theta$. Sketch the nullclines and thereby infer the shape of certain key trajectories that can be used to bound the periodic solutions. For instance, sketch the trajectory that passes through $(t, \theta) = (\frac{\pi}{2}, \frac{\pi}{2})$.)

8.7.6 Give a mechanical interpretation of the system $\dot{\theta} + \sin \theta = \sin t$ considered in the previous exercise.

8.7.7 (Computer work) Plot a computer-generated phase portrait of the system $i = 1$, $\dot{\theta} = \sin t - \sin \theta$. Check that your results agree with your answer to Exercise 8.7.5.

8.7.8 Consider the system $\dot{x} + x = F(t)$, where $F(t)$ is a smooth, T -periodic function. Is it true that the system necessarily has a stable T -periodic solution $x(t)$? If so, prove it; if not, find an F that provides a counterexample.

+ 8.7.9 Consider the vector field given in polar coordinates by $\dot{r} = r - r^2$, $\dot{\theta} = 1$.

- Compute the Poincaré map from S to itself, where S is the positive x -axis.
- Show that the system has a unique periodic orbit and classify its stability.
- Find the characteristic multiplier for the periodic orbit.

8.7.10 Explain how to find Floquet multipliers numerically, starting from perturbations along the coordinate directions.

8.7.11 (Reversibility and the in-phase periodic state of a Josephson array) Use a reversibility argument to prove that the in-phase periodic state of (8.7.1) is not attracting, even if the nonlinear terms are kept.

+ 8.7.12 (Globally coupled oscillators) Consider the following system of N identical oscillators:

$$\dot{\theta}_i = f(\theta_i) + \frac{K}{N} \sum_{j=1}^N f(\theta_j), \text{ for } i = 1, \dots, N,$$

where $K > 0$ and $f(\theta)$ is smooth and 2π -periodic. Assume that $f(\theta) > 0$ for all θ so that the in-phase solution is periodic. By calculating the linearized Poincaré map as in Example 8.7.4, show that all the characteristic multipliers equal $+1$.

Thus the neutral stability found in Example 8.7.4 holds for a broader class of oscillator arrays. In particular, the reversibility of the system is not essential. This example is from Tsang et al. (1991).